Ford Motor Company
AERONUTRONIC DIVISION

Publication No. U-1951

ADVANCED TECHNOLOGY
ENGINEERING OPERATION

TECHNICAL REPORT

EMPIRE - A STUDY OF EARLY MANNED INTERPLANETARY MISSIONS

FINAL REPORT

Prepared for: George C. Marshall Space Flight Center
National Aeronautics and Space Administration
Huntsville, Alabama

Under Contract: NAS8-5025
Control No. TP-2-74-011 (1)

Reporting Period: 26 May 1962 - 25 November 1962

Prepared by: F. P. Dixon, Program Manager
M. H. Caldwell
D. P. Johnson
R. P. Nagorski
E. W. Onstead
R. K. Simmons
L. D. Stimpson
C. E. Van Emon

21 December 1962

Newport Beach, California

ABSTRACT

16078 over

This report summarizes the investigations and results of the EMPIRE Study Program undertaken by Aeronutronic Division of Ford Motor Company for the Future Projects Office, Marshall Space Flight Center, under Contract NAS8-5025.

The dual planet flyby missions of the Crocco and Symmetric trajectory classes are discussed. The Crocco mission with an August 1971 launch window requires an interplanetary injection velocity increment of 10.1 km/sec, has a return velocity of 13.5 km/sec, and takes approximately 400 days. The Symmetric mission with a July 1970 launch window has an injection velocity increment of 5.3 km/sec, a return velocity of 15.8 km/sec, and takes approximately 630 days. Additional results of the trajectory studies and abort trajectories are reported. The guidance and navigation subsystem, midcourse corrections, and planetary approach corrections are discussed.

A detailed analysis of the reentry phase of EMPIRE includes consideration of an Apollo-type, a Drag Brake, and a lifting-type reentry vehicle to return the six-man crew at mission completion or in an aborted condition. The High L/D reentry vehicle is used in the missions considered.

The various technological areas required for design criteria are developed and several spacecraft designs are considered. The all chemical propulsion Crocco system is discarded due to weight, complexity, and cost. The nuclear injected Crocco is treated in a similar manner. The lower energy injection for the Symmetric Mission leads to the feasibility of a nuclear injected vehicle with an Earth orbit weight of about 180,000 kilograms (400,000 pounds) before interplanetary transit. In addition, two chemical symmetric vehicles are treated. Conservative radiation exposures are derived, for the 630 day mission, of less than 200 REM and a polyethelene radiation shelter is designed. Scientific aspects of the missions are discussed.

Mission Success Probabilities are presented for the various missions considered and for Saturn C-5, Nova, and Super-Nova Earth launch vehicles in light of possible development.

The need for acceleration of nuclear rocket engine developments and auxiliary power developments is indicated. Definition of a larger nuclear engine of the order of 200,000 pounds thrust and about 800 seconds

burning time or 50,000 pound thrust and 3600 seconds burning time is indicated for the Symmetric Mission in 1970 (energy requirements are higher in 1972 and for later launch due to the less favorable position of Mars). Immediate development of this advanced nuclear propulsion capability is recommended.

A Development Plan and Funding Schedule is given for the 1970 launch window pinpointing the critical development areas and indicating a total program cost of $12.6 billion independent of other programmed R&D costs.

In conclusion, technological feasibility for an early manned dual planet Mars-Venus flyby is believed to be demonstrated in this study. Several areas of accelerated development and experimental confirmation of theory are pinpointed. The necessary funding and development of Nova or orbital operations capability with Saturn C-5's is required. The 1970 launch window appears to offer the least expensive Symmetric Mission for several years into the 1980's.

ACKNOWLEDGEMENTS

In addition to the authors listed on the title page, the following Aeronutronic personnel made valuable contributions during various phases of the EMPIRE Study:

W. K. Aron
J. Arsenault
R. R. Auelmann
W. H. Bachle
L. J. Barbieri
D. C. Black
I. H. Blifford
A. A. Gammal
D. H. Geipel
M. R. George
S. E. Golian
V. H. Henderson
C. G. Hilton
R. E. Irwin
P. E. Koskela
S. Lampert
W. T. Lemm
V. A. Marple
W. D. Marsing
T. W. Neumann
P. W. Peterson
J. T. Rehak
W. C. Robinson
D. A. Rodriquez
D. B. Ruhmel
J. W. Simmons
I. F. Sobczak
L. G. Walters
E. A. Ward
R. L. Weir, M.D.
D. G. Younger

Contributions to the study effort were also made through discussions with the following companies:

Aerojet-General Corporation, Azusa, California
AiResearch Division of Garrett Corp., Los Angeles, California
Hamilton Standard Division of United Aircraft, Windsor Locks, Conn.
Ionics, Inc., Cambridge, Massachusetts
Mechanics Research Division of General American Transportation, Niles, Ill.
Rocketdyne, Division of North American Aviation, Canoga Park, California
Sundstrand Corp., Denver, Colorado
Systems Division, Whirlpool Corp., St. Joseph, Michigan
The Jet Propulsion Laboratory, Pasadena, California

Ford Motor Company
AERONUTRONIC DIVISION

CONTENTS

CONTENTS (Continued)

CONTENTS (Continued)

ILLUSTRATIONS

ILLUSTRATIONS

ILLUSTRATIONS (Continued)

ILLUSTRATIONS (Continued)

ILLUSTRATIONS (Continued)

ILLUSTRATIONS (Continued)

TABLES

TABLES (Continued)

TABLES (Continued)

LIST OF SYMBOLS

A	-	Section 5 - Reentry vehicle cross-sectional area Section 6 - Surface Area; square feet
$[A]$	-	Miss coefficient matrix
$[A]^T$	-	The transpose of the miss coefficient matrix
a	-	Semi-major axis
C_B	-	Reentry vehicle mass ballistic coefficient; lb-sec^2/ft^3
C_D	-	Section 4 - Dimensionless parameter dependent on the several physical aspects of taking a position fix Section 5 - Reentry vehicle drag coefficient
$\overline{C}_D$	-	Mean drag coefficient
cg	-	Center of gravity
D	-	Diameter; feet
ELV	-	Earth Launch Vehicle
e	-	eccentricity
F	-	Thrust; pounds
F_p	-	Reentry perigee parameter
g	-	Gravitational constant
$[H]$	-	Moment matrix or variance · covariance matrix
HTP	-	Hyperbolic turn program
I_{sp}	-	Propellant specific impulse; lb-sec/lb
K_i	-	Heating relation coefficients
L	-	Length; feet
L/D	-	Lift-to-drag ratio
MTF	-	Mean time to failure
m	-	Mass; slugs
N	-	Minimum number of Earth launch vehicles required for mission

LIST OF SYMBOLS (Cont.)

$[N]^{-1}$	-	Noise moment matrix of the uncertainties in determining injection conditions.
NL	-	Integer indicating number of transfer legs
n	-	Section 4 - Number of backup systems Section 6 - Number of vehicle steps
OLO	-	Orbital Launch Operations
P	-	Probability of mission success up to, and including interplanetary injection
PD	-	Date of arrival or launch from planet
PTP	-	Planetary transfer program
Q	-	Aerodynamic heating; Btu/ft^2
$\overline{Q}$	-	Nondimensional heating parameter
q	-	Hyperbolic perigee distance; measured in planet radii
$\dot{q}$	-	Aerodynamic heating; Btu/ft^2
$\overline{q}$	-	Nondimensional heating rate parameter
R	-	Section 4 - System reliability factor Section 5 - Stagnation point nose radius; feet Section 7 - Reliability of launch and orbital operations
r_p	-	Radial distance from center of Earth to return trajectory perigee; feet
T	-	Section 3 - Flight time Section 6 - Temperature; scale noted
t	-	Operating time
$\overline{t}$	-	Equivalent aerodynamic heat pulse duration
t_s	-	Skin thickness; inches
Δt	-	Increment of flight time
V	-	Vehicle velocity; km/sec
V_a	-	Aerodynamic entry velocity; km/sec
V_c	-	Circular satellite velocity; 7.92 km/sec

LIST OF SYMBOLS (cont.)

$\bar{V}_i$	-	Entry velocity ratio
ΔV	-	Velocity increment
V_∞	-	Asymptotic velocity relative to planet
v	-	Velocity
W	-	Section 4 - Number of corrections Section 5 - Aerodynamic reentry vehicle weight; pounds
W_{GD}	-	Payload weight; pounds
W_{HS}	-	Heat shield weight; pounds
W_i	-	Cryogenic insulation weight; pounds
W_o	-	Section 5 - Total entry system weight; pounds Section 6 - Total weight; pounds
W_{PL}	-	Reentry vehicle payload weight; pounds
W_{ps}	-	Propulsion system weight; pounds
W'_{ps}	-	Propellant system weight (tank, bladder, lines, engine, etc.); pounds
W_R	-	Retro-grade reentry rocket weight; pounds
W_{ST}	-	Reentry vehicle structural weight; pounds
W_8	-	Usable propellant; pounds
α	-	Section 3 - Angle between hyperbolic asymptotes Section 5 - Angle of attack Section 6 - Absorptivity
β	-	Section 3 - Angle between planet - sun line and vector defining perifocus of planetocentric trajectory Section 5 - Earth atmospheric decay constant (4.25×10^{-5} ft^{-1})
ϵ	-	Emissivity
ϵ_{V_∞}	-	Maximum tolerable value of $\left\|\left\|\underline{V}_{\infty A}\right\| - \left\|\underline{V}_{\infty D}\right\|\right\|$
Θ	-	Angular distance from stagnation point at R center; degrees

LIST OF SYMBOLS (cont.)

λ	-	Section 5 - Ratio of total entry system weight to aerodynamic entry vehicle weight Section 6 - Propellant loading fraction
ρ	-	Section 4 - Distance from vehicle to planet Section 5 - Density Section 6 - Density
σ_h	-	Final rms altitude dispersion
σ_{h_o}	-	Initial rms altitude dispersion
σ_{MEAS}	-	Sighting accuracy (rms) in the measurement of the star reference angles
τ	-	Time of exposure to meteoroid impact; hours
ψ_s	-	Step payload ratio
ψ_t	-	Total payload ratio
μ	-	Section 4 - Gravitational constant Section 6 - Mass ratio

SUBSCRIPTS

A	-	Arrival condition
c	-	Convective heating
D	-	Departure condition
E	-	Earth
M	-	Mars
max	-	Maximum
p	-	Perigee value
r	-	Radiative heating
st	-	Stagnation point
T	-	Total (convective plus radiative heating)
V	-	Section 3 - Vehicle Section 5 - Venus
1,2,3,4	-	Refer to legs 1,2,3, and 4 or 1st,2nd 3rd, or 4th planet encountered.

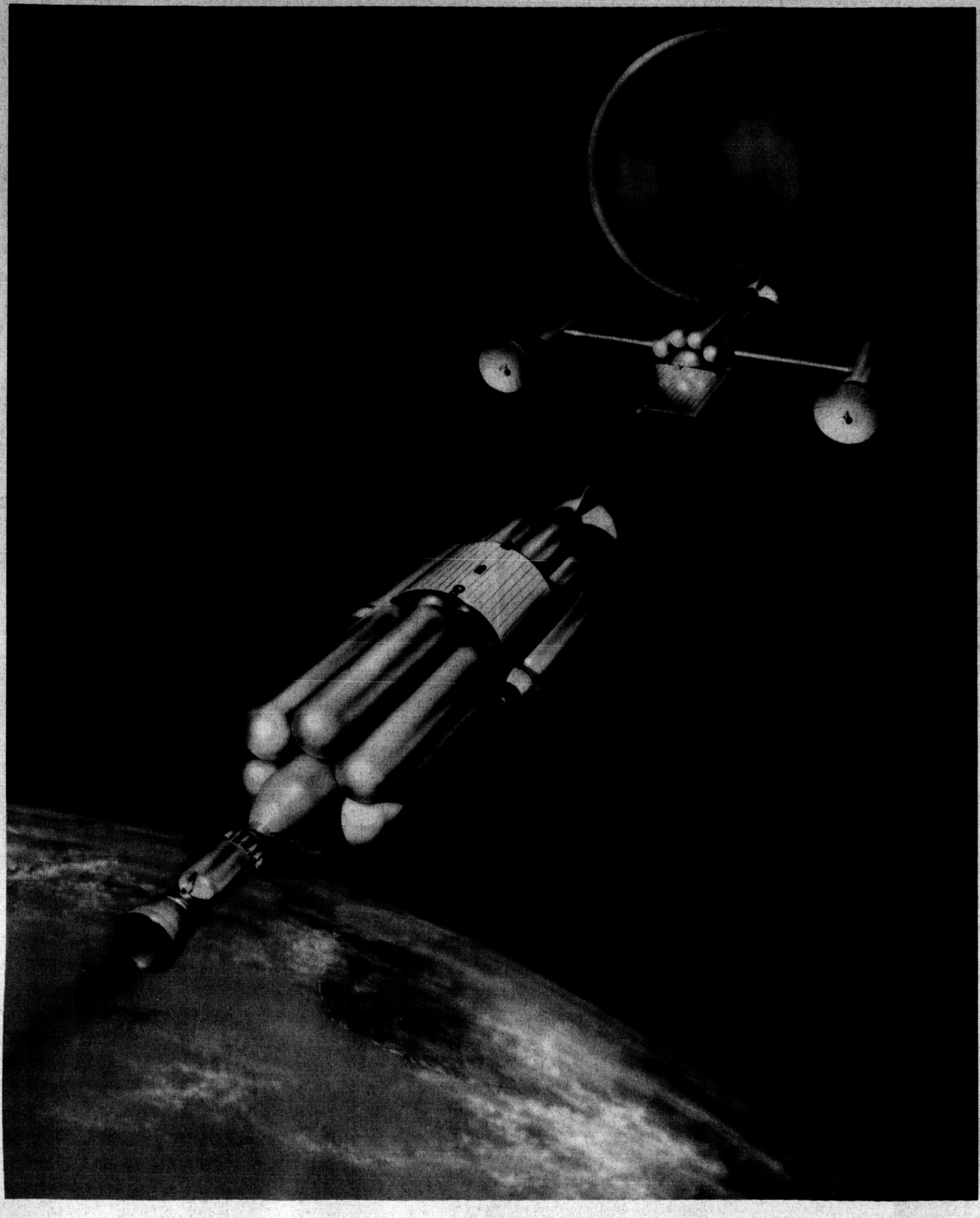

Ford Motor Company
AERONUTRONIC DIVISION

ERRATA TO EMPIRE FINAL REPORT DATED 21 DECEMBER 1962

PAGE	LINE	CORRECTION
xviii	15	Should read $\dot{q}$ - Aerodynamic heating rate; Btu/ft^2-sec
xviii	29	Change V_a to V_e
xix	2	Should read $\overline{V}_i$ - Entry velocity ratio (V_i/V_c)
xix	3	Should read ΔV - Velocity increment ($V_i - V_e$)
xx	19	After c- Convective heating add: (superscript in Section 5)
xx	29	Under V should read - Section 4-Venus
List of Symbols:		Add ⊕ - Earth, ♂ - Mars, ♀ - Venus
1-2	23	Comma after program
3-5	16	Should read "forth well into August"
3-11	5	"hpyerbolic" should read "hyperbolic"
3-19	20	"V_i" should read "v_i"
3-21	9	The second $1_{\oplus_4}$ should read $1_{\sigma^{\nearrow}_4}$
3-29	11	Table 5.2 should read Table 3.2
4-1	5	"as suitable" should read "a suitable"
4-8	35	"An obvious limit on" should read "An obvious limit on $\Delta \bar{V}$"
4-10	16	"Friendlander" should read "Friedlander"
5-5		Figure 5-2, Ordinate should be labled - "Reentry Corridor Depth"

ERRATA (cont.)

PAGE	LINE	CORRECTION
5-6	5	"exessive" should read "excessive"
5-11	9	Should read $\rho^{1.7} V_i^{21.2}$
5-11	15	"leanding" should read "leading"
5-12		Note at bottom of page should read "pyrolytic graphite"
5-22	19	"that these" should read "than these"
5-29	20	"30,00 lb." should read "30,000 lb."
6-2		Add this note to Table 6.1 - Note: The Crocco Vehicle was sized using an injection ΔV = 11.95 km/sec prior to the time the finalized value of 10.1 km/sec (Table 3.2) was obtained.
6-27	1	Add asterisk - 6.3 REENTRY SYSTEMS* Footnote should read: * Reentry systems weights shown in this section include propulsion system weights which are based on larger, more conservative, velocity requirements than finally determined and discussed in Section 5, Earth Reentry.
6-44		Table 6.9: Change -

Earth Reentry Systems		17,300
First Stage Entry Propellant	2,000	
First Stage Entry Booster	300	
Second Stage Entry Propellant	1,760	
Second Stage Entry Booster	240	

To read:

Earth Reentry System		17,300
Entry Propellant	3,760	
Entry Booster	540	

6-59		Figure 6-23 - "Hydorgen" should read "Hydrogen"	
7-1	17	"P_{ELV}" should read "R_{ELV}"	

ERRATA (cont.)

PAGE	LINE	CORRECTION
7-10	23	"liklihood" should read "likelihood"
8-12	2	"requirement" should read "requirements"
A8-5	15 & 16	Asterisks refer to the following footnote to be added below the table: * Duplicate (or similar) automatic tests/ checkout and related data acquisition, processing, and display equipment employed at all test/checkout locations.

SECTION 1

INTRODUCTION

1.1 EMPIRE PROGRAM DEFINITION

The EMPIRE* Study is a unique program to examine the problem areas associated with the goals of early manned interplanetary missions in the early 1970's. Aeronutronic has concentrated its efforts on the dual planet flyby missions under contract NAS8-5025 for the Future Projects Office, Marshall Space Flight Center, Huntsville, Alabama. The work reported in this volume represents the efforts of many persons. It utilizes their varied technologies and diverse experience in defining the problem areas for further attention related to the manned flights by Mars and Venus and safe return to the surface of the Earth.

It should be noted that the interest in dual planet missions prohibited this contractor from exploring other varieties of missions in the present study. This does not mean that single planet flyby missions, planetary orbital missions, and planetary landing missions are less important. However, having obtained the results oriented toward low and medium energy trips in a free-fall interplanetary transit through the dual flyby mission, the relative cost and utility of the latter versus the larger energy demands of landing and orbiting missions can be evaluated.

Much credit must be given to the forward thinking approach shown by the NASA effort on this program in 1962. By attacking the

---

* Early Manned Planetary-Interplanetary Roundtrip Expedition.

areas of interest at this early date it will be possible to obtain a clearer picture of the requirements for early manned planetary and interplanetary flight. Thus the nation's resources, and the NASA and other United States space programs can be oriented toward long range goals at an early date. This present effort represents an unusually early attack on this type of analysis. The conclusions, which indicate the need for acceleration of certain related development programs to meet the earliest possible low energy Venus-Mars Flyby launch date of July, 1970, justify this early definition of potential problem areas.

A Development Plan and Funding Schedule for the design point mission (Nuclear Symmetric) is presented in Section 8 Use of the selected mission for this purpose does not indicate that Aeronutronic believes such a program will be undertaken and funded in time to utilize the July-August 1970 Symmetric Orbit Launch Window. It is however, an effort to define in some detail enough of the development, test, and funding requirements to show the critical areas. This effort will provide information for appraisal of technical and financial considerations for discussions and decisions related to the early manned planetary programs.

1.2 SCOPE OF THE AERONUTRONIC EMPIRE STUDY

a. Objectives of EMPIRE

The primary goals of the EMPIRE Study Program are to establish requirements for the NOVA booster development program to provide inputs to the nuclear rocket program, and explore any advanced space operational concepts necessary for implementation of the mission under study. To define the requirements in these areas a detailed systems analysis, mission analysis, and program planning exercise was performed. The final goals of these analyses are the Development and Funding Plans given in Section 8.

b. Study Areas

In order to obtain the above results it was necessary to concentrate on several areas for analysis and system integration. The areas requiring specific attention included:

(1) Trajectories - Crocco* and other useful interplanetary trajectories.

(2) Propulsion - Nuclear and/or chemical rockets

---

* Trajectory types are discussed in Section 3.

(3) Operations - Orbital operations and mission staging development requirements.

(4) Earth Reentry

(5) Crew Requirements

(6) Scientific Aspects

(7) Life Support Requirements

(8) Cryogenics

(9) Subsystem Definition - Electronics, Guidance, Control and Power Supply Requirements

(10) Emergency Operations

As the study program progressed, some of the specific areas required more concentrated investigation due to the critical nature of the system and mission constraints, due to the lack of current technological solutions, or due to other characteristics tending to render the particular area a "problem area". Some of these concentrations of effort became passe' for the final mission choice when the nuclear injection symmetric mission was selected as the design mission over the Crocco Nuclear, Symmetric Chemical I (I_{sp} = 410 seconds), and the Symmetric Chemical II (I_{sp} = 300 seconds) to be discussed in Sections 3 and 6 in more detail. The selection of the lightest payload in Earth orbit for the dual planet flyby mission eliminated the requirement for long term cryogenic storage, and for orbital operations, such as rendezvous, assembly, and fueling, if a NOVA Earth launch vehicle is used. It is evident that such areas required more attention in the early phases of this study when the Crocco mission was being investigated, than at a later time when the nuclear symmetric mission appeared most feasible. In light of the effort spent in some of these "non-design" areas, some data appears in later sections which was not specifically generated to meet the requirements of the design mission. It is, however, of interest for planetary flights requiring these particular technologies.

1.3 APPROACH TO THE EMPIRE STUDY

As historic background it might be useful to outline the course of the present study program. In the early phase an effort was made to examine the Crocco orbit in a three dimensional analysis to confirm its desirability for a dual planet flyby mission. A launch window was

obtained in 1971 which fell in the 1970-72 era under investigation. Velocity requirements, launch dates, and flight times around 400 days were derived. A search was made for alternate trajectories and the symmetric trajectory was found to have a launch window in the middle of 1970 with a much lower velocity requirement for injection, but a higher return velocity after about 600 days.

The detailed investigations resulted in the data presented in Section 3.

In addition the crew requirements, life support, radiation protection, and environment analyses were performed. Also, emergency operations were considered with the derivation of abort trajectories for return from an unsatisfactory injection phase of the earth departure leg. A detailed analysis of the reentry technique with evaluation of Apollo developed technology was performed. A selection of a reentry vehicle of the high lift-to-drag aerodynamic type with some rocket deceleration was made. This study and its results are discussed in Section 5.

The problem of guidance and navigation with the related midcourse and planetary approach velocity vector corrections was studied to define the overall system requirements. The results are shown in Section 4. The goal was to arrive at sufficient design data to allow a system synthesis of a suitable interplanetary spacecraft. All of the above detailed studies and several other areas were integrated to provide inputs for the interplanetary vehicles. These design considerations and various system parametric studies are discussed in Section 6. It should be emphasized that four useful systems were provided in the various designs and the all Chemical Crocco vehicle was investigated and discarded as impractical due to excessive size, weight, and cost.

The examination of the various possible approaches to an early manned interplanetary vehicle for the missions studied led to the choice of the Nuclear Symmetric Mission for 1970, as indicated above. This allowed a more detailed subsystem and vehicle definition and provided a program for the operational analysis in Section 7 and the Development Plan and Funding Program in Section 8.

The assignment of scientific payloads was not made because of the early nature of the present study and the many questions yet to be answered by unmanned space probes. A discussion of the scientific aspects will be given in Section 2.

The general conclusions and relevant recommendations based on this study are given in Section 9 to focus attention on the feasibility of the mission considered and the necessary developments to accomplish a useful program.

SECTION 2

MISSION CONSIDERATIONS

2.1 GROUND RULES FOR EMPIRE

In the present study several points were established to provide guidelines for the study. The trajectory was to provide a multiple planet flyby of Venus and Mars. The launch time was set for the early 1970's. Propulsion was to be nuclear and/or chemical. The boosters to be considered for Earth launch were Saturn and/or NOVA to be launched from AMR with mission staging to be investigated in Earth orbit or in interplanetary transit.

It was specified that survival of the crew was essential and that the design should allow for a 3 percent growth in velocity requirements and a 10 percent growth in payload weight when booster and injection systems are selected.

Also, the scientific aspects were to be considered from the point of view of desirability, compatibility with the mission profile, and only in sufficient detail to establish spacecraft support requirements essential to the overall mission design.

Use was to be made of systems, concepts, and techniques currently under development with an effort to avoid extension of capabilities beyond those developments programed for Apollo. Although not specifically set as a ground rule, ability to actually perform the mission selected in this study required a conservative approach to selection of system parameters and capabilities for the 1970 period and this approach was taken for all areas of this study where feasible.

2.2 SCIENTIFIC EXPERIMENTS

a. General

While a detailed system integration was not performed on the scientific payload, an investigation was made in order to arrive at a useful weight and power assignment for spacecraft synthesis. Investigation of past and future experiment requirements in the unmanned military and space programs supported the finding that a useful payload weight of 1000 to 2500 pounds and an average power of 200 to 300 watts represents the best estimate of the requirements for an integrated payload package. This considers three phases of experimentation in 6 steps: interplanetary (and Earth departure), Mars approach and departure, interplanetary, Venus approach and departure, interplanetary (and Earth approach).

Many decisions remain in the choice of experiments, delivery techniques, data processing and other areas. The detailed selections will undoubtedly be based largely on data to be obtained in the 1962-1968 planetary experiment programs using unmanned spacecraft and automatic equipment, therefore a general allocation for spacecraft support requirements appears sufficient. However, in order to show possible areas for future consideration a group of experiments for the unmanned planetary applications has been accumulated, discussions have been held with JPL, and potential experiments, as reported in a recent Air Force study, will be presented.

b. Unmanned Planetary Experiments

Mars, Venus, and interplanetary probes are currently planned by NASA, under the cognizance of the Jet Propulsion Laboratories. The programs include various Mariners and planning is in progress for large payloads of the Voyager class. The experiments listed in Table 2.1 represent an accumulation from several sources and are assigned weights and power requirements consistent with the experiences of JPL and Aeronutronic scientists and engineers.

c Later Experiments

These early experiments, which now have well defined weight and power requirements will be followed by orbital and landing payloads which are presently less well defined in detail. The Voyager payloads to be landed in part on the nearer planets later in the 1960's or early 1970's are in this category. In order to bridge the gap for EMPIRE planning a list of possible experiments are presented in Table 2.2. This is merely a listing of measurements and some instrument techniques which seem reasonable in light of our present knowledge. Undoubtedly, many others will be considered and additions can be made later as more detailed investigations take place.

TABLE 2.1 EARLY PLANETARY EXPERIMENTS NOW UNDER CONSIDERATION

Experiment	Interplanetary	Venus	Mars	Wt Lbs	Power Watts
Magnetometer	X	X	X	11	8
Micrometeorite Detector	X			8	1
Cosmic Ray Spectrometer	X			18	3
Ionization Chamber	X			5	1
Particle Flux Detector	X			5	1
High Energy Proton Angular Distribution	X			4	1
Medium Energy Proton Angular Distribution	X			3	1
High Energy Plasma Probe	X			10	1
Low Energy Plasma Probe	X			18	4
Faraday Cup Collector	X			3	3
Narrow Angle Plasma Probe	X			5	1
Low Frequency RF Receiver	X	X	X	9	2
Ionizing Particle Spectrometer	X			10	2
IR Radiometer		X		4	2
Mircowave Radiometers		X		30	7
UV Spectrometer		X		25	6
Trapped Radiation Detectors		X	X	5	1
IR Surface Temperature Detector			X	3	2
IR Spectrometer (High Resolution)			X	25	9
Television			X	40	17
UV-Visual Polarimeter			X	10	3
Topside Sounder			X	25	1

TABLE 2.2

POSSIBLE EXPERIMENTS ON PLANETARY MISSIONS
(After de Vaucouleurs, Reference 1)

I. Space Probe Vehicles

a. Magnetic Fields and Radiation Belts

b. Optical Search for Planetary Satellites (at 10^6km)*

c. Search for Gaseous Trails (Flourescence) (10^5 to 10^6km)

d. High Resolution Photography and Television of Planetary Surfaces (10^4 to 10^5 km)

(1) Mars - wavelengths above 0.5 microns

e. Measure Planetary Masses and Diameters

f. Photometry, Spectroscopy, and Polarimetry (Complete Phase curves require passage outside the planetary orbit)

(1) Mars & Venus

(2) Earth Observations to Establish Solar Albedo Vs. Radiation Balance

g. Sunset and Twilight Phenomena Across Planetary Limb

(1) Transit of Planet in front of Sun (10^6 to 10^7 km)

(a) Diameter of Solid Globe of Mars

(b) Diameter of Opaque Cloud Layer of Venus

(c) Ingress and Egress Phases of Refracted Light from Planetary Atmosphere

(2) Eclipse of the Sun (10^5 to 10^6 km)

(a) Absorption, Refraction, and Composition data on the Lower Atmospheres

* Represents distance from experiment to observed phenomena.

TABLE 2.2 (Continued)

(3) Normal Sunset (10^4 to 10^5km)

(a) Cloud Altitudes

(b) Haze Conditions

(c) Atmospheric Transmission

(d) Search for Minor Constituents (Spectroscope)

(e) High Dispersion Line Profile Studies in Atmospheric Absorption Bands for Temperature versus Altitude

(f) Absorption and Refraction Studies to Obtain Atmospheric Scale Heights.

(4) Observations in the Planet Shadow (10^3 to 10^4km)

(a) Upper Atmosphere Scattering and Twilight Phenomena

(b) Search for High Altitude Scattering Layers by Twilight Zone Photometry

(c) Scattering Phase Functions of Aerosols

(d) Flourescent Effects of Minor Atmospheric Constituents by UV Spectroscopy

h. Dark Side Optical Observations (10^4km)

(1) Permanent Atmospheric Glow and Auroral Activity

(2) Lightening and Corona Effects of Venus

i. Infrared Thermal Emissions at 2 to 20 microns on Venus

(1) Scan the Light and Dark Sides at several Wavelengths (Absorption Windows)

(2) Observe in Absorption Bands to Measure CO_2 and H_2O Above Radiating Layers

TABLE 2.2 (Continued)

(3) Spectrophotometry of Mars at Good Resolution

(4) Spectral Scans from 5 to 40 microns on Mars to get Height-Time-Temperature variations

j. Microwave Thermal Emissions of Venus and Mars (10^4km)

(1) Scans of Bright and Dark Sides from 1 mm to 10 cm Wavelengths (Particularly at 1.34 cm, the H_2O Resonance)

k. Non-thermal Radio Emission in the Meter Range

(1) Dipole Search for Cyclotron or Synchrontron Emission in trapped Radiation Belts, Ionosphere or from atmospherics.

(2) Power Spectrum and Ionospheric Absorption Cut Off Frequency to Determine Maximum Electron Density of Ionosphere.

l. Ionospheric Sounding and Radar Probing

(1) Sweep frequency transceiver for topside sounding

(a) Probable maximum electron density of 10^6 to 10^7 per cm^3 (fo $\approx$ 10 to 30 mc/s) for Venus.

(b) Probable maximum electron density of 10^5 to 10^6 electrons per cm^3 (fo $\approx$ 3 to 10 mc/s) for Mars. Measure echo times for $f > fo$ and $f < fo$ to get altitude of electron density layers.

(2) Transceiver at $\sim$ 1 cm to 50 cm may be able to receive echoes from lower atmospheric cloud layers on Venus for a determination of altitude for the opaque cloud layers.

II. Artificial Satellite Observations

a. Track to determine period and semi-major axis for measurement of mass and radius by apparent diameter of solar eclipse.

TABLE 2.2 (Continued)

b. Orbital Radius plus altitude measured by an altimeter could give surface radius.

c. Optical Mapping (2000 km)

d. Surveys

(1) Photometric

(2) Spectroscopic

(3) Infrared

(4) Microwave

(5) Radar - Doppler scan perpendicular to Venus Orbit would give axis location

(6) Magnetic surveys

e. Low Orbit Satellites

(1) Drag gives atmosphere density, down to about 120 km on Venus and 200 km on Mars where burn up should occur.

f. Low Altitude X-Ray and UV detectors would give absorption as a function of depth in the atmosphere.

(1) Photon Counters: Be window $\lambda < 8$ Å

Al window 8 Å $< \lambda < 20$ Å

mylar window 44 Å $< \lambda < 60$ Å

(2) Photo electric Scanning 60 Å to 1000 Å with grazing incidence grating monochromator

(3) Ionization chambers with appropriate gas fillers and windows to cover 1000 to 1500 Å

NO with LiF window 1050 to 1350 Å
NO with CaF window 1225 to 1350 Å
Xylene with Sapphire window 1425 to 1500 Å

TABLE 2.2 (Continued)

(4) High resolution studies of Lyman α line profile as a function of altitude to give a measure of neutral atomic hydrogen.

g. Ionization Phenomena Using Low Satellites at 200 to 500 km altitude for Venus and 400 to 1000 km for Mars.

(1) Multiple or sweep frequency transceivers for electron density critical frequencies from above and below.

(2) Mass Spectrometers, ionization gauges, and Langmuir Probes for ion densities and masses, and kinetic temperatures.

(3) Photometry and Spectral Analysis of the night airglow above and below satellite to get altitude distribution of the luminescent layers. Line width measurements would give kinetic temperatures.

h. Measure Upper Atmosphere Winds and Turbulence

(1) Release of sodium and other metallic vapors with optical and radio observation from a higher satellite for relaying data. Best at twilight for optical observations against the night side of planet.

III. Penetrating Probes

Slowed by retro-rockets, drag parachutes, winged gliders, etc.

a. Atmospheric pressure, density, temperature, dielectric constant. Monitor deceleration by accelerometer or Doppler radar tracking.

b. Atmospheric transmission

(1) H_2O- ρ, σ, ψ, Ω near infrared bands

(2) CO_2- 0.8 μ for Venus, 1.6 and 2.0 μ for Mars

(3) O_2 A-band

TABLE 2.2 (Continued)

(4) Near UV to study continuous absorption at 4500 Å, wavelength dependence of absorption would indicate composition and particle size of clouds.

c. Atmospheric Scattering

Brightness distribution of solar aureole from sun pointing satellite by photoelectric scanning of sky area surrounding the sun.

d. Twilight Photometry - Altitude Distribution of Luminescence

IV Hard Landings on Planet Surface
Slowed by retros, parachutes, gliding, etc.

a. Ballistic Landings

(1) Spectrum of High temperature compression wave gives indication of atmospheric density and composition.

(2) Radio or Radar Observations of the Ionized Wake may provide (if feasible) diffusion and recombination rates.

(3) Separate detector and observe impact to get sound and flash from impacting probe to obtain velocity of sound in the lower atmosphere.

b. Penetrometer and Hardness Tests

c. Passive and Active Seismometer Nets.

d. Television of Surface at Impact and Post Impact Observations.

e. Surface Temperature Measurements
Diurnal and seasonal variations would give axis orientation of Venus - at least 3 stations would help to average local conditions.

TABLE 2.2 (Continued)

V. Soft Landings

a. Atmospheric Absorption

(1) Solar Spectrum 0.3 to several microns (e.g. 20)

(2) Radio measurements 1 mm to 30 m

b. Atmospheric Surface Phenomena

(1) Thermal

(2) Pressure

(3) Photosensors

(4) Wind velocity and direction.

c. Thermal Radiation

(1) Surface spectra

(2) Sky Spectra

d. Light Emission at Night

(1) Aurora, Airglow, Lightening, etc.

(2) Photometric and Spectroscopic Observations of eclipses of Deimos and Phobos, Mars satellites from a ground station. Period: Phobos 7 hrs. 39 min.
Deimos 30 hrs. 21 min.

e. Atmospherics and Radio Noise: Ionospheric Soundings

f. Magnetic Field

(1) Long term drifts

(2) Vector

(3) Daily magnetic activity

(4) Anomalies on Mars at times of inferior conjunction of the earth

TABLE 2.2 (Continued)

g. Gravity Measurements

In at least 3 latitudes: equator, pole, and intermediate latitude.

h. Atmospheric Electricity

(1) Potential gradient

(2) Conductivity

(3) Ion density and mobility

(4) Rate of ion formation

i. Surface Radioactivity
Abundance of Uranium, Thorium, and Potassium.

j. Surface Composition

(1) Spectroscopic analysis

(2) X-ray flourescence

(3) Neutron activation (small Ra-Be source)

(4) γ-ray spectroscopy

(5) Mass Spectrograph

(6) Gas Chromatography

k. Close-up TV and Microscopy
Long period observations to derive:

(1) Wind effects

(2) Phototropic effects

(3) Changes of form

(4) Mobility of features

TABLE 2.2 (Continued)

1. Listening Devices

m. Biological Sampling and Detection of particular species.

2.3 OTHER MISSION CRITERIA

There are many considerations which tend to dictate spacecraft design criteria other than those mentioned in Section 2.1 and 2.2. In view of the complex nature of the interplay with design, most of the important factors are treated in the discussions of Section 6. The most important studies are broken out in separate sections to follow. Hence, the reader is referred to those later sections for more detailed mission considerations related to the interplanetary spacecraft and its operational performance.

SECTION 2

References

1. de Vaucouleurs, G., "Reconnaissance of the Nearer Planets", AFOSR/DRA-61-1, November 1961.

SECTION 3

TRAJECTORIES

3.1 INTRODUCTION

The principal effort by Aeronutronic in the area of trajectory analysis during this contract period has been the examination of those multiple planet flyby trajectories (Earth, Venus, Mars) whose launch dates occur in the time period 1970-72. The salient features of these trajectories are presented in the several sections to follow.

3.2 ANALYTICAL PROCEDURE

The method of solution initially used in the determination of nominal EMPIRE transfer orbits was one that employed a combination of graphical and analytical techniques. Figure 3-1 depicts schematically the entire procedure.

The representations PTP and HTP refer to the Planetary Transfer Program and the Hyperbolic Turn Program respectively. PTP, a three-dimensional program requires, as input, the ephemerides of the launch and target planets, launch date, and trip time (T) to the target planet. The output of this program consists of the transfer orbital elements as well as the vehicular planetocentric approach and departure velocities (V_{∞}). The latter quantities are entered into the HTP which in turn calculates the distance of closest approach to the planet (q - in radii of that particular planet) along with other data of interest. The subscripts E, 1, and 2 respectively refer to the Earth, first planet encountered after launch, and the second planet encountered after launch.

PROCEDURE FOR OBTAINING EMPIRE NOMINAL ORBITS
(SYMMETRIC AND NON-SYMMETRIC)

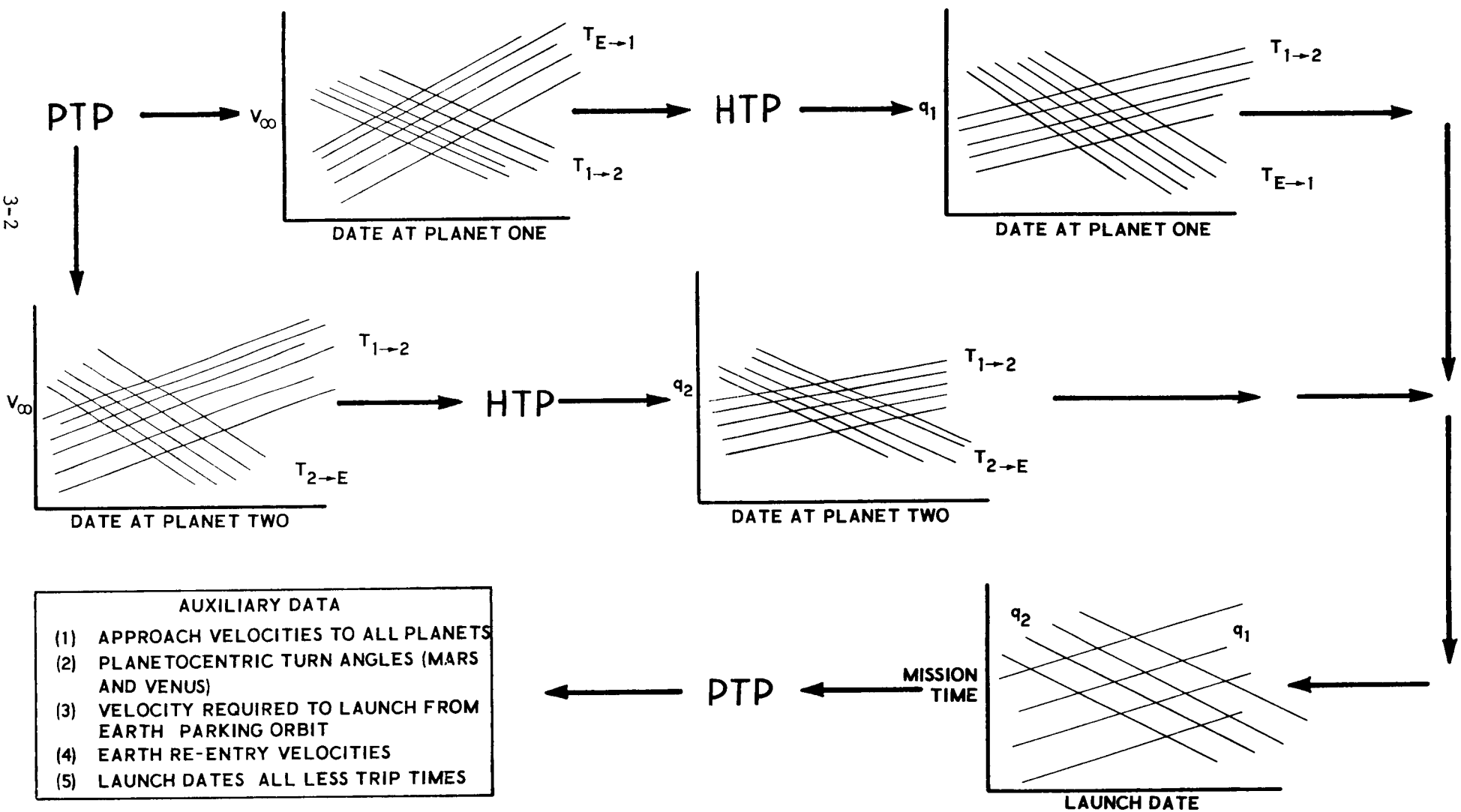

FIGURE 3-1

This procedure was subsequently automated by the development of a computer program that utilized the basic principles previously described in the development of suitable trajectories. A detailed description of this computer program and its application to the EMPIRE program is described in the Section 3 Appendix.

3.3 MISSION CHARACTERISTICS

In the following sections, the classes of interplanetary flyby missions are defined, the procedure for preliminary definition of launch windows for each class is discussed, and the results of a detailed investigation of these launch windows is presented.

a. Orbit Classes

Two types of multiple planet transfer oribts have been considered for the EMPIRE mission: symmetric and non-symmetric (Crocco).

A Crocco orbit is defined as one whose period is approximately one year. The symmetric class has a characteristic of symmetry in that the longitude of the vehicle and the launch planet are approximately equal at the mission half-period. Figure 3-2 depicts each orbit class in simplified unperturbed form.

b. Crocco Orbit Class

(1) Preliminary Launch Window

Crocco(1) has stated that the geometry favorable for a non-symmetric free-fall orbit (Earth-Mars-Venus-Earth) will occur during the year 1971. In particular, he indicates launch should occur during June of that same year. An investigation of the heliocentric longitudes of the planets for the year 1971 revealed a situation quite different from those stated by Crocco. A brief summary of Crocco's conditions for the first leg (Earth-Mars) of the interplanetary transfer and how they differ with the conditions dictated by the current analysis is discussed in the following paragraphs.

For intercept of Mars to occur near its perihelion, when Mars is approximately 1.38 a.u.'s from the Sun on 7 September 1971, Crocco indicates that a longitude difference of approximately 68^{0} must exist between the the position of Earth at launch and Mars at arrival. The flight time required to traverse this distance is stated by Crocco as approximately 113 days. These figures pertain to a simplified case;

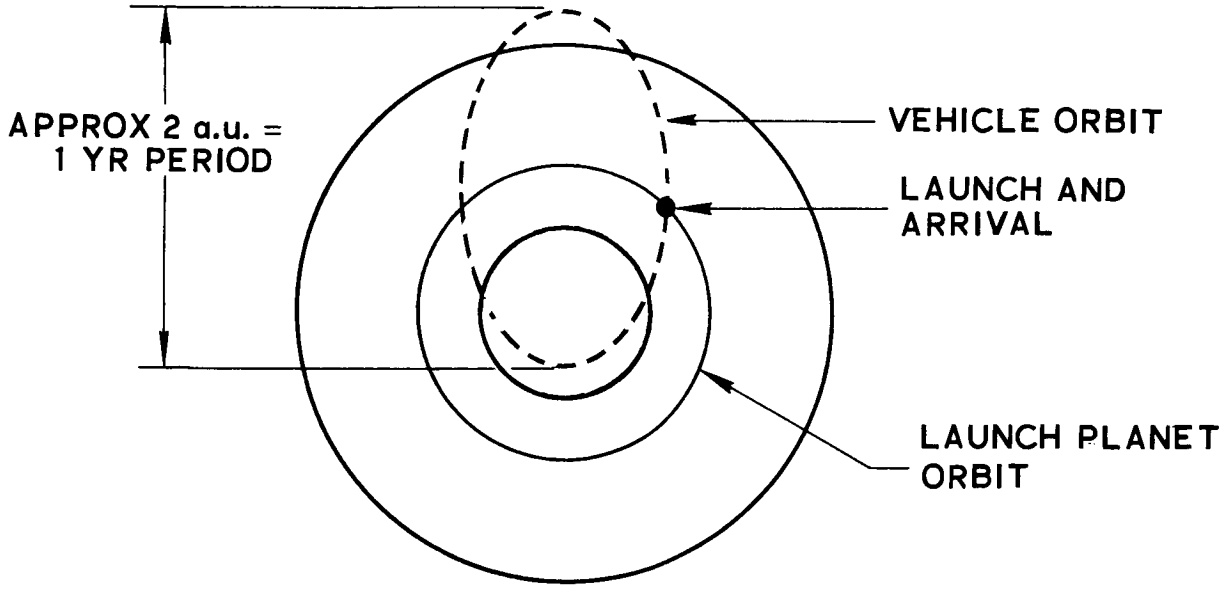

(a) UNPERTURBED NON-SYMMETRICAL (CROCCO) TRAJECTORY

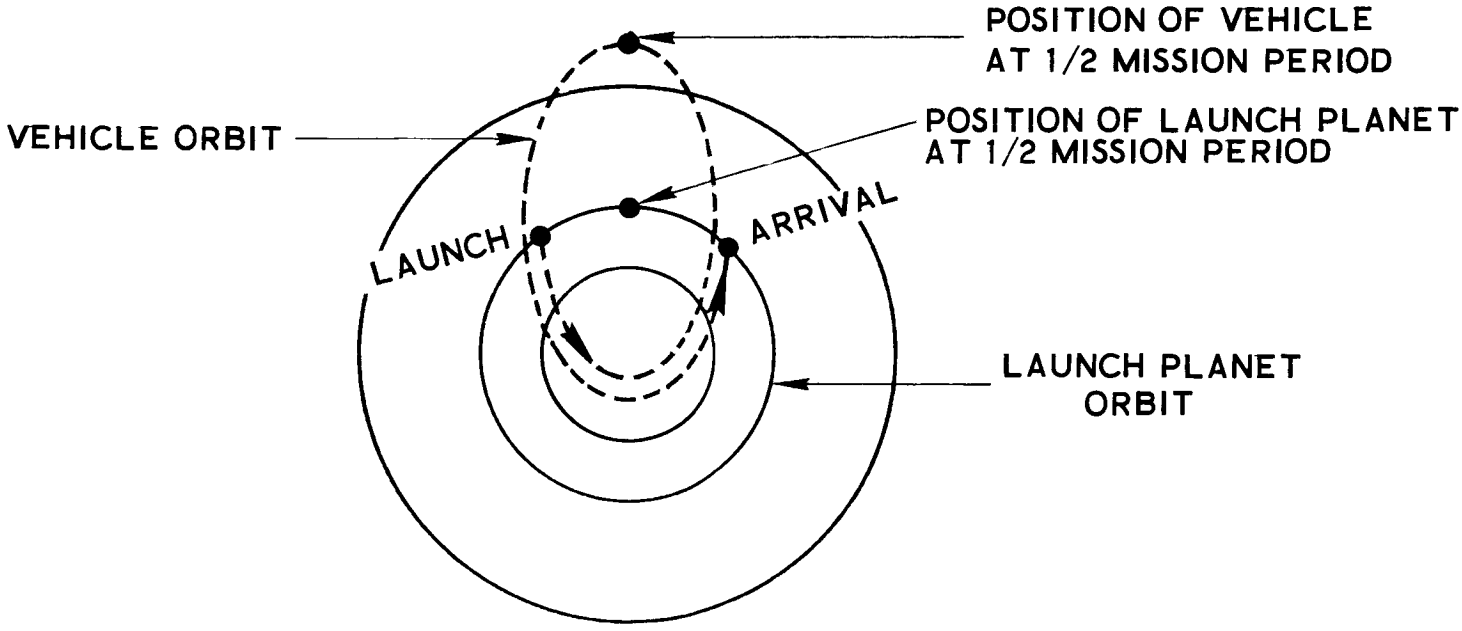

(b) UNPERTURBED SYMMETRICAL TRAJECTORY

FIGURE 3-2

that is, all orbits being coplanar and all planets considered as massless bodies. The transfer orbit is defined to have a semi-major axis of 1 a.u. (i.e., an exact one year period). Crocco further states that a longitude difference between Earth at launch and Mars at arrival of approximately 74^{o} must exist when the perturbational effect of Mars is accounted for. However, for this case Crocco still assumes the orbits to be coplanar although he does discuss the fact that they are not coplanar. Crocco uses the mean motion of Mars in his orbits, 0.52 deg/days, to determine the angular motion over 113 days, or approximately 59^{o}. His study implies that at launch the Earth-Sun-Mars angle, projected into the ecliptic plane, would be 9^{o}. A check of the heliocentric longitudes of Earth and Mars indicates a launch date in the middle of July 1971, rather than the June date mentioned by Crocco. Mars moves approximately 0.6 deg/day in the vicinity of perihelion or 68^{o} in 113 days. This situation implies that at launch Mars and Earth are in opposition and the launch date set for well into August. The controversy in time of launch apparently due to the different rates of motion of Mars about perihelion is carried over in a more complicated analysis when perturbations and non-coplanar planetary orbits are considered. A June launch is favorable for subsequent contact with Venus; but unfortunately, delaying the launch date into the July-August period makes a contact with Venus more difficult.

As a check on Crocco's work, the heliocentric longitude differences between Earth at launch and Mars at arrival were calculated utilizing the table of planetary coordinates[2] and plotted as a function of flight time for given Earth launch dates. Launch dates between 9 May 1971 and 6 September 1971 were investigated. This information is contained in Figure 3-3. It is obvious, by examination of this graph, that neither of the two conditions set forth by Crocco can be met <u>anytime</u> during the month of June 1971. However, both conditions (longitude difference and time of flight) are met for a launch from Earth on approximately 20 August 1971. The other condition set forth by Crocco--semi-major axis of 1 a.u.--is met for Earth launches of 6 September 1971 and 14 September 1971, for flight time of 113 days and 125 days respectively. The corresponding longitude differences are 62 and 64 degrees. These trajectories intercept Mars at positions of 68^{o} and 79^{o} <u>beyond</u> its perihelion position.

As a result of the inconsistencies displayed between Crocco's work and the analysis done to date, it was deemed necessary to investigate launch dates covering from 1 April 1971 to 1 October 1971. The restriction that a (i.e., the semi-major axis) be equal to 1 a.u. on the first leg of the transfer orbit was lifted.

HELIOCENTRIC LONGITUDE CHANGE VERSUS LAUNCH DATE
FOR VARIOUS EARTH TO MARS FLIGHT TIMES

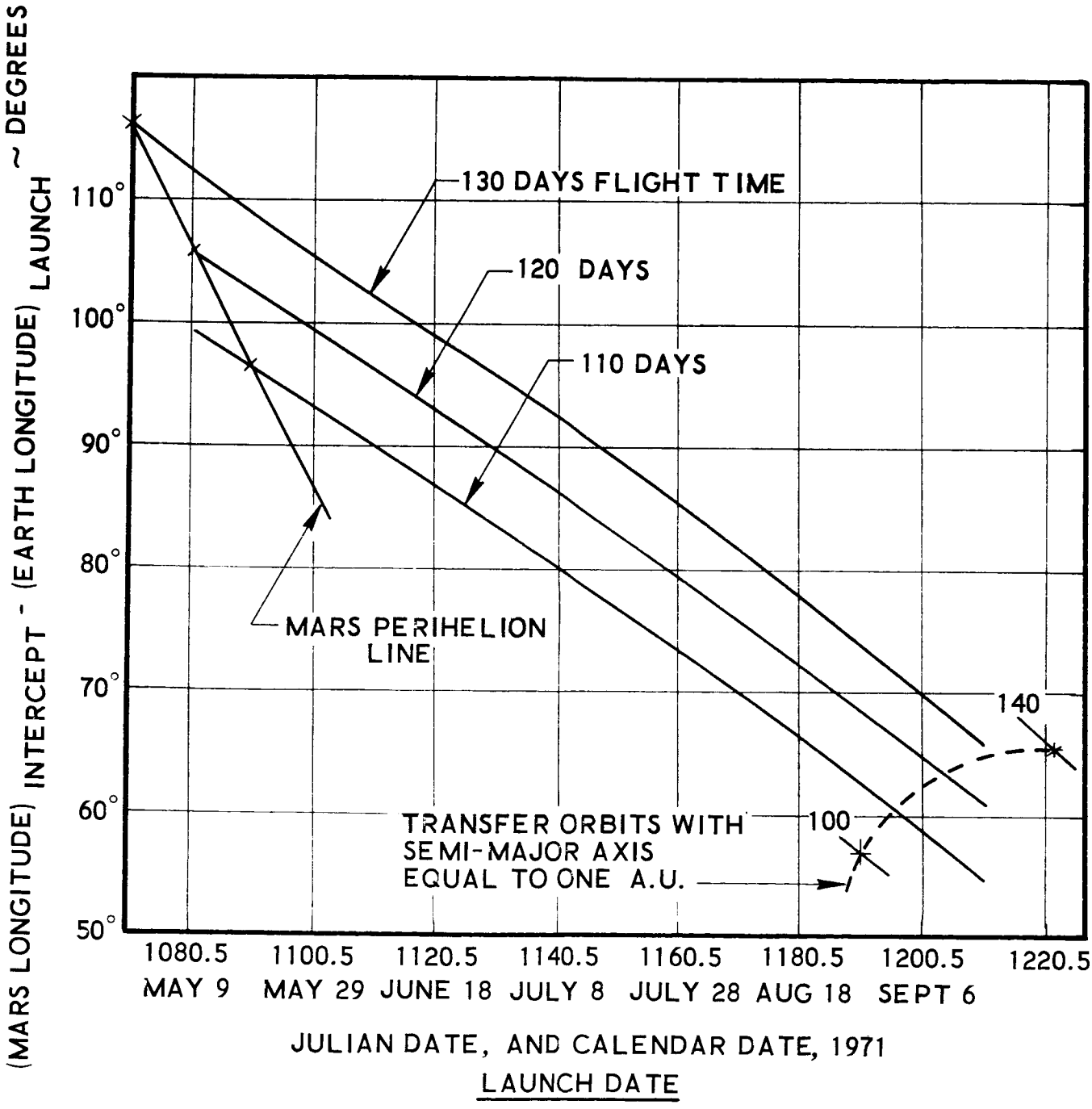

FIGURE 3-3.

Subsequent to these efforts, a graphical technique for finding other possible launch dates was reported in Reference (3) (Section 5). This technique uses a circular-coplanar planetary model for Earth, Mars and Venus. Solution for possible launch dates in the 1970-1972 era yields the following:

ORBIT NO.	CALENDAR DATE	JULIAN DATE, DAYS	LAUNCH ELEVATION ANGLE (Θ), DEG.
1	9 February 1970	2440626	+63
2	2 April 1970	2440678	-87
3	27 June 1970	2440764	+89
4	8 January 1972	2441324	+83
5	25 February 1972	2441372	-55
6	27 May 1972	2441464	+52
7	23 September 1972	2441584	+32

Several interesting points come to mind when examining this list.

(1) No launch date appears in 1971 as suggested by Crocco.

(2) For all Crocco (1 year) orbits the launch evaluation angle (angle between Earth's heliocentric velocity vector and the vehicle's launch heliocentric velocity vector) is a direct measure of the hyperbolic excess which must be produced at launch. Thus the minimum energy launch date in this list is in late September 1972.

On the first point it should be stated that the accuracy of such a procedure can be ascertained by reviewing the repeatability of the period of opposition for Mars and Earth and the period of conjunction for Venus and Earth. The value of the opposition period for Mars is 779+ days based on a mean radius, but when ephemeric values are used, the period varies as follows:

OPPOSITION DATES	OPPOSITION PERIOD
15 April 1967	
	770
2 June 1969	
	801
19 August 1971	
	807
25 October 1973	

Also the conjunction period of Venus and Earth has some variation about its mean value of 584 days.

CONJUNCTION DATES	CONJUNCTION PERIOD
9 April 1969	
	581
10 November 1970	
	585
18 June 1972	
	585
24 January 1974	

Thus, the difference between an analysis based upon mean periods and actual periods may be as much as 30 days. This amount of error is enough to explain the absence of an August 1971 solution using the results of Reference (3). This window was indeed found to exist in August and September of 1971.

(2) Launch Window and Trajectory Characteristics

Figures 3-4 through 3-12 contain the salient characteristics for the three planet encounter of the Crocco Orbit Class-Earth to Mars to Venus and return.

Figure 3-4 defines the launch window for the Crocco mission and is defined in terms of total mission time and the parameters q_{MARS} and q_{VENUS}, the perigee - or distance of closest approach - measured in planet radii.

Specific points of interest are:

(1) For $1.1 \leq q_{MARS}$ and $q_{VENUS} \leq 1.5$, the launch date from Earth is restricted to lie between 14 August 1971 and 11 September 1971.

(2) Total mission time, for the orbits defined in (1) varies between 395 days and 404 days.

(3) Total mission time varies directly with q_{MARS} (i.e., as q_{MARS} increases, so does total mission time.)

Figure 3-5 dictates the amount of characteristic velocity, ΔV, required to place the vehicle into a heliocentric orbit. The vehicle is injected from a 300 KM circular Earth parking orbit. This graph also defines the amount of velocity that must be dissipated upon return to an Earth surface landing. The high points may be summarized as follows:

CROCCO MISSION TIME VERSUS EARTH LAUNCH DATE

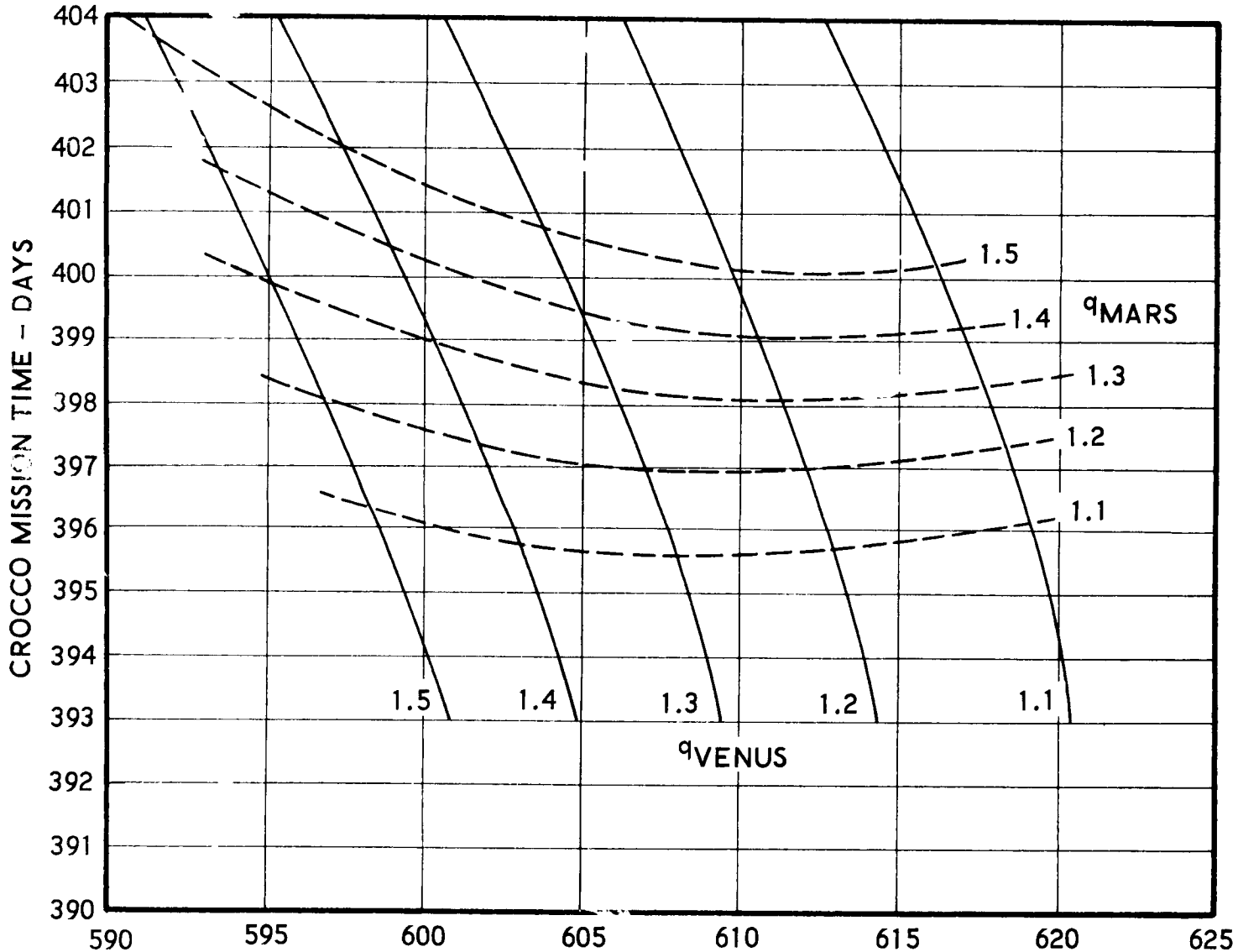

FIGURE 3-4

CROCCO LAUNCH AND RE-ENTRY VELOCITIES AS A FUNCTION OF q_{MARS} q_{VENUS}

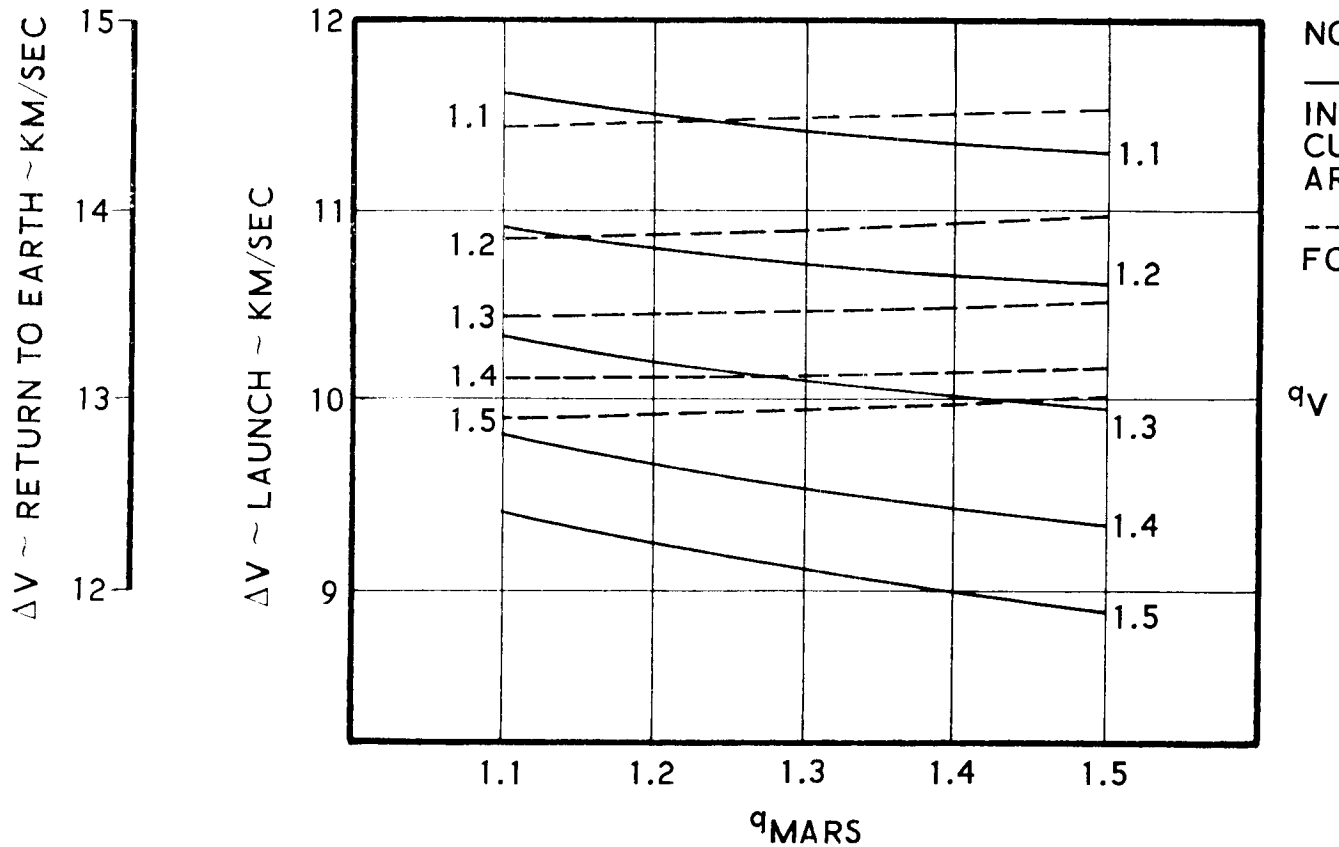

NOTE:

—— ΔV NECESSARY TO LAUNCH INTO CROCCO ORBIT FROM A CIRCULAR 300 KM PARKING ORBIT AROUND EARTH

---- ΔV NECESSARY TO ABSORB FOR RETURN TO EARTH SURFACE

FIGURE 3-5

(1) Reentry velocities are relatively insensitive to q_{MARS}; however, maximum q_{MARS} yields minimum launch ΔV

(2) Maximum q_{VENUS} (for the trajectories studied) yields minimum ΔV on both launch and reentry.

Figure 3-6 depicts the hpyerbolic excess velocity (V_∞) after launch and the excess velocity dictated upon return to Earth, for the Crocco mission. The salient characteristic of this figure is that the departure excess velocities are greater than arrival excess velocities, for all combinations of q_{MARS} and q_{VENUS}.

Figure 3-7 illustrates the hyperbolic excess velocities relative to the individual planets at time of encounter.

Figure 3-8 is a graphical representation of the hyperbolic turn angle as a function of the distances of closest approach to the respective planets. A few points of interest in this figure are:

(1) Turn angles about Venus are relatively insensitive to variations in q_{MARS}.

(2) The turn angle about Mars varies by nearly a factor of two, depending upon the particular combination of q_{MARS} and q_{VENUS}.

Figure 3-9 depicts the included angle between the line of apsides of the planetocentric hyperbola and the sun line. For this particular launch window, the Martian flyby will occur on the "dark" side of the planet ($\beta \cong 180^o$) and the Venutian flyby will be such that the vehicle will "fall" inward toward the sun and then depart on the sunny side of the planet ($\beta \cong 90^o$).

Figures 3-10 through 3-12 give the nominal time of flight for the several trajectory legs.

c. Symmetric Orbit Class

(1) Preliminary Launch Window

The techniques used for finding an approximate launch date were based on an analytical approach, assuming that the three planets were in co-planar non-circular orbits and that no perturbation occurs during planetary passage.

CROCCO ASYMPTOTIC VELOCITIES WITH RESPECT TO EARTH ON ARRIVAL AND DEPARTURE AS A FUNCTION OF q_{MARS} AND q_{VENUS}

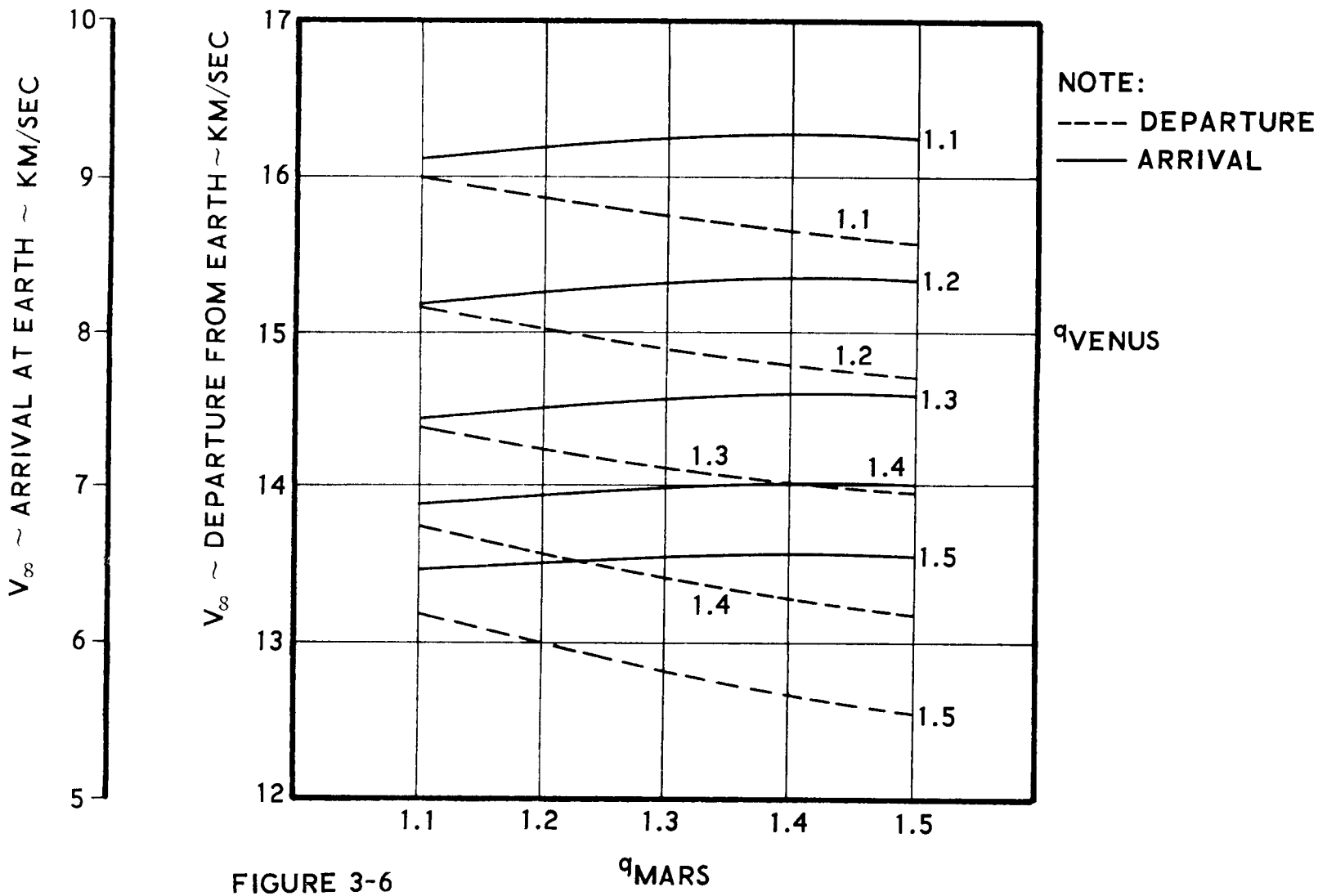

FIGURE 3-6

CROCCO ASYMPTOTIC VELOCITIES WITH RESPECT TO MARS AND VENUS AS A FUNCTION OF q_{MARS} AND q_{VENUS}

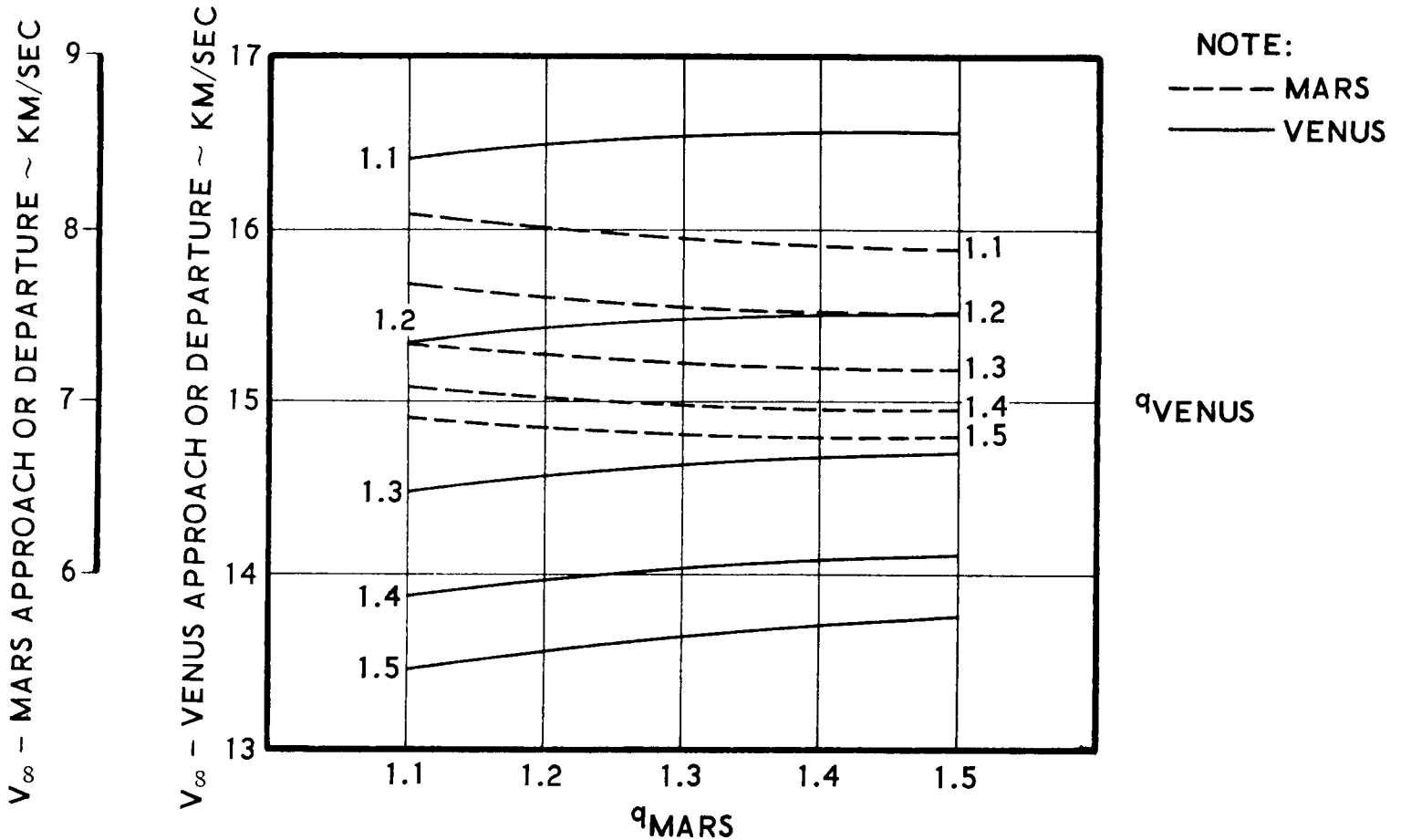

FIGURE 3-7

CROCCO TURN ANGLE ABOUT MARS AND VENUS
AS A FUNCTION OF q_{MARS} AND q_{VENUS}

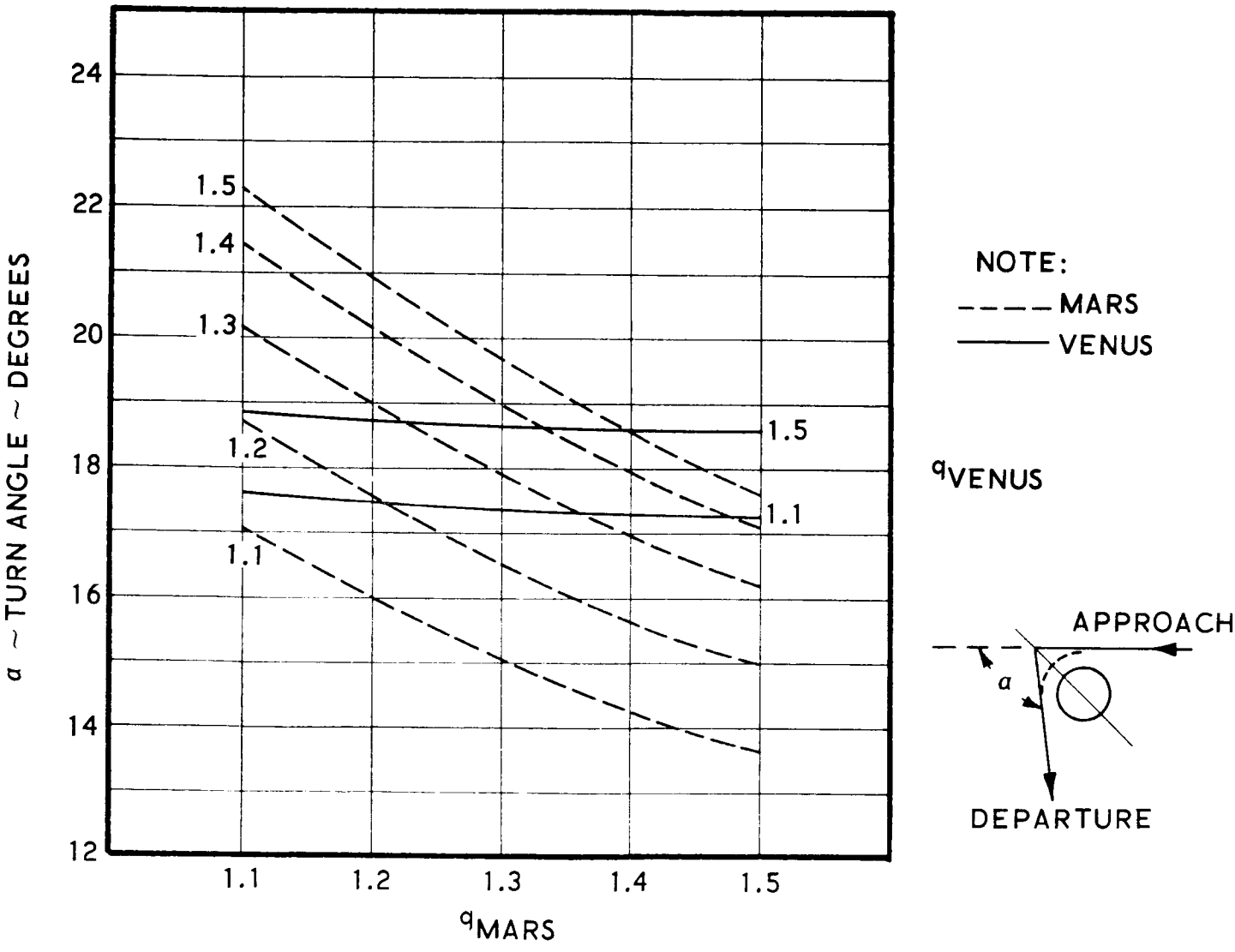

FIGURE 3-8

CROCCO

PERIFOCUS/SUN-LINE ANGLE AS A FUNCTION OF q_{MARS} AND q_{VENUS}

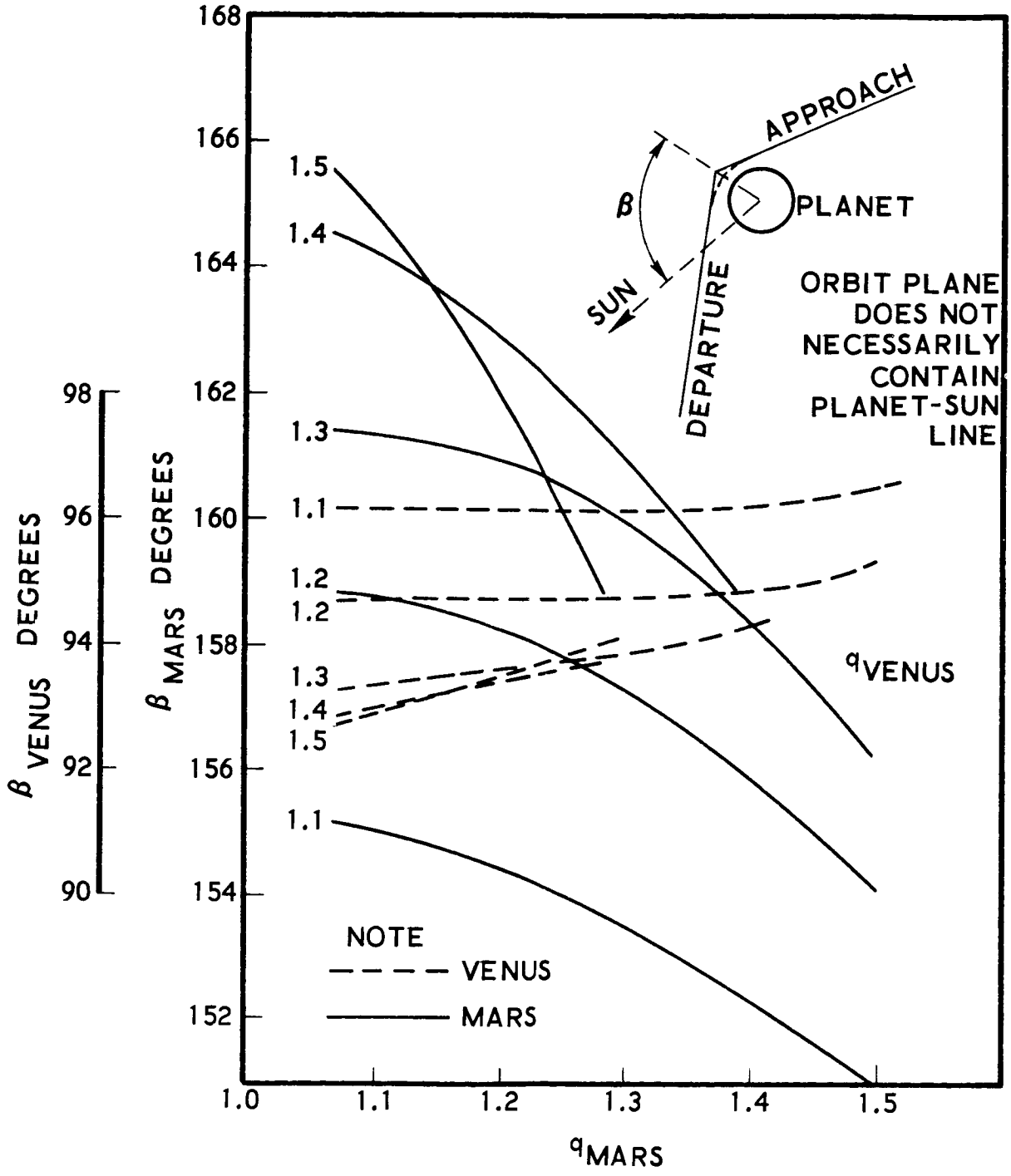

FIGURE 3-9

CROCCO EARTH TO MARS TRIP TIME AS A FUNCTION OF q_{MARS} AND q_{VENUS}

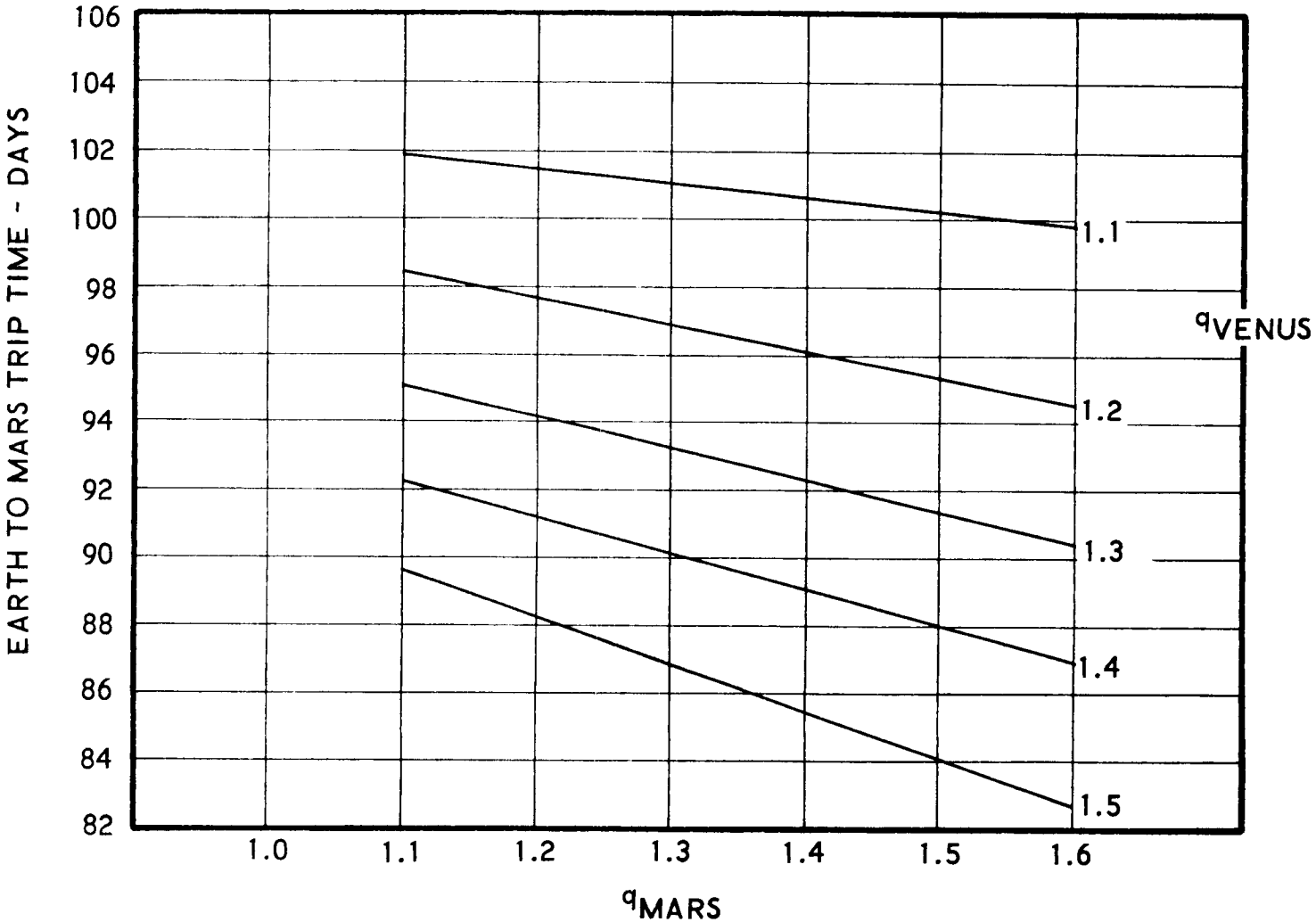

FIGURE 3-10

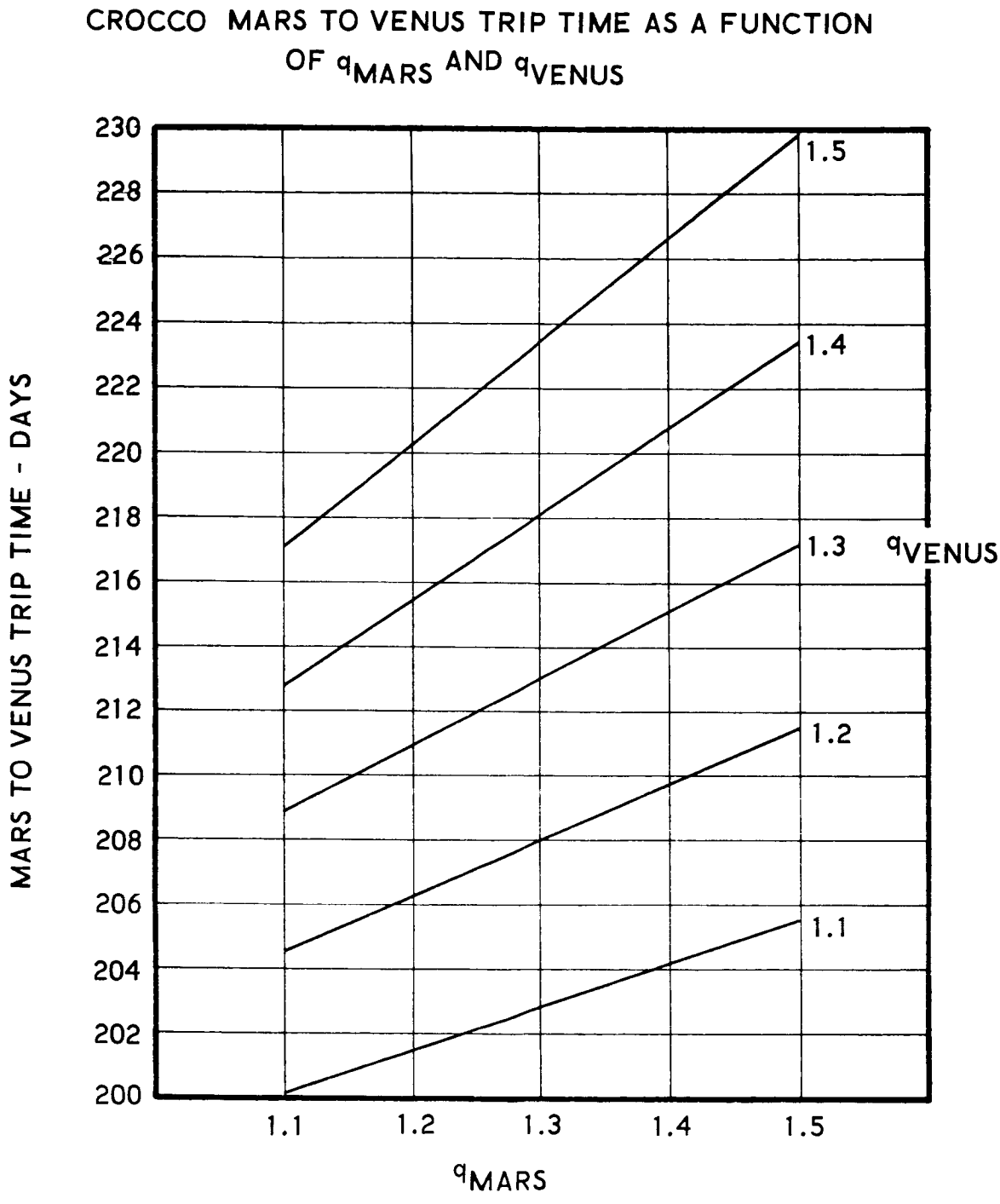
CROCCO MARS TO VENUS TRIP TIME AS A FUNCTION OF q_{MARS} AND q_{VENUS}
MARS TO VENUS TRIP TIME - DAYS
230
228
226
224
222
220
218
216
214
212
210
208
206
204
202
200
1.1
1.2
1.3
1.4
1.5
q_{MARS}
1.5
1.4
1.3
1.2
1.1
q_{VENUS}

FIGURE 3-11

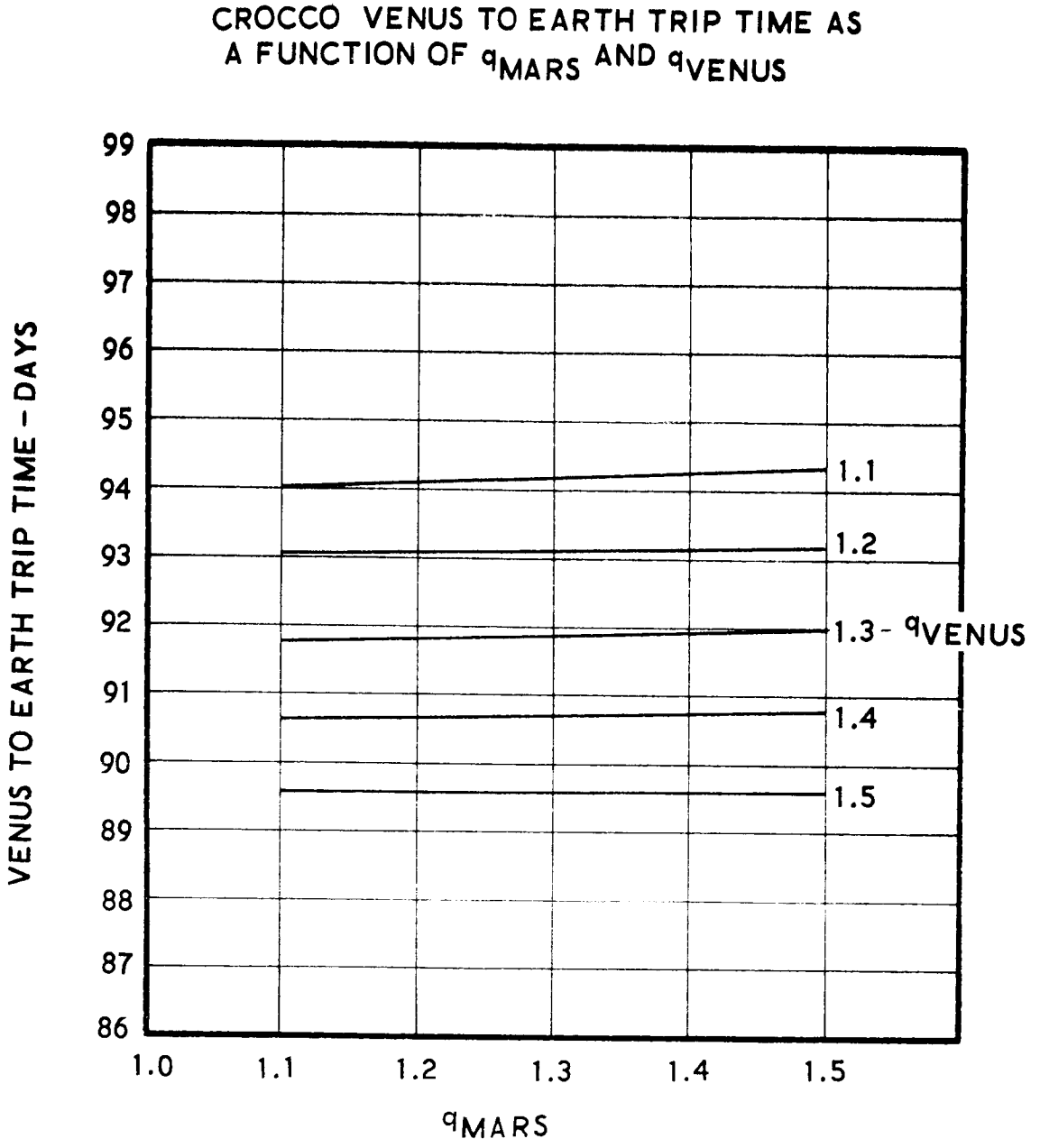
CROCCO VENUS TO EARTH TRIP TIME AS A FUNCTION OF q_{MARS} AND q_{VENUS}
VENUS TO EARTH TRIP TIME - DAYS
99
98
97
96
95
94
93
92
91
90
89
88
87
86
1.0
1.1
1.2
1.3
1.4
1.5
q_{MARS}
1.1
1.2
1.3 - q_{VENUS}
1.4
1.5

FIGURE 3-12

For an Earth-Venus-Mars Symmetric mission, the orbit (Figure 3-13) is as follows:

(1) Launch from Earth at time t_1

(2) Intercept Venus at time t_2 or t_2^*

(3) Intercept Mars at time t_3 or t_3^*

(4) The vehicle's longitude must equal the Earth's longitude at t_4

(5) Return to Earth at time t_5

The aphelion distance of the vehicle orbit, Q, was taken to be 1.387 a.u., which is nearly the perihelion distance of Mars. This aphelion distance was used with perihelion distances, q, of 0.650, 0.700, and 0.719 a.u. The symbol t_1 specifies the launch date from the Earth; t_2 is the time at which the vehicle is at a radial distance of 0.719 a.u., the heliocentric distance of Venus; and t_4 is the time the vehicle arrives at aphelion.

The time intervals $(t_2 - t_1)$ and $(t_4 - t_1)$ were calculated according to:

Semi-major axis $\quad a = \frac{q + Q}{2}$, a.u.

Eccentricity $\quad e = \frac{Q - q}{Q + q}$

True anomaly $\quad V_i = \cos^{-1}\left[\frac{1}{e}\left(\frac{qQ}{ar_i} - 1\right)\right] \quad i = 1, 2$

Eccentric anomaly $\quad E_i = \cos^{-1}\left[\frac{1}{e}\left(1 - \frac{r_i}{a}\right)\right] \quad i = 1, 2$

Interval of mean anomaly

$$(M_i - M_1) = (E_i - E_1) - e(\sin E_i - \sin E_1), \text{ radians}$$

Time interval $\quad (t_i - t_1) = \frac{(M_i - M_1)}{0.017202} a^{3/2}$, days.

SYMMETRIC ORBIT PROFILE

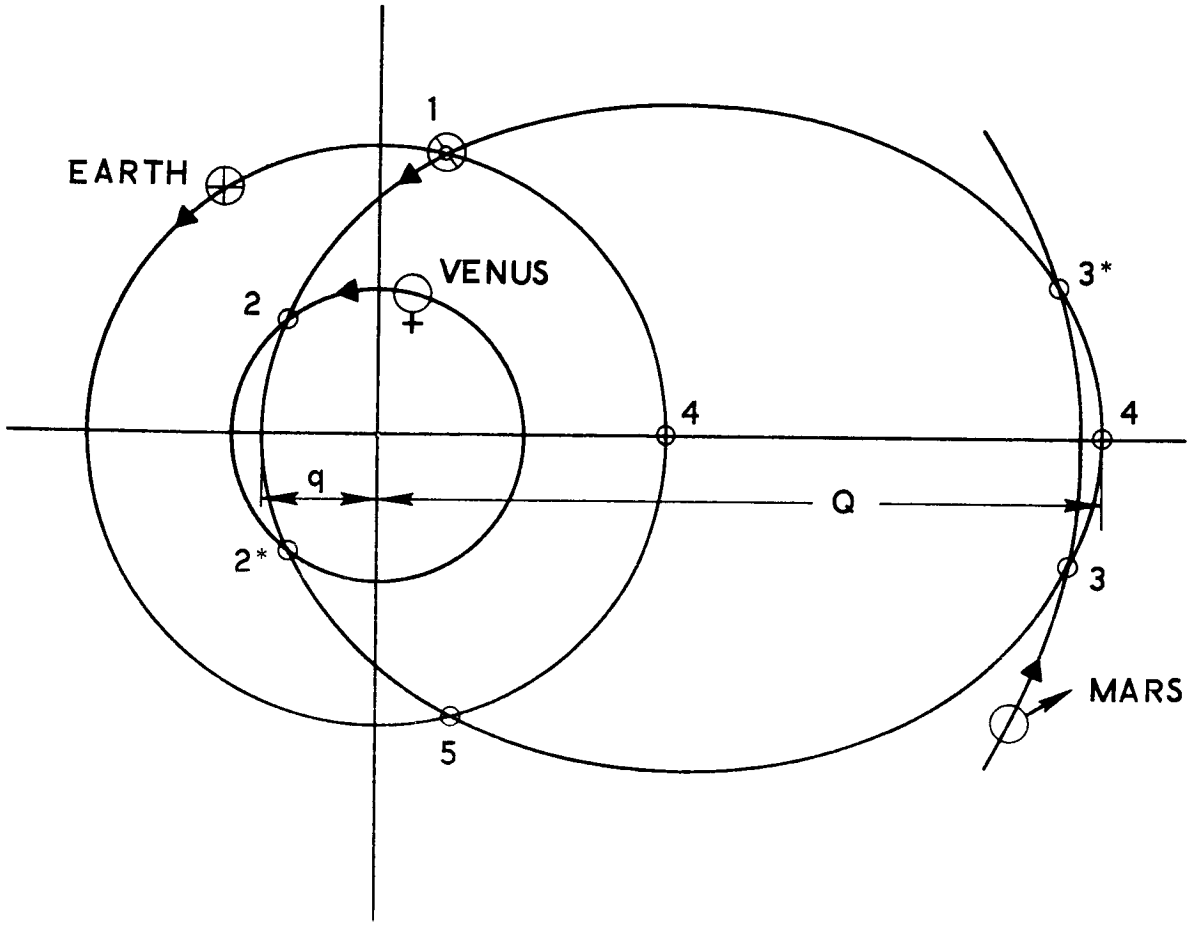

FIGURE 3-13.

The adoption of values for t_1 specifies t_2 and t_4. The longitude of the vehicle, l_{v_2}, at t_2 is then

$$l_{v_2} = l_{\oplus_1} + (360 - v_1) - (360 - v_2)$$

where $l_{\oplus_1}$ is the longitude of the Earth at takeoff, as given by the ephemeris. The true longitude of Venus at time t_2, l_{q_2}, is also taken from the ephemeris and compared with l_{v_2}. Similarly, the longitude of the vehicle at t_4 is

$$l_{v_4} = l_{\oplus_1} + (360 - v_1) + 180$$

This is compared with $l_{\oplus_4}$ and $l_{\oplus_4}$, both taken from the ephemeris. The results are shown in Table 3.1. Times are given in Julian date.

For a symmetric orbit, it is necessary that $l_{\oplus_4} = l_{v_4}$. In the cases considered here, the vehicle always reached its aphelion before the Earth reached the same longitude. Note in particular that for $q = 0.719$ a.u., a t_1 slightly later than 244 0880 (21 October 1970) would enable the vehicle to intercept Venus at t_2 and, if Q were slightly larger the vehicle would reach its aphelion somewhat later, thus enabling the vehicle to match its longitude with Earth at t_4. Furthermore, the longitude of Mars will also be very close to l_{v_4} and $l_{\oplus_4}$ at this later time, permitting the desired rendezvous with Mars at t_3 or t_3^*. For $q < 0.719$, it appears that Venus might possibly be intercepted at t_2^*, and Mars at t_3 or t_3^* in addition to satisfying the symmetric condition for return to Earth. These cases appear to warrant more detailed numerical study.

TABLE 3.1

VEHICLE AND PLANET LONGITUDES FOR SYMMETRIC MISSION

	LONGITUDES AT t_2		LONGITUDES AT t_4		
LAUNCH DATE	VEHICLE	VENUS	VEHICLE	MARS	EARTH
$q = 0.650$, $(t_2 - t_1) = 44^d.7$, $(t_4 - t_1) = 257^d.1$					
244 0880	$84^\circ.6$	$85^\circ.5$	$314^\circ.9$	$294^\circ.0$	$282^\circ.0$
0890	94.6	101.7	324.9	300.0	292.0
0900	104.6	117.9	334.9	306.0	302.0
0910	114.6	134.2	344.9	312.0	312.0
$q = 0.700$, $(t_2 - t_1) = 55^d.6$, $(t_4 - t_1) = 264^d.0$					
244 0880	$102^\circ.6$	$103^\circ.0$	$308^\circ.6$	$296^\circ.0$	$288^\circ.4$
0890	112.6	119.2	318.6	305.0	298.4
0900	122.6	135.4	328.6	311.0	308.4
0910	132.6	151.8	338.6	317.0	318.4
$q = 0.719$, $(t_2 - t_1) = 68^d.9$, $(t_4 - t_1) = 266^d.4$					
244 0880	$126^\circ.0$	$124^\circ.6$	$306^\circ.0$	$299^\circ.0$	$291^\circ.0$
0890	136.0	140.8	316.0	306.0	301.0
0900	146.0	157.1	326.0	312.0	311.0
0910	156.0	73.0	336.0	317.0	321.0

The approximate graphical technique of Reference (3) is also available for the Symmetric orbits. This technique was applied in the 1970-1972 era and the following possible dates were determined.

ORBIT NO.	LAUNCH DATE	FIRST FLYBY IS AT:	θ (DEG.)
I	15 February 1970	VENUS	67
II	30 October 1970	VENUS	22
III	15 November 1970	MARS	23
IV	15 December 1970	MARS	28
V	30 May 1971	MARS	68
VI	15 January 1972	VENUS	63
VII	15 April 1972	MARS	62
VIII	25 May 1972	VENUS	57
IX	15 October 1972	VENUS	36

It may be seen that Orbit II agrees well with the orbit previously suggested, and it appears to be near minimum in hyperbolic excess velocity using the launch evaluation angle (θ) as a criterion. This criterion is not completely valid in the Symmetric cases, since the semi-major axis of the transfer orbit is not a constant (i.e., period is not fixed but is bounded between 1 and 2 years).

(2) Launch Window and Trajectory Characteristics

Figures 3-14 through 3-22 represent the Symmetric class of trajectories. These trajectories have a duration of somewhat more than a year and a half, with passage about Venus occurring prior to passage about Mars. The reference illustrations utilize the same general parameters and format as the previously described Crocco class.

Figure 3-14 shows the effect of closest approach distance to Mars and Venus upon the launch date and total mission time. Note especially that:

1. The launch will occur in an interval from July 16, 1970 to August 16, 1970 for approach distances less than 2.0 planet radii.

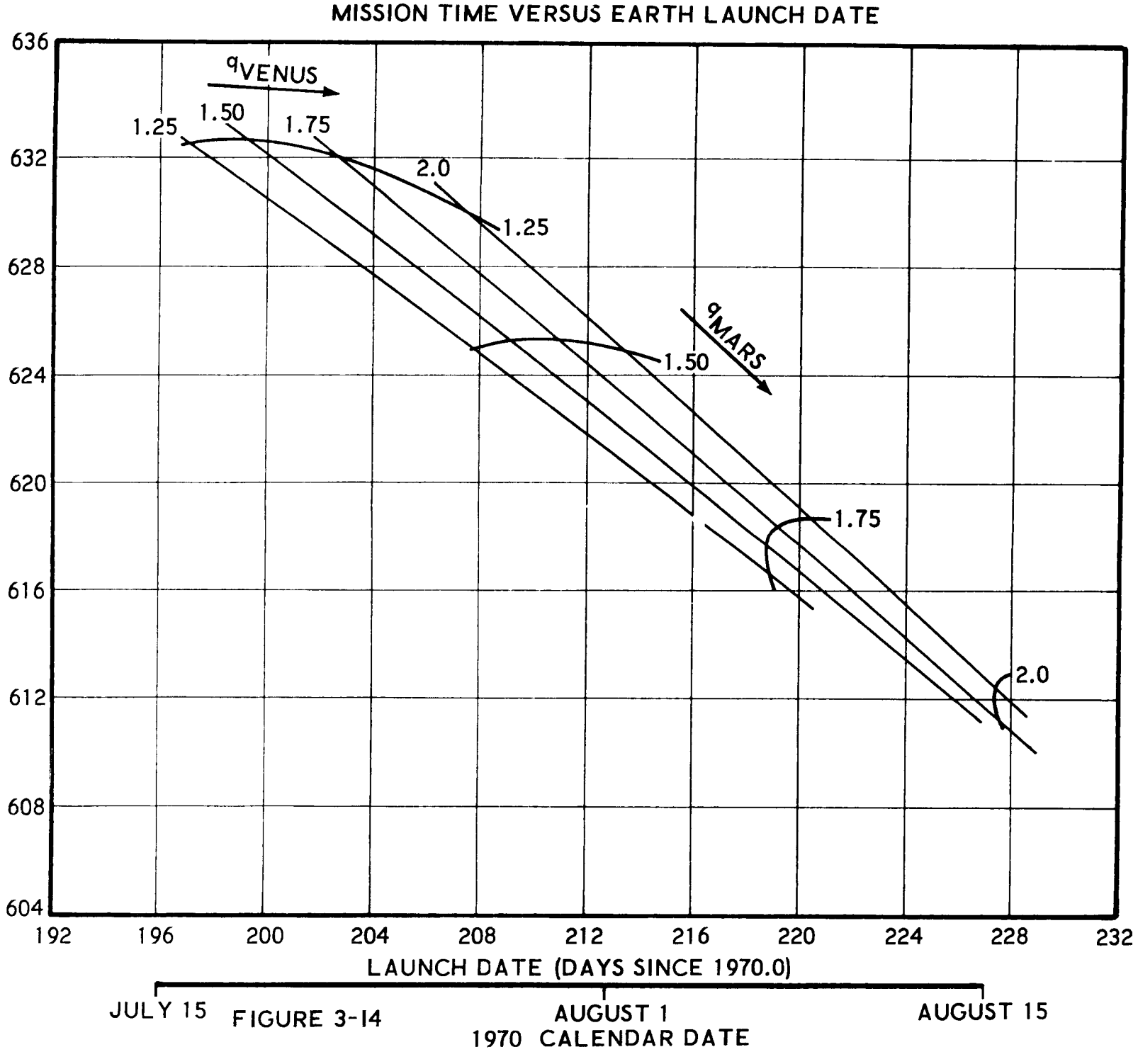
MISSION TIME VERSUS EARTH LAUNCH DATE
636
632
628
624
620
616
612
608
604
q_{VENUS}
1.25
1.50
1.75
2.0
1.25
q_{MARS}
1.50
1.75
2.0
192
196
200
204
208
212
216
220
224
228
232
LAUNCH DATE (DAYS SINCE 1970.0)
JULY 15
AUGUST 1
AUGUST 15
1970 CALENDAR DATE

FIGURE 3-14

2. Flight times range from 611 to 633 days, with a trend toward a lower value as the closest approach distance to Mars increases. Trip time is rather insensitive to closest approach distance to Venus.

3. Launch date is strongly dependent upon closest approach distance to Venus.

Figure 3-15 presents the characteristic velocity required to initiate the mission from a 300 KM parking orbit; as well as the velocity upon reentry at the completion of the mission. It is of interest to observe the following:

1. Launch velocity increases as the closest approach distance to Mars or Venus is decreased.

2. The required launch velocity of from 4 to 5½ KM/sec is considerably less than that for the Crocco mission.

3. Reentry velocity increases as the closest approach distance to Venus is reduced, but is not strongly dependent upon the closest approach distance to Mars.

4. Reentry velocities are somewhat larger than for the Crocco mission.

Figure 3-16 gives the hyperbolic excess velocity at launch and upon return to a non-rotating Earth for the Symmetric mission. The outstanding characteristic of this figure is that the departure velocities are significantly smaller than those for arrival for all combinations of nominal planetary miss distances. This is attributable to perturbations which occur at planet encounters. These perturbations result (in this case) in an increase of orbit energy and a greater heliocentric flight path angle on return to Earth. In general, multiple planet flyby missions can be expected to have differing departure and arrival asymptotic velocities. Like velocities would imply the existence of negligible or negating planetary perturbations - a situation which would also imply a planar mission. In short, an actual trajectory differs considerably from the simplified, planar, unperturbed versions of Figure 3-2.

Figure 3-17 gives the hyperbolic excess velocities relative to the individual planets at time of encounter.

SYMMETRIC

LAUNCH AND RE-ENTRY CHARACTERISTIC VELOCITIES AS A FUNCTION OF q_{VENUS} AND q_{MARS}

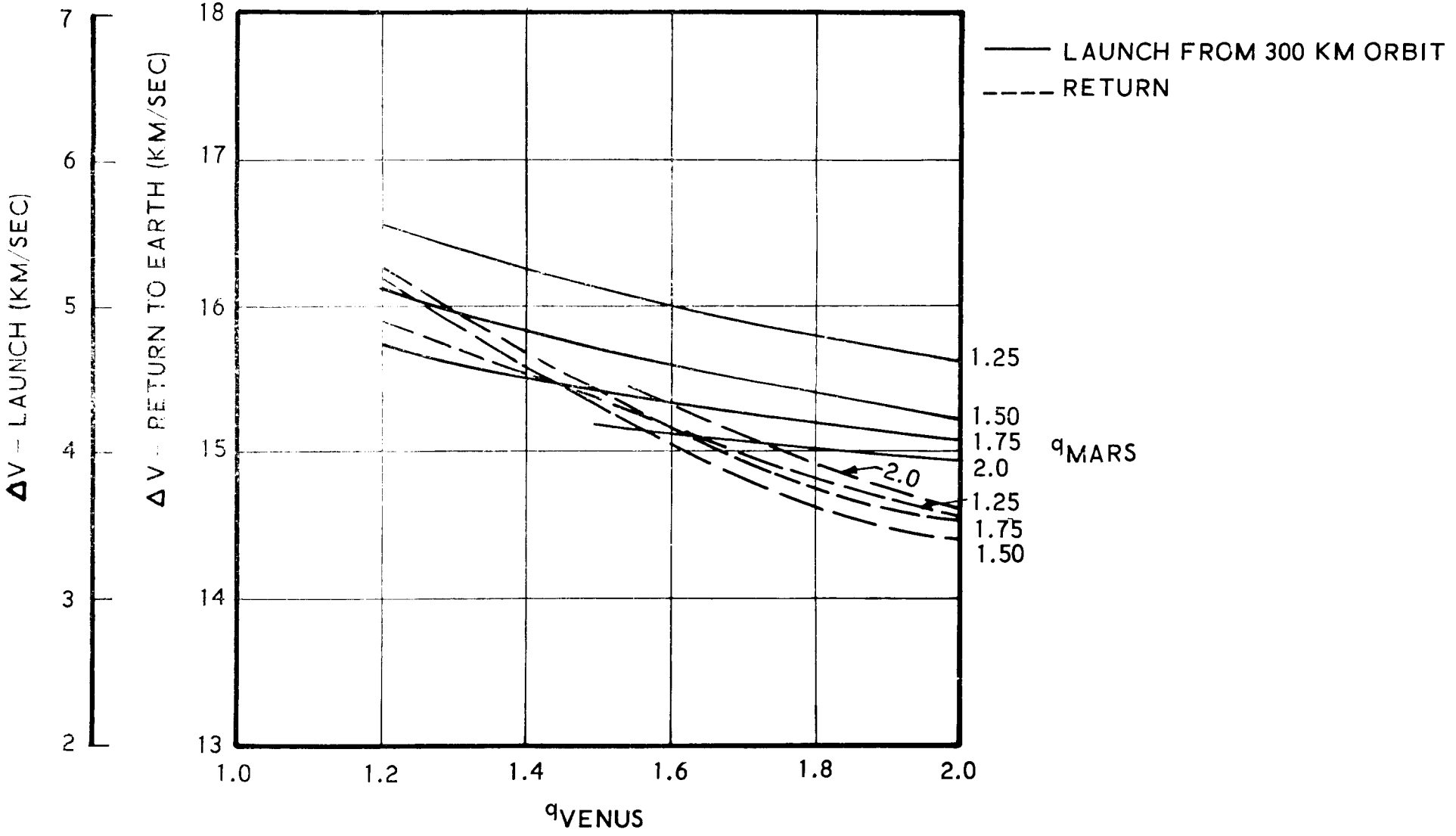

FIGURE 3-15

SYMMETRIC

ASYMPTOTIC VELOCITIES WITH RESPECT TO EARTH ON ARRIVAL AND DEPARTURE AS A FUNCTION OF q_{VENUS} AND q_{MARS}

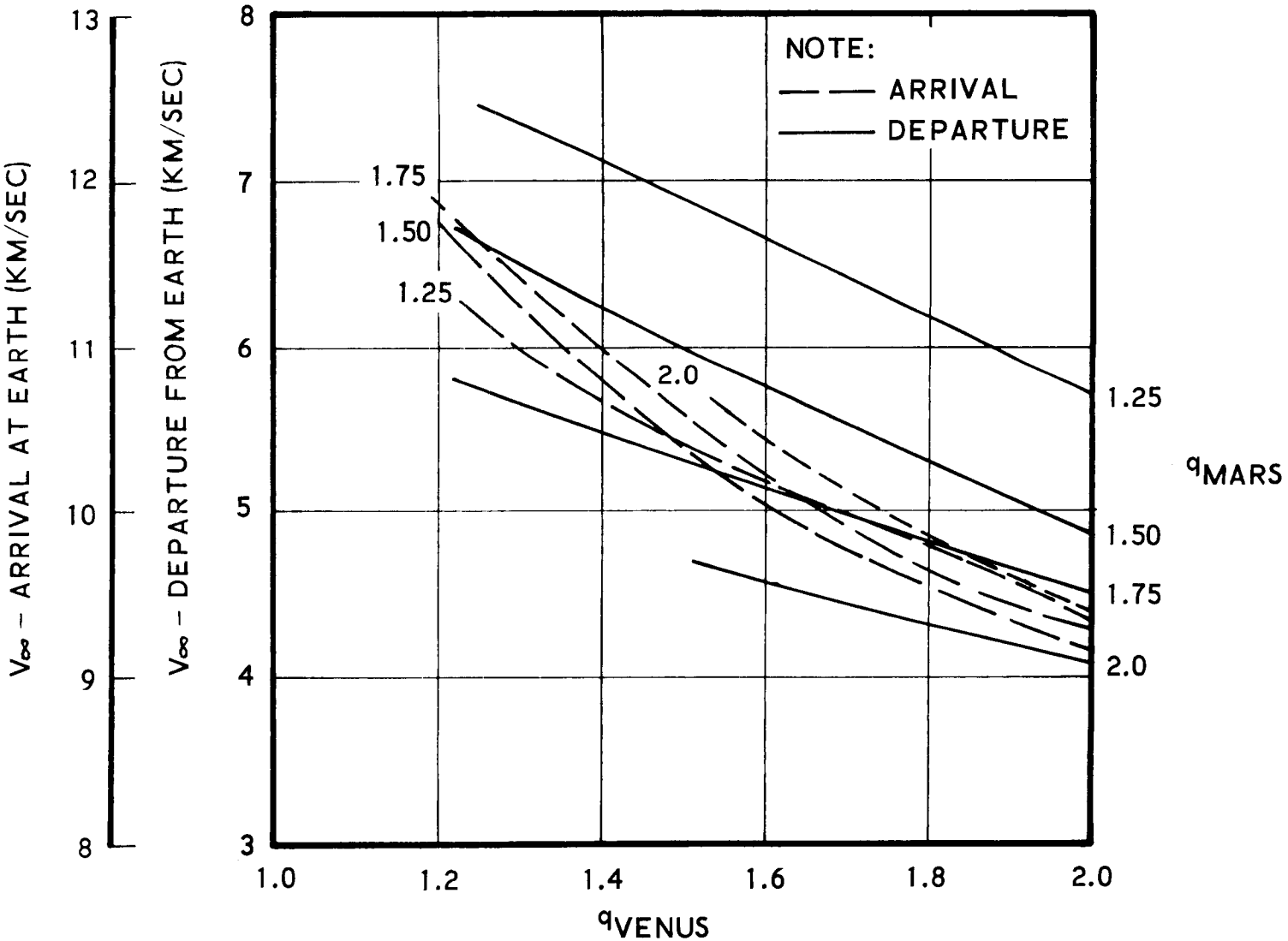

FIGURE 3-16

SYMMETRIC

ASYMTOTIC VELOCITIES WITH RESPECT TO MARS AND VENUS AS A FUNCTION OF q_{MARS} AND q_{VENUS}

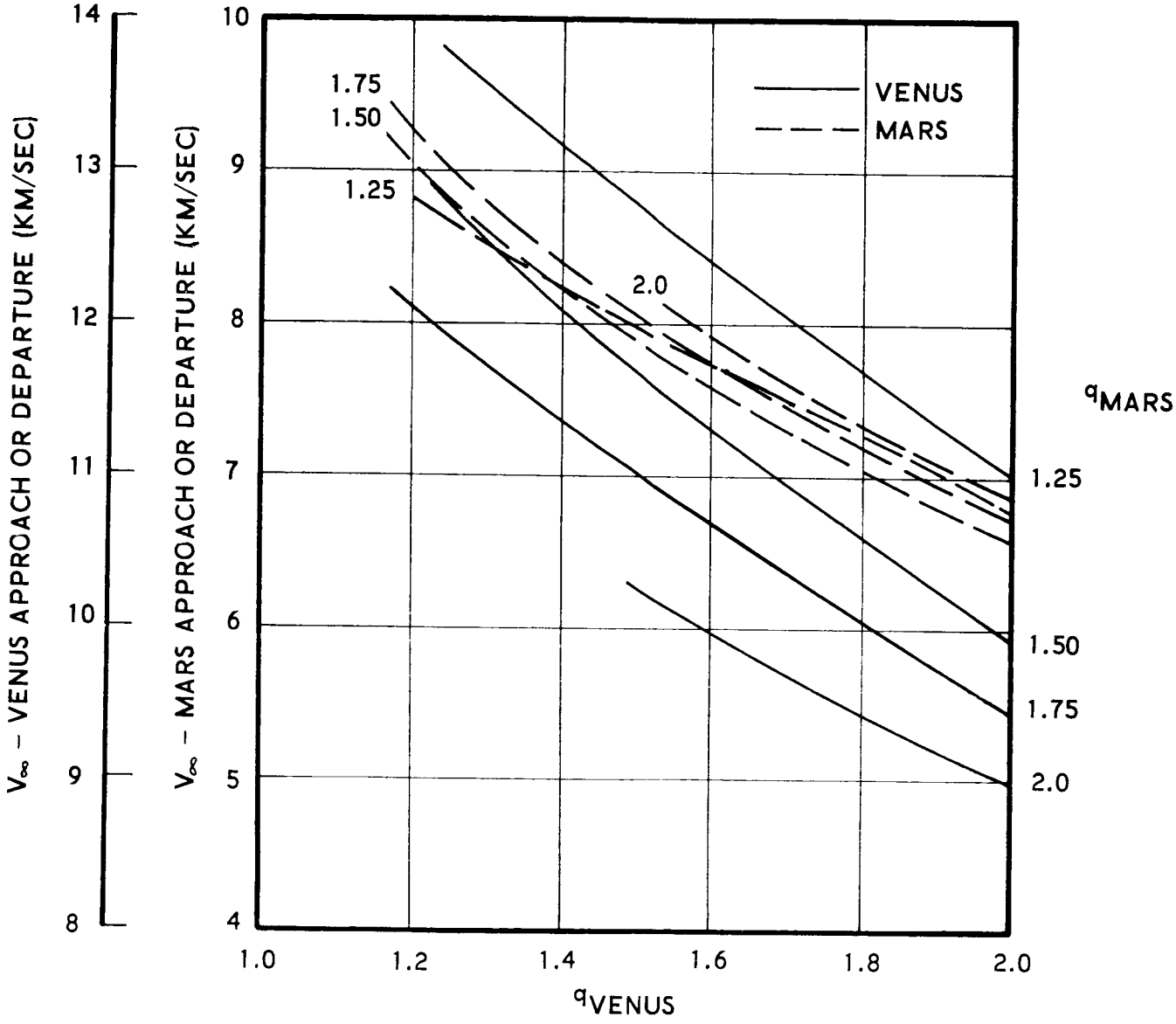

FIGURE 3-17.

Figure 3-18 depicts the hyperbolic turn angle as a function of the distances of closest approach to the respective planets.

Figure 3-19 illustrates the included angle between the line of apsides of the planetocentric hyperbola and the sun line. For this launch window, the vehicle will fly on the sunnyside ($\beta < 90^{o}$) about Mars and fall toward the sun ($\beta \cong 90^{o}$) from the dark side for the Venutian encounter.

Figures 3-20 through 3-22 give the nominal flight times for the several trajectory legs.

d. Comparative Evaluation

Table 5.2 contains in tabular form, the salient features of several arbitrarily selected trajectories in the Crocco and Symmetric class. The one important feature to note is the marked reduction in characteristic velocities as the nominal distance of closest approach to the planets is increased within the limits of the windows.

3.4 ABORT CAPABILITIES

Single impulse abort maneuvers from a geocentric escape trajectory have been investigated to determine the velocity increment necessary to accomplish a successful return to Earth in a specified time after abort. Escape trajectories have been assumed to have a perigee radius of 1.1 Earth radii, with hyperbolic excess velocities varying between zero and sixteen KM/sec. Abort trajectories are assumed to be elliptical, with a perigee radius of 1.005 Earth radii. The escape trajectory and abort trajectory are assumed to be co-planar with the same rotational sense. Abort action is initiated at distances between 1.5 and 10.0 Earth radii. Times from abort to arrival at perigee (an indication of flight time) vary from 15 minutes to 10,000 minutes. Parametric plots have been formed which relate the required velocity increment to abort radius, escape trajectory excess velocity, and time from abort to arrival at perigee. Reentry velocities are, of course, less than parabolic in magnitude, and the reentry flight path angles are mainly between 5 and 7 degrees.

The problem of mission abort at less than Earth escape velocity has already received considerable treatment in the open literature. A summary of such studies is given in Reference (4). For the EMPIRE mission, however, it is necessary to extend the abort capability to escape trajectories with a considerable excess velocity. Since the abort propulsion requirement will be governed by the extent of this capability, it was

SYMMETRIC

JRN ANGLE ABOUT MARS AND VENUS AS A FUNCTION OF q_{VENUS} AND q_{MARS}

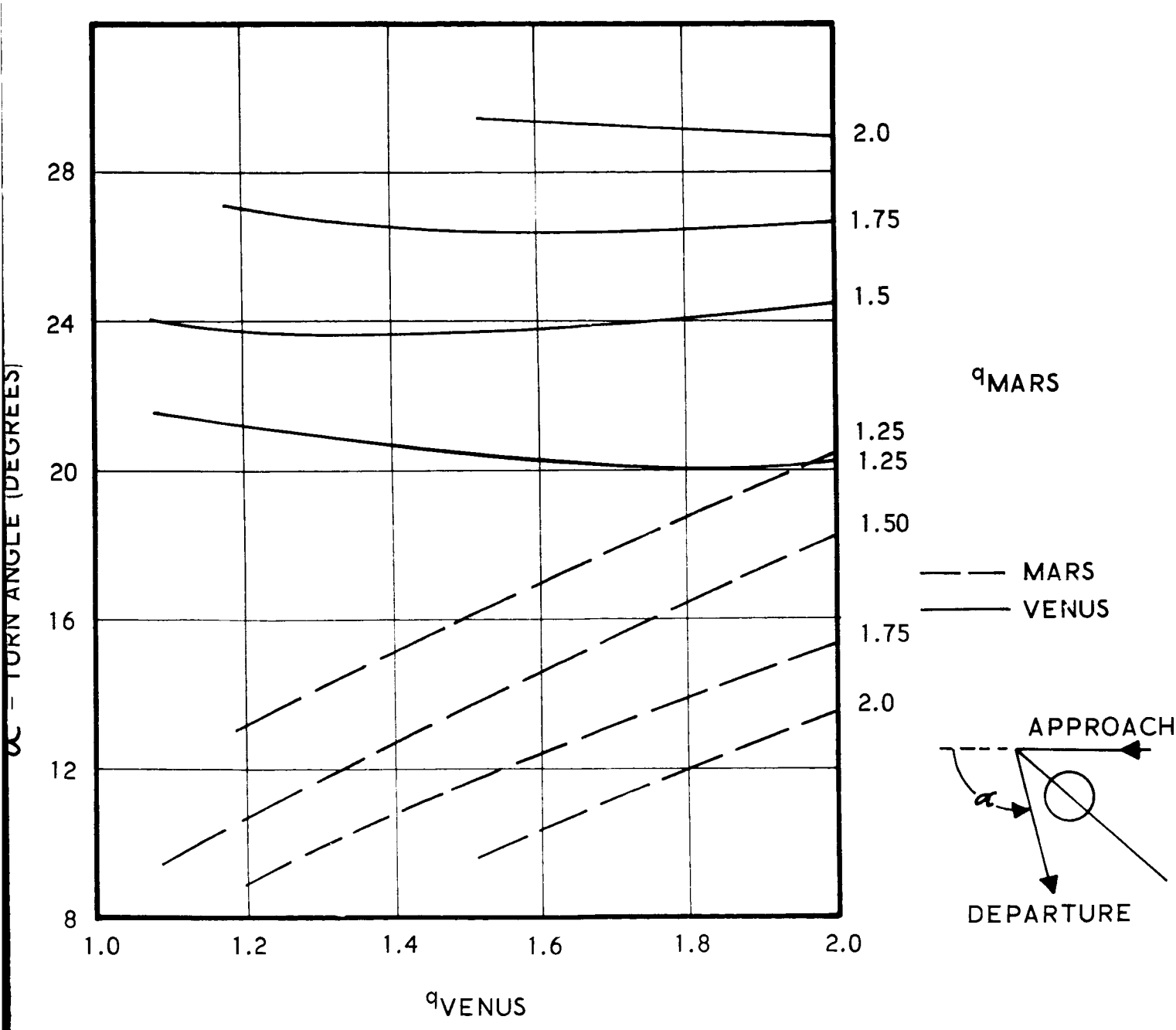

FIGURE 3-18

SYMMETRIC

PERIFOCUS / SUN-LINE ANGLE AS A FUNCTION OF q_{MARS} AND q_{VENUS}

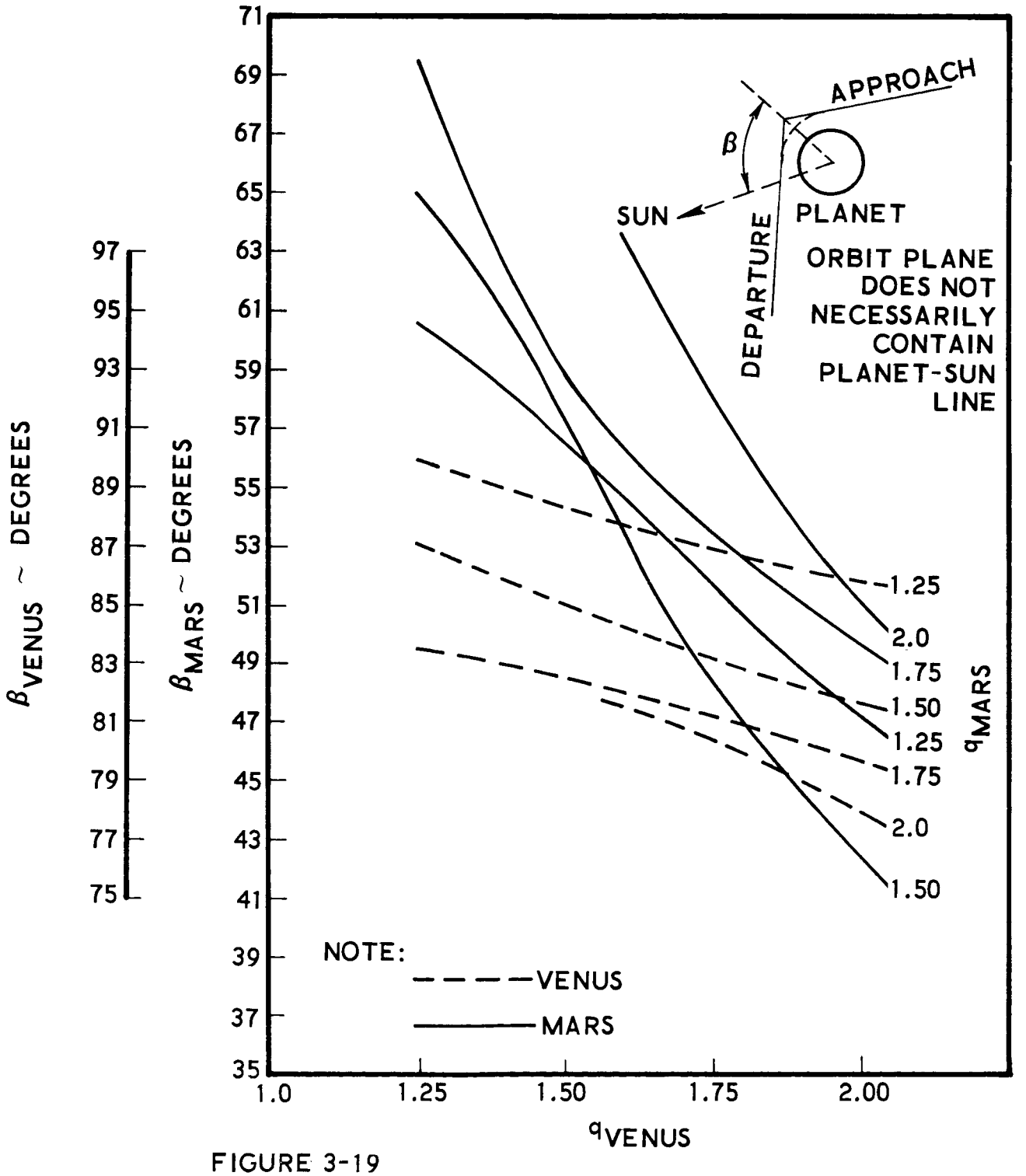

FIGURE 3-19

SYMMETRIC

EARTH TO VENUS TRIP TIME

AS A FUNCTION OF q_{VENUS} AND q_{MARS}

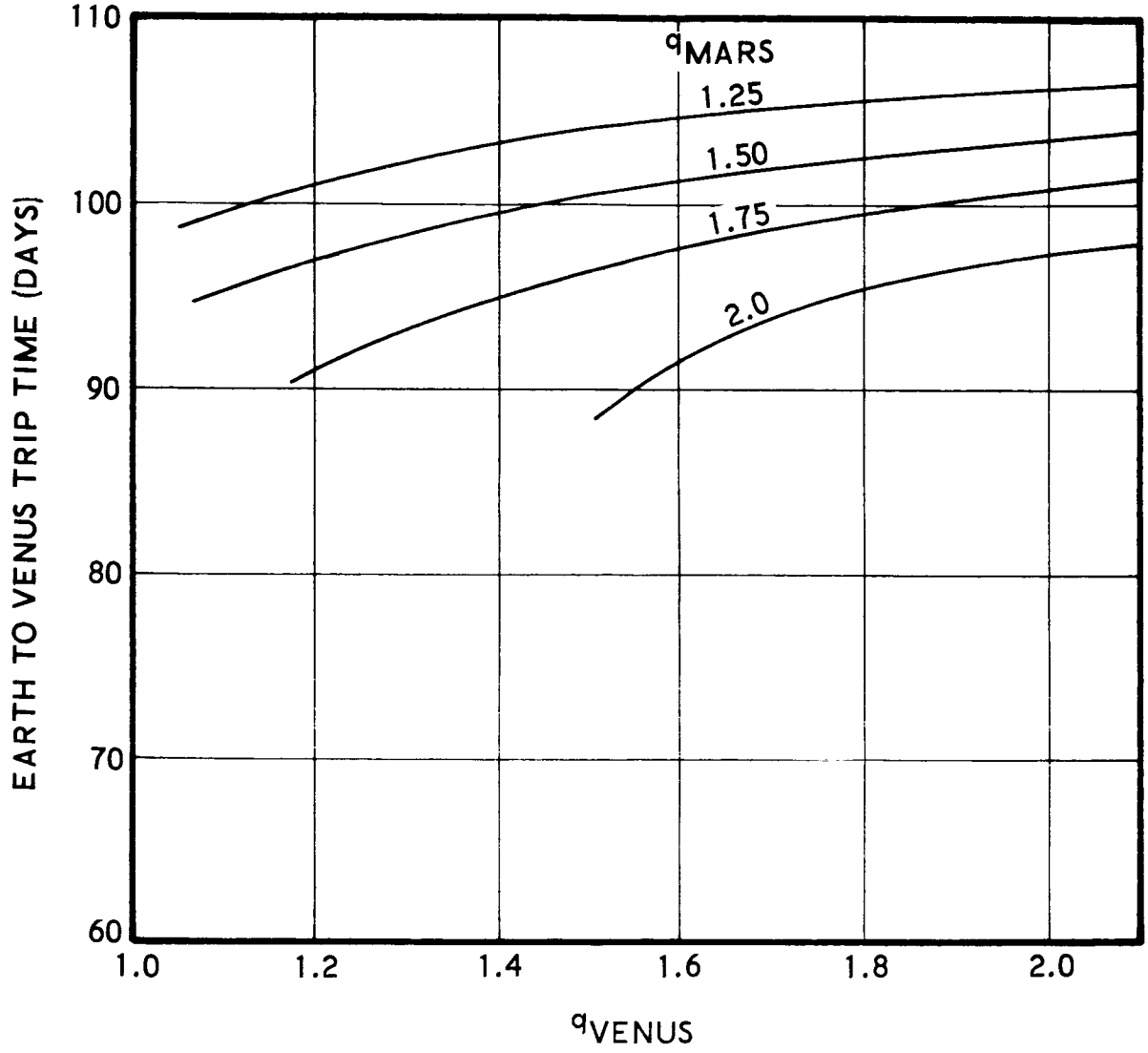

FIGURE 3-20

SYMMETRIC

VENUS TO MARS TRIP TIME
AS A FUNCTION OF q_{VENUS} AND q_{MARS}

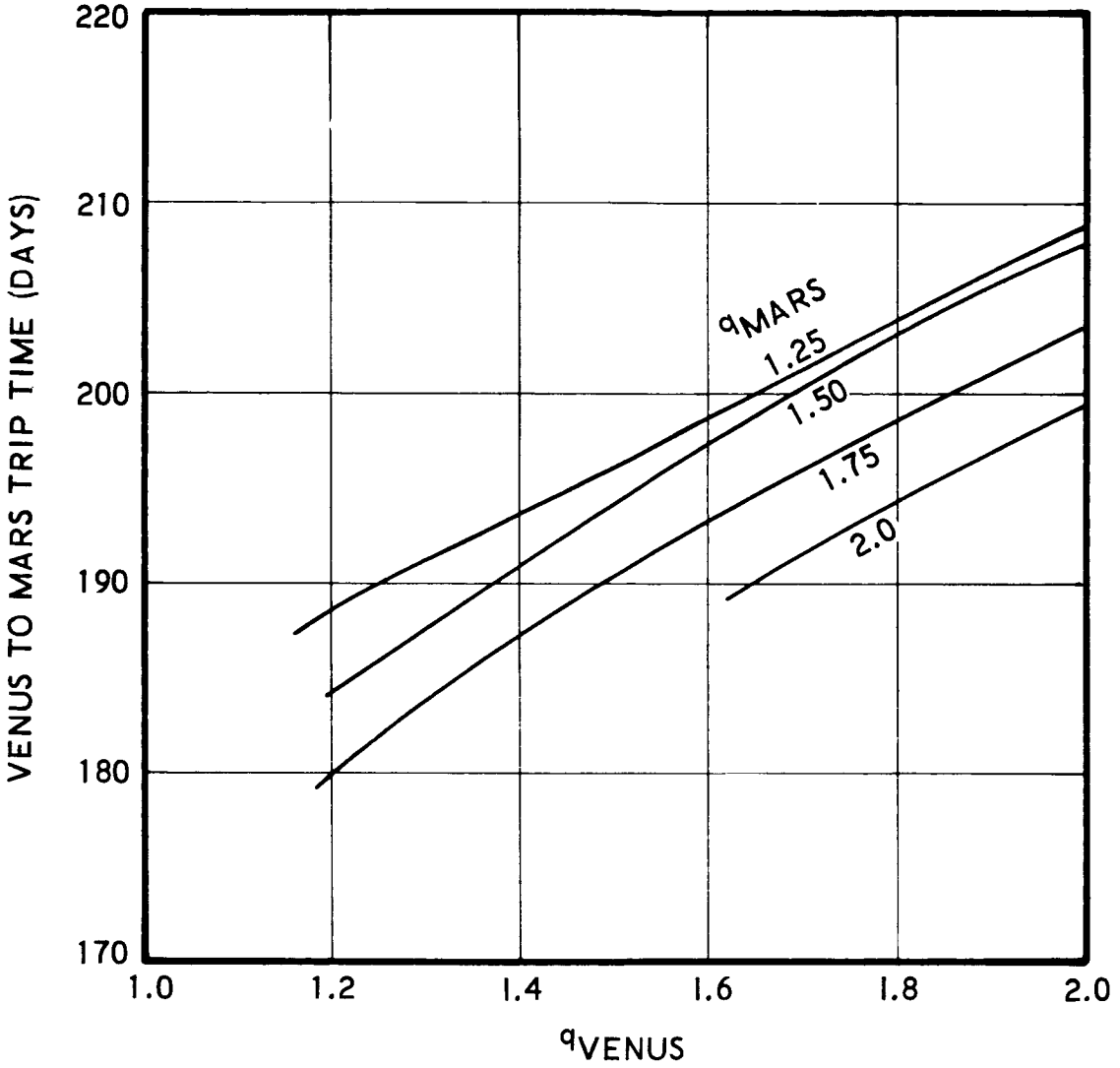

FIGURE 3-21

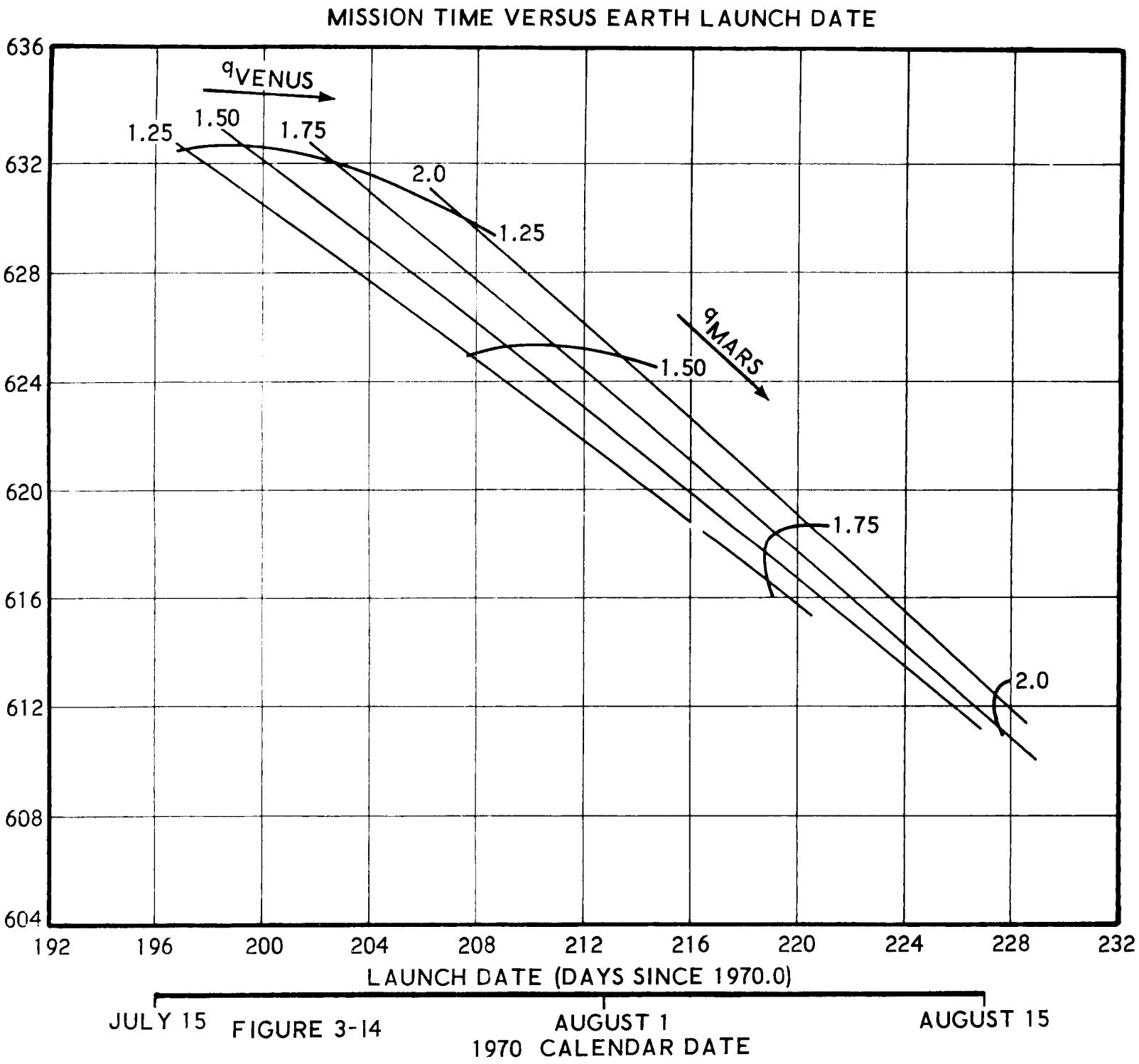
MISSION TIME VERSUS EARTH LAUNCH DATE
636
632
628
624
620
616
612
608
604
q_{VENUS}
1.25
1.50
1.75
2.0
1.25
q_{MARS}
1.50
1.75
2.0
192
196
200
204
208
212
216
220
224
228
232
LAUNCH DATE (DAYS SINCE 1970.0)
JULY 15
AUGUST 1
AUGUST 15
1970 CALENDAR DATE

FIGURE 3-14

TABLE 3.2

TYPICAL EMPIRE MISSION CHARACTERISTICS

	CROCCO		SYMMETRIC	
$q_{MARS} = q_{VENUS}$	1.3	1.5	1.3	2.0
Characteristic Launch Velocity Requirement (300 KM Parking Orbit)	10.1 KM/Sec	8.9 KM/Sec	5.3 KM/Sec	3.9 KM/Sec
Reentry Velocity (Neglecting Earth Rotation)	13.5 KM/Sec	13 KM/Sec	15.8 KM/Sec	14.7 KM/Sec
Total Trip Time	398.2 Days	403.8 Days	631.0 Days	613 Days
Earth Launch Date	8-29-71	8-13-71	7-19-70	8-16-70

necessary to parametrically investigate the propulsive requirements for such aborts. In performing the study, it has been assumed that a single thrust application would be used, that the abort trajectory is co-planar with the escape trajectory and that the reentry corridor is specified by an unperturbed perigee location. Abort trajectories are assumed to be elliptical, and with the same rotational sense as the escape trajectory. No attempt has been made to specify landing locations, since such considerations would be difficult to apply without decreasing the generality of the results.

Figure 3-23 shows the relevant geometry for performing an abort maneuver from a hyperbolic (or parabolic) escape trajectory. The escape trajectory is defined by its perigee radius q_1, and hyperbolic excess velocity V_h. The abort ellipse is defined by its perigee radius q_2, and major semi-axis a. The dashed abort ellipse is identical in geometry to the solid one but differs in that the flight path angle at abort is negative, resulting in a quicker return to Earth at the expense of additional abort velocity. The other two solutions, those involving retro-grade motion, have not been considered in view of their greater propulsive requirements. The velocity vector diagram defines the abort velocity requirement ΔV. For this study, the perigee radius of the escape trajectory q_1, has been held constant at 1.10 Earth radii.

In order to specify reasonable reentry conditions for the abort trajectory, a perigee radius q_2 of 1.005 Earth radii has been utilized.

Figure 3-24 through 3-26 parametrically define the abort propulsive requirements. Time from abort to arrival at perigee is used as the abscissa in deference to its importance in the abort problem. The parameter is the hyperbolic excess of the escape trajectory V_h. The range shown is sufficient to apply to almost any currently envisioned space mission. Abort radii of 1.5, 3.0, and 10 Earth radii have been investigated. From inspection of the figures, the following conclusions may be drawn.

(1) Except for very small excess velocities and abort radii, a reduction in the time parameter always results in an increased velocity increment.

(2) For small and moderate abort radii, a significant reduction in the time parameter may be obtained with a modest increase in velocity increment.

(3) Regardless of excess velocity, the abort velocity requirement will ultimately increase with abort radius for a given value of the time parameter.

GEOCENTRIC ABORT MANEUVER GEOMETRY

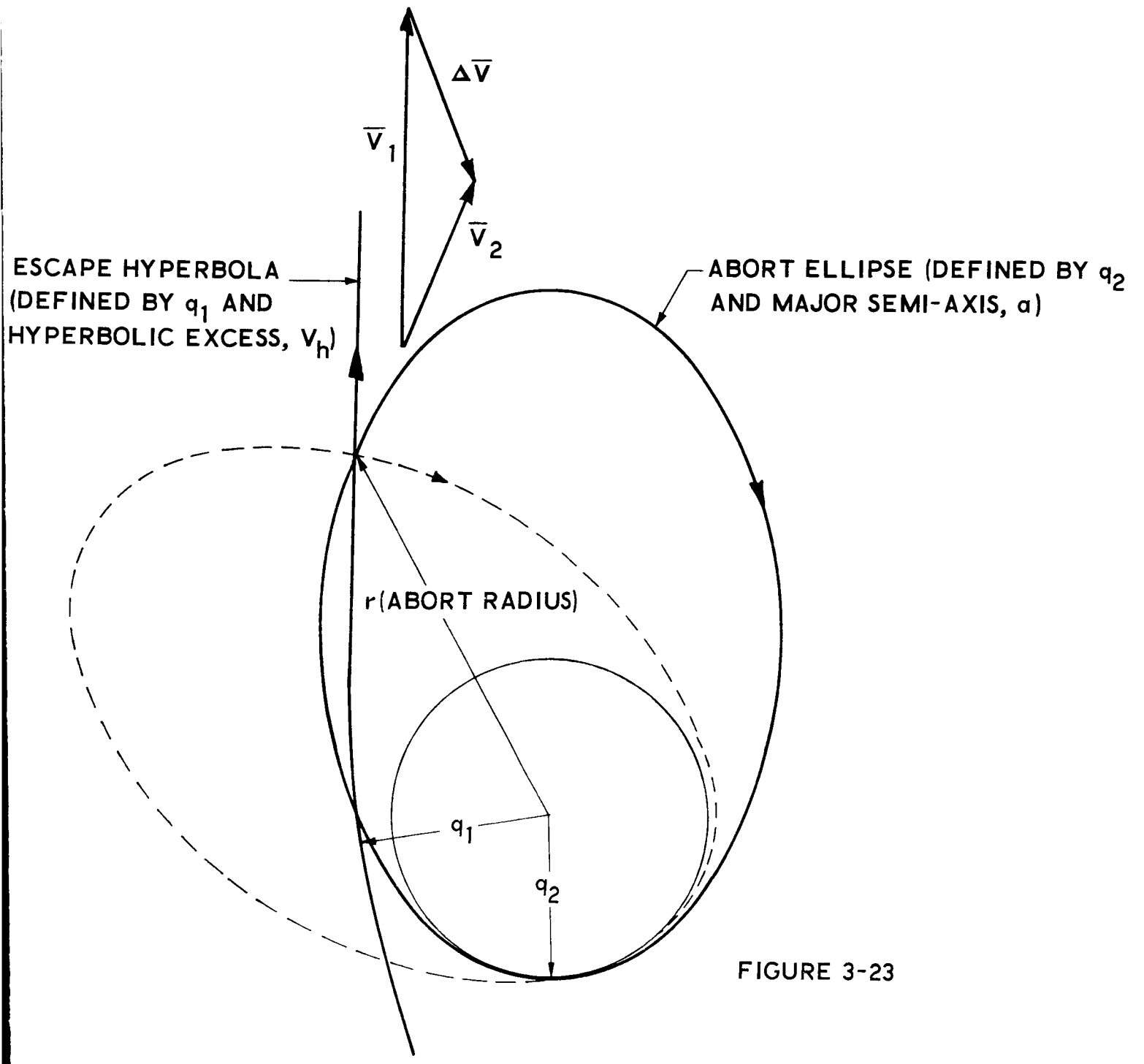

FIGURE 3-23

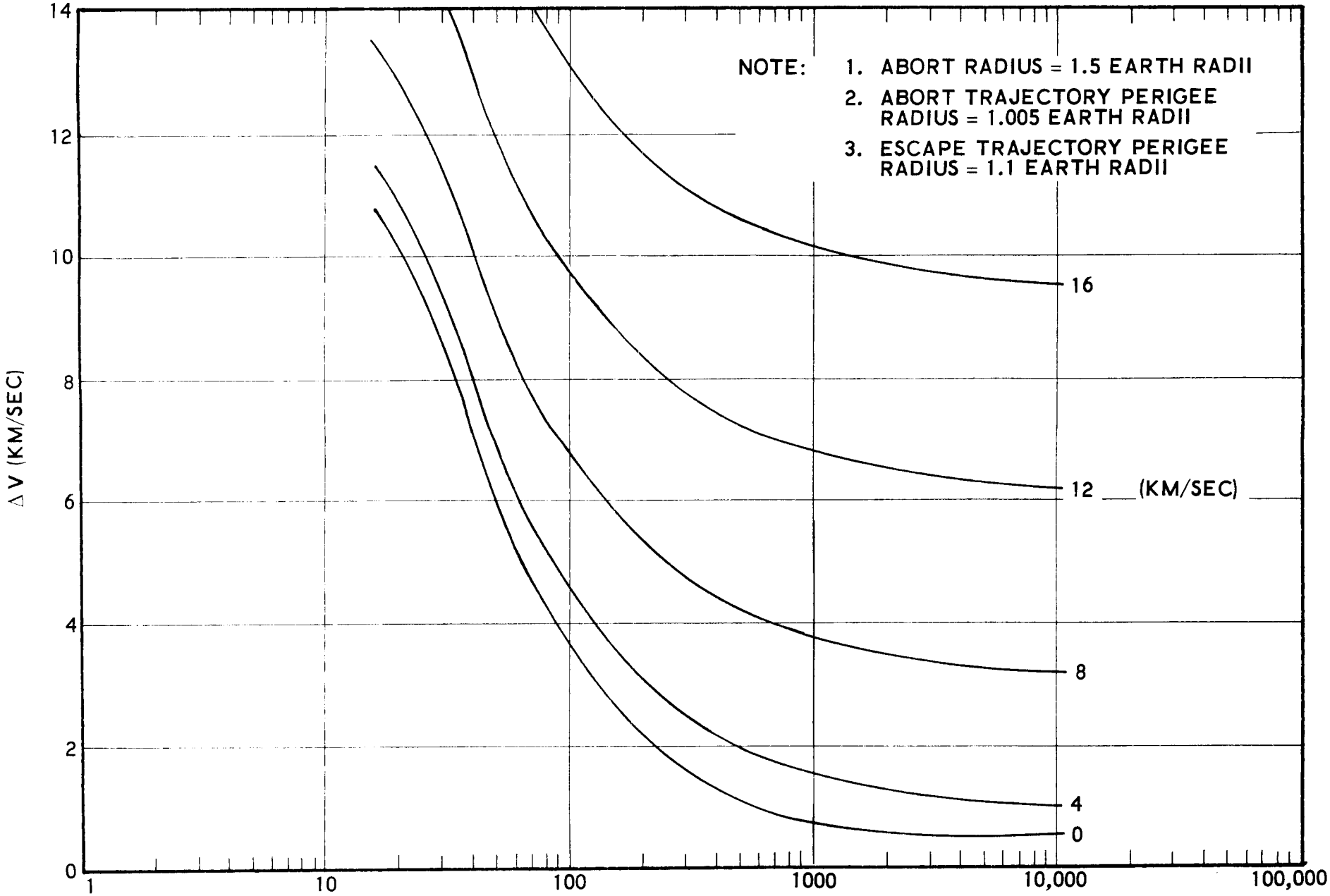
NOTE:
1. ABORT RADIUS = 1.5 EARTH RADII
2. ABORT TRAJECTORY PERIGEE RADIUS = 1.005 EARTH RADII
3. ESCAPE TRAJECTORY PERIGEE RADIUS = 1.1 EARTH RADII
16
12 (KM/SEC)
8
4
0
ΔV (KM/SEC)
0
2
4
6
8
10
12
14
1
10
100
1000
10,000
100,000
TIME FROM ABORT TO PERIGEE (MIN)

FIGURE 3-24

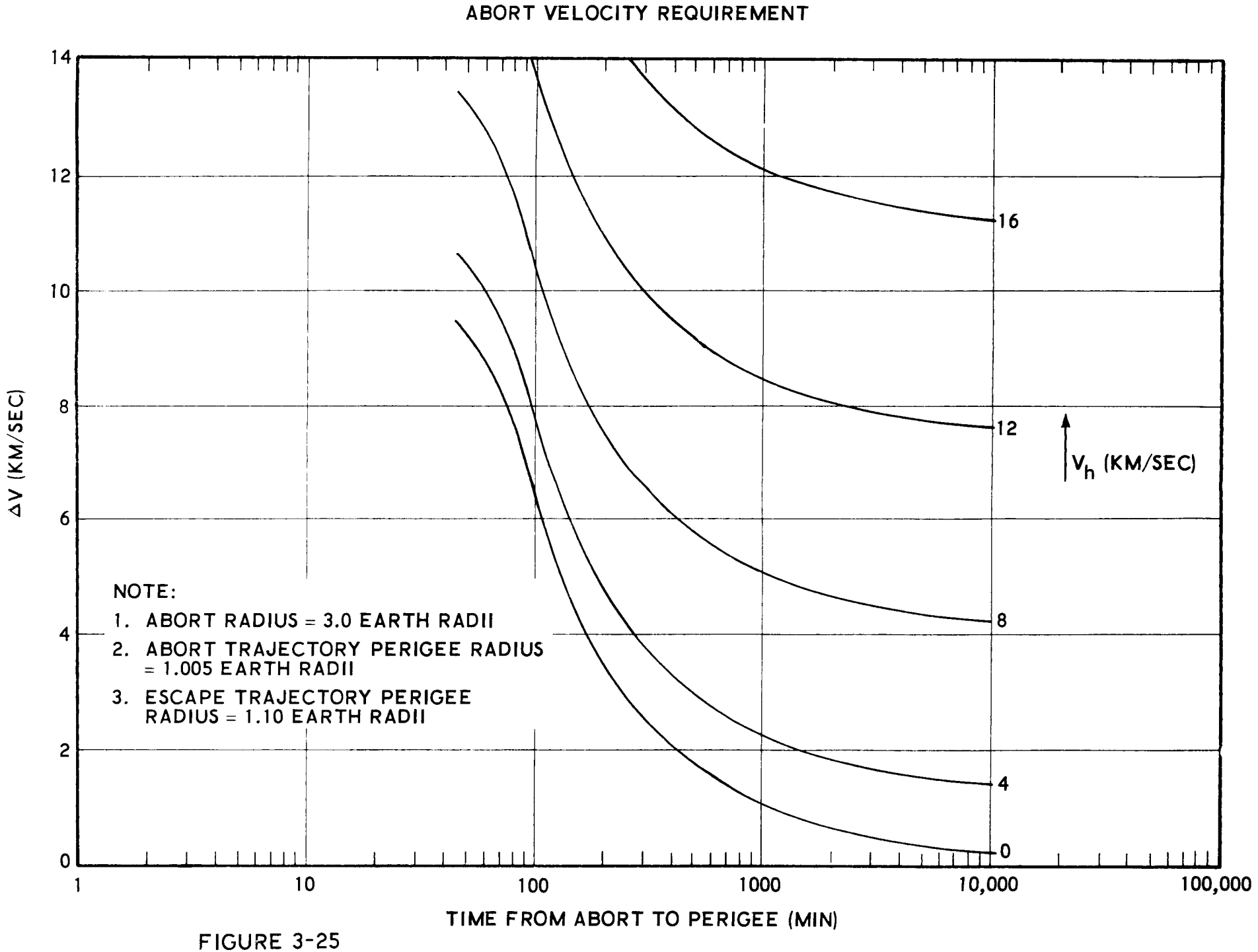
ABORT VELOCITY REQUIREMENT
ΔV (KM/SEC)
TIME FROM ABORT TO PERIGEE (MIN)
14
12
10
8
6
4
2
0
1
10
100
1000
10,000
100,000
16
12
8
4
0
V_h (KM/SEC)
NOTE:
1. ABORT RADIUS = 3.0 EARTH RADII
2. ABORT TRAJECTORY PERIGEE RADIUS = 1.005 EARTH RADII
3. ESCAPE TRAJECTORY PERIGEE RADIUS = 1.10 EARTH RADII

FIGURE 3-25

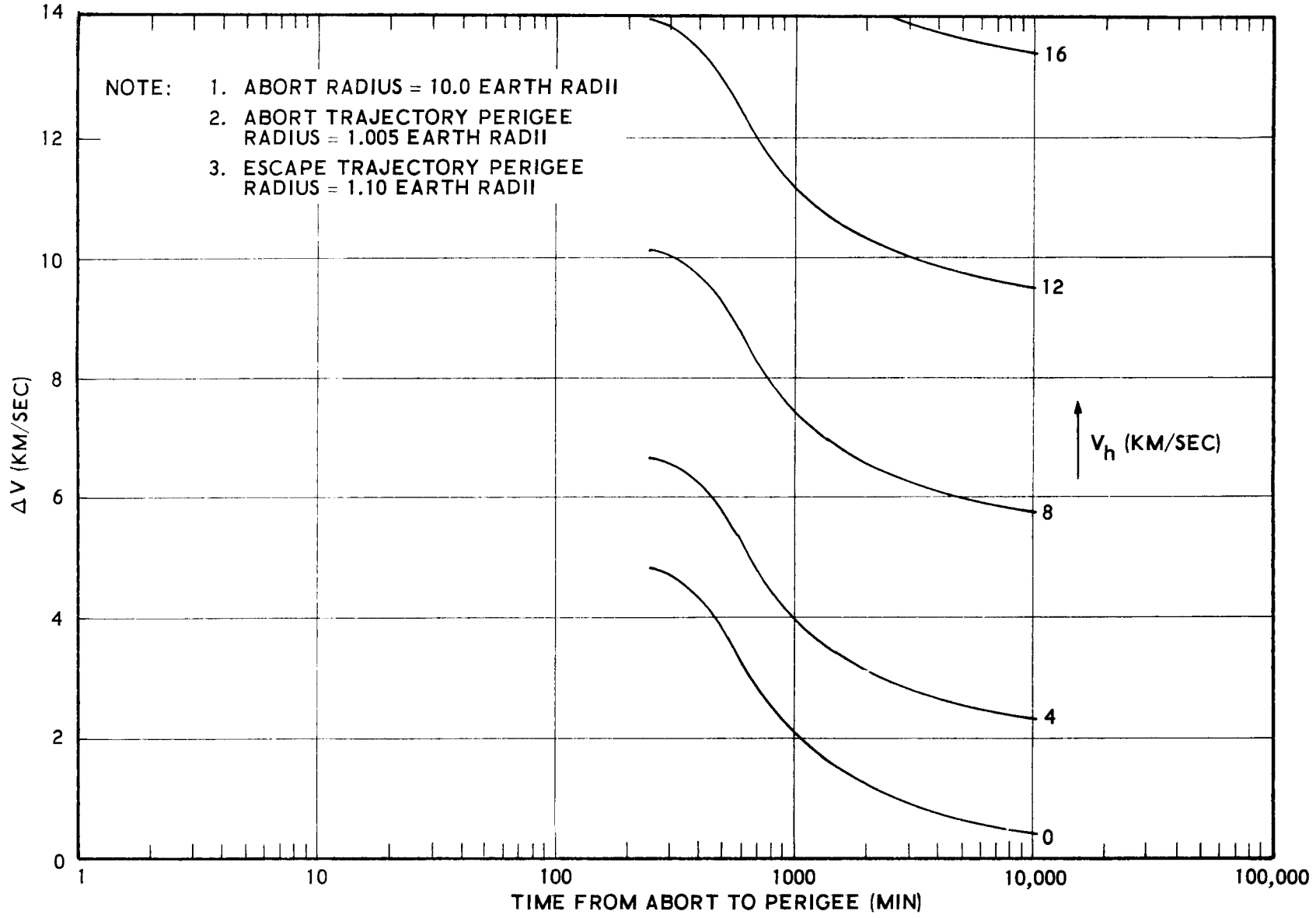
NOTE:
1. ABORT RADIUS = 10.0 EARTH RADII
2. ABORT TRAJECTORY PERIGEE RADIUS = 1.005 EARTH RADII
3. ESCAPE TRAJECTORY PERIGEE RADIUS = 1.10 EARTH RADII
16
12
8
4
0
V_h (KM/SEC)
ΔV (KM/SEC)
TIME FROM ABORT TO PERIGEE (MIN)
0
2
4
6
8
10
12
14
1
10
100
1000
10,000
100,000

FIGURE 3-26

Item (1) suggests that there is a practical lower limit on the time from abort to arrival at perigee. Item (2) suggests, however, that a fairly low time to perigee (say 1000 minutes) can be achieved without an excessive abort propulsion requirement. For example, for a typical Symmetric class trajectory ($q_{\alpha} = q_{\beta} = 1.3$) with an excess velocity of 7.1 KM/sec, an abort velocity capability of 4 KM/sec would permit a return to Earth in 1000 minutes if abort action were taken at a distance of 3 Earth radii. At 5 Earth radii, this velocity increment would still permit return to Earth in about 5000 minutes or about 3½ days.

An additional consideration which affects the abort problem is the radius at which thrusting along the escape trajectory is completed. Except for very low thrust trajectories (e.g., electrical propulsion) or very large escape velocities, it is anticipated that burning will be completed within less than 3 Earth radii[5].

3.5 EFFECTS OF FINITE BURNING TIME

The ideal launch velocity requirements in the preceding sections have presumed that thrust would be impulsively applied. For finite burning times, the velocity requirements would be somewhat larger. Figure 3-27 has been included to illustrate this effect. The figure has been derived from the work of W. E. Moeckel [5], who has numerically integrated the appropriate equations of motion in a non-dimensional form. Values shown are applicable to a single stage vehicle with a specific impulse of 790 seconds. The thrust vector is assumed to be colinear with the velocity vector--a procedure yielding a near optimum trajectory for large hyperbolic excess velocities. The figure should not be construed to imply that high thrust to weight ratios are necessarily advisable, for this would depend upon structural considerations, and upon the fact that thrust levels will be limited for practical reasons. The necessary propellant fraction can be determined from the classical rocket equation,

$$V_{IDEAL} = g_o I_{sp} \ln (M_{INITIAL}/M_{FINAL}).$$

VELOCITY REQUIREMENT FOR ESCAPE
FROM 300 KM CIRCULAR ORBIT ABOUT EARTH

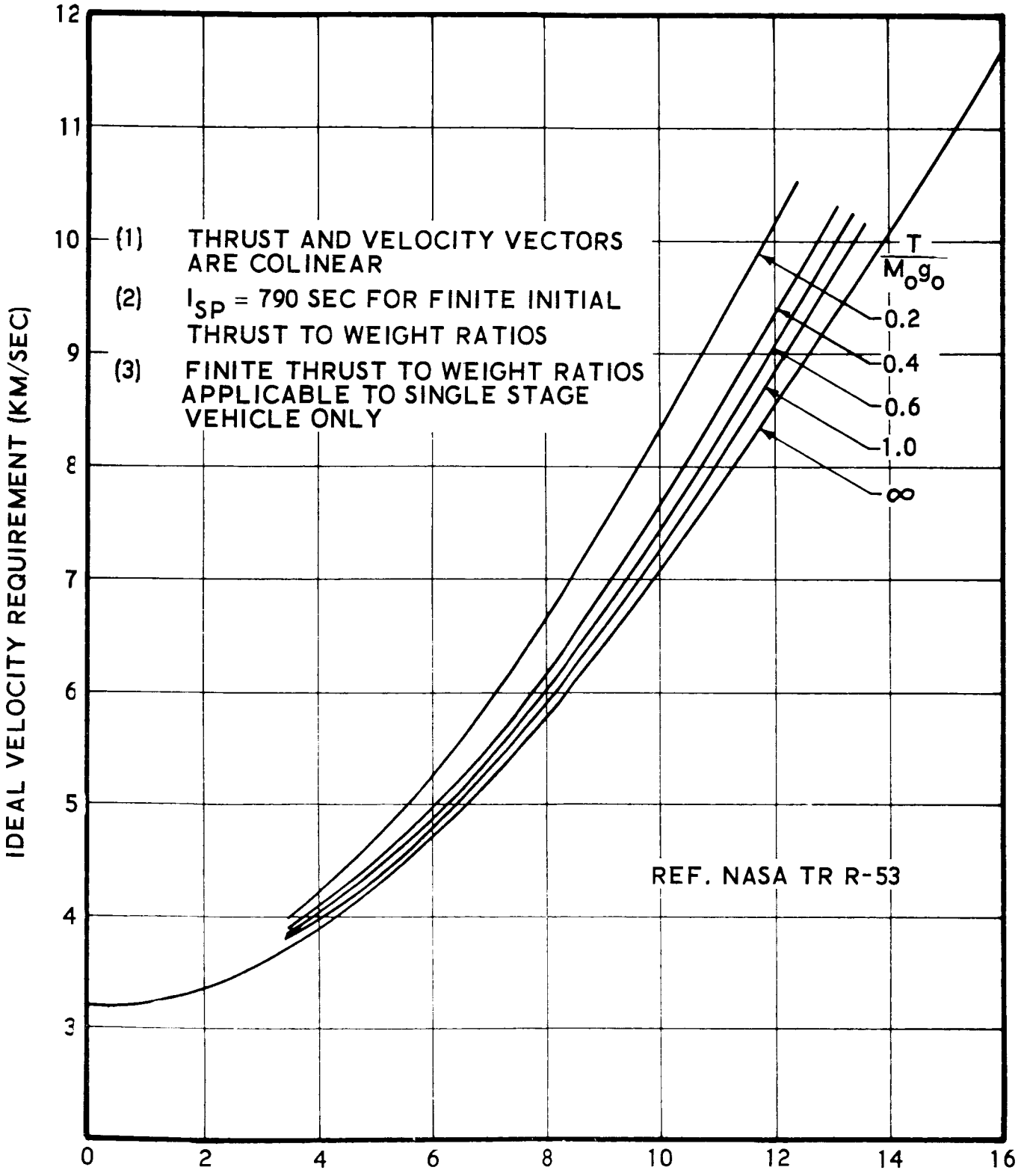

FIGURE 3-27

REFERENCES

1. G. A. Crocco, Proceedings of the VIIth International Astronomical Congress, Roma 1956, p. 201.

2. Planetary Coordinates for the Year 1960-1980 prepared by H. M. Stationary Office, London, 1958.

3. A Study of Interplanetary Transfer Systems, Lockheed Missile and Space Company Report 3-17-62-1, June 2, 1962.

4. J. M. Eggleston, "Some Abort Techniques and Procedures for Manned Spacecraft", Aerospace Engineering, November 1962.

5. W. E. Moeckel, "Trajectories with Constant Tangential Thrust in Central Gravitational Fields", NASA TR R-53, 1959.

SECTION 3
APPENDIX

PATCHED-CONIC INTERPLANETARY MISSION PROGRAM
(PCIMP)

The Patched-Conic Interplanetary Mission Program was formulated and programmed for the IBM 7090 Computer in order to permit rapid exploration and expansion of launch windows for interplanetary missions consisting of one, to a maximum of three planet flybys. The target planets may or may not be different, i.e., a mission may have more than one flyby of a given planet.

An information flow diagram for the two planet flyby mission computation is illustrated in Figure 3-28 and describes the information flow within PCIMP, omitting the additional logic available to handle the three planet encounter. Briefly, the operation of PCIMP is as follows: (Steps below correspond to circled numbers on flow diagram)

(1) A given launch date, T_{E-1}, $T_{1\rightarrow 2}$, T_{2-E}, and ϵ_{V_∞} are input to the program.

(2) $V_{\infty 1_A}$ and $V_{\infty E_D}$ are computed.

(3) $V_{\infty 1_D}$ and $V_{\infty 2_A}$ are computed for the given $T_{1\rightarrow 2}$.

(4) The quantity $|\epsilon_c|$ is compared with ϵ_{V_∞}.

(5) If $|\epsilon_c|$ is larger than ϵ_{V_∞}, $T_{1\rightarrow 2}$ is stepped accordingly until the quantity $|\epsilon_c|$ is less than ϵ_{V_∞}.

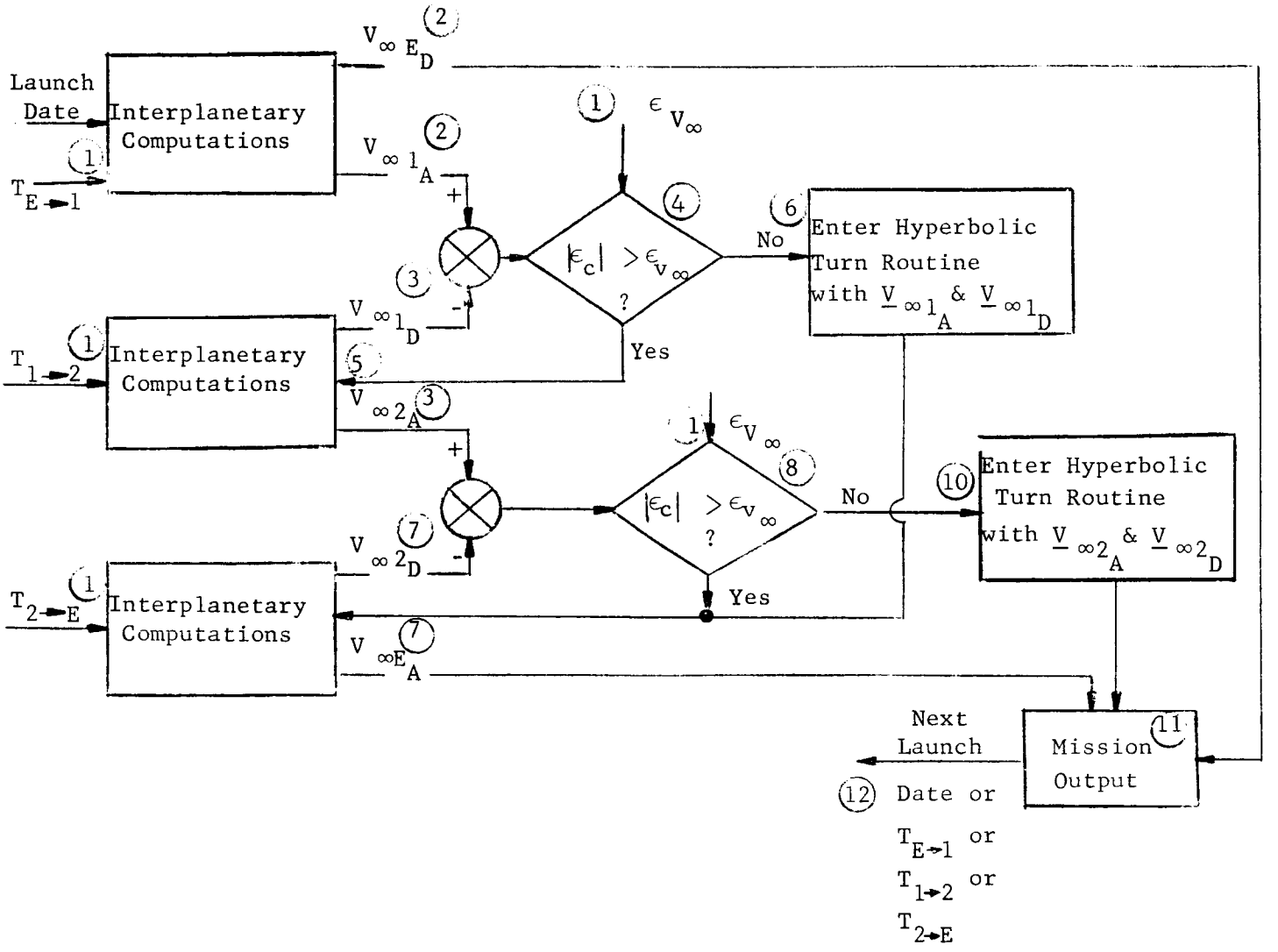

FIGURE 3-28

Information Flow Diagram for two planet flyby mission computation. (A single planet flyby or three planet flyby would be the next logical reduction or extension, respectively, of the above flow diagram.)

(6) The hyperbolic turn routine computes planetocentric quantities needed for the mission definition and output. It also computes and checks the magnitude of q to insure a safe planet flyby.

(7) $V_{\infty\ 2_D}$ and $V_{\infty\ E_A}$ are computed (functions of $T_{2 \rightarrow E}$).

(8) $|\epsilon_c|$ is compared with ϵ_{V_∞}.

(9) If $|\epsilon_c|$ is larger than ϵ_{V_∞}, $T_{2 \rightarrow E}$ is stepped accordingly until $|\epsilon_c|$ is less than ϵ_{V_∞}.

(10) This step is identical to step (6).

(11) The pertinent mission parameters are accumulated or computed and output.

(12) The above (11) steps are repeated for the next $T_{2 \rightarrow E}$, or $T_{1 \rightarrow 2}$, or $T_{E \rightarrow 1}$, or new launch date.

Figure 3-29 is a simplified logical flow diagram of PCIMP. It identifies the subroutines used in PCIMP and the necessary logic connecting them.

PCIMP permits almost an order of magnitude reduction in manpower requirements for exploring a launch window, over the semi-graphical methods previously used. In addition, the accuracy obtainable is limited only by the errors inherent to the patched conic method. The Symmetric mission launch window was verified and expanded considerably with PCIMP using only fifteen minutes of IBM 7090 time.

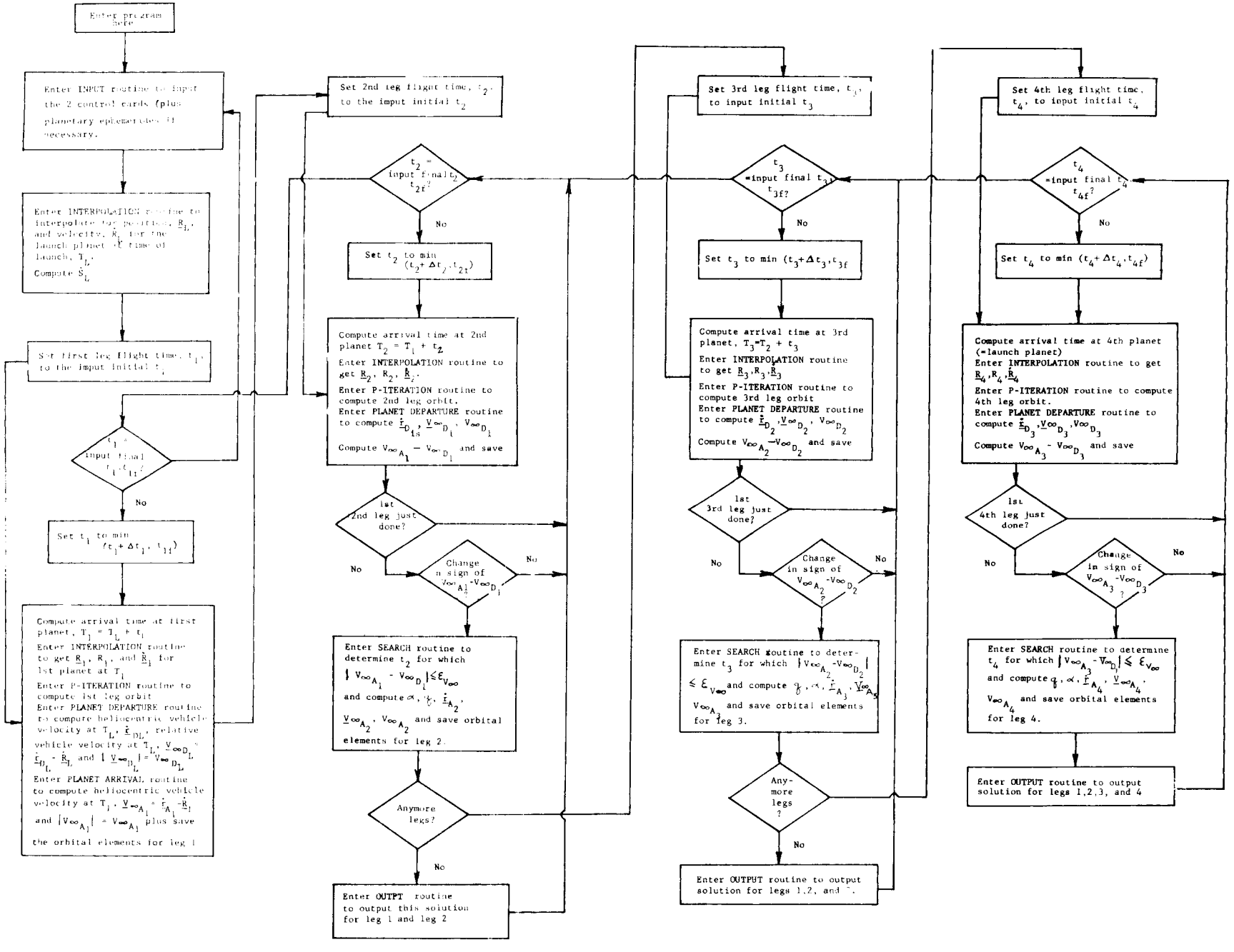
Enter program here
Enter INPUT routine to input the 2 control cards (plus planetary ephemerides if necessary.
Enter INTERPOLATION routine to interpolate for position, $\underline{R}_L$, and velocity, $\dot{\underline{R}}_L$, for the launch planet at time of launch, T_L.
Compute $\dot{S}_L$
Set first leg flight time, t_1, to the input initial t_1
t_1 = input final t_{1f}?
No
Set t_1 to min ($t_1+\Delta t_1$, t_{1f})
Compute arrival time at first planet, $T_1 = T_L + t_1$
Enter INTERPOLATION routine to get $\underline{R}_1$, R_1, and $\dot{\underline{R}}_1$ for 1st planet at T_1
Enter P-ITERATION routine to compute 1st leg orbit
Enter PLANET DEPARTURE routine to compute heliocentric vehicle velocity at T_L, $\dot{\underline{r}}_{D_L}$, relative vehicle velocity at T_L, $\underline{V}_{\infty D_L} = \dot{\underline{r}}_{D_L} - \dot{\underline{R}}_L$ and $|\underline{V}_{\infty D_L}| = V_{\infty D_L}$
Enter PLANET ARRIVAL routine to compute heliocentric vehicle velocity at T_1, $\underline{V}_{\infty A_1} = \dot{\underline{r}}_{A_1} - \dot{\underline{R}}_1$ and $|V_{\infty A_1}| = V_{\infty A_1}$ plus save the orbital elements for leg 1
Set 2nd leg flight time, t_2, to the input initial t_2
t_2 = input final t_{2f}?
No
Set t_2 to min ($t_2+\Delta t_2$, t_{2f})
Compute arrival time at 2nd planet $T_2 = T_1 + t_2$
Enter INTERPOLATION routine to get $\underline{R}_2$, R_2, $\dot{\underline{R}}_2$.
Enter P-ITERATION routine to compute 2nd leg orbit.
Enter PLANET DEPARTURE routine to compute $\dot{\underline{r}}_{D_1}$, $\underline{V}_{\infty D_1}$, $V_{\infty D_1}$
Compute $V_{\infty A_1} - V_{\infty D_1}$ and save
1st 2nd leg just done?
No
Change in sign of $V_{\infty A_1} - V_{\infty D_1}$?
No
Enter SEARCH routine to determine t_2 for which $|V_{\infty A_1} - V_{\infty D_1}| \leq \epsilon_{V_\infty}$ and compute α, γ, $\dot{\underline{r}}_{A_2}$, $\underline{V}_{\infty A_2}$, $V_{\infty A_2}$ and save orbital elements for leg 2.
Anymore legs?
No
Enter OUTPT routine to output this solution for leg 1 and leg 2
Set 3rd leg flight time, t_3, to input initial t_3
t_3 =input final t_{3f}?
No
Set t_3 to min ($t_3+\Delta t_3$, t_{3f})
Compute arrival time at 3rd planet, $T_3=T_2 + t_3$
Enter INTERPOLATION routine to get $\underline{R}_3$, R_3, $\dot{\underline{R}}_3$
Enter P-ITERATION routine to compute 3rd leg orbit
Enter PLANET DEPARTURE routine to compute $\dot{\underline{r}}_{D_2}$, $\underline{V}_{\infty D_2}$, $V_{\infty D_2}$
Compute $V_{\infty A_2} - V_{\infty D_2}$ and save
1st 3rd leg just done?
No
Change in sign of $V_{\infty A_2} - V_{\infty D_2}$?
No
Enter SEARCH routine to determine t_3 for which $|V_{\infty A_2} - V_{\infty D_2}| \leq \epsilon_{V_\infty}$ and compute γ, α, $\dot{\underline{r}}_{A_3}$, $\underline{V}_{\infty A_3}$, $V_{\infty A_3}$ and save orbital elements for leg 3.
Any-more legs ?
No
Enter OUTPUT routine to output solution for legs 1,2, and 3.
Set 4th leg flight time, t_4, to input initial t_4
t_4 =input final t_{4f}?
No
Set t_4 to min ($t_4+\Delta t_4$, t_{4f})
Compute arrival time at 4th planet (=launch planet)
Enter INTERPOLATION routine to get $\underline{R}_4$, R_4, $\dot{\underline{R}}_4$
Enter P-ITERATION routine to compute 4th leg orbit.
Enter PLANET DEPARTURE routine to compute $\dot{\underline{r}}_{D_3}$, $\underline{V}_{\infty D_3}$, $V_{\infty D_3}$
Compute $V_{\infty A_3} - V_{\infty D_3}$ and save
1st 4th leg just done?
No
Change in sign of $V_{\infty A_3} - V_{\infty D_3}$?
No
Enter SEARCH routine to determine t_4 for which $|V_{\infty A_3} - V_{\infty D_3}| \leq \epsilon_{V_\infty}$ and compute γ, α, $\dot{\underline{r}}_{A_4}$, $\underline{V}_{\infty A_4}$, $V_{\infty A_4}$ and save orbital elements for leg 4.
Enter OUTPUT routine to output solution for legs 1,2,3, and 4

FIGURE 3-29.

SECTION 4

GUIDANCE AND NAVIGATION

4.1 MODE OF NAVIGATION

The following "modus operandi" has been hypothesized as most appropriate for the EMPIRE missions.

The space navigator would be supplied an updated ephemeris by means of as suitable network of ground tracking stations. A secondary, or backup system, consisting of an on-board stellar tracker and associated auxiliary equipment will be available as the redundant system for the transit trajectory determination. This optical system would also be employed as the principal guidance sensor for the planetary approach phase as will be described later. An additional benefit would be the availability of vehicular attitude information as a redundant sensor to the attitude control system.

The mission may be expected to be initiated by the placement of the vehicle into a suitable, precomputed Earth parking orbit. Injection into the heliocentric transfer orbit will be initiated as the vehicular position and velocity vectors are appropriate to the specified initial conditions. As a consequence of the uncertainties at injection, due primarily to the errors in monitoring the thrusting phase and the errors in determining the parking orbit ephemeris, one may expect a significant variation of the nominal heliocentric orbit, hence, some mid-course maneuver would be required to redirect the vehicle onto a new nominal orbit so as to accomplish the prescribed terminal conditions, i.e., the intercept of the target planet. Again, as a consequence of the uncertainties in determining the actual vehicular heliocentric orbital parameters and the monitoring of the applied characteristic velocity during the mid-course maneuver, one would further expect some trajectory variations at the target planet. To attenuate this error we have recommended a planetary approach corrective maneuver for the EMPIRE missions.

Obviously, a full simulation study would be required for a definitive quantitative solution to the error propagations and propulsion requirements for any particular design trajectory. Aside from the fact that this would be unrealistic for the present study program one may extract some reasonable approximations from prior studies.

4.2 MIDCOURSE MANEUVER VELOCITY REQUIREMENTS

From prior studies conducted by JPL (Reference 1), it has been estimated that the midcourse maneuver for each of the several legs of the trajectory would require a corrective impulse of approximately 200 fps.

The basis for this estimate, using the data given in Table 1 of Reference 1, is contingent on the following assumed rms variations in the injection conditions:

velocity vector magnitude	4 fps
velocity vector orientation	2 milliradians
altitude variation	1 km

These assumptions may be expected to be a conservative estimate of the state of the art in the 1970-1980 period. While it is recognized that this estimate is based on the study of a particular trajectory, the total velocity capability required was found to be a relatively insignificant perturbation on the other requirements of the mission, i.e., the planetary approach maneuver. Hence the conservative estimate made of the characteristic velocity required -- 200 fps -- is expected to be representative of that required for each of the three legs of the heliocentric orbits.

4.3 VARIATION IN APPROACH CORRIDOR

An excellent report by JPL (Reference 2) has provided the basic material for the estimate of the nominal dispersion corridor at the target planet due to the variations evident during the midcourse maneuver.

Basically, the two principal sources of error, when considering a particular form of radio-command midcourse guidance system are as follows:

- errors which are developed as a result of the uncertainties in the estimate of the vehicular ephemeris, and

- errors which occur during the thrusting phase of the mid-course maneuver.

The individual contributions of these errors when projected as miss coefficients in an rms manner constitute the total trajectory variations to be expected. These contributions may be represented by the general moment matrix defined by

$$\left[H\right] = \left[A\right]\left[N\right]^{-1}\left[A\right]^{T} \qquad (4\text{-}1)$$

This moment matrix is sometimes referred to as the variance-covariance matrix (note especially References 3 and 4).

In the evaluation of the moment matrix $\left[H\right]$, the matrix $\left[A\right]$ represents the several partials relating the miss variations at the terminus to the variations in (a) the orbital parameters due to tracking uncertainties, and (b) the principal parameters of the thrusting phase, i.e., the velocity components. The matrix $\left[N\right]^{-1}$ is simply the noise matrix (or a least squares matrix as it is sometimes called) of the errors due to the particular error sources.

A quantitative evaluation of the several error sources has been developed (Reference 2) for several representative trajectories and is summarized in Table 4.1. On the basis of these studies it has been estimated that a nominal approach corridor variation of 8000 km (rms) would be realistic at each of the approaches to the target planets.

TABLE 4.1

REPRESENTATIVE FIGURES FOR THE ACCURACY*
OF MIDCOURSE GUIDANCE

Destination	Orbit Determination Miss, Mi**	ΔV Coefficient Mi/Ft/Sec	Assumed Error Ft/Sec	ΔV Miss Mi	ΔV Orientation Coefficient Mi/Deg	Assumed Error Deg	Orientation Error	Total Miss (RMS) Mi
Mars	1500	3570	1	3570	6230	1/2	3115	5000
Venus	700	1970	1	1970	3430	1/2	1715	2700

*RMS Quotations of errors with Δ V correction in the critical plane

**The uncertainty in the astronomical unit assumed as 1 part in 20,000

Reference: JPL Technical Report No. 32-28

4.4 THE PLANETARY APPROACH MANEUVER

a. Introduction

The primary problem of the approach guidance system is to make corrections in the altitude of closest approach to the target planet. Using values quoted by JPL (Reference 5) for the Mariner missions, the injection guidance errors can be expected to lead to an error on the order of 10^5 km in the altitude of closest approach. Midcourse guidance can be expected to reduce this error to on the order of 8000 km. In this study a rms error of 8000 km in the altitude of closest approach will be assumed at the start of each of the three phases of planetary approach guidance. This is thought to be a conservative estimate for the early 1970's. In particular, one is interested in determining the velocity increments which may be required at each of the planets to correct the assumed error in the altitude of closest approach. These increments will not all be equal, principally because the asymptotic approach velocities are different at each of the planets. These values are -- 8.1 km/sec near Mars, 16.3 km/sec near Venus, and 9.0 km/sec near Earth -- for the nominal Crocco orbit ($q_{\varphi} = q_{\sigma^{\prime}} = 1.1$) under consideration in this study.

The approach guidance system is assumed to be completely self-contained. The feasibility of using an optical system which measures the angles between the target planet and two judiciously selected stars, and the angle diameter of the target planet to determine the characteristics of the planetary approach trajectory has been demonstrated by workers at JPL (see References 6, 7, and 8), and by Harry and Friedlander (Reference 9) at the Lewis Research Center. These systems will be described at a later point.

b. Accuracy Requirements

The vehicle will enter the atmosphere of the Earth at approximately $\sqrt{(11.2)^2 + (9.0)^2} = 14.4$ km/sec, which is significantly greater than escape velocity, 11.2 km/sec. Chapman (Reference 10) has determined the entry corridor requirements for supercircular atmospheric entry. For the low-lift configuration assumed in this report, the allowable rms error in the altitude of closest approach to the Earth is taken as 10 km.

The necessary accuracy requirements for the altitude of closest approach to Mars and Venus are somewhat arbitrary because the vehicle simply "flies by" these planets. In these cases errors in the directions of the outgoing velocity asymptotes are especially critical. However, as will be shown presently, the errors in these asymptotes are directly related to the uncertainties in the altitudes of closest approach.

The geometry for a planetary encounter is shown in Fig. 4-1 where $\bar{v}_1$ is the approach velocity vector and $\bar{v}_2$ is the exit velocity vector. At equal distances from the planet the magnitudes of $\bar{v}_1$ and $\bar{v}_2$ are equal (this is really an approximation because the perturbation of the sun has been ignored), but the direction has been changed by an angle ψ ; that is, $\bar{v}_1 \cdot \bar{v}_2 = v^2 \cos \psi$. It is useful to recognize that ψ and the radius of closest approach q are, for practical purposes, independent of ρ_1 and ρ_2 to the points 1 and 2 when ρ_1 and ρ_2 are orders of magnitude greater than the planet radius. Then ψ and q only depend on $v_1 = v_2 = v$ and the miss distance b. The approach trajectory is assumed to be a perfect hyperbola with the mass center of the target planet at a foci. The following elementary relations hold:

$$a = \mu / v^2 , \qquad e = \sqrt{1 + \left(\frac{b}{a}\right)^2} , \qquad \psi = 2 \sin^{-1} \left(\frac{1}{e}\right) \tag{4-2}$$

where a is the semi-major axis, e is the eccentricity and μ is the product of the universal constant of gravitation and the mass of the target planet.

The principal error in the approach trajectory is in the magnitude of b. Errors in the magnitude and direction of the approach velocity vector $\bar{v}_1$ will also be present and must be detected, however, for purposes of determining the size of the velocity correction increments, the error in b is overwhelming. The reason for the large expected value ($\sim$ 8000 km) for Δb lies in the fact that Δb is essentially an error in timing. Since the mean orbital velocities of Venus, Earth and Mars are approximately 35, 30 and 24 km/sec, respectively, an error of only 1 hour in the time of arrival may lead to an error in b on the order of 10^5 km. Since the time of travel between planets in the Empire mission is on the order of 100 days, an error of 1 hour corresponds to an uncertainty of only 4 parts in 10^5. Furthermore, since the orbit planes of the planets and of the approach trajectories differ by only a few degrees, the error problem is basically a two dimensional problem.

For approach velocities to Mars, Venus and Earth greater than a few km/sec, an error in q is approximately equal to an error in b. Initially $(\Delta b/b)$ may be on the order of 1. The first approach guidance correction will make $\Delta b/b \ll 1$. Then after the first (and all subsequent) corrections

$$\Delta \psi \approx - 2 (\Delta b/b) \sin \psi \tag{4-3}$$

where b and ψ are understood to be nominal values. The above relation specifies the directional error $\Delta \psi$ in the outgoing velocity vector $\bar{v}_2$ in

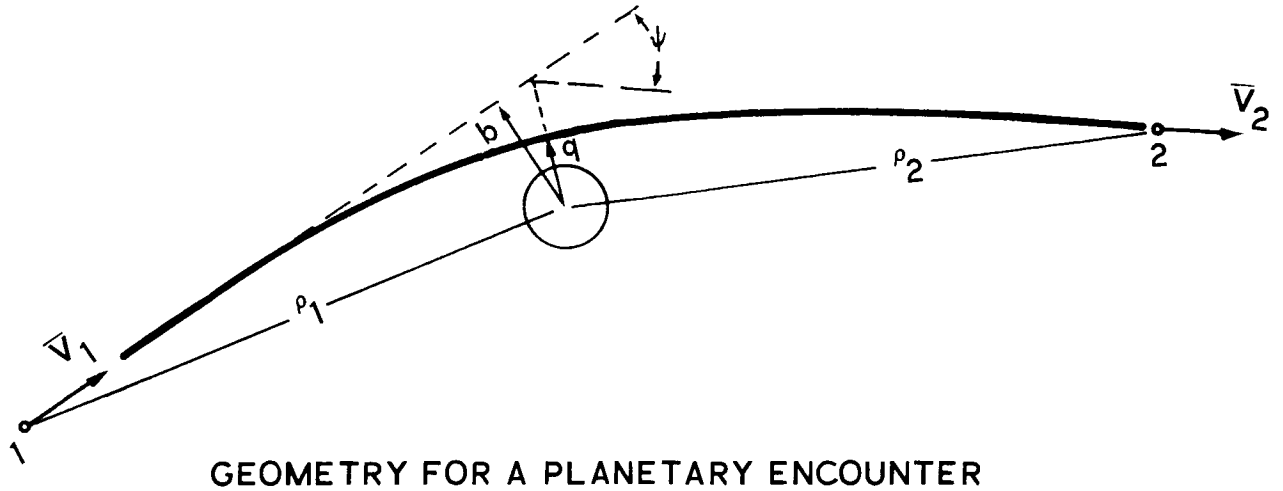

GEOMETRY FOR A PLANETARY ENCOUNTER

FIGURE 4-1

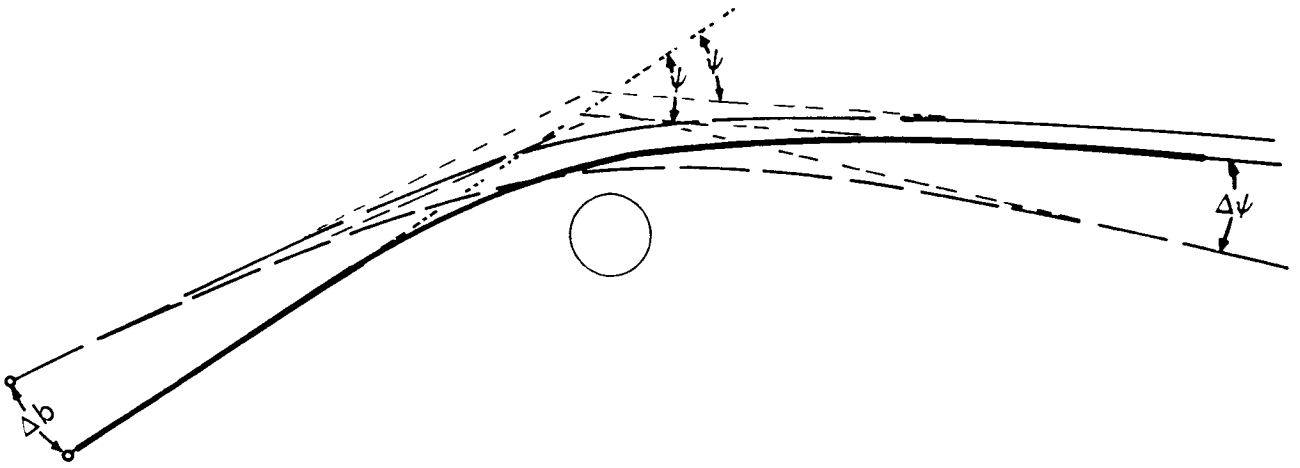

CORRECTIONS TO ORIGINAL AND NEW NOMINAL VALUES FOR MISS DISTANCE b

FIGURE 4-2

terms of the error $\Delta b \approx \Delta q$ after the last approach guidance correction has been made. Therefore $\Delta\psi$ represents an initial error to subsequent midcourse guidance phase. We will require $\Delta b \approx \Delta q$ to be less than 10 km. Then, for the typical values of ψ = 20 deg. and b = 10^4 km, we would have $\Delta \psi < .04$ deg.

Closely related to the problem of accuracy, is the question whether or not a new nominal miss distance b should be calculated after each correction. We have concluded that a new nominal should be computed in the case of the fly-by trajectories past Mars and Venus but not for the return trajectory to Earth. The geometry is shown in Fig. 4-2. The solid line denotes the nominal trajectory. The short-dashed line denotes a perfect correction to the initial nominal b while the long-dashed line denotes a perfect correction to a new nominal b, which was selected so that the corrected outgoing velocity vectory asymptote is parallel to the nominal outgoing velocity vector asymptote. It is evident that for an initial b smaller than the nominal b_0, the new nominal b_1 must be smaller than b_0, and vice versa. Clearly b_0 must be sufficiently large that $b_1, b_2, \ldots b_N$ will not have corresponding $q_1, q_2, \ldots q_N$ smaller than the planet radii (plus some margin to avoid atmospheric penetration at Mars or Venus). The main purpose for bringing up this topic is to indicate that by simply changing (slightly) the nominal b after each correction, the approach guidance problem for accomplishing a fly-by mission can be reduced to the problem of achieving a given altitude of closest approach. In other words, the fuel requirement to achieve a desired error from the nominal b is repeatedly changed by known, small amounts.

c. System Selection

The problem of determining the velocity increments needed to correct an error in the miss distance b when there are no errors in the approach guidance scheme itself is trivial. The velocity correction would be applied perpendicular to the approach velocity asymptote and at as great a distance from the target planet as possible. The actual increment Δv would be given by

$$\Delta v \approx \frac{\Delta b}{\rho} v_1 \qquad (4\text{-}4)$$

where ρ is the distance from the planet at which the correction is made, and v_1 is the magnitude of the approach velocity. An obvious limit on occurs when the perturbation of the approach trajectory hyperbola due to the mass of the sun becomes significant. In the actual case the distance from the planet at which the first correction can be applied depends upon

the accuracy with which the approach guidance scheme can determine b. Obviously it would be fruitless to attempt a correction when the uncertainty in determining b is of the same order as the maximum expected value of the Δ b residual from the midcourse guidance phase. Thus the sum of the velocity corrections made near the planet is closely related to the accuracy of the approach guidance scheme.

A number of different approach guidance schemes for determining the approach velocity trajectory relative to the target planet have been investigated by Harry and Friedlander (References 9, 11, and 12). A scheme based on the use of range, range rate and the rate of rotation about the target planet is described in (11). Such a scheme would utilize radar (or radio) and a gyroscopically stabilized reference direction. The basic disadvantage of this scheme is that the orbit determination degrades very rapidly at increasing distances from the target planet. This means that one would have to be relatively near the target planet before imparting the first correction.

Also described in (11) is a scheme based on the radar determined range and range rate data obtained at two successive points. Since this scheme is not directly capable of determining the orientation of the orbit relative to the stars, it is not especially attractive for the fly-by-hyperbolas near Mars and Venus where the orientation information is needed to insure rendezvous at the next planet. This difficulty would not be important for Earth return.

A third scheme using three successive range and angular-position measurements, obtained by means of an optical system with planet scanner and star tracker, is described in (12). Though no rates are used, accuracy is dependent upon second differences in the measured quantities.

A fourth scheme, and the one which is proposed for the Empire mission, is described in (6, 7, 8, and 9). This is an optical scheme which measures the angle diameter of the target planet and the angles between the center of the target planet and two, preselected stars at successive intervals of time. While the accuracy which can be realistically expected of this scheme is about the same as the accuracies of the other schemes mentioned at short range, the accuracy of this scheme at long ranges from the target planet is significantly greater. Since the amount of fuel expended for approach guidance corrections is closely related to the range at which the first correction is made, the fourth scheme was selected for the Empire mission.

In view of the considerable research, which has been performed at both Lewis Research Center and JPL, on the problems of approach guidance, it was decided to base the Empire approach guidance analysis on the results generated at the two NASA centers. The work performed at Lewis Research Center is documented in great detail and is considered first in this report. It will show that a basic shortcoming of the Lewis work is the restriction that the first velocity correction be performed at no greater than 100 planet radii from the target planet. This restriction leads to relatively large velocity corrections. No such restriction is made in the JPL studies and for this reason the velocity corrections are smaller. For this reason the velocity corrections for Empire are determined on the basis of the JPL model. It is interesting to note that the weight of fuel needed to perform the necessary corrections is much greater than the expected weight of the guidance components themselves.

d. Lewis Research Center Studies

Harry and Friendlander have summarized some of their results in Fig. 20 of (9). Nondimensionalized units are used throughout their report, for example, velocity is expressed in units of escape velocity for the particular planet and distance is expressed in units of planet radii. Fig. 4-3 of this report was generated from the data contained in Fig. 20 of (9) but in units more directly applicable to the Empire study.

Fig. 4-3 is a plot of the sum of the velocity corrections as a function of the asymptotic approach velocity for the three planets and for given accuracies of the star angle measurements. The following important assumptions were made:

(1) The nominal altitude of closest approach is zero. (This is conservative for the Empire mission.)

(2) The initial errors in the altitude of closest approach are equal to 2 planet radii: 12,756 km for Earth, 12,400 km for Venus and 6,620 km for Mars. (Since an 8000 km error is postulated for all three planets in the Empire study, use of Fig. 4-3 would lead to overly conservative results. Therefore, modifications will be made.)

(3) The final errors in the altitude of closest approach are less than .005 planet radii: 32 km for Earth, 31 km for Venus and 16.5 km for Mars. For values of $\sigma_{MEAS} \leq .0002$ the final errors are less than .0015 planet radii. (If $\sigma_{MEAS} \leq .0002$, the final accuracies indicated are probably sufficient for the Empire mission.)

VELOCITY INCREMENTS BASED ON DATA
GENERATED AT LEWIS RESEARCH CENTER

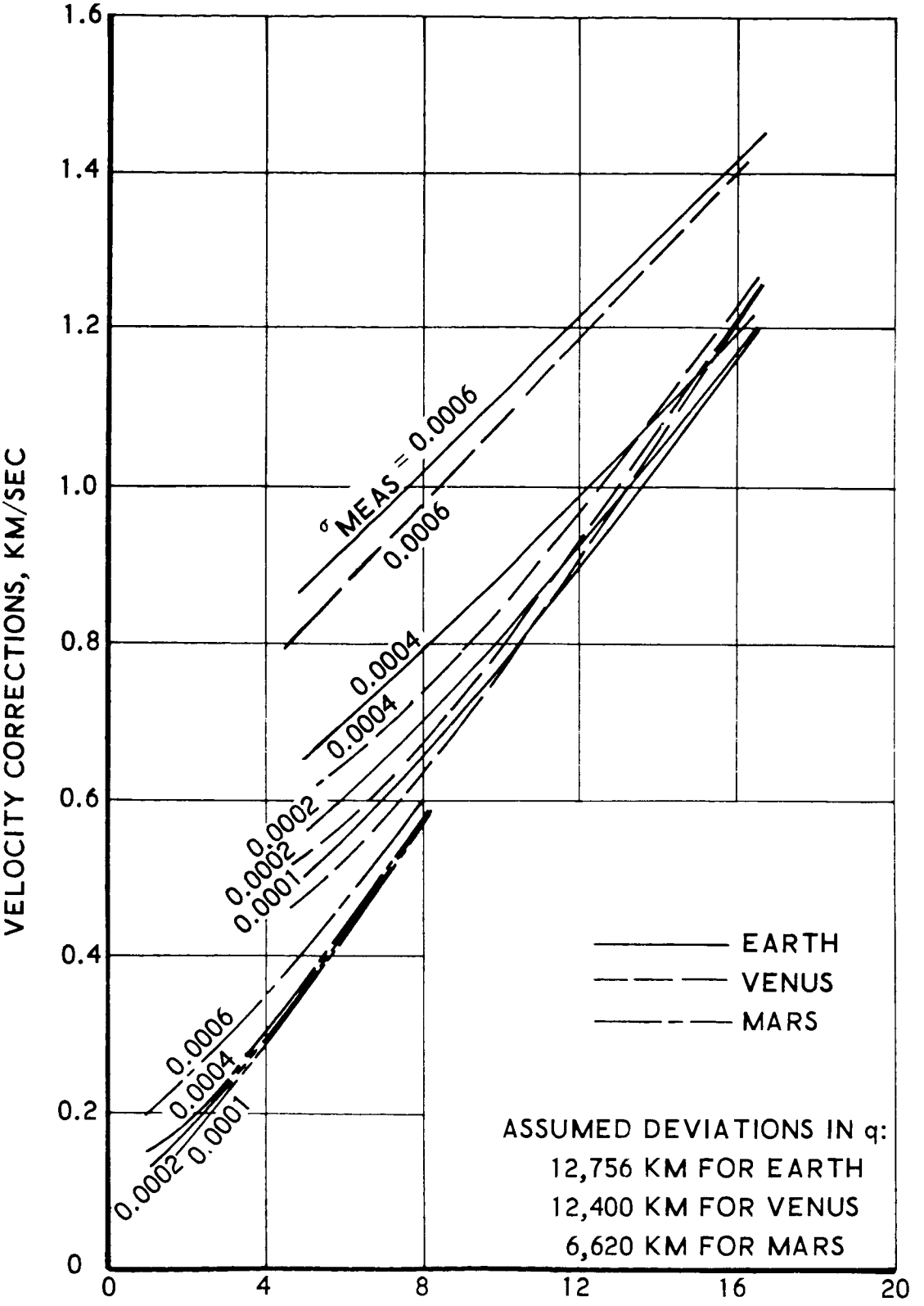

ASYMPTOTIC APPROACH VELOCITY, KM/SEC
FIGURE 4-3.

(4) The first velocity correction is made at 100 planet radii. The initial sampling interval is 15 planet radii and all subsequent sampling intervals at 10 radii. (These restrictions lead to relatively large approach guidance velocity requirements for the Empire mission.)

(5) The control of the direction of Δ v is equal to twice the instrument accuracy σ_{MEAS}.

In generating Figure 4-3 for use in the Empire study, it was necessary to extrapolate the data given in (9) to obtain those portions of the curves for Mars with values of the asymptotic approach velocities greater than approximately 4 km/sec. Since the velocity correction for Venus is expected to be dominant, small errors due to this extrapolation are not expected to be critical.

The asymptotic approach velocities are taken as 8.1, 16.3, and 9.0 km/sec for Mars, Venus and the Earth, respectively. From Fig. 4-3 we see that the curves for σ_{MEAS} = .0001, .0002, and .0004 rad are rather closely grouped. Using this figure we obtain the following velocity increments:

	Δv for σ_{MEAS} = .0002	Δv for σ_{MEAS} = .0006
Mars	.58 km/sec	.60 km/sec
Venus	1.23	1.42
Earth	.76	1.08

which must be corrected to an initial rms altitude dispersion of 8000 km rather than 2 planet radii. The appropriate corrections were determined by using Fig. 18 of (9). The corrected values are given below.

	Δv for σ_{MEAS} = .0002	Δ v for σ_{MEAS} = .0006
Mars	.65 km/sec	.67 km/sec
Venus	1.03	1.19
Earth	.64	.91

The Δv's determined were thought to be relatively large. Therefore, a study was undertaken to determine legitimate ways to reduce the velocity requirements. The following conclusions were reached:

1 A relatively small reduction in Δv can be achieved by relaxing the final corridor accuracy requirement.

2 Increasing the angle accuracy from $\sigma_{MEAS} = .0002$ rad to $\sigma_{MEAS} = .0001$ rad gives a negligible reduction in velocity requirements.

3 Increasing the range at which the first correction is made, along with an increase in the data sampling interval, would seem to reduce Δv by a sizable amount. This conclusion is based on the trend indicated in Fig. 6 of (9). It is further conjectured that conclusions 1 and 2 only hold because a fixed upper limit on the range for the first correction was made in (9).

The work (References 6-8) done at JPL seems to confirm these conclusions. The velocity increments based on the latter work are determined in the next section.

e. JPL Studies

The approach guidance scheme proposed by JPL is essentially the same as the one proposed by Lewis Research Center; that is, the orbit determination is based on the optical measurement of the planet diameter and the angles between the target planet and two stars taken at two successive times. While the Lewis scheme is restricted to operate at distances less than 100 planet radii from the target planet, the JPL scheme may commence operation at a few million kilometers from the target planet.

An approximate equation for the total velocity requirements necessary to reduce the final error in the miss distance b to a specified ratio of the initial error in b for 99% of the events on any one planetary encounter is given in (8):

$$\Delta v = v \ \sigma_{MEAS} \ C_0 \ W \left(\frac{0.475 \ \sigma_h}{\sqrt{2} \ \sigma_{h_0}} \right)^{-\frac{1}{W}} \qquad (4\text{-}5)$$

where

v	- asymptotic approach velocity
σ_{MEAS}	- rms sighting accuracy in measuring the star reference angles. (Same meaning as in (9))
C_0	- a dimensionless parameter which depends on the relative physical locations of the various fixes, the number of fixes, the correlation between the errors in the various celestial measurements, and the relative accuracy of the angular diameter measurement in comparison to the other angular measurements. A value of 1.4 is thought to be conservative based on Fig. 23 of (8).
W	- number of corrections
σ_{h_0}	- initial rms altitude dispersion, which is approximately equal to the initial error in b
σ_h	- final rms altitude dispersion

Plots of Δv as functions of v for $W = 3$, $C_0 = 1.4$, $\sigma_{MEAS} = .0002$ and .0006 rad, and $\sigma_h / \sigma_{h_0} = .04, .02, .01, .004, .002$ and .001 are shown in Fig. 4-4. The velocity corrections at the three planets assuming $\sigma_{MEAS} = .0002$ and .0006 rad, and requiring $\sigma_h / \sigma_{h_0} = .001$ are given below.

	Δv for $\sigma_{MEAS} = .0002$	Δv for $\sigma_{MEAS} = .0006$
Mars	.10 km/sec	.30 km/sec
Venus	.20	.61
Earth	.11	.33

The lower values obtained from the JPL analysis is attributed to the fact that no restriction is placed on the distance at which the first correction can be applied.

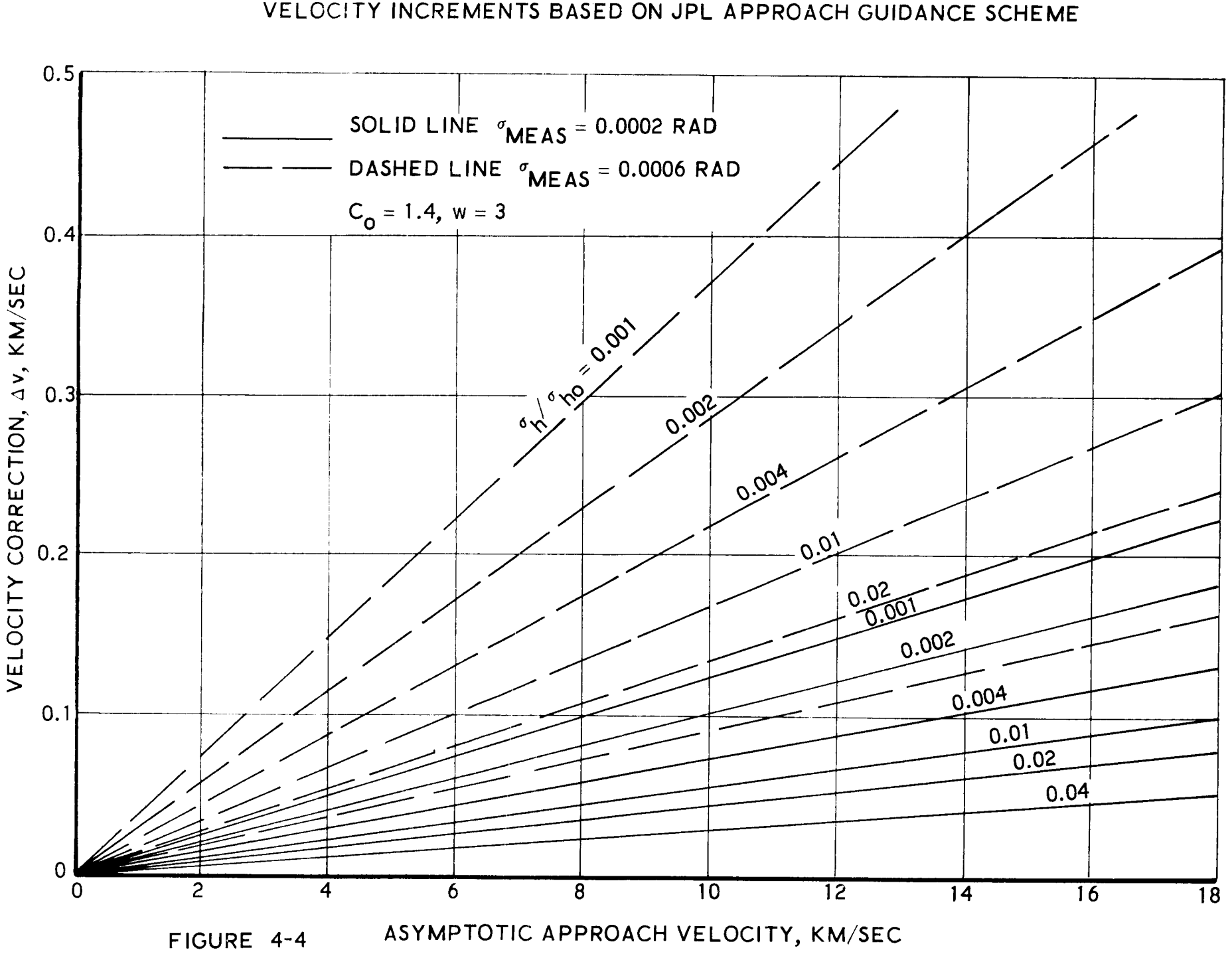
VELOCITY INCREMENTS BASED ON JPL APPROACH GUIDANCE SCHEME
SOLID LINE σ_{MEAS} = 0.0002 RAD
DASHED LINE σ_{MEAS} = 0.0006 RAD
C_o = 1.4, w = 3
σ_h/σ_{ho} = 0.001
0.002
0.004
0.01
0.02
0.001
0.002
0.004
0.01
0.02
0.04
VELOCITY CORRECTION, Δv, KM/SEC
ASYMPTOTIC APPROACH VELOCITY, KM/SEC
0.5
0.4
0.3
0.2
0.1
0
0
2
4
6
8
10
12
14
16
18

FIGURE 4-4

The design criteria selected for the EMPIRE mission, based on the results extracted from the JPL studies for σ_{MEAS} = .0002, produced a total velocity requirement of 0.41 km/sec for the planetary approach maneuver.

4.5 COMPONENT RELIABILITY

An examination of the several system components required for the guidance and control functions for the EMPIRE missions was conducted. In particular, the subsystem reliability requirements have been derived and an estimate of the present day reliability standards for each subsystem determined.

Assuming a subsystem reliability, R, of 0.95, the necessary mean-time to failure was calculated using the well known relationship

$$R = e^{-\frac{\text{operating time (t)}}{MTF}} \qquad (4\text{-}6)$$

An added measure of reliability may be achieved through the use of backup systems either by allowing complementary systems to back each other up or by multiple systems. In that event the reliability is expressed as

$$R = 1 - \left(1 - e^{-\frac{t}{MTF}}\right)^{n} \qquad (4\text{-}7)$$

where n is the number of backups.

The following components will form the principal subsystems for the EMPIRE mission.

a. Attitude Control Package

Consisting of rate and displacement gyro sensors, the subsystem will provide the required attitude signals during the thrusting phases of the injection, midcourse and planetary approach maneuvers as well as the reentry phase. Since each of the two forms of sensors may be required to provide an alternate output (rate or displacement) in addition to its principal function, the MTF of the entire attitude control package was increased by a factor of two.

b. Star Tracker and Computer

This subsystem will operate in two principal modes of operation. Basically the star tracker and computer will provide the space navigator the capability to establish the vehicular ephemeris during the heliocentric transfer and the planetary approach maneuvers.

c. Sun and Planet (Earth) Tracker

These sensors provide the orientation data required to stabilize the omni-directional antenna in the Earth-vehicle communication link.

A summary of the reliability estimates of the several subsystems is contained in Table 4.2.

TABLE 4.2

RELIABILITY ESTIMATES OF EMPIRE GUIDANCE SUBSYSTEMS

System	Operating Time (Hours)	Single System MTF (R=0.95) (Hours)	System with Standby Backup MTF (R=0.95) (Hours)	State of the Art (Hours)	Remarks
Attitude Control Package	80	3,200	Less than 1,000	Greater than 1,000	Displacement and rate gyro reference
Sun Sensor	14,500	290,000	65,900	75,000	
Planet (Earth) Sensor	14,500	290,000	65,900	75,000	Reliability may be enhanced by carrying replacement units
Star Tracker	1,450	29,000	6,590	80,000 for R=0.90	ADF proposal to STL
Guidance Communication Link	1,450	29,000	6,590	10,000 (narrow B.W.)	
Guidance Computer	1,450	29,000	6,590	10,000	Minuteman Program Spec

REFERENCES

1. Noton, A. M., "Interplanetary Post-Injection Guidance", JPL External Publication No. 653, 1959

2. Noton, A. M.; Cutting, E.; Barnes, F. L.; "Analysis of Radio-Command Mid-Course Guidance", JPL Technical Report No. 32-28, 1960

3. Johnston, T., and Onstead, E., "Orbital Error Analysis," Aeronutronic Technical Report U-1831, 1962

4. Noton, A., "The Statistical Analysis of Space Guidance Systems," JPL Technical Memorandum No. 33-15, 1960

5. JPL Research Summary No. 37-10, Vol. I, August 1, 1961, pp 39-40

6. JPL Research Summary No. 36-2, Vol. I, April 15, 1960, pp 47-48

7. JPL Research Summary No. 36-3, Vol. I, Part I, June 15, 1960, pp 63-64

8. JPL Research Summary No. 36-4, Vol. I, August 15, 1960, pp. 22-24

9. Harry, D. P., III, and Friedlander, A. L., "An Analysis of Errors and Requirements of an Optical Guidance Technique for Approaches to Atmospheric Entry with Interplanetary Vehicles", NASA TR R-102, 1961

10. Chapman, D. R., "Analysis of the Corridor and Guidance Requirements for Supercircular Entry into Planetary Atmosphere," NASA TR R-55, 1960

11. Harry, D. P., III, and Friedlander, A. L., "Exploratory Statistical Analysis of Planet Approach Guidance Schemes Using Range, Range Rate and Angle Rate Measurements", NASA TN D-268, 1960

12. Friedlander, A. L., and Harry, D.P., III, "An Exploratory Statistical Analysis of a Planet Approach - Phase Guidance Scheme Using Angular Measurements with Significant Error", NASA TN D-471, 1960

SECTION 5

EARTH REENTRY

5.1 INTRODUCTION

The purpose of this phase of the work was to compare the feasibility of various Earth reentry modes involving the higher approach velocities expected from the EMPIRE Mars-Venus flyby mission and to estimate reentry vehicle weights. Alternate reentry modes were investigated and possible use of a modified Apollo command module was considered. In addition, the trade-off in weight between aerodynamic heat shield and retro-propulsive braking was evaluated.

Three basic types of vehicles: Apollo, High L/D (Lift/Drag), and Drag Brake; were considered for reentering the Earth's atmosphere at initial velocities well above the Earth escape velocity. These vehicles were sized for the crew of six. The nominal reentry velocities for the EMPIRE Crocco and Symmetric orbits are 13.5 km/sec and 15.8 km/sec, respectively for a non-rotating Earth. At these velocities, radiative aerodynamic heating from ionized gas just ahead of the vehicle begins to predominate over the convective heating for which Mercury, Gemini, and Apollo are designed. Radiative heating is minimized if vehicles are more pointed, whereas convective heating requires blunting of the vehicle.

An Apollo-type configuration would enter with its edge tilted in the direction of travel, as shown in Figure 5-1, for two reasons. One is that of reducing the radiative heating at the expense of some increase in convective heating. The other reason for the upward pitched attitude of Apollo is that of creating lift through an offset c.g., which is necessary to achieve a satisfactory reentry corridor depth. A purely ballistic reentry at these velocities would result in the tragic incineration of the vehicle, since the heating rates would exceed thermal protection materials capability.

TYPES OF RE-ENTRY VEHICLES

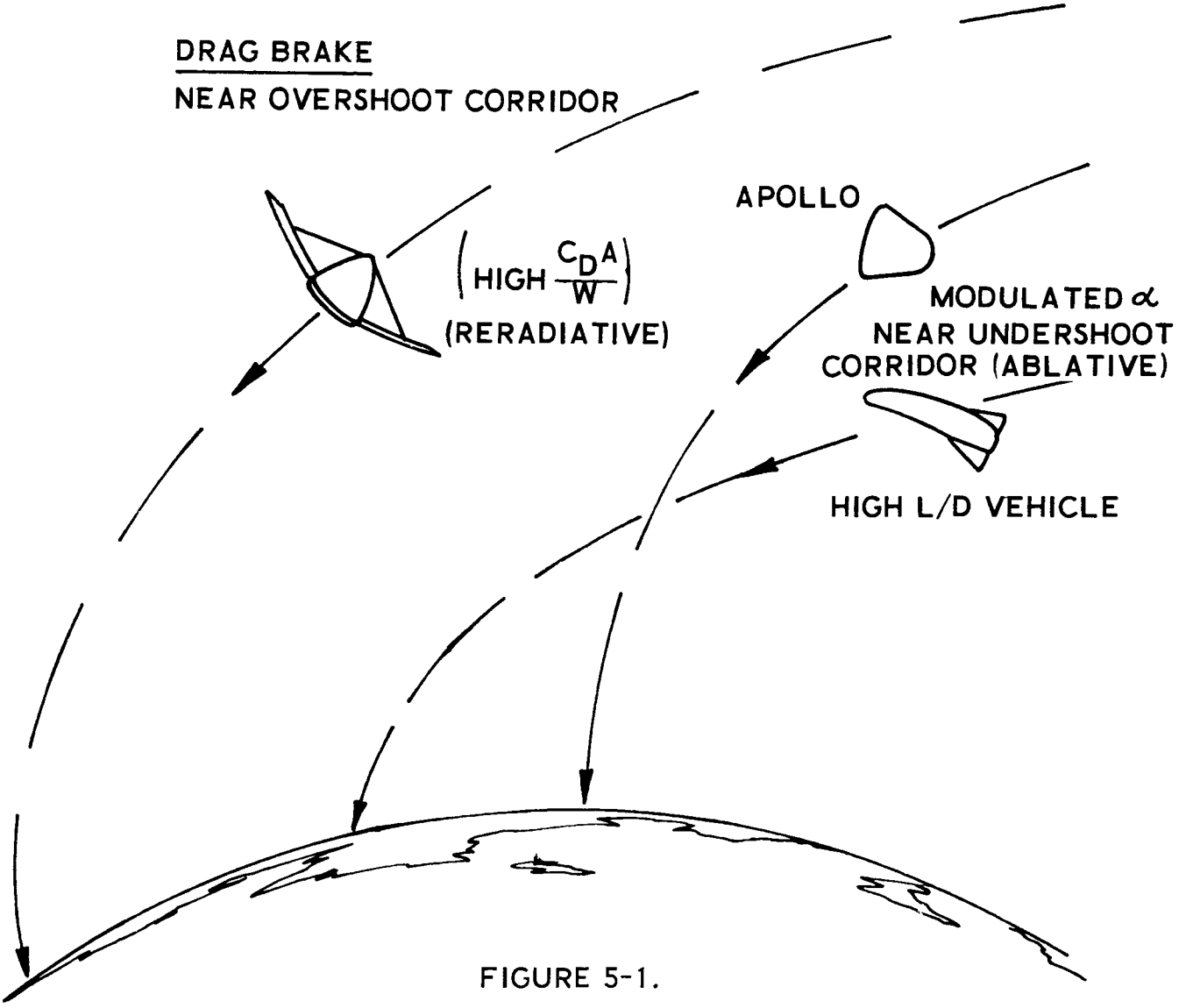

FIGURE 5-1.

A High L/D Vehicle, as shown in Figure 5-1, would open up the reentry corridor considerably. Again it would have a pointed nose to minimize the radiative heating. As was the case with Apollo, the High L/D Vehicle would initially enter at a high angle-of-attack (α) until a certain g-limit is reached. After that, the vehicle would gradually pitch forward toward zero α maintaining this constant g-limit. Beyond that it would maneuver to select a suitable landing site. This modulated lifting program would enable reentry at high velocities with a higher degree of certainty of survival, provided the crew have been preconditioned to one g or so for some time during the last few weeks of planetary flight. A 10 g maximum is experienced for approximately one minute during the reentry maneuvers investigated in this study.

An entirely different reentry concept is that of the Drag Brake system which modulates its drag near the overshoot corridor to maintain a constant g-load as well as maintaining control. Also distinctly different is the concept that the surface of the Drag Brake reradiates heat almost as rapidly as it is receiving it, whereas the other two vehicles dissipate the heat through ablation of heat shield material. One difficulty with the present Drag Brake configuration is that the highest heating is taking place on the face of the Apollo requiring a large heat shield there. Pointing the body and trimming back the brake would minimize the heating, but this would mean higher brake weight. In addition, there are the problems of effecting a satisfactory heat reradiation at these high velocities and the difficulty of controlling the flight path angle with sufficient accuracy to avoid dipping too deeply into the atmosphere or, alternately, that of skipping out when not desired.

It will be shown later that the Apollo and High L/D Vehicle cannot reenter the atmosphere much above the Crocco reentry velocity of 13.5 km/sec using only an ablative heat shield without exceeding expected ablative materials and transpiration technology. Consequently, retros are used initially to decelerate from the symmetric reentry velocity of 15.8 km/sec. The minimum total weight, including the trade-off of heat shield and retro, is determined for both the Apollo and the High L/D Vehicle. The Drag Brake is analyzed for complete aerodynamic (heat shield and reradiation) braking along the overshoot boundary.

5.2 TRAJECTORIES

Reference 1 points out the attractiveness of a direct lifting reentry into the Earth's atmosphere from a Mars mission using the modulated angle-of-attack program originally proposed by Lees, Hartwig, and Cohen in Reference 2 and subsequently studied in considerable detail by other investigators (Ref. 3-7). Luidens presents a simple closed-form solution and compares the modulated α with the constant α reentry programs in Reference 3 and compares them with other flight paths in Reference 4. He finds the modulated α program for constant g-loading gives reentry corridor depths* two to four times larger than the fixed α program and results in lower convective heating than along the other flight paths, where maximum negative lift is used on the overshoot and the modulated α is used on the undershoot. Grant (Ref. 5-7) points out the advantage of high drag on the reduction of peak g-loading and recommends modulated α reentry beginning with a maximum lift condition ($\alpha \sim 45^{\circ}$) which corresponds to high drag but is above the maximum lift-to-drag peak ($\alpha \sim 10^{\circ}$-20°) for most lifting vehicles.

Levy (Ref. 8) analyzes the modulated drag (non-lifting) reentry showing that the 10 g-limit ballistic escape reentry corridor of 7 miles can be extended to 30 miles with a ballistic coefficient change of 21. Thus, the Drag Brake configuration would modulate its drag to widen the reentry corridor and maintain constant g's, much in the same manner as the lifting vehicles modulate α (or lift). Reference 9 contains an analysis of the AVCO Drag Brake designed to enter near the overshoot boundary and to reradiate most of its heat.

Smith and Menard (Ref. 10) advocate the use of a high lift-to-drag ratio glider for reentry from parabolic speed and list three advantages: wider tolerance of reentry angle (i.e., deeper corridor), possibility of reducing maximum g-loading at the expense of a smaller but adequate corridor, and better landing site selection capability. A presupposed penalty for pointed vehicles of more severe heating no longer exists at the higher reentry velocities expected from the EMPIRE mission. This is a consequence of the predominance of radiative heating which leads to sharp leading edge vehicle designs for minimum heating.

The effect of increasing the maximum L/D ratio of the reentry vehicle on corridor depth is shown in Figure 5-2. As it turns out, retro rockets are required on both Apollo and the High L/D Vehicle for the Symmetric mission to slow them down to about 13.5 and 13.0 km/sec, respectively. (Small rockets are required for the Crocco reentry.)

* Reentry corridor depth is the fictitious difference in altitude between the overshoot and undershoot perigee points, assuming no atmosphere. The overshoot is that boundary above which the vehicle would skip out, whereas the undershoot is specified as that boundary below which the g-loading exceeds 10 or the heating becomes excessive.

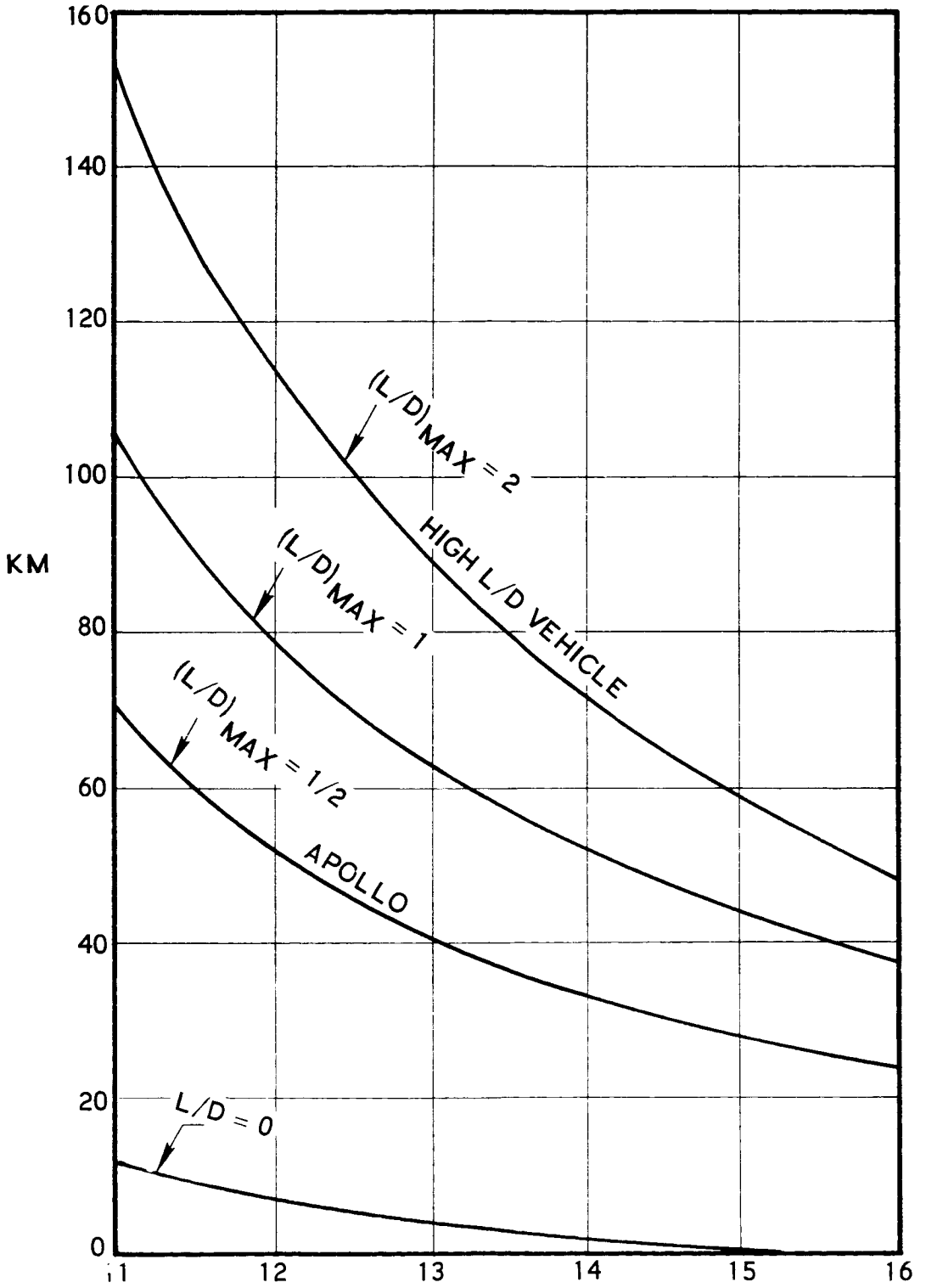
160
140
120
100
80
60
40
20
0
KM
11
12
13
14
15
16
(L/D)MAX = 2
HIGH L/D VEHICLE
(L/D)MAX = 1
(L/D) MAX = 1/2
APOLLO
L/D = 0
INITIAL RE-ENTRY VELOCITY, KM/SEC

FIGURE 5-2.

At this velocity Apollo has a total corridor potential of about 36 km in depth, whereas the High L/D Vehicle has a corridor of about 90 km. The Drag Brake effective corridor is estimated to be less than that of Apollo, primarily because it doesn't have quite the flexibility to approach as near the undershoot limit (exessive g's and heating), whereas Apollo and the High L/D Vehicle can enter near the overshoot by incorporating a relatively small amount of additional heat shield (this also would reduce the g-level).

In addition, these lift-modulating vehicles designed to enter near the undershoot are assured of Earth capture, whereas the Drag Brake could skip out should the guidance or control not function accurately. Considerable rocket impulse is necessary to minimize the tendency for a skip out. Actually, the Drag Brake appears to be more suited to skip out maneuvers, with a reentry effected upon the next pass. The High L/D Vehicle has this same capability by entering deeper near the overshoot at high α .

Chapman (Ref. 11) has developed a general nonlinear differential equation which includes the effects of gravity, centrifugal and lift forces upon an arbitrary vehicle entering an exponential atmosphere of any planet. This report includes graphical data on deceleration, velocity, convective heating,and range for satellite reentry into the atmospheres of Earth, Mars, Venus, and Jupiter. Also included are some data on atmospheric skips from parabolic reentry. Chapman (Ref. 12) has extended his analysis to twice the circular satellite initial reentry velocity, and in collaboration with Arline Kapphahn (Ref. 13), has presented an extensive set of tabular trajectory data which were very useful in the EMPIRE study.

The procedure used to obtain trajectory data on Earth reentry was first to determine perigee parameters:

$$F_p = \frac{\rho_p}{2(m/C_D A)} \sqrt{\frac{r_p}{\beta}} \qquad 5\text{-}1$$

for a range of reentry velocities and maximum L/D values for the modulated lifting entry along the undershoot from Figures 17 and 18 of Reference 12. Corresponding F_p values for the Drag Brake entering along the overshoot (L/D = 0) were obtained from Figure 13. With these F_p values and their corresponding L/D and reentry velocity ratios:

$$\bar{V}_i = V_i/V_c, \; V_c = 7.92 \text{ km/sec}, \qquad 5\text{-}2$$

use was made of the tabular data in Reference 13. Data were interpolated, and when the maximum 10 g's were reached, approximate matching with lower L/D (or $\alpha \longrightarrow 0$) data was accomplished by assuming equivalent velocity $\bar{V}$ and Z parameter (analogous to F) at that point of the trajectory:

$$Z = \frac{\rho \bar{V}}{2(m/C_D A)} \sqrt{\frac{r}{\beta}} \qquad 5\text{-}3$$

Thus mathematical solutions were matched and adjustments were made in accumulated angle, heating, range, and time.

5.3 AERODYNAMIC HEATING

Two basically different types of aerodynamic heating are of interest: convective and radiative. Convective laminar heating predominates at the lower supercircular reentry velocities and is given by Chapman (Ref. 12) proportional to $\sqrt{\rho}\ V^3\ \sqrt{C_B/R}$*. Turbulent heating is not significant above 30 km altitude where convective laminar and radiative heating predominate. Radiative heating has been related to air density, velocity and nose radius in proportion to $\rho^{1.7}\ V^{21.2}\ R$ by Wilkinson (Ref. 14)**.

Recently, Scala (Ref. 16) has developed a theoretical model involving a four component gas which leads to a convective heating rate at parabolic velocity about twice that predicted by Fay and Riddell (Ref. 17) or Wilkinson (Ref. 14)***. There is a debate on now as to the accuracy of Warren's (Ref. 16) experimental verification of Scala's theory. Should the ionization prove to be experimentally evident as professed in Reference 15, this could have the effect of more than doubling the convective heat transfer obtained by Chapman at velocities above parabolic. However, radiative heating would still predominate as velocities approached twicecircular velocity.

---

* A mass ballistic coefficient: $C_B = m/C_D A$, is used throughout the analysis and referred to simply as the ballistic coefficient.

** Lovelace (Ref. 15) gives a similar form with a 19.5 power law on velocity such that his radiative heating matches Wilkinson's at about 13.5 km/sec reentry.

*** British units are used throughout this section rather than mks in order to maximize the utility of all the data which appears in British units.

In the discussion to follow, use is made of the heating at the stagnation point. The variation in heating away from the stagnation point for both convective and radiative heating is shown in Figure 5-3 for a simple hemisphere-cylinder body. Two-dimensional leading edge effects and angle-of-attack shifting of the heat load onto the underside can be inferred from wind tunnel tests and simplified aerodynamic concepts.

Chapman (Ref. 12) has related the maximum stagnation point convective heating rate over a wide range of reentry conditions as follows:

$$\dot{q}_{c_{max}} = 630\sqrt{C_B/R}\ \ \bar{q}_{max} \quad (Btu/ft^2\text{-sec}) \qquad 5\text{-}4$$

where

$$\bar{q}_{max} \doteq \frac{(0.9\ \bar{V}_i)^2\sqrt{g_{max}}}{\sqrt{30}\left[1 + (L/D)^2\right]^{1/4}} \qquad 5\text{-}5$$

showing a velocity-squared dependence as well as the variation with maximum g's and maximum vehicle lift-to-drag ratio. The nose radius and ballistic coefficient dependencies remain the same. Chapman (Ref. 12) gives a similar relationship for total convective heating absorbed during the supercircular portion of the reentry (by far the largest amount):

$$Q_c = 17{,}000\ \sqrt{C_B/R}\ \ \bar{Q}, \quad (Btu/ft^2) \qquad 5\text{-}6$$

where

$$\bar{Q} \doteq \frac{\sqrt{30}\ (\bar{V}_i^{\,3})\left[1 + (L/D)^2\right]^{1/4}}{4\ (3/4)\sqrt{g_{max}}} \qquad 5\text{-}7$$

showing the $V^3\ \sqrt{C_B/R}$ dependence indicated before as well as an opposite effect of g_{max} and L/D compared to that on $\dot{q}_{c_{max}}$.

Thus, in summary, the convective heating at the stagnation point can be related to three basic parameters* by:

$$\dot{q}_{c_{max}} = K_1\ \bar{V}_i^{\,2}\ \sqrt{C_B/R} \quad (Btu/ft^2\text{-sec}) \qquad 5\text{-}8$$

* $\bar{V}_i$ = initial reentry velocity/(7.92 km/sec), $C_B = m/C_D A$ ($lb\text{-}sec^2/ft^3$), R in feet.

HEAT TRANSFER DISTRIBUTION FROM STAGNATION POINT

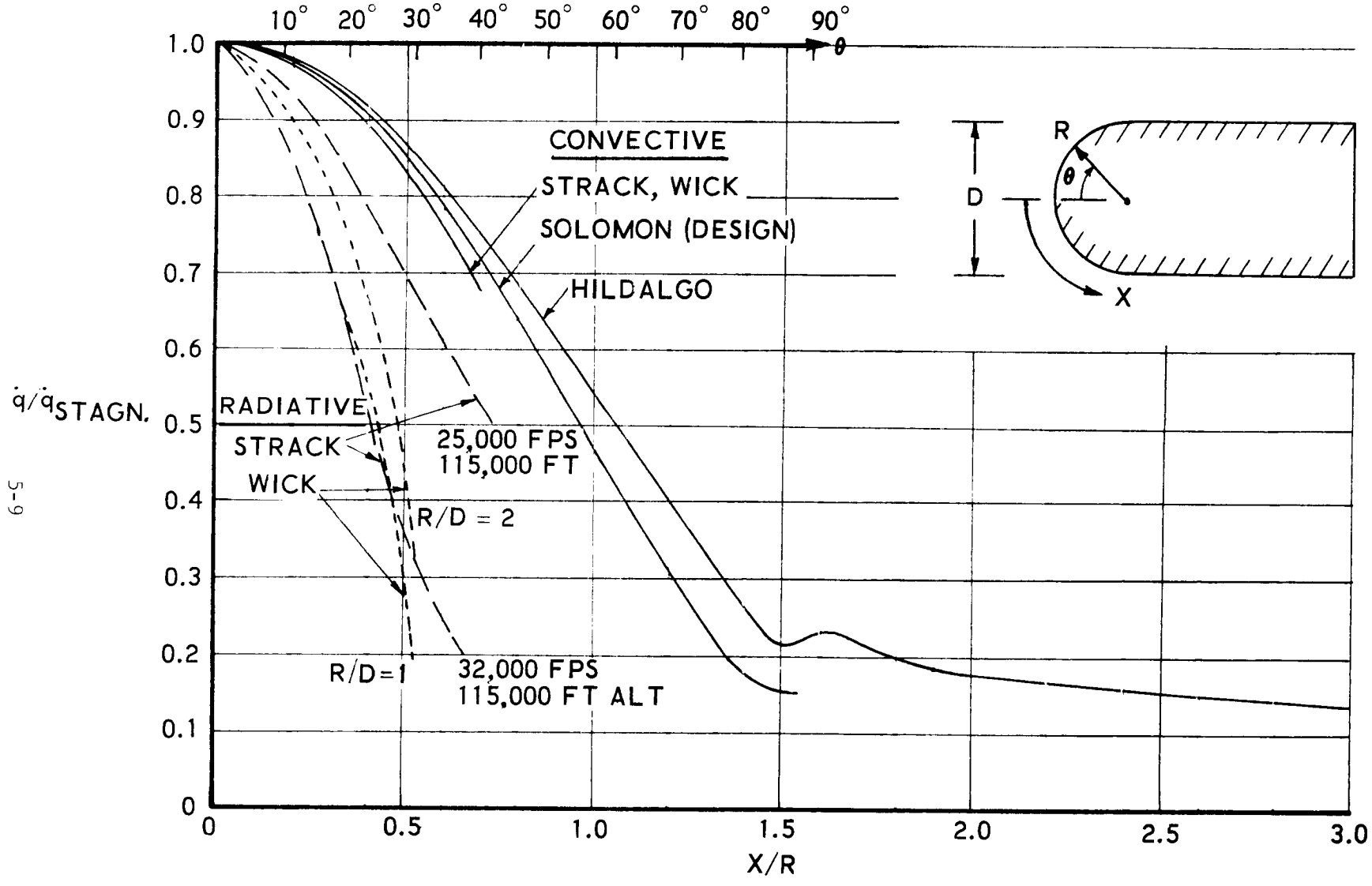

FIGURE 5-3.

$$Q_c = K_2 \bar{V}_i^3 \sqrt{C_B/R} \quad (\text{Btu/ft}^2) \qquad 5\text{-}9$$

where	Apollo (2-D)	High L/D Vehicle	Drag Brake
K_1	250	250	250
K_2	6,500	13,000	7,300

Maximum g-loading is 10, and $(L/D)_{max}$ is 0.5, 2 and zero for the above vehicles, respectively. The coefficients, K_1 and K_2, were actually obtained from empirical fitting of reentry trajectory data interpolated from data in Chapman and Kapphahn (Ref. 13), where Apollo and the High L/D Vehicle entered along undershoot boundaries at their respective L/D values (modulated) and the Drag Brake entered at zero L/D along the overshoot boundary.

The radiative heating at the stagnation point also can be related to the three basic parameters.*

* The equivalence of C_B and ρ can be argued by assuming the following constant under only a scaled change in vehicle size (principle C_B variation source):

$$F_P = \frac{\rho_p}{2 C_B} \sqrt{\frac{r_p}{\beta}} = \text{constant (fixed by Ref. 12)} \qquad 5\text{-}10$$

where the radius from Earth center, r_p, and the atmospheric decay parameter, β, remain nearly constant. Extension to ρ, in general not at the perigee point, can be inferred from:

$$Z = \frac{\rho \bar{V}}{2 C_B} \sqrt{\frac{r}{\beta}} = \text{constant (point-by-point)} \qquad 5\text{-}11$$

where $\bar{V}$ differs only a small amount during the initial phase of reentry for the two differently sized vehicles.

$$q_{r_{max}} = K_3 C_B^{1.7} V_i^{21.2} R \quad (Btu/ft^2\text{-sec}) \qquad 5\text{-}12$$

$$Q_r = K_4 C_B^{1.7} V_i^{21.2} R \quad (Btu/ft^2) \qquad 5\text{-}13$$

where

	Apollo (2-D)	High L/D Vehicle	Drag Brake
K_3	0.090	0.003	0.0023
K_4	1.700	0.055	0.042

These relationships follow from Wilkinson (Ref. 14) and the numerical coefficients result again from empirical fitting of velocity and density data, assuming the $^{1.7}\ V_i^{21.2}$ proportionality.

The Apollo stagnation region is considered as a two-dimensional cylinder which reduces the total convective heating through both the dimensionality change as well as a reduced L/D effect (these effects counteract each other in the case of convective heating rate leaving K_1 unchanged). More than an order of magnitude increase in radiative heating is expected when changing from a three- to a two-dimensional leanding edge. The somewhat smaller coefficients for the Drag Brake are a consequence of entering along the overshoot rather than the undershoot boundary.

Some additional simplifications were found to be reasonable for estimating thermal protection system capability and the consequent heat shield weights. The first was to limit the total heat rate (convective plus radiative) at the stagnation point to ten thousand Btu/ft^2-sec which seems to be a realistic ablative (plus transpiration) materials technology limitation for a pyrolytic graphite* in the 1970 time period.

$$\dot{q}_{T_{max}} = \dot{q}_{c_{max}} + \dot{q}_{r_{max}} \leq 10^4 \quad (Btu/ft^2\text{-sec}) \qquad 5\text{-}14$$

Using the maximum heat rate possible at the stagnation point results in the lightest total heat shield.

The second simplification is the approximate ablative heat shield area density shown to be proportional to the two-thirds power of the total heat at any point on the vehicle.

* Or phenolic and fiber or other materials.

$$\rho \doteq 0.0112 \quad Q_T^{2/3} \qquad 5\text{-}15$$

Also, the radiative component of the total heat is concentrated quite close to the stagnation point so that it can be neglected in estimating the total heat shield weight (except for the case of the blunt face forward on the Drag Brake).

$$Q_T = Q_C \quad \text{(except at stagnation point)} \qquad 5\text{-}16$$

There remains the task of estimating the distribution of total convective heat over the vehicle which is dependent upon the stagnation convective magnitude, the angular distance from the stagnation point, the angle of attack and the vehicle shape:

$$Q_c = F\ (Q_{st},\ \theta,\ \alpha\ ,\ \text{Shape}) \qquad 5\text{-}17$$

The variations of heating rates around the body surface away from the stagnation point are shown in Figure 5-3. The data presented are from some of the most recent summaries (Ref. 18-21). There is close agreement among the authors on the convective heating distribution. Hildalgo (Ref. 19) extends his data beyond the others showing a very slow decay along the cylinder. Hildalgo also gives a comparative turbulent heating rate distribution which more than doubles the stagnation heating, but it appears much later than the laminar and radiative peaks, and consequently is negligible. Strack (Ref. 20) also shows the radiative heating distribution for two reentry velocity conditions, whereas Wick (Ref. 21) gives the effect of overall vehicle geometry on the radiative distribution.

5.4 THERMAL PROTECTION SYSTEMS

The thermal protection systems most promising for an aerodynamic deceleration along the undershoot reentry corridor appear to be the ablative types,* possibly including some transpiration (or film) cooling or an auxiliary internal heat sink system at the stagnation point.

---

* Some of the candidates are pyrolytic graphie, phenolic nylon and other derivatives.

The significant heating parameters for estimating ablative heat shield weight requirements are:

Q = total heat absorbed during flight (at stagnation point),

$\dot{q}_{max}$ = maximum heating rate (at stagnation point), and

$\bar{t}$ = effective duration = $\frac{2Q}{\dot{q}_{max}}$ (triangular pulse)

Table 5.1 summarizes the stagnation point heating conditions for the three types of reentry vehicles which result from further considerations yet to be discussed. Apollo and the High L/D Vehicles are first decelerated from the symmetric planetary orbit return by retros and enter along the undershoot corridor, whereas the Drag Brake absorbs all the energy along the overshoot corridor.

TABLE 5.1

STAGNATION POINT HEATING FOR REENTRY VEHICLES

	$\dot{q}_{T_{max}}$ (Btu/ft^2-sec)	Q_T (Btu/ft^2)	$\bar{t}$ (sec)
Apollo	10^4	2.27×10^5	45
High L/D	10^4	3.70×10^5	74
Drag Brake	10^4	1.65×10^5	33

Anderson and Swann (Ref. 22) have correlated the feasible types of thermal protection systems with maximum heating rate and total heat load. Figure 2 of their report suggests the above reentry vehicles require systems which border on absorption and ablation. (An ablative type system is being considered (Ref. 23) for Apollo under the present lunar program.)

Since the above vehicle heating conditions exceed Figure 2 of Reference 22, the results of this study are only approximate. This is an area for future studies involving simulated heating tests at these higher rates and loadings on the more promising materials, including such backup systems as transpiration cooling, film cooling, and internal heat sink systems of both the passive or active (liquid circulation) type.

Some preliminary estimates of ablative type heat shield weights are available from Reference 23 stemming from the Lunar Apollo vehicle, also from Reference 24 and most recently from Reference 25. The latter reference is a comprehensive review of the thermal protection state-of-the-art as related to materials, and in particular, Figure 11 in this reference is quite useful, since it relates the various types of thermal protection to the maximum heating rate and the effective time duration. Reference 26 also reviews the subject but not as inclusive as the above.

5.5 VEHICLE CONFIGURATIONS

The aerothermodynamic equations previously given are applied to derive minimum heat shield weights for the three basic reentry vehicles: Apollo, High L/D, and Drag Brake. Heat shield thickness distributions based upon the data of Figure 5-3 are determined for each vehicle taking into account shape, angle-of-attack and distance from the stagnation point. The optimum stagnation point radii are determined for the minimum total vehicle weight, including heat shield and retro weights.

a. Apollo

An Apollo type vehicle sized to contain a crew of six men is shown in Figure 5-4. The heat shield area density distribution is shown where it is decreased to one-half the stagnation value at the upper corner (since the blunt face effectively is a flat-plate). On the underside of the vehicle, which is exposed to angle-of-attack heating, an average thickness is taken as one-fifth the stagnation thickness and one-tenth at the top (these surfaces effectively are cylinders). The total heat shield weight is estimated to be 150 times the convective stagnation area density, and is related to reentry velocity ratio, mass ballistic coefficient and nose radius (2-dimensionally) through the use of the formulas previously given.

$$W_{HS} \doteq 150 \; \rho_{st}^{c} = 927 \; \bar{V}_i^{2} \; C_B^{1/3} \; R^{-1/3} \qquad 5\text{-}18$$

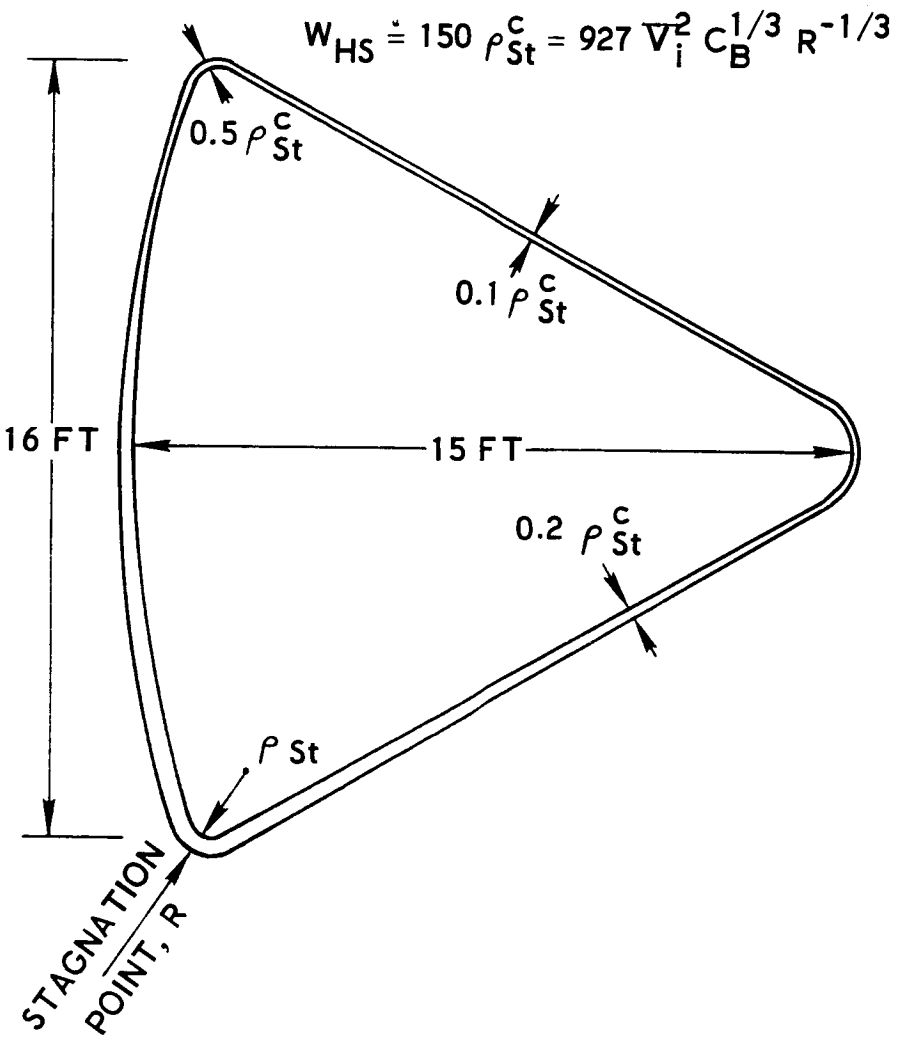
$W_{HS} \doteq 150\ \rho^{c}_{St} = 927\ \overline{V}_i^2\ C_B^{1/3}\ R^{-1/3}$
$0.5\ \rho^{c}_{St}$
$0.1\ \rho^{c}_{St}$
16 FT
15 FT
$0.2\ \rho^{c}_{St}$
ρ_{St}
STAGNATION POINT, R

FIGURE 5-4.

where

ρ_{st}^{c} = area density of heat shield at the stagnation point required for the convective heating component (lb/ft^2).

$\bar{V}_i$ = initial reeentry velocity/circular velocity (=7.92 km/sec).

C_B = $\sqrt{\bar{C}_D A}$ ($lb\text{-}sec^2/ft^3$)

R = stagnation point radius (ft)

$\bar{C}_D = \frac{1}{T}\int_0^T C_D(t)dt$

Equation 5-18 neglects the heat shield weight required for radiative heating which is small relative to the total convective heating requirements. Figure 5-3 demonstrates how the radiative component is concentrated in the region of the stagnation point, particularly for small nose radii as are being considered here.

The radiative heating influences the configuration design through the maximum total heating rate which can be tolerated at the stagnation point; given by equation 5-14, using equations 5-8 and 5-10.

$$\dot{q}_{T_{max}} = 250\ \bar{V}_i^{\,2}\sqrt{C_B/R} + 0.090\ C_B^{\,1.7}\ \bar{V}_i^{\,21.2}\ R \leq 10^4 \qquad 5\text{-}19$$

Thus, the job remains to minimize the heat shield weight given by equation 5-18 with the side condition given by the equality in equation 5-19. A minimum total heat shield weight is realized when maximum heat shielding capability is used at the stagnation point (represented by the equality), since this minimized ρ_{st}^{c} in equation 5-18. The optimum trade-off between radiative and convective heating is determined primarily by the nose radius, R, which will be chosen subsequently by a minimum total weight condition

The initial reentry velocity ratio, $\bar{V}_i$, could be specified now for either the Crocco ($\bar{V}_i = 1.7$) or symmetric ($\bar{V}_i = 2$) cases, however, a subsequent trade-off is to be made between heat shield weight and retro weight, so that a range of $\bar{V}_i$ values will be investigated (in addition, it will be shown that the symmetric all-aerodynamic reentry is beyond anticipated ablative materials capability, thus necessitating a retro).

Now that a vehicle size is fixed for six men in Figure 5-4, the mass ballistic coefficient, C_B, can be reduced to total vehicle weight, given $\bar{C}_D$.

$$\bar{C}_D = \frac{1}{100}\left[20(1) + \int_{20}^{60} C_D(t)\,dt + 40(1.4)\right] = 1.27 \qquad 5\text{-}20$$

$$C_B = \frac{W}{(32.2)(1.27)(64\,\pi)} = 1.22 \times 10^{-4} W \qquad 5\text{-}21$$

The total vehicle weight is composed of heat shield, structure and internal equipment or payload.

$$W = W_{HS} + W_{ST} + W_{PL} = W_{HS} + 2{,}300 + 7{,}000 \text{ (lb)} \qquad 5\text{-}22$$

where structure is 4 lb/ft^2 and payload is 7,000 lb.

Consequently, the unknowns C_B and W_{HS} are replaced by factors of W, and equation 5-18 is substituted into equation 5-19.

$$W = 46.3\,\bar{V}_i^{\,2}\,W^{1/3}\,R^{-1/3} + 9{,}300 \qquad 5\text{-}18'$$

$$\dot{q}_{T_{max}} = 2.76\,\bar{V}_i^{\,2}\,W^{1/2}\,R^{-1/2} + 2.067 \times 10^{-8}\,\bar{V}_i^{\,21.2} W^{1.7} R=10^4 \qquad 5\text{-}19'$$

Eliminating R:

$$0.875 \times 10^{-6}\,\bar{V}_i^{\,(-1)}(W-9{,}300)^{3/2} + 2.05 \times 10^{-7}\bar{V}_i^{\,2.72} W^{2.7}(W-9{,}300)^{-3} = 1$$

5-23

Given a range of values for $\bar{V}_i$, then total vehicle weights can be found from equation 5-23. These are listed in Table 5.2 along with the corresponding heat shield weights, nose radii, and ballistic coefficients.

TABLE 5.2

APOLLO AERODYNAMIC VEHICLE PARAMETER VALUES

$\bar{V}_i$	W (lb)	W_{HS} (lb)	R (ft)	C_B (slugs/ft^2)
1.6	11,170	1,870	2.85	1.36
1.65	11,940	2,640	1.30	1.46
1.7	13,180	3,880	0.54	1.61
1.75	15,280	5,980	0.20	1.86

b. High L/D Vehicle

A reentry vehicle, with a maximum hypersonic L/D of 2, and its heat shield distribution are shown in Figure 5-5. The aerodynamic controls which are indicated come into action after initial jet control, and are included only for purposes of estimating their weights and shield requirements. Extensive control studies are required to further define their configuration. The vehicle has an internal volume of about a thousand cubic feet similar to the previous Apollo command module. A heat shield weight of only about 82 times the stagnation point shield area density is required. (This is a little over one-half the Apollo coefficient given in equation 5-18, because of the elimination of the blunt Apollo face.)

$$W_{HS} \doteq 82 \rho_{st}^{c} = 510 \bar{V}_i^{2} C_B^{1/3} R^{-1/3} \qquad 5\text{-}24$$

The corresponding heating rate limitation from equations 5-8, 5-10, and 5-14 is:

$$\dot{q}_{T_{max}} = 250 \bar{V}_i^{2} \sqrt{C_B/R} + 0.003 C_B^{1.7} \bar{V}_j^{21.2} R \leq 10^4 \qquad 5\text{-}25$$

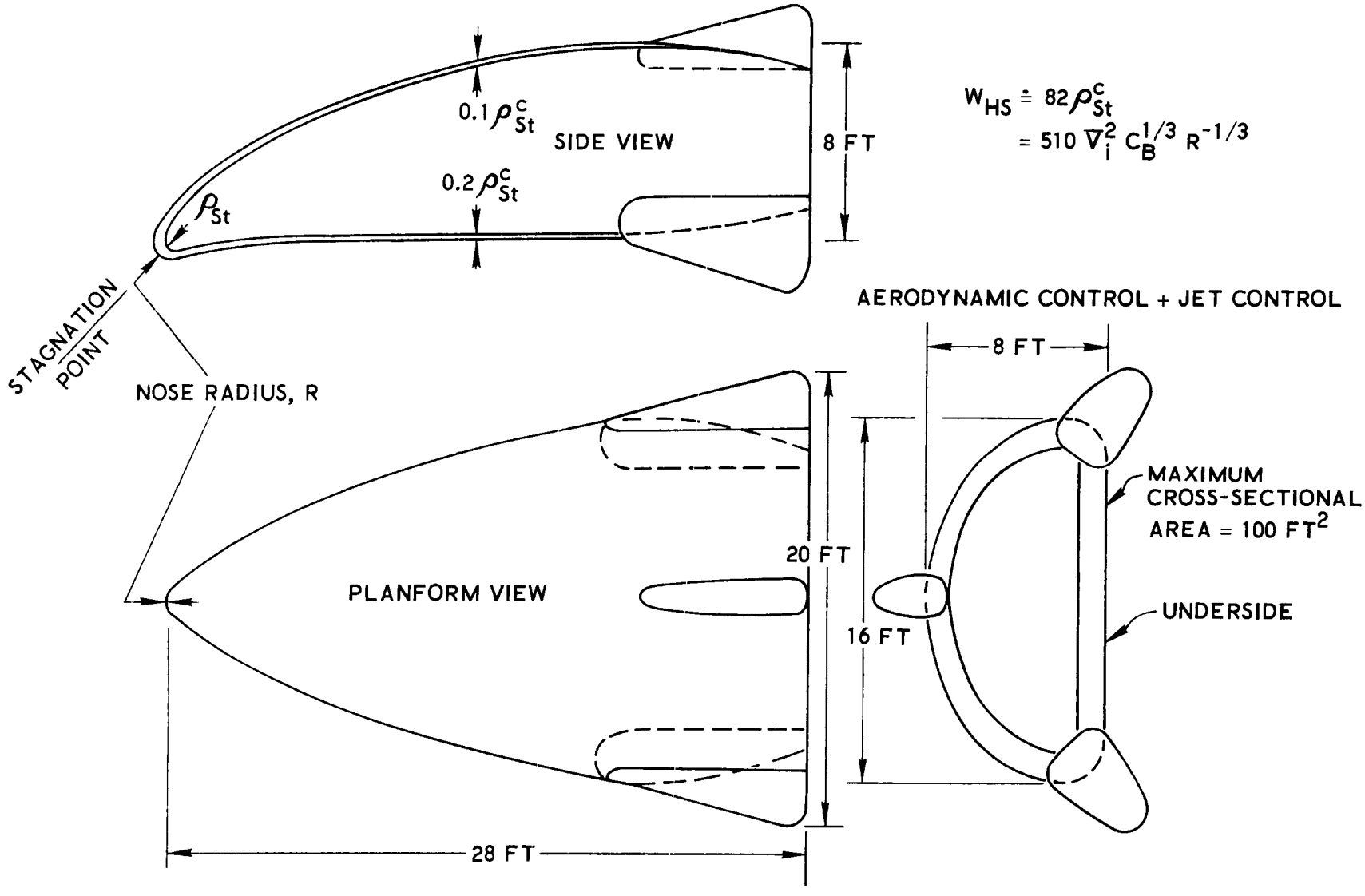
$W_{HS} \doteq 82 \rho_{St}^{c}$
$= 510\ \overline{\nabla}_i^2\ C_B^{1/3}\ R^{-1/3}$
$0.1 \rho_{St}^{c}$
SIDE VIEW
8 FT
$0.2 \rho_{St}^{c}$
ρ_{St}
STAGNATION POINT
NOSE RADIUS, R
AERODYNAMIC CONTROL + JET CONTROL
8 FT
MAXIMUM CROSS-SECTIONAL AREA = 100 FT^2
20 FT
PLANFORM VIEW
16 FT
UNDERSIDE
28 FT

FIGURE 5-5.

and the configurational relations (analogous to equation 5-21 and 5-22) are:

$$C_B = 0.932 \times 10^{-3} W \qquad 5\text{-}26$$

$$W = W_{HS} + W_{ST} + W_{PL} = W_{HS} + 2{,}800 + 7{,}000 \text{ (lb)} \qquad 5\text{-}27$$

so that the final relationship involving initial velocity and total weight becomes:

$$2.245 \times 10^{-6} \bar{V}_i^{(-1)} (W-9{,}800)^{3/2} + 2.64 \times 10^{-7} \bar{V}_i^{27.2} W^{2.7} (W-9{,}800)^{-3} = 1 \qquad 5\text{-}28$$

Table 5.3 shows the total vehicle weights resulting from a range of reentry velocity ratios, along with some of the other parameter values.

TABLE 5.3

HIGH L/D AERODYNAMIC VEHICLE PARAMETER VALUES

$\bar{V}_i$	W (lb)	W_{HS} (lb)	R (ft)	C_B (slugs/ft^2)
1.55	11,390	1,590	4.78	10.6
1.60	12,095	2,295	2.05	11.3
1.62	12,450	2,650	1.48	11.6
1.65	13,245	3,445	0.75	12.3
1.68	14,550	4,750	0.38	13.6
1.69	15,580	5,780	0.22	14.5

c. Drag Brake

With the Apollo command module imbedded in the Drag Brake as shown in Figure 5-1, the Apollo itself must have a heat shield, even through the brake is assumed capable of reradiating most of its heat. The vehicle enters along the overshoot corridor at $\overline{V}_i = 2$ (15.8 km/sec) for the return from the symmetric orbit, where a ballistic coefficient $C_B = 0.1$ or about one-tenth of the Apollo. With a stagnation point radius of 25 feet for the Apollo, the heating at that point becomes:

$$\dot{q}_{c_{max}} = 90 \text{ Btu/ft}^2\text{-sec} \qquad 5\text{-}29$$

$$\dot{q}_{r_{max}} = 9{,}000 \text{ Btu/ft}^2\text{-sec} \qquad 5\text{-}30$$

$$\dot{Q}_T = 165{,}000 \text{ Btu/ft}^2 \qquad 5\text{-}31$$

Thus from equation 5-15, a requirement for 34 lb/ft^2 is apparent at the stagnation point. Taking into account the heating distributions shown in Figure 5-3, an average heat shield area density of about 25 lb/ft^2 results, or a total Apollo heat shield weight of 12,000 lb.

At this point, it is evident that a savings in heat shield weight could be made by pointing the Apollo face to minimize the high radiative heating at the expense of some increase in convective heating. However, it must be realized that an increase in convective heating will show up on the Drag Brake surface. Coning back the brake would help minimize heating there but at the expense of additional structure to maintain the same drag characteristics.

The advantage of initial retro-braking does not pay off to the extent that it did for the lifting vehicles. As it is the Drag Brake requires a considerably larger share of its propulsion capability to maintain a tighter control near its overshoot to prevent skip out or dipping too deeply into the atmosphere, which would increase both its heating and deceleration loading.

The state-of-the-art in Drag Brake control simply is not as advanced as the lifting control, but under detailed study might prove to be the lighter vehicle due to some possible innovations in control at much higher altitudes as well as the deliberate use of its skip out capability. For purposes of this analysis, where emphasis was upon estimating total reentry vehicle system weight, the more conservative approach was taken of using lifting vehicles which appear to be within ablative materials capability, can result in deeper reentry corridors and give a greater landing site selection capability.

d. Comparison of Vehicle Weight Trends

Figure 5-6 shows that the total weight of the Apollo with its heat shield is less than that of the High L/D Vehicle which is the consequence of a higher drag coefficient (1.27 versus 0.33) and additional structure required (the total weights without heat shields are 9,300 and 9,800 lb., respectively). The rapid growth of heat shield weight for both vehicles is indicated as the reentry velocity increases. The High L/D Vehicle appears to be ablative materials limited slightly below 13.5 km/sec, whereas the Apollo limit is limited just above 14 km/sec. At reentry velocities higher that these, retros are definitely required for these vehicles. Note the rapid change of nose radius from blunt to sharp in the region of 13 km/sec, indicating the rapid transition from convective to radiative heating as would be expected from the 21.2 power law assumed.

A comparison of the stagnation point heating is shown in Table 5.4 for the three basic reentry vehicles where the Apollo is retro thrusted down to 13.5 km/sec and the High L/D Vehicle is retro thrusted down to 13 km/sec, but the Drag Brake aerodynamically descends all the way from 15.8 km/sec. Note the much higher radiative heating on the Drag Brake as compared to the convective heating. This will result in a very heavy heat shield for the exposed Apollo blunt face on the Drag Brake Vehicle. Some weight advantage could be gained if the stagnation radius were sharpened. Note the wide range of mass ballistic coefficient explored in this study.

e. Retro Weights

Figure 5-7 gives the payload ratio as a function of velocity increment required for a retro, where:

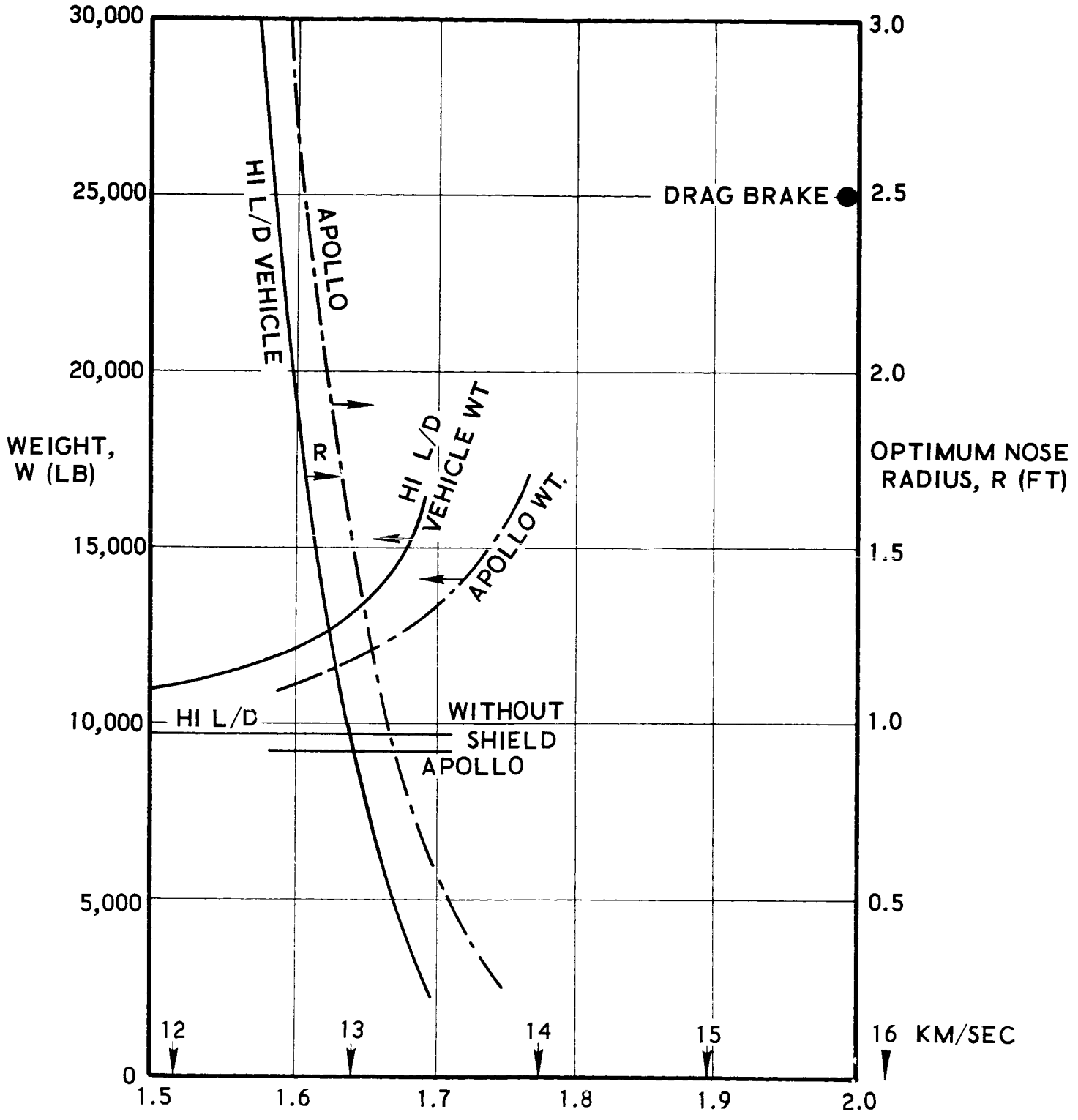
30,000
25,000
20,000
15,000
10,000
5,000
0
WEIGHT, W (LB)
3.0
2.5
2.0
1.5
1.0
0.5
OPTIMUM NOSE RADIUS, R (FT)
DRAG BRAKE
HI L/D VEHICLE
APOLLO
R
HI L/D VEHICLE WT
APOLLO WT.
HI L/D
WITHOUT SHIELD
APOLLO
12
13
14
15
16 KM/SEC
1.5
1.6
1.7
1.8
1.9
2.0
RE-ENTRY VELOCITY RATIO, $\overline{V}_i$

FIGURE 5-6.

PAYLOAD RATIO VS VELOCITY INCREMENT
(I_{sp} = 410 SEC, ONE STAGE)

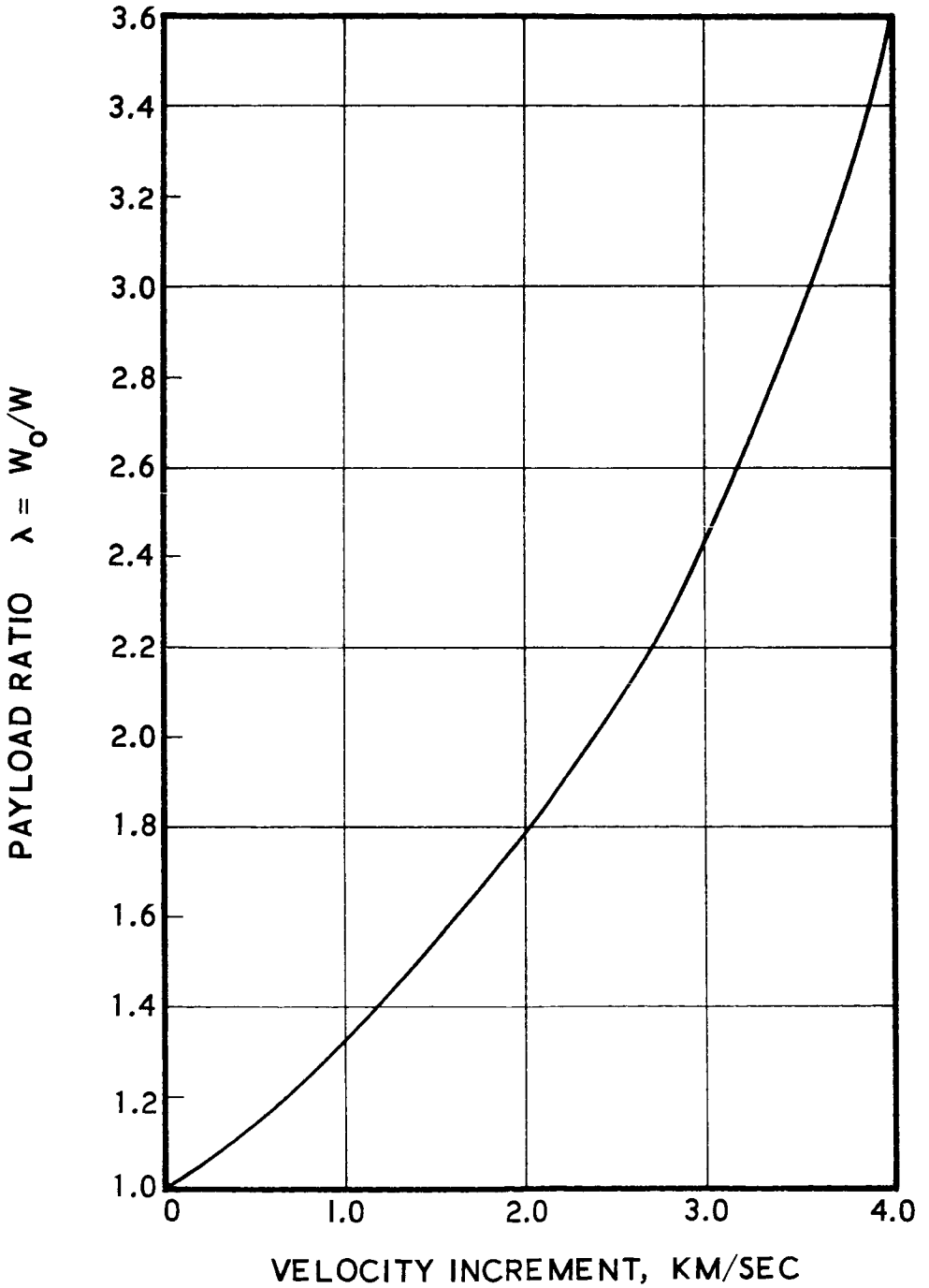

FIGURE 5-7.

TABLE 5.4

COMPARISON OF REENTRY VEHICLE STAGNATION POINT HEATING

	Apollo	High L/D Vehicle	Drag Brake
Maximum Stagnation Point Heating			
$\dot{q}_c$ (BTU/FT^2-SEC)	1,200	2,800	90
$\dot{q}_r$ (BTU/FT^2-SEC)	8,800	7,200	9,000
Q_C (BTU/FT^2)	56,500	240,000	5,200
Q_r (BTU/FT^2)	170,000	130,000	160,000
Stagnation Radius, R(FT)	0.54	0.75	25.
Ballistic Coefficient, C_B (m/C_DA, LB-SEC^2/FT^3) (After Retro)	1.6	12.5	0.2

$$\lambda = W_o/W \qquad 5\text{-}32$$

W_o = Total reentry vehicle weight including retro

W = Total reentry vehicle weight excluding retro

$\Delta V = V_i - V_e$

V_i = Initial reentry velocity before retro

V_e = Entry velocity after retro

The curve shown in Figure 5-7 assumes a one-stage chemical with an I_{sp}= 410 sec. Other types of propulsion and additional staging are covered in Section 6.

The total reentry system weight, including retro, is:

$$W_o = \lambda W \qquad 5\text{-}33$$

and the retro weight is:

$$W_R = (\lambda - 1) W \qquad 5\text{-}34$$

Figure 5-8 shows the additional weight for retros required to decelerate the lifting vehicles down to the velocity at which they can then enter the atmosphere more efficiently using ablative heat shields. The aerodynamic vehicle weight trends shown are from Figure 5-6. A one stage chemical rocket is added for both vehicles for the Crocco requirement of 13.5 km/sec and the Symmetric requirement of 15.8 km/sec. Minimum trade-off points between heat shield and retro are shown as encircled X's for the two vehicles and two missions. The Apollo shows some slight weight advantages over the High L/D Vehicle.

5.6 EVALUATION

Since the reentry velocity has such a decided affect upon the reentry vehicle weight as well as its overall reliability, there is some possible trade-off with other requirements of the EMPIRE mission. For the Symmetric mission the initial reentry and orbit injection velocities were found to be strong functions of the approach distance to the planet Venus, whereas changing the distance of Mars approach would cause smaller opposing changes in injection and return velocities. Figure 5-9 demonstrates the reduction of reentry vehicle weight as a consequence of more distance passes by the planets, where both relative distance ratios are changed by the same ratio. Design points are shown encircled where the nominal flyby distances were taken as 30 percent of the planet radius. Thus, a twenty-five percent reduction in total reentry vehicle weight (including retro) could be realized if the flyby ratio were changed to 2.0 (one planet radius altitude) rather than the design value of 1.3 planet radii from the center of each planet.

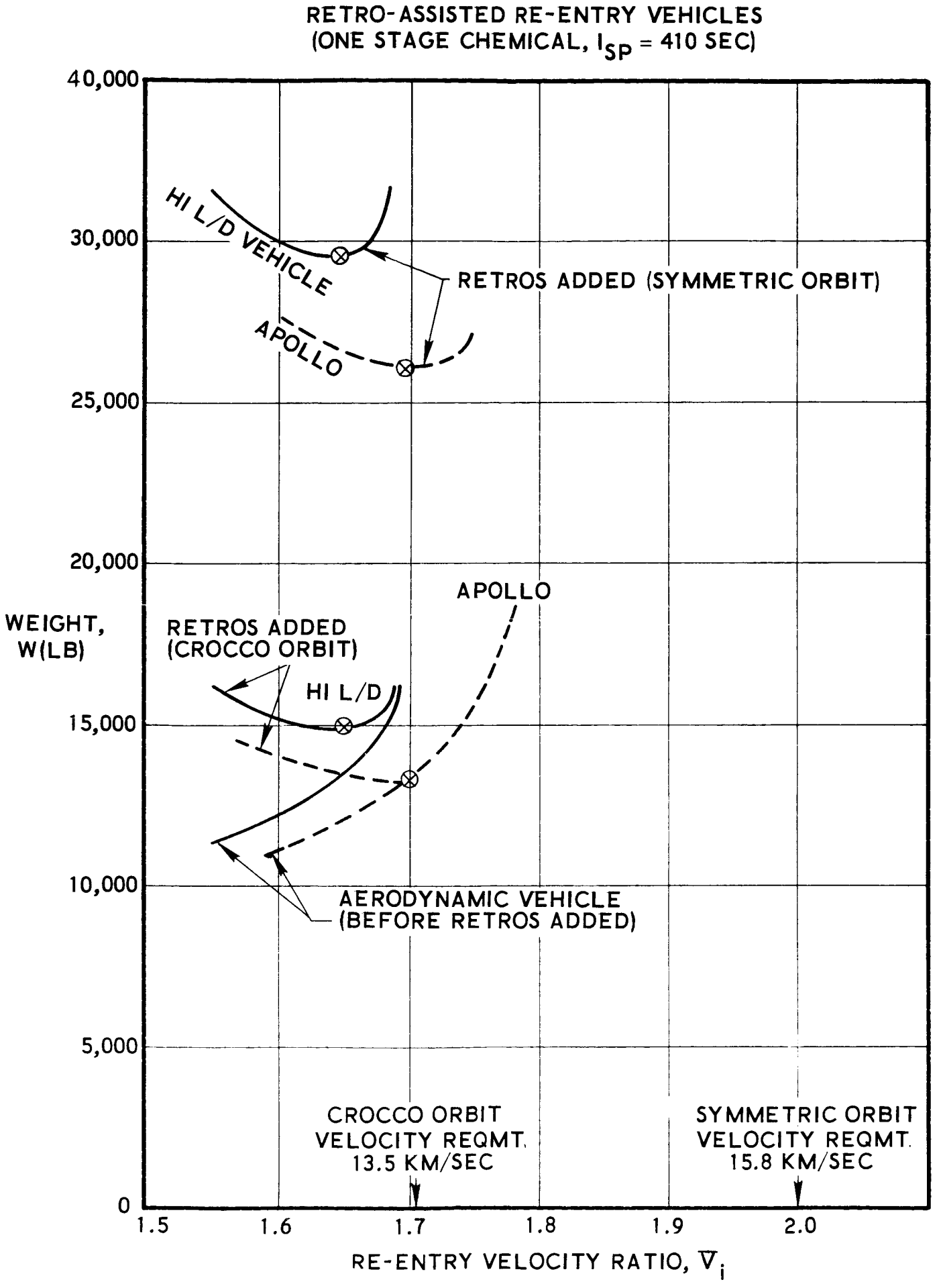
RETRO-ASSISTED RE-ENTRY VEHICLES
(ONE STAGE CHEMICAL, I_{SP} = 410 SEC)
40,000
30,000
25,000
20,000
15,000
10,000
5,000
0
WEIGHT, W(LB)
HI L/D VEHICLE
APOLLO
RETROS ADDED (SYMMETRIC ORBIT)
APOLLO
RETROS ADDED (CROCCO ORBIT)
HI L/D
AERODYNAMIC VEHICLE (BEFORE RETROS ADDED)
CROCCO ORBIT VELOCITY REQMT. 13.5 KM/SEC
SYMMETRIC ORBIT VELOCITY REQMT. 15.8 KM/SEC
1.5
1.6
1.7
1.8
1.9
2.0
RE-ENTRY VELOCITY RATIO, $\overline{V}_i$

FIGURE 5-8.

RE-ENTRY VEHICLE WEIGHTS VERSUS PLANET MISS DISTANCES
(SYMMETRIC ORBIT, INCLUDES RETRO)

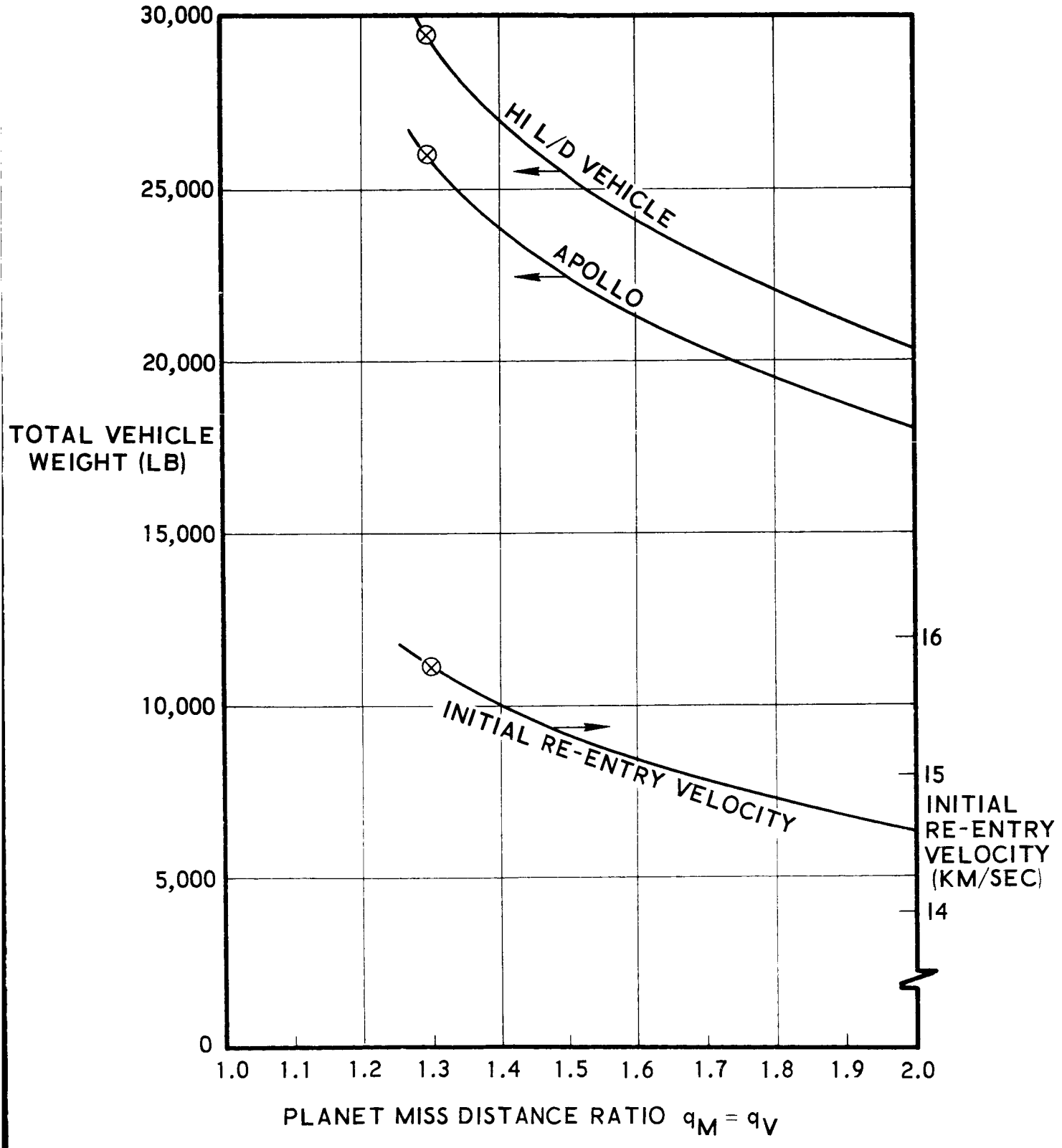

FIGURE 5-9.

The three basic return vehicles are compared in Table 5.5. Total estimated weights, including retros, drag brake, heat shield and control system requirements are quite competitive with each other. Further weight refinements are in order, particularly for the Drag Brake, however, the ultimate comparisons should be made on overall reentry system reliability.

Two important factors in making a reliability evaluation are shown below. The High L/D Vehicle has the widest corridor depth to operate within as well as the best potential flexibility for landing site selection. Quantitative data on the latter would be desirable. This was not included in the present study, however.

In summary, the Drag Brake requires some extensive work beyond the scope of this study and might provide a suitable alternative to the other vehicles. Particularly attractive is its potential for operating at lower g-levels and/or in a skip mode, thus opening up its reentry corridor as well as its landing site selection capability.

5.7 CONCLUSIONS

The conclusions of this phase of the study are:

- The Earth reentry is feasible for the EMPIRE mission with nominal weights of approximately 15,000 and 30,00 lb. for the Crocco and Symmetric orbits, respectively.
- The three types of reentry vehicles are competitive in weight, since no single one is more than a 20 percent variation from the others.
- Reentry vehicle weights required for the dual planet missions will vary about $\pm$ 25 percent from the nominal values depending upon planetary approach distance and launch window flexibility.
- The High L/D Vehicle has a deeper reentry corridor and more flexibility in landing site selection than Apollo or the Drag Brake vehicle.

TABLE 5.5

REENTRY VEHICLE COMPARISONS

	Apollo		High L/D Vehicle		Drag Brake
	Symmetric	Crocco	Symmetric	Crocco	Symmetric
Total Weight (lb)	26,100	13,300	29,500	14,920	30,000
Retro Weight (lb)	12,920	-0-	16,300	1,675	-0-
Heat Shield Wt.(lb)	3,880	4,000	3,455	3,455	12,000
Control Sys. Wt. (lb)	500	500	500	500	5,000
Initial Velocity (km/sec)	15.8	13.5	15.8	13.5	15.8
Landing Site Selection					
Longitudinal	Fair		Good		Good
Lateral	Poor		Good		Fair

- Apollo and the High L/D Vehicle require retros for reentry. otherwise they would experience conditions exceeding ablative materials capability, especially in the Symmetric orbit mission.

- The High L/D Vehicle was chosen for more complete analysis over the Apollo or Drag Brake Vehicle because it exhibits a more conservative reentry mode in light of our present knowledge.

5.8 RECOMMENDATIONS

The recommendations for additional effort from this phase of the EMPIRE study are:

- Model testing in ionized gas streams are required to simulate the radiative heating and to establish both the radiative heating relationships and the thermal protection materials technologies in the EMPIRE reentry regime.

- Aerodynamic wind tunnel tests are in order for the High L/D Vehicle to study flow field behavior during reentry maneuver and to study control effectiveness down to landing.

- Detailed control system studies are desirable not only to establish more accurate weights but to further define their actual requirement, particularly in the case of the Drag Brake, as well as to estimate the effect of long storage time.

- The Drag Brake system needs further study to explore reductions in weight which could result from lower g-levels and from less radiative heating. Also the skip potential of this system should be explored in depth.

SECTION 5

REFERENCES

1. Himmel, S. C., Dugan, J. F., Luidens, R. W., and Weber, R. J., "A Study of Manned Nuclear-Rocket Missions to Mars", Aerospace Engineering, July 1961.

2. Lees, L., Hartwig, F. W., and Cohen, C. B., "The Use of Aerodynamic Lift During Entry Into the Earth's Atmosphere", GM-TR-0165-00519, Space Tech. Labs., Inc., Nov. 20, 1958.

3. Luidens, R. W., "Approximate Analysis of Atmospheric Entry Corridors and Angles", NASA TN D-590, Lewis Research Center, January 1961.

4. Luidens, R. W., "Flight-Path Characteristics for Decelerating from Supercircular Speed", NASA TN D-1091, Lewis Research Center, December 1961.

5. Grant, F. C., "Importance of the Variation of Drag with Lift in Minimization of Satellite Entry Acceleration", NASA TN D-120, Langley Research Center, October 1959.

6. Grant, F. C., "Analysis of Low-Acceleration Lifting Entry from Escape Speed", NASA TN D-249, Langley Research Center, June 1960.

7. Grant, F. C., "Modulated Entry", NASA TN D-452, Langley Research Center, August 1960.

8. Levy, L. L., "The Use of Drag Modulation to Limit the Rate at Which Deceleration Increases During Nonlifting Entry", NASA TN D-1037, Ames Research Center, September 1961.

9. Hayes, J. E., Rose, P. H., and Vander Velde, W. E., "Analytical Study of a Drag Brake Control System for Hypersonic Vehicles", WADD Technical Report 60-267, January 1960.

10. Smith, R. H. and Menard, J. A., "Supercircular Entry and Recovery with Maneuverable Manned Vehicles", Boeing Airplane Company, Paper No. 64-114-1808, presented at the National IAS-ARS Joint Meeting in Los Angeles, June 13-16, 1961.

11. Chapman, D. R., "An approximate Analytical Method for Studying Entry Into Planetary Atmospheres", NASA TR R-11, Ames Research Center, 1959.

12. Chapman, D. R., "An Analysis of the Corridor and Guidance Requirements for Supercircular Entry Into Planetary Atmospheres", NASA TR R-55, Ames Research Center, 1960.

13. Chapman, D. R., and Kapphahn, A. K., "Tables of Z Functions for Atmosphere Entry Analyses", NASA TR R-106, Ames Research Center, 1961.

14. Wilkinson, H. R., "Stagnation Point Heating for Steep Angle Entry into the Earth's Atmosphere at Supercircular Velocities", Space Technology Labs. Report 9751-0008-MU-000, May 1961.

15. Lovelace, V. M., "Charts Depicting Kinematic and Heating Parameters for a Ballistic Reentry at Speeds of 26,000 to 45,000 Feet per Second", NASA TN D-968, Langley Research Center, October 1961.

16. Scala, S. M. and Warren, W. R., "Hypervelocity Stagnation Point Heat Transfer", ARS J., Jan. 1962,pp. 101-102.

17. Fay, J. A. and Riddell, F. R., "Theory of Stagnation Point Heat Transfer in Dissociated Air", J. Aero. Sci., vol. 25, 1958, pp. 78-85.

18. Solomon, J. M., "Approximate Calculation of the Equilibrium Laminar Boundary Layer on Blunt Bodies at Hypersonic Speeds", ARS Journal, March 1962, pp. 422-4, Fig. 2.

19. Hildalgo, H., "Closing Reply", Technical Comments, ARS Journal, April 1962, pp. 647-8, Fig. 1.

20. Strack, S. L., "Radiant Heat Transfer Around Reentry Bodies", ARS Journal, May 1962, pp. 744-748, Fig. 4.

21. Wick, B. H., "Radiative Heating of Vehicles Entering the Earth's Atmosphere", NASA (Ames), Presented to the Fluid Mechanics Panel of Advisory Group for Aeronautical Research and Development NATO, Brussels, Belgium, April 3-6, 1962.

22. Anderson, R. A. and Swann, R. T., "Structures for Reentry Heating", NASA TM X-313, September 1960 (Confidential).

23. Brooks, W. A., Wadlin, K. L., Swann, R. T. and Peters, R. W., "An Evaluation of Thermal Protection for Apollo", NASA TM X-613, December 1961 (Confidential).

24. Swann, R. T., "Composite Thermal Protection Systems for Manned Re-Entry Vehicles", ARS Journal, February 1962, pp. 221-6.

25. "Thermal Protection Systems", NASA TM X-650, February 1962 (Conf.)

26. Allen, H. J., "Hypersonic Aerodynamic Problems of the Future", NASA (Ames), Presented to the Fluid Mechanics Panel of AGARD, Brussels, Belgium, April 3-6, 1962.

SECTION 6

VEHICLE REQUIREMENTS

This section presents the significant results of the Vehicle Configuration and System studies. Vehicle configurations are defined for both Crocco and Symmetric orbits based on careful evaluation of system and mission requirements. A symmetric nuclear injection vehicle weighing less than 400,000 pounds and using a single 50,000 pounds thrust engine is shown and compared with a Crocco nuclear injection vehicle weighing over 2,000,000 pounds and requiring a 700,000 pounds thrust engine with a 3600 second burn time. In addition two symmetric chemical injection vehicles weighing 701,000 and 1,859,000 pounds respectively are briefly discussed.

The design criteria for system and vehicle design is presented first, followed by a section presenting system design considerations. Using the information presented in these two subsections, vehicle synthesis is then discussed. In addition, the work on cryogenic storage, which is not directly applicable to the design vehicles, is presented.

6.1 DESIGN CRITERIA

System and vehicle design criteria are composed primarily of Mission Requirements, Environmental Effects, and Crew Requirements. Also of importance, primarily in subsystem design, are such considerations as reliability, availability, and weight.

a. Mission Considerations

Mission considerations consist of energy requirements for orbit establishment, guidance, control, and abort maneuvers, and length of mission. Specific energy requirements in the form of velocity increments for each mission phase are shown in Table 6.1. These requirements were presented in previous sections of this report but are summarized here for convenience.

TABLE 6.1

MISSION VELOCITY REQUIREMENTS

	ΔV Km/Sec	
	Crocco	Symmetric
Injection	11.95	5.30
Midcourse	0.62	0.62
Reentry	13.50	15.80
Abort	11.95	3.00

Mission length varies with launch date and type of orbit as discussed in the Trajectories section of this report. For design purposes the mission lengths chosen are:

Crocco	396 Days
Symmetric	611 Days

b. Environment

The major environment factors affecting vehicle design include meteoroids, zero gravity, space vacuum, and thermal radiation. Additional criteria are the solar flare and cosmic radiation which are discussed in the section on Crew Requirements.

(1) Meteoroids

The magnitude of the meteoroid puncture and erosion hazard for the missions studied is relatively unknown. Because of the possible serious effects of a meteoroid puncture on crew life and mission success, Aeronutronic has used (Reference 1) what it considers to be conservative design criteria in the light of present knowledge. Figure 6-1 is a plot of required shield thickness as a function of the parameter $A\tau$ for different probabilities of penetration of a dual wall aluminum structure. The parameter A is area (square feet) of tank or living module wall exposed to meteoroid puncture. The parameter τ is exposure time in hours. The data shown on the figure were taken from Aeronutronic studies presented in WADD Report TR 60-503.

(2) Zero Gravity

All components must be designed to operate in a weightless condition. Of greatest concern are operations which involve liquid-gas separation and those heat transfer processes which are dependent on film contact. The problem of weightlessness as it affects the crew is discussed under Crew Requirements.

(3) Space Vacuum

Although no detailed system design has been done during this study, the effects of the high vacuum of space on sublimation of thermal coatings, material properties, and mechanical systems operation has been considered.

(4) Thermal Environment

The spacecraft operates in a thermal environment consisting primarily of solar radiation. Planetary radiation and reflected solar radiation are important only during the brief periods of launch and flyby. In addition to these heat sources, the heat sink of outer space must also be considered in designing for thermal protection and in the design of space radiators.

Figure 6-2 shows the variation of solar heat flux as a function of distance from the sun. This curve is based on data from Reference 2.

SOLAR HEAT FLUX AS A FUNCTION OF DISTANCE FROM THE SUN

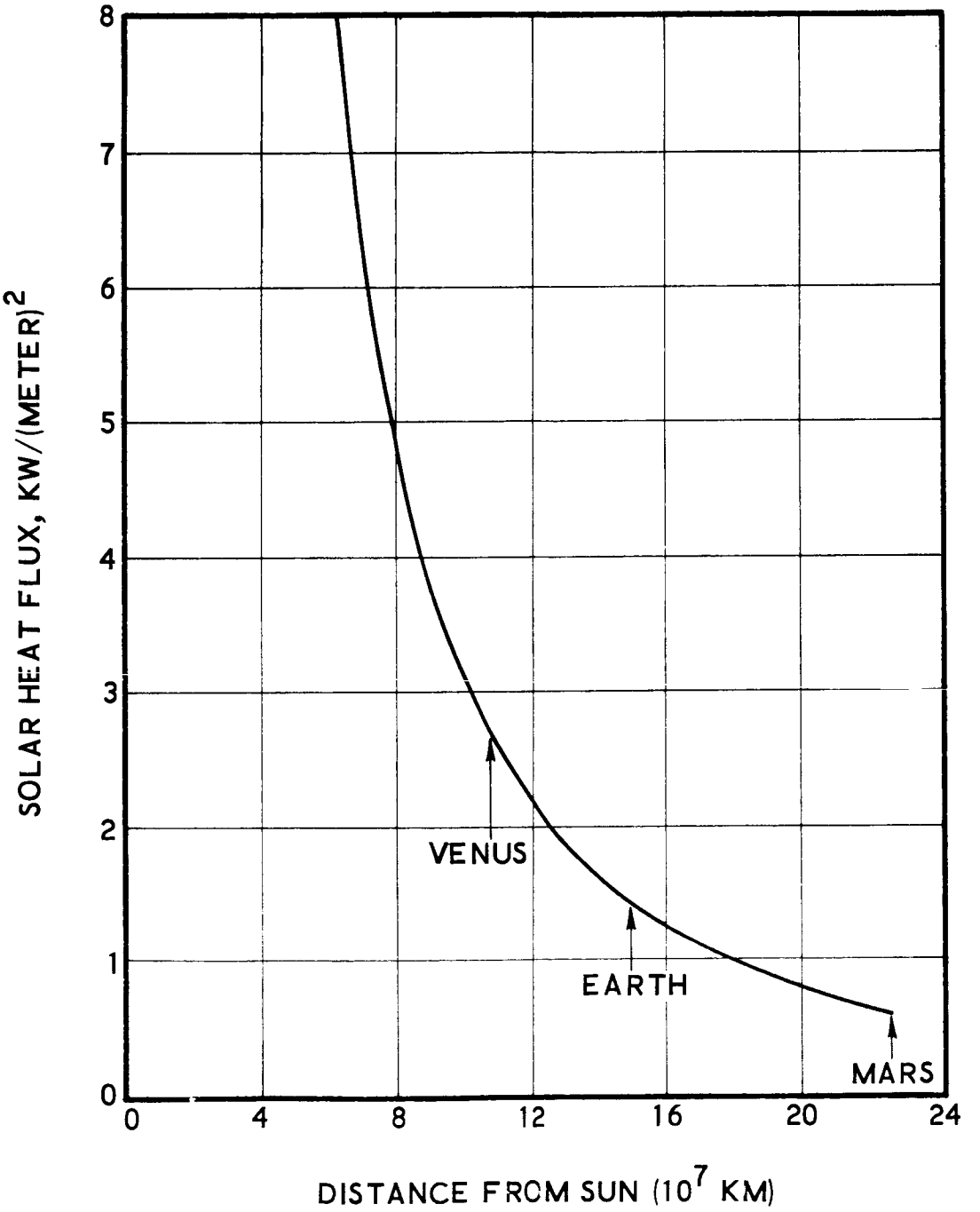

FIGURE 6-2

c. Crew Requirements

Crew requirement criteria which affect vehicle design include life support and thermal control system considerations, requirements for radiation protection, the total crew size, and the need for artificial gravity.

(1) Life Support

Life support considerations pertinent to this study fall into two broad categories--physiological and psychological considerations. Physiological considerations further breaks down into Environmental Factors and Support Requirements.

Most of the requirements such as metabolic criteria and human tolerances to acceleration, noise, vibration, etc., are well defined in the literature. One task has been to interpret and select those requirements which appear to be most reasonable, and key vehicle design to them.

Metabolic data for an average man was obtained from ASD TR 61-161, "Space Vehicle Environmental Control Requirements Based on Equipment and Physiological Criteria". The data used is summarized:

O_2	Required per man	- 1.8 lb/day
H_2O	Required per man	
	Food & Drinking	- 4.84 lb/day
	Other	- 20.00 lb/day
Urine Produced		- 3.08 lb/day
CO_2	Produced (Respiratory quotient = 0.80)	- 2.25 lb/day
H_2O	Produced in Respiration (Perspiration)	- 2.20 lb/day

(2) Gravity

It cannot be positively stated that an artificial gravity is or is not required for the EMPIRE length mission. Therefore it seems most reasonable to provide it. Providing gravity not only removes an area of doubt as to crew comfort (and possibly even survival) it also establishes the most severe design and weight constraint. The vehicle designed to provide some level of artificial gravity is more conservative than a zero gravity vehicle.

(3) Crew Size

Because of its importance on vehicle size, an analysis was made to establish a definite limit to the crew size. The steps taken in this analysis were:

- Literature search was made for data pertaining to human factors for crews of nuclear submarines and simulated space vehicles (References 2 through 4). Particular emphasis was placed upon work/rest cycles, function and task assignment, prevention of boredom and fatigue, and maintenance of high performance level. The company physician, Dr. R. L. Weir (30 years of experience as Flight Surgeon, USMC) was contacted relative to crew function and task, and contributed data based upon long experience with cramped quarters and low interest problems attendant with small naval vessels.

- These data led to a set of basic assumptions that were used to define the crew functions.

  - The Commanding Officer of the vehicle will have responsibility for the overall performance of the vehicle and its crew.

  - The Commanding Officer will be assisted by the Executive Officer, who will assume command in the event of incapacitation of the Commanding Officer.

  - The Flight Surgeon will be responsible for the physical and mental health of all crew members.

  - The remainder of the crew will have equal status with the Flight Surgeon.

  - Duty posts for all on watch personnel were divided into three functions; duty officer, maintenance and repair officer, and scientific activity officer. The responsibility of each post is shown in Table 6.2.

TABLE 6.2

CREW COMPOSITION

Commanding Officer — Flight Surgeon

Executive Officer — Three Crew Members

Watch Personnal	Responsibility
Duty Officer - On watch in control room located in solar radiation cellar.	Monitors all systems. Maintains Communications Records Key Data. Initiates Repair Activity. Alerts Scheduled Scientific Activity. Maintains Spacecraft Integrity.
Maintenance & Repair Officer -	Performs Regular Preventive Maintenance on All Systems. Performs Repair. Supervises Emergency Procedures. Assists in Scientific Activity.
Scientific Activity Officer -	Performs, Records, & Evaluates Scheduled Scientific Activity. Plans & Executes Unscheduled Activity as Warranted.
Waste Management, Meal Preparation, etc., Scheduled Informally For Off-Duty Crew. All Personnal Perform All Functions Except Hazardous Repair Is Not Done By Commanding Officer or Flight Surgeon.	

The data and the assumptions listed above were combined, and forty-eight hour schedules prepared for different crew sizes within the specified range. One area of question which influences the desirability of a crew schedule is the utility level required by the maintenance/repair and scientific activity watches. If the nature of those watches is such that one man can monitor both watches, the smaller crew sizes (4 to 6) appear adequate. If, however, these activities require full duty of two crewmen, crews of seven or eight will become necessary.

A typical schedule for the selected six man crew is shown in Table 6.3.

TABLE 6.3

TYPICAL SCHEDULE FOR SIX MAN CREW

	Duty Officer	Maintenance & Repair	Scientific Activity	Sleep	Rest
0000 - 0200	A	E	D	F	C,B
0200 - 0400	B	D	C	F,E	A
0400 - 0600	A	D	C	F,E	B
0600 - 0800	B	A	D	E	F,C
0800 - 1000	C	A	F	B	E,D
1000 - 1200	D	F	E	A,B	C
1200 - 1400	C	F	E	A,B	D
1400 - 1600	D	C	F	A	B,E
1600 - 1800	E	C	B	D	A,F
1800 - 2000	F	B	A	C,D	E
2000 - 2200	E	B	A	C,D	F
2200 - 2400	F	E	B	C	A,D

This schedule provides the following for the six man crew:

- No more than two hours continuous duty at a constant vigil post.
- Duty for no more than six hours at one time.
- Six hours of unbroken sleep during each 24 hours.
- Two hours rest preceding duty officer watch.
- One hour between meals and beginning of a watch.

(4) Living Area

Volume of living areas must be sufficient to provide comfortable surroundings for the long mission times involved. Based on space allocations in nuclear submarines, a volume allocation of 750 cubic feet per man (free volume) appears to be adequate for the primary living modules. Volume allocation for the radiation protection area can be much less because of the relatively short periods of occupancy by the entire crew. Fifty cubic feet (free volume) per man appears to be adequate. This latter number is based on data in Reference 5.

(5) Radiation Protection

The protection of the EMPIRE crew from the debilitating effects of high energy radiation is one factor which strongly influences the total mass of the vehicle and which demands careful design to utilize the shielding afforded by tankage, propellants, and other structures in order to keep the mass to a minimum.

There are many uncertainties in this area as in the meteoroid hazard area. Because of the expected high level of sun spot (hence solar flare) activity during the period of the EMPIRE mission for 1970-72 (see Figure 6-3) very conservative design criteria are required. The two basic criteria selected are:

- Selection of the May 10, 1959 solar flare as the maximum intensity flare to be encountered during the mission.
- Establishment of 200 REM as the maximum desirable accumulated dose to be received by the crew during the mission.

CYCLICAL VARIATION OF SUNSPOTS

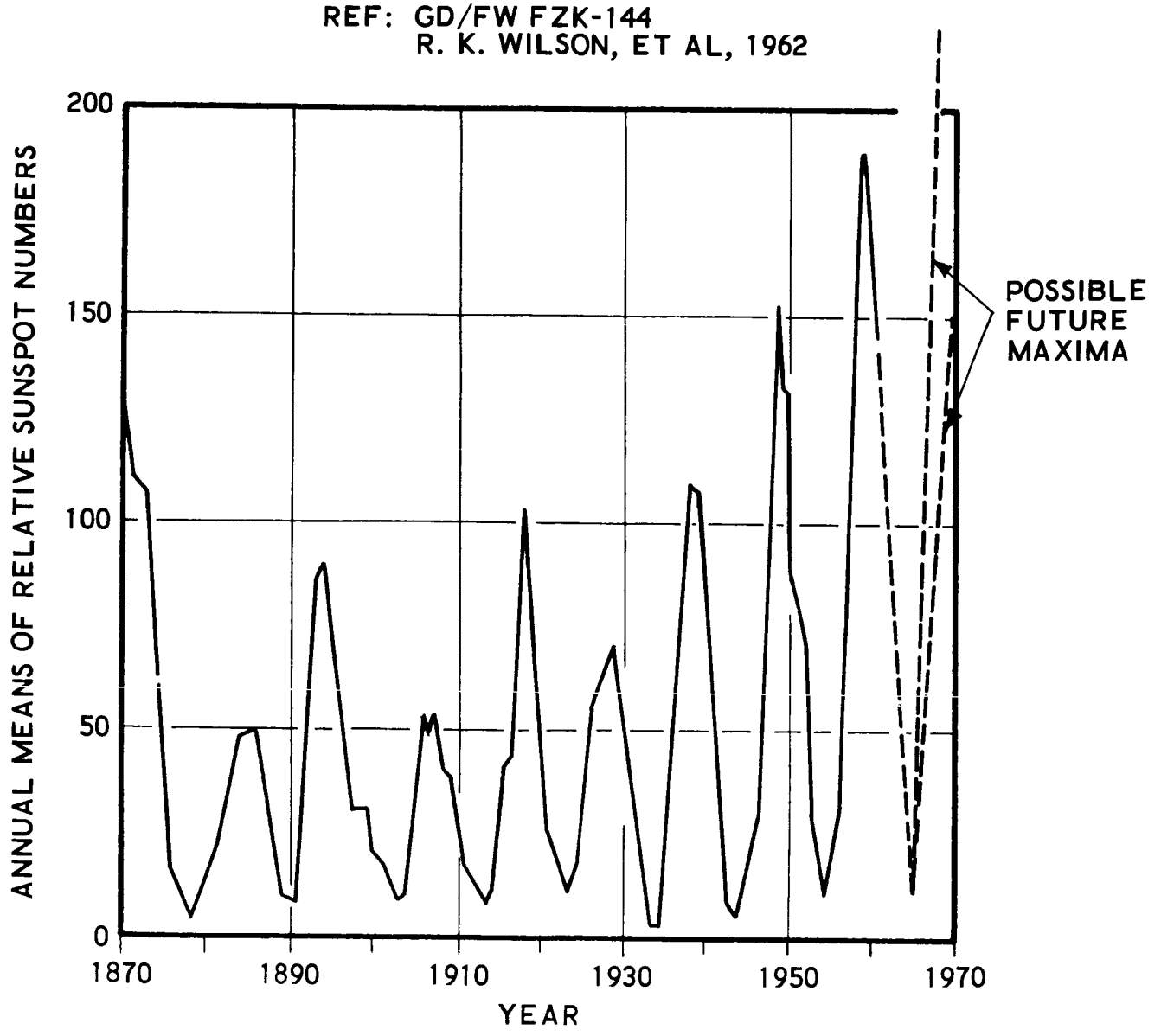

FIGURE 6-3

6.2 SYSTEM DESIGN

This section briefly presents design and weight summaries of major on-board systems and the living areas. These data, which were generated using the design criteria discussed in the preceeding section, are then used along with the reentry system weights (discussed in the Reentry System section) to size the vehicle.

a. Life Support

A preliminary system was conceived for use in defining a total system weight. The system (shown in Figure 6-4) was used in determining system weight for both Crocco and Symmetric missions.

Water produced by the crew in respiration and perspiration is electrolyzed (or otherwise broken into H_2 and O_2) and the produced oxygen is reused to provide metabolic oxygen. The hydrogen produced by the process is combined with CO_2 (which is removed from the atmosphere in another process) to produce water and carbon. This water plus water from humidity control and urine are then processed for reuse. A store of emergency (makeup) water is also provided.

For this system concept to work, the water balance, oxygen requirement, and CO_2 production of the crew must be compatible. That is, sufficient H_2O must be available in the atmosphere to produce breathing oxygen, and the H_2 (from the electrolyzed H_2O) must be sufficient to reduce the metabolic CO_2 produced by the crew.

All the H_2O produced in respiration and perspiration must be removed from the atmosphere, to maintain a constant relative humidity, and therefore is available to provide oxygen. Assuming 100 percent efficiency of all processes the following data were obtained:

H_2O Required to produce 1.8 lbs. O_2/day (electrolysis)	- 2.0 lb/day
H_2 Produced from electrolysis of H_2O	- 0.22 lb/day
H_2 Required to reduce 2.25 lbs. CO_2/day	- 0.20 lb/day
H_2O Produced by reduction of 2.25 lbs. CO_2/day	- 1.84 lb/day

The water balance on one man (not including water in feces) then is:

LIFE SUPPORT SYSTEM SCHEMATIC

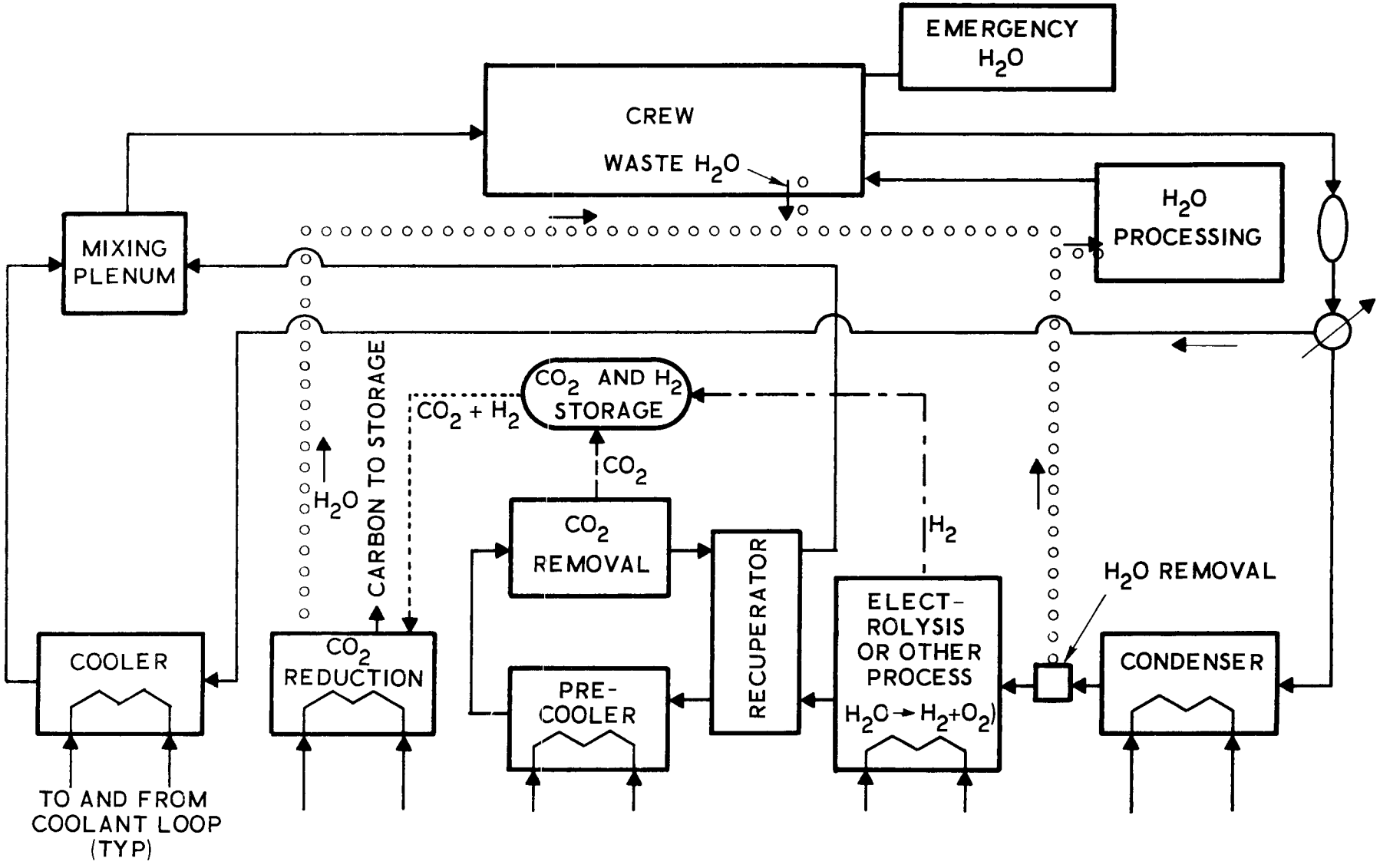

FIGURE 6-4

Fresh Water Required		Required to be Processed	
Food & Drink	4.84 lbs/day	Urine	3.08 lbs/day
Other (Utility)	20.00 lbs/day	Hum. Control	0.20 lbs/day
		CO_2 Reduction	1.84 lbs/day
		Utility H_2O	20.00 lbs/day
TOTALS	24.84 lbs/day		25.12 lbs/day

It appears that this system concept is feasible, and even allowing for process inefficiencies and other losses, should provide a low weight system.

System information for estimating weight was obtained from the following companies:

Ionics, Incorporated
Cambridge, Massachusetts

AiResearch Division of Garrett Corp.
Los Angeles, California

Hamilton Standard Division of United Aircraft Corp.
Windser Locks, Connecticut

Mechanics Research Division of General American Transportation
Niles, Illinois

Whirlpool Corporation Research Laboratories
St. Joseph, Michigan

System weights tabulated in Table 6.4 were obtained based on the following

(1) 3 complete atmospheric constituent and thermal control systems (one in each living module and one in the radiation shelter).

(2) Water reprocessed

(3) Oxygen regenerated

(4) CO_2 reduced

(5) Makeup and emergency atmosphere stored cryogenically

(6) 5 complete repressurizations allowed for (total air filled volume - 8,350 cubic feet)

(7) 30-day supply of emergency O_2

(8) Cabin leakage 1.5 lb/day

(9) Food plus container weight 2.5 lb/man-day

TABLE 6.4

LIFE SUPPORT SUBSYSTEM WEIGHTS

	Weight - Lbs	
	Crocco	Symmetric
Food & Packaging	6340	9945
Feeding System	1153	1153
Waste Management	200	200
Water Reclamation	68	68
Personal Hygiene	444	444
Atmospheric Constituent & Thermal Control	6000	6000
Pressurization System	3500*	4000*
Total Weight	17,705	21,810

* Omitted from previous reports.

The effect on spacecraft weights of the addition of pressurization system weight which was inadvertently omitted in obtaining the total spacecraft weight can be determined from Figure 6-19 for the Symmetric Nuclear and Chemical Vehicle Configurations.

Estimated power requirement for the total system is 3700 watts continuous with peaks up to 7300 watts.

b. Living Modules

The living areas of the structure have been examined to establish the major variables involved, and determine their influence on vehicle size and mass. The living area is divided into two distinct areas, the living module (discussed in this section) and the radiation shelter (discussed in the following section).

The living module is defined as all areas designed specifically for manned occupancy and use with the exception of the radiation shelter and reentry vehicle. This area includes all work, rest, recreation, and laboratory facilities. Passageways between modules are not included. The design weight shown in Table 6.5 was based on the following assumptions:

- 750 cubic feet per man (free volume)
- Length to diameter ratio of module = 3
- Equipment density 25 lbs/ft^3
- Meteoroid protection based on the 90 percent probability curve on Figure 6-1.

TABLE 6.5

LIVING MODULE WEIGHTS

Crocco	7500 lbs.
Symmetric	9000 lbs.

c. Radiation Protection

Within the energy ranges of interest charged particles lose energy principally by excitation and ionization of the atoms in their paths. For this purpose low-Z materials are best on a mass basis, with hydrogen being about a factor of two better than the second best material, helium. For practical purposes materials containing large weight percentages of hydrogen in their composition, such as water, polyethylene, butyl rubber,

etc., are desirable not only because they serve as excellent shield but also because of their abundance, low cost, and ease of handling. Other low-Z materials, such as aluminum, attenuate high energy charged particles almost as well on a mass per unit area basis (gm/cm^2).

Two radiation protection shield materials were examined during the study, water and polyethylene. The polyethylene shelter was chosen primarily on the basis of weight. Figure 6-5 shows a weight comparison of the water and polyethylene shelters as a function of free shelter volume per man. The design point is at 50 cubic feet per man using a 50 cm thick polyethylene shield.

The radiation dose in Rads received by the crew in the design shelter from a May 10, 1959, type flare is shown in Figure 6-6. Added to the protection of the polyethylene is three inches of aluminum provided by the second stage injection tanks and inner structure. Although not included in this study an inner layer of neutron absorbing material such as boron could be useful in reducing secondary neutron effects.

The data in Figure 6-6 was taken from work done at the General Dynamics, Fort Worth Division (Ref. 6). This work takes into consideration nuclear processes wherein secondary particles are produced. At the design point shown, secondary particles contribute significantly to the total dose.

The flare of 10 May 1959 used in this study was an especially large one. Adequate protection against it will therefore provide even better protection against the less intense though more numerous ones.

Table 6.6 lists the dose contributions of the various particles at three shield thickness near the design point. The dose in Rads is converted to REM by combining it with the appropriate relative biological effectiveness (RBE). The RBE of high energy radiation is not well known and is perhaps the area of greatest uncertainty. The RBE used, however, appear to be acceptable in light of current knowledge.

It is expected that the design point shielding will allow exposure of the astronauts to 70-80 REM from a May 10, 1959 type flare.

The total dose which the crew receives during the mission will come from solar flares, cosmic radiation, and the on-board nuclear reactor in the power system. Shielding the SNAP-8 reactor to produce no more than 2 millirem/hour at the living modules, and adding an estimated 0.5 millirem/hour from cosmic radiation gives a total accumulated dose for the 611 day symmetric mission of 37.5 REM.

RADIATION SHELTER WEIGHT
AS A FUNCTION OF SHELTER VOLUME

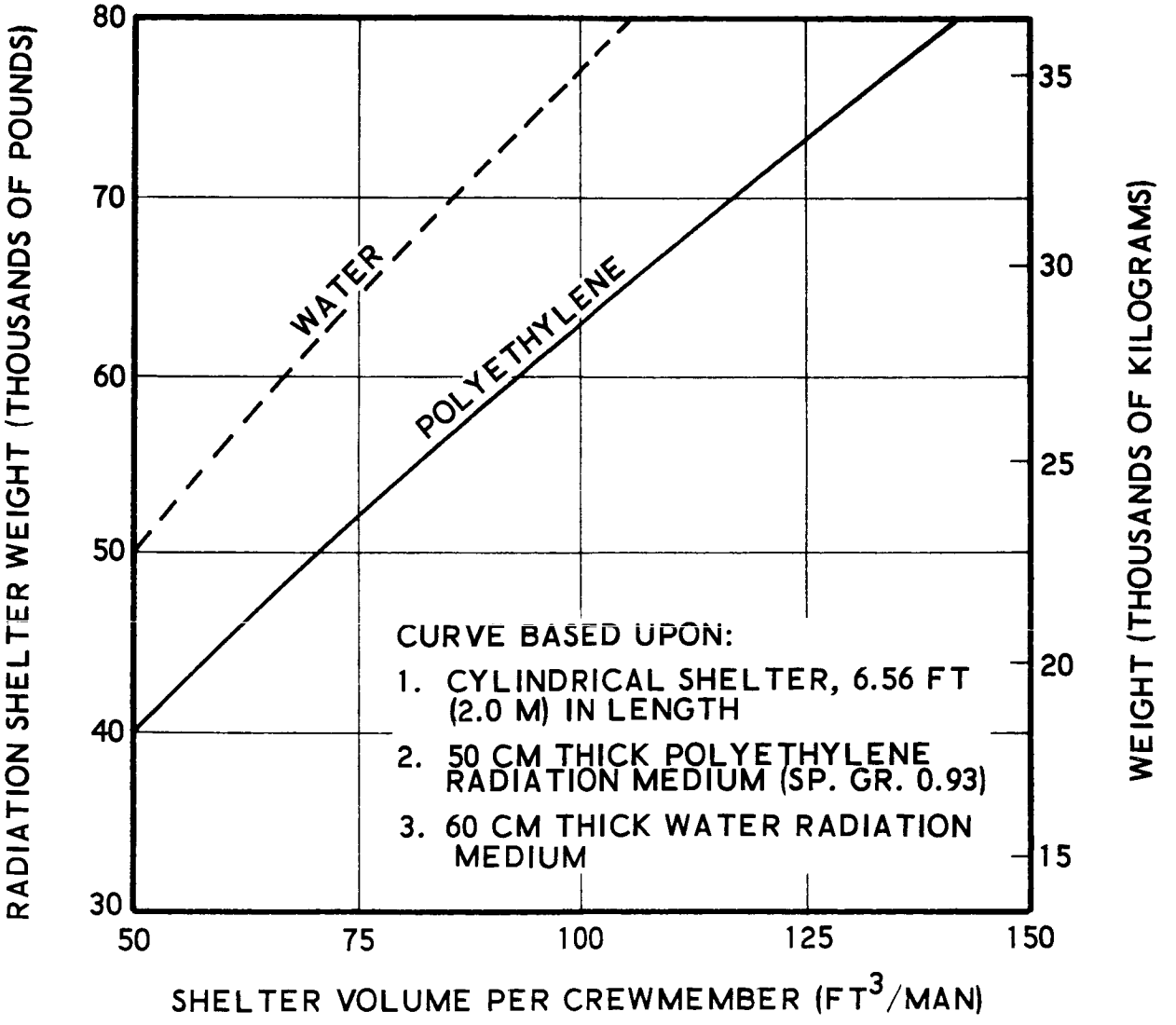

FIGURE 6-5

RADIATION DOSE FOR SOLAR FLARE EQUIVALENT OF 10 MAY 1959

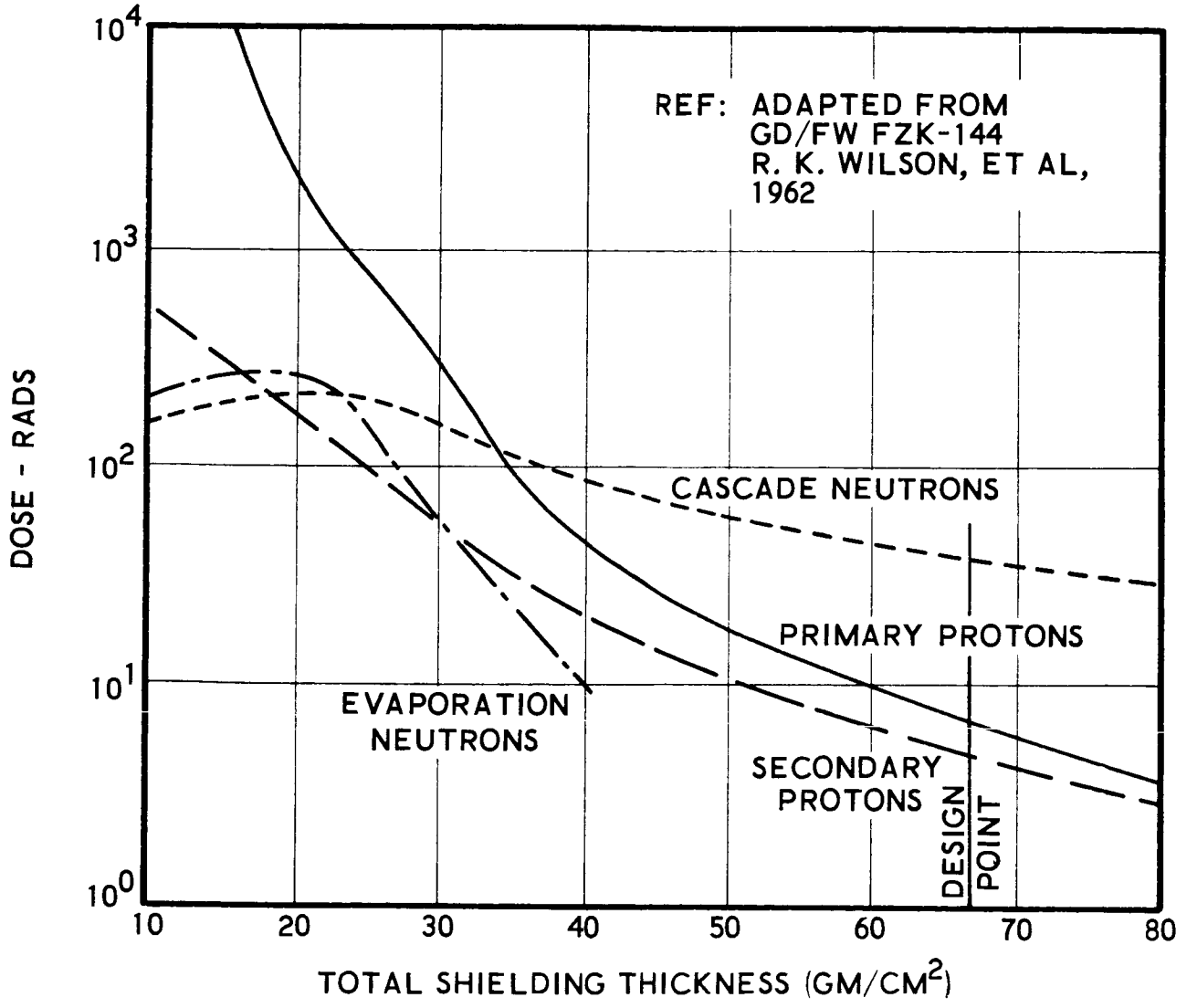

FIGURE 6-6.

TABLE 6.6

RADIATION DOSAGES FOR THE 10 MAY 1959 FLARE

TYPE OF RADIATION	TOTAL DOSE - RADS			RELATIVE BIOLOGICAL EFFECTIVENESS RBE	TOTAL DOSE - REM		
	TOTAL SHIELD THICKNESS				TOTAL SHIELD THICKNESS		
	80 GM/CM^2	70 GM/CM^2	60 GM/CM^2		80 GM/CM^2	70 GM/CM^2	60 GM/CM^2
PRIMARY PROTONS	4.1	5.8	9.8	2	8.2	12	20
SECONDARY PROTONS	3.0	4.4	6.8	5	15	22	34
CASCADE NEUTRONS	32	36	44	1	32	36	44
EVAPORATION NEUTRONS	$<10^{-1}$	$\sim 10^{-1}$	<1	5	<0.5	~ 0.5	<5

Assuming that one flare such as that of 10 May 1959 will occur adds another 70-80 REM bringing the total up to 108 to 118 REM. The difference between this dose and the 200 REM selected as the maximum desirable dose for the entire mission is 82 to 92 REM. It is expected that this difference is sufficient to provide for the more common 3 and 3+ flares.

d. Communications

A spacecraft communication installation was postulated as a contribution to the EMPIRE system description. It is subject to refinement as mission conditions and information-transmission requirements are further clarified, but the basic communication functions should remain essentially the same.

In the launch and boost phases, some tracking aids compatible with AMR facilities (radar, doppler, and interferometer) will be required to establish the staging orbit. However, the airborne components involved will be carried in the booster rather than in the payload and need not be of concern at this time.

The EMPIRE communications capabilities may be roughly divided into three categories. The first is that required for operation within 10,000 km of Earth. The functions required (voice, telemetry, command, and tracking) will be extensions of (and very similar to) those to be utilized by Apollo, and should be compatible with the Earth facilities being developed and improved for the next decade of space probes. Furthermore, this first category of equipment would be especially useful for inter-vehicle communications (at reduced power) if the expedition be composed of more than one spacecraft.

The second category of communications equipment is that required for the longer distances. The cooperating Earth equipment is that of the Deep Space Instrumentation Facility (DSIF) developed and operated by Jet Propulsion Laboratory for NASA.

The third general category is that of internal communications. This is to be the network providing the various manned stations of the spacecraft with voice communications and tie-ins to external communications.

Figure 6-7 is a block diagram of the conceptual EMPIRE communications installation. For the purpose served by this study the short-range category is assumed to be a 1970 evolution of the present Mercury installation. Propagation time (as much, possibly, as 22 minutes each way) may introduce an operational problem but does not affect the basic equipment.

CATEGORIES OF REQUIRED CAPABILITY

1. OPERATION WITHIN 10,000 KM OF EARTH EXTENSION OF APOLLO SYSTEM.
2. OPERATION BEYOND 10,000 KM FROM EARTH DEPENDENT ON DSIF DESIGN IN 1970-1972.
3. INTERNAL COMMUNICATIONS STANDARD EQUIPMENT.

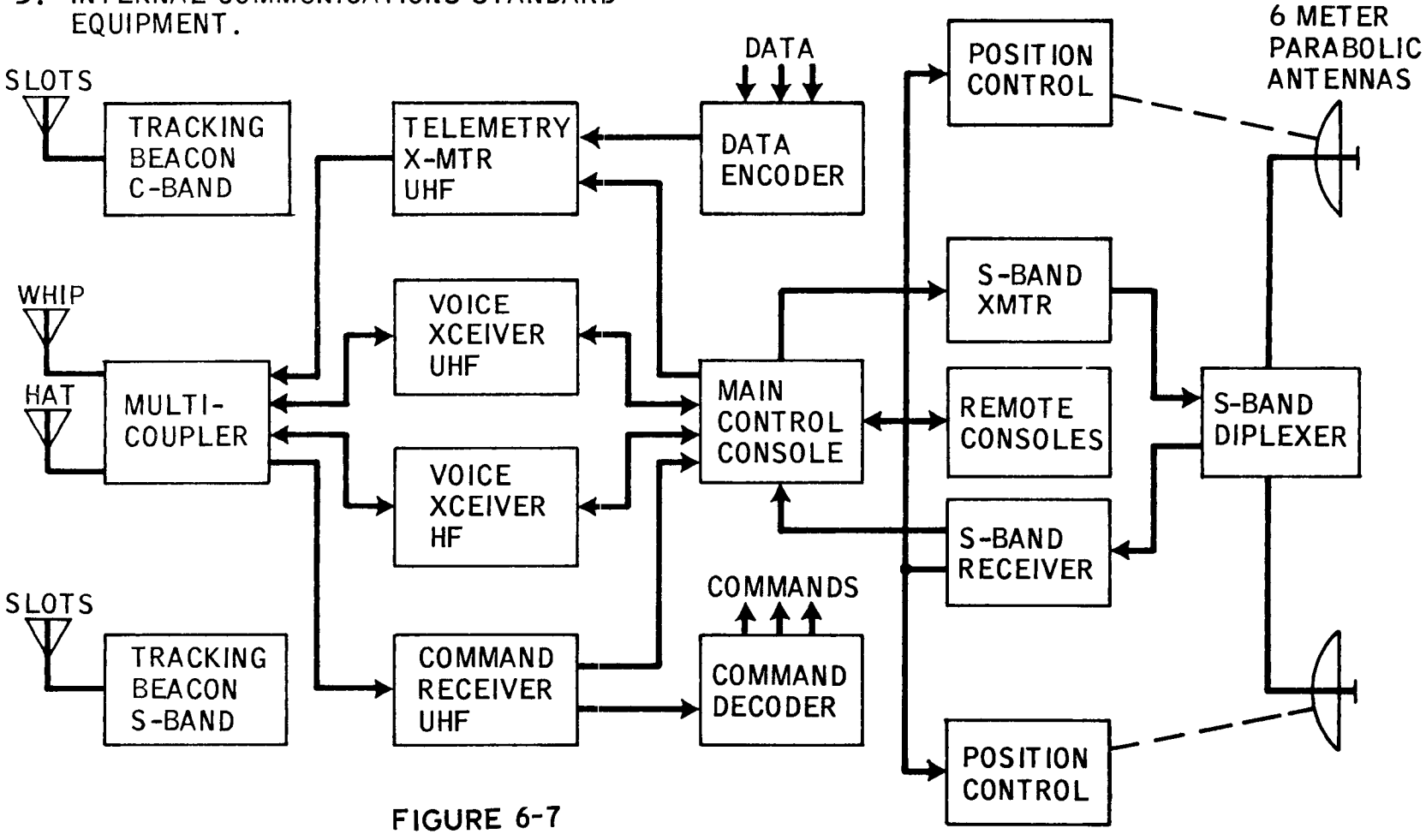

FIGURE 6-7

Since functions are largely implied by the nomenclature of Figure 6-7, a complete functional description is not given here. However, a few observations on the long-range communication problem are in order.

The Earth-to-spacecraft traffic is assumed to be voice, digital data, or ranging interrogation occupying an information bandwidth of about 4000 cps. Since all other factors in the range equation are known approximately, a spacecraft antenna gain of about 40 db is required. At 2115 mc, the diameter of a parabolic reflector should be 6 meters to achieve this gain.

The spacecraft-to-Earth problem, having the directive antenna of 40 db gain, yields a trade among distance, information bandwidth, and transmitter power. As distance from Earth increases, transmitter power should be increased or information rate decreased, or both.

Two antennas, which may be used in any combination for transmission and reception, are indicated for redundancy. It is quite likely, however, that one would be sufficiently reliable. Because beamwidth is less than 2°, fairly accurate pointing (at Earth) would be required. This could probably be achieved by slewing antennas to an optical sight and/or by closed-loop automatic tracking.

Because of the long duration of the mission, very good equipment reliability must be postulated. However, for the sake of a conservative estimate, it is best to assume a number of spare components to be required and on-board repair to be feasible.

Communication system weight including spares is estimated at 300 pounds. Estimated power is 150 watts with peaks to 200 watts.

e. Guidance and Navigation

The system used for spacecraft guidance and navigation is described in Section 4.5 of this report. Estimated system weight is 1000 pounds.

f. Attitude Control

Attitude control will be provided by a reaction control propulsion system. Little effort was devoted to the detailed study of this system. The estimated system weights for both Crocco and Symmetric missions is 1500 pounds.

g. Scientific Activity

A discussion of possible scientific activities is presented in Section 2 of this report. A system weight of 1000 pounds was allowed for an unspecified combination of experiments.

h. Power

Two SNAP-8 systems are used to provide continuous power during both Crocco and Symmetric missions. One unit would remain inactive unless its use be required eut to a failure of the first system. Backup emergency power is provided by batteries. There is some question whether the estimated 10,000 pounds system weight is sufficient to include both SNAP-8 systems, the emergency systems, and the shielding required to limit radiation to the living modules.

Although no detailed study of total power requirement has been made, it appears that it will not exceed 15 KW for a six man vehicle for either Crocco or Symmetric missions. A more detailed study of power requirements may show that a solar turboelectric system such as that currently being developed by the Sundstrand Corporation may be applicable.

Sundstrand has a contract with the Air Force to develop a 15 KW solar turboelectric system. At the current rate of funding flight prototype hardware will be available by 1968 and a man rated system available by 1970.

i. Propulsion

Two types of propulsion system have been studied for the EMPIRE mission, Nuclear and Chemical. Because of the classified nature of the required information, they are only briefly discussed here.

A study was made to determine nuclear engine and shield weights as a function of thrust level (Refs. 7-11). A typical spacecraft configuration was used to provide separation distance between crew and engine during the injection phase. Figure 6-8 shows engine plus shield weights as a function of thrust level. Tungsten shielding was used. The design vehicles were sized using an estimated nuclear engine specific impulse of 760 seconds.

Reentry and midcourse guidance propulsion is provided by chemical systems. Two specific impulse levels were used for the study, the currently

VARIATION OF NUCLEAR ENGINE PLUS SHIELD WEIGHT WITH THRUST

TUNGSTEN SHIELD DESIGNED TO LIMIT GAMMA RAY DOSE RATE TO 50 RADS/HR

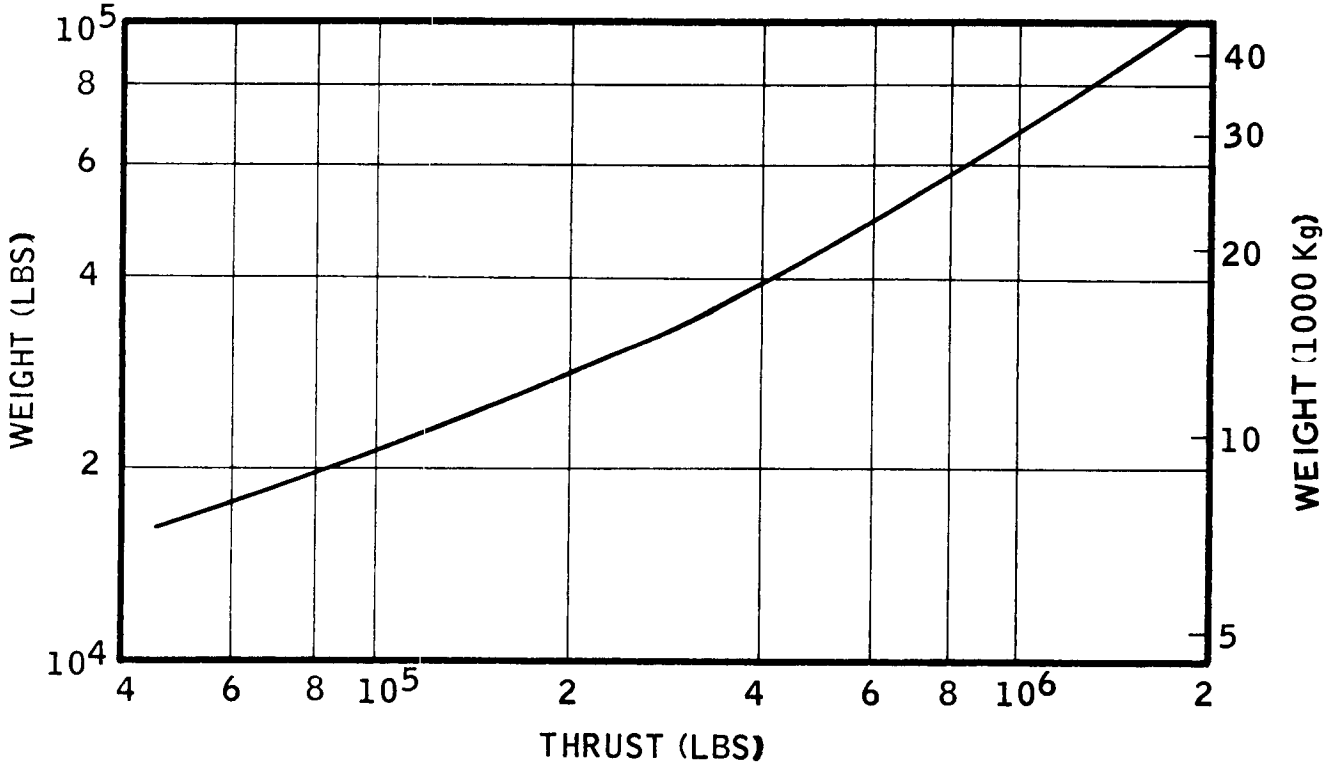

FIGURE 6-8

available storable chemical system impulse of 300 seconds (conservative) and an estimated 410 seconds which appears to be a reasonable value for tripropellant combinations. At the current level of development the tripropellant systems should be available in the EMPIRE time period*. Density of both types of propellant was assumed to be approximately that of water.

j. Summary of System Weights

A summary of all system weights is presented in Table 6.7.

TABLE 6.7

SUMMARY OF SUBSYSTEM WEIGHTS

	Weight (lbs)	Weight (Kg)
CROCCO TRAJECTORY		
Life Support	17,705	8,048
Thermal Control	1,000	455
Power	10,000	4,545
Attitude Control	1,500	682
Guidance	1,000	455
Communication	300	136
Furnishings	500	227
Instrumentation	1,000	455
Emergency Gear	1,200	545
Scientific Payload	1,000	455
	35,205	16,003
SYMMETRIC TRAJECTORY		
Life Support	21,810	9,914
Thermal Control	1,000	455
Power	10,000	4,545
Attitude Control	1,500	682
Guidance	1,000	455
Communication	300	136
Furnishings	500	227
Instrumentation	1,000	455
Emergency Gear	1,200	545
Scientific Payload	1,000	455
	39,310	17,869

* Based on Reference 12 and conversation with Aerojet-General personnel at Azusa facility.

6.3 REENTRY SYSTEM

Data presented in Section 5 showed the weight variation of an all-aerodynamic entry vehicle as a function of the parameter $\overline{V}_i$, the ratio of entry to circular velocity. It can be seen from Figure 5-6 that both Crocco and Symmetric missions require the addition of some type of energy dissipation system. This system is required to slow the entry from approach velocity to a velocity at which entry can be successfully executed.

A trade-off study was made on the variation of reentry system weight as a function of $\overline{V}_i$, assuming that a chemical propulsion system is used for energy dissipation. The system weight includes the weight of aerodynamic and propulsive systems required to provide the proper entry velocity for both Crocco and Symmetric entry conditions. The velocity increment that must be provided by the propulsion system under consideration was found from:

$$\Delta V_e = 7.92\,\overline{V}_i - V_a \qquad 6\text{-}1$$

where V_a = aerodynamic entry velocity = 11.5 km/sec for Crocco
= 15.8 km/sec for Symmetric

Using the velocity increments from equation 6-1, values of payload ratio, and the ratio of step launch weight to payload weight, were calculated as shown below, using the method outlined in Reference 13.

Mass ratio per step:
$$\mu = e^{\left(\frac{\Delta V}{g I_{sp}}\right)} \qquad 6\text{-}2$$

where ΔV = velocity increment per step

g = gravitational constant, 9.807 m/sec^2

I_{sp} = propellant specific impulse.

Payload ratio per step:
$$\psi_s = \frac{\lambda}{\frac{1}{\mu} - (1-\lambda)} \qquad 6\text{-}3$$

where λ = propellant loading fraction = $\dfrac{\omega_8}{\omega_o - \omega_{gd}}$

μ = mass ratio from step 1 above.

Total payload ratio:
$$\psi_t = \left(\psi_s\right)^n \qquad 6\text{-}4$$

where n = number of steps.

This total payload ratio was then applied to the aerodynamic entry vehicle weight consistent with the $\overline{V}_i$ originally under examination, and the total entry system weight calculated.

This trade-off was made for both Crocco and Symmetric trajectories and the results are shown in Figures 6-9 and 6-10, respectively. Chemical propulsion systems, with specific impulses of 300 and 410 seconds, and using one, two, and three stages were examined, and are shown on the figures noted.

It can be seen from Figure 6-9 that for a system with a specific impulse of 410 seconds, a minimum system weight occurs in the area of $\overline{V}_i$ = 1.64. Little decrease in weight can be realized by the use of staging. Thus, the design point entry vehicle for the Crocco trajectory was selected as a single stage, chemical system (I_{sp} = 410 seconds) with a total system weight of 17,300 pounds. Similarly, from Figure 6-10 the design point entry vehicle for the Symmetric trajectory was selected as a two stage, chemical system (I_{sp} = 410 seconds), with a total system weight of 33,600 pounds. In both curves, the advantage of increasing propellant specific impulse is obvious.

Multi-stage nuclear systems were also examined, but they were discarded because of the long term cryogenic storage problem and large tank sizes attendant with liquid hydrogen.

6.4 VEHICLE DESIGN

The data presented in the previous sections and in the preceeding portions of this section were used as the basis for the systematic development of the vehicle weight. Vehicle configurations were developed as necessary to assist in, as well as justify the vehicle weight synthesis. The Earth entry vehicle described in Section 6.3 was used as final payload for the EMPIRE vehicle, and the vehicle was developed, in reverse, along the trajectory.

The EMPIRE vehicle was assumed to have three distinct phases; (1) injection into interplanetary trajectory; (2) on interplanetary trajectory; and (3) Earth entry. To the Earth entry system then, was added those components necessary for crew survival and mission objective completion during the interplanetary trajectory. This weight was used as payload for the trajectory correction system, which includes both midcourse correction and planetary approach correction energy requirements.

REENTRY SYSTEM WEIGHT AS A FUNCTION OF
VELOCITY REMOVED AERODYNAMICALLY
CROCCO TRAJECTORY

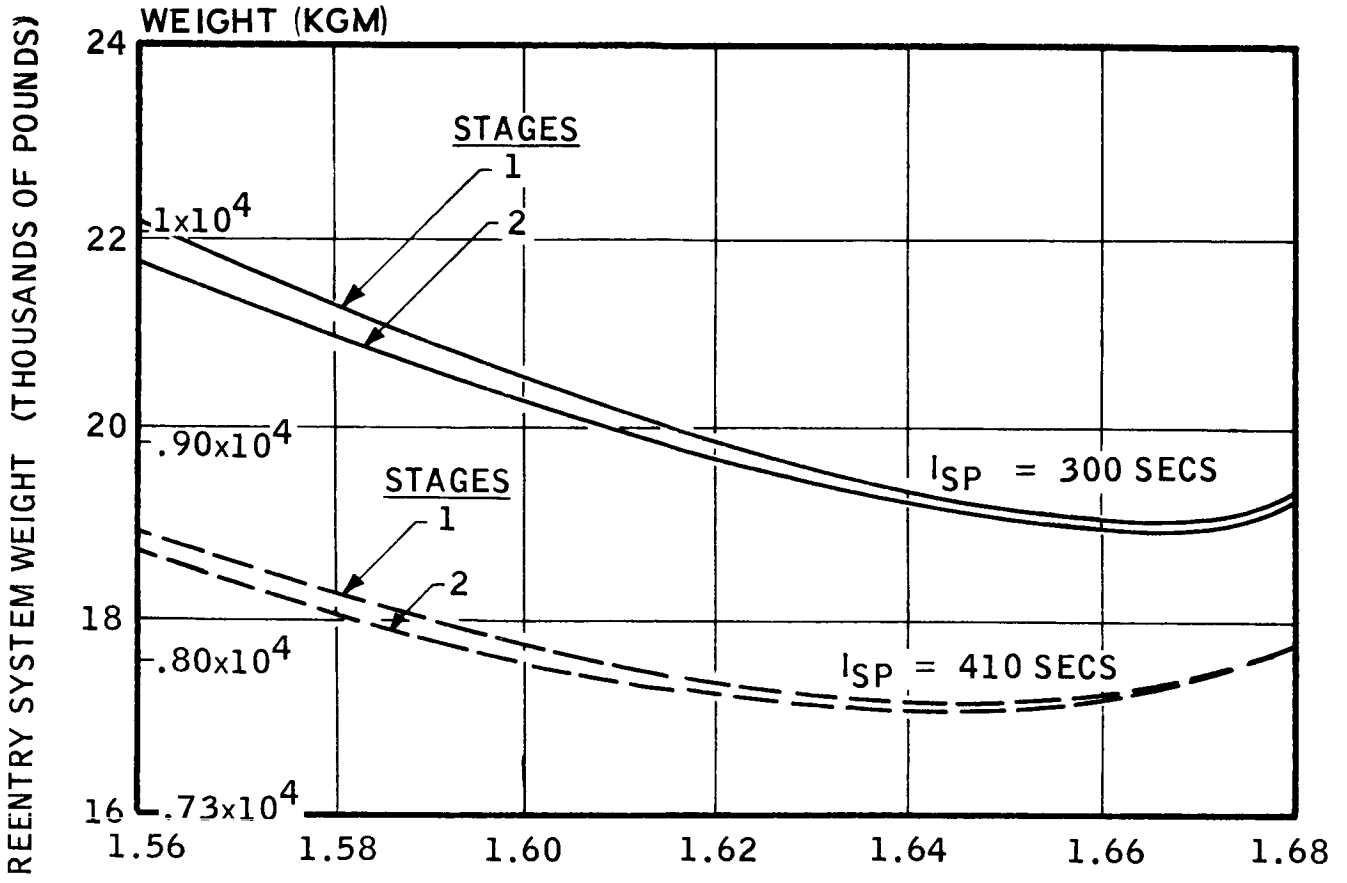

FIGURE 6-9

REENTRY SYSTEM WEIGHT AS A FUNCTION OF VELOCITY REMOVED AERODYNAMICALLY SYMMETRIC TRAJECTORY

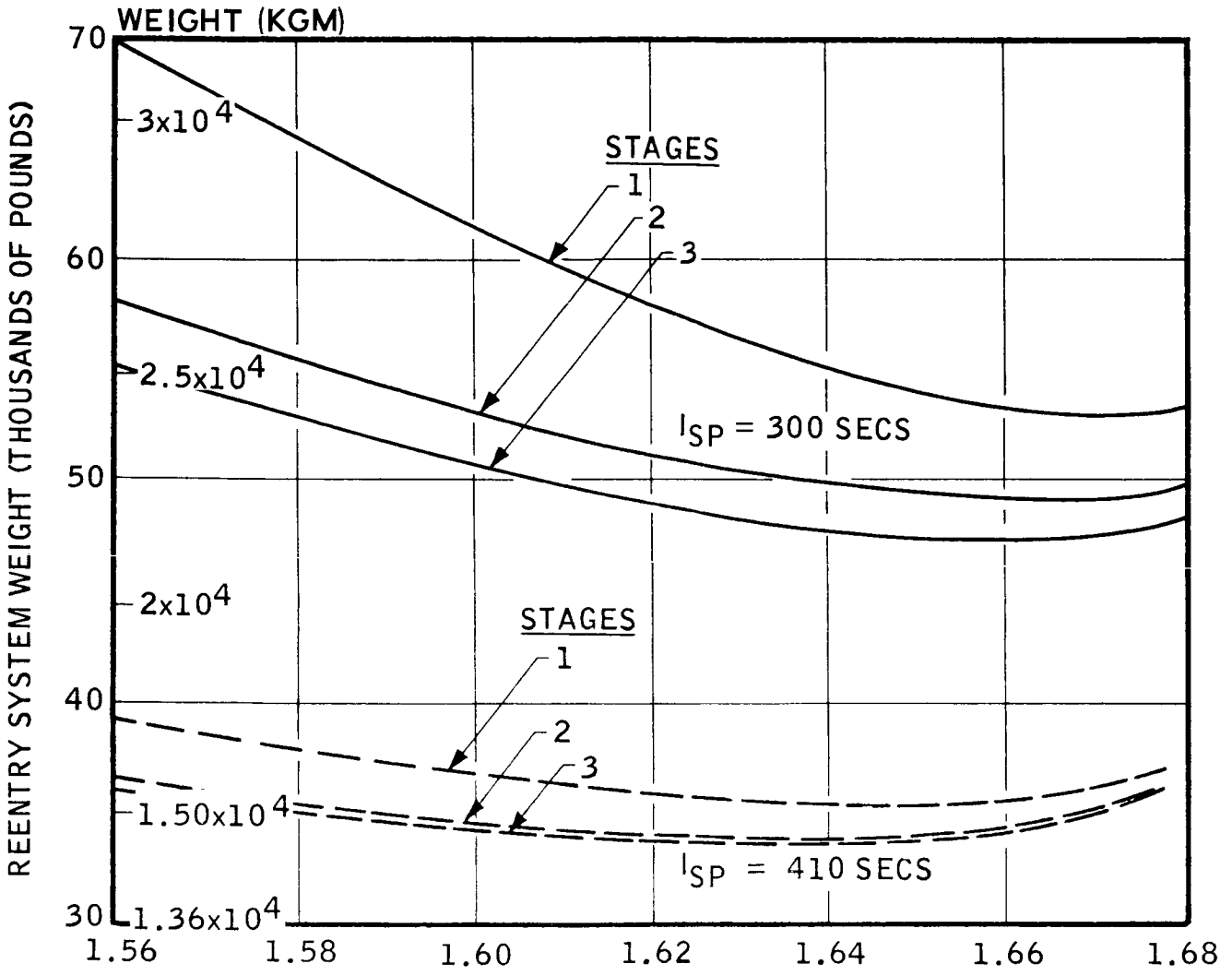

FIGURE 6-10

The vehicle weight on interplanetary trajectory was then used as the payload for the injection system, and the Earth orbit weight of the spacecraft calculated using the same technique outlined for the Earth entry vehicle in Section 6.3

a. Nuclear Symmetric Injection Vehicle

Vehicle weights and configurations for both Crocco and Symmetric vehicles were derived using the method described above. This method will be shown in detail for the design point vehicle, a nuclear injection symmetric trajectory vehicle.

(1) Weight Synthesis

· Trajectory Correction System

The propulsion system was required to provide trajectory correction velocity increments of .62 km/sec to the spacecraft on its planetary trajectory. A chemical system with a specific impulse of 410 seconds and a propellant loading fraction of .90 was used. The relatively high value of propellant loading fraction was made possible by using the vehicle shell structure to provide meteoroid protection for the trajectory correction system. The propulsion system was sized using the fixed weights as listed.

Component	Weight (Pounds)	
Entry System	33,600	
Radiation Shelter	40,000	
Living Module	9,000	
On-Board Systems	35,300	
Upper Stage Injection Tanks	12,000	
Fixed Weight (1)		129,900 pounds

The propulsion system weight was calculated using the technique described in Section 6.3, Equations 6-1, 6-2, 6-3, and 6-4.

$$W_{ps} = W_{gd} \ (\psi - 1) \qquad 6\text{-}5$$

where W_{ps} = Propulsion system weight

W_{gd} = Payload weight

ψ = Payload ratio = $\frac{W_o}{W_{gd}}$

W_o = Total weight

W_{ps} = 129,900 (1.186-1) = 24,100 pounds

The propellant weight was calculated from:

$$W_8 = W_{ps} \lambda \qquad 6\text{-}6$$

W_8 = 21,700 pounds

The weight of engine, tanks, lines, etc., was found from:

$$W'_{ps} = W_{ps} - W_8 = 2{,}400 \text{ pounds} \qquad 6\text{-}7$$

Thus the weight of the on-trajectory spacecraft was:

Fixed Weight (1)	129,900	
Trajectory Correction Propellant	21,700	
Trajectory Correction Propulsion Sys.	2,400	
Fixed Weight (2)		154,000 pounds

- Abort

The energy requirements for the abort system were established in Section 6.1 at 3.0 km/sec. The trade-off study made on the Earth entry vehicle system indicated that the minimum system weight occurs slightly below a $\overline{V}_i = 1.64$. Thus the reentry propulsion system, already included in the fixed weight listed must supply approximately 3.0 km/sec ΔV during reentry and therefore is capable of providing the energy required for the abort operation for distances within about 3 Earth radii.

- Trajectory Injection

The injection propulsion system was required to provide a velocity increment of 5.3 km/sec to the entire spacecraft. A nuclear engine system using liquid hydrogen propellant and having a specific impulse of 760 seconds was used. The effect of staging was considered by calculating the payload ratio (launch weight to payload weight) for a one, two, and three stage system. Values of propellant loading fraction of .88 were used, assuming that the weight of the nuclear engine and shield were a part of the payload. This was assumed throughout the study because of the tenuous nature of nuclear engine and shield weights. The payload ratios were calculated by using the expression shown in Section 6.3, Equation 6-3.

$$\psi = \frac{\lambda}{\frac{1}{\mu} - (1-\lambda)}$$

The values are shown in tabular form below.

Number of Stages (n)	Payload Ratio (ψ)
1	2.438
2	2.301
3	2.284

The decrease in payload ratio, and hence in total vehicle weight, is marked between the one and two stage systems. While there is some further reduction in a three stage system, it was felt that this reduction was offset by an increase in functional complexity and a possible reduction in reliability. For this vehicle, then a two-stage tank system was used, with the second-stage tank retained for meteoroid protection for subsequent propellant systems. A single injection engine system was assumed, and a portion of the first stage tanks retained as structural support for the engine system. This is reflected in the manipulation of system weights outlined below. The fixed weights used in sizing the injection second stage were:

Component	Weight (Pounds)	
Fixed Weight (2)	154,000	
Less Second Stage Tanks	- 12,000*	
First Stage Support Tank	8,000	
Engine and Shield	18,300	
Fixed Weight (3)		168,300 pounds

The propulsion weight was calculated from:

$$W_{ps} = W_{gd} (\psi - 1) \qquad \text{6-5 (repeated)}$$

$$= 168,300 \ (.517)$$

$$W_{ps} = 87,000 \text{ pounds}$$

The propellant and propellant system weights were calculated as before;

$$W_8 = W_{ps} \lambda \qquad \text{6-6 (repeated)}$$

$$W_8 = (87,000) \ (.88) = 76,600 \text{ pounds}$$

$$W'_{ps} = W_{ps} - W_8 = 10,400 \text{ pounds} \qquad \text{6-7 (repeated)}$$

The spacecraft weight at the completion of first stage burning is:

Fixed Weight (3)	168,300	
Second Stage Injection Propellant	76,600	
Second Stage Injection Propellant Sys.	10,400	
Fixed Weight (4)		255,300 pounds

* Second stage tank weight is included in second stage propellant loading fraction parameter.

The fixed weights used in sizing the injection first stage were:

Component	Weight (Pounds)	
Fixed Weight (4)	255,300	
Less First Stage Tank	- 8,000	
Fixed Weight (5)		247,300 pounds

As before, the propellant system weights were calculated and found to be:

W_8 = 112,400 pounds
W'_{ps} = 15,300 pounds

Thus the on-orbit spacecraft weight was calculated from:

Component	Weight (Pounds)	
Fixed Weight (5)	247,300	
First Stage Injection Propellant	112,400	
First Stage Injection Propellant Sys.	15,300	
On-Orbit Spacecraft Weight		375,000 pounds

A summary of the weights derived above is presented in Table 6.8.

(2) Spacecraft Configuration

The configuration developed during the vehicle weight synthesis is shown in three view form in Figure 6-11. The in-board profile depicts the interior arrangement of the trajectory spacecraft. The Earth reentry vehicle is oriented so that injection and separation g forces will be received by the crew in the optimum manner (chest to back). The entry retro-pack is a two-stage chemical propellant system which also functions as the abort system in the event of a cataclysmic failure within a 3 Earth radii range. The command center/radiation shelter is located so as to provide centralized location from the living modules, which are extended through telescoping cylinders. Protection for the crew from

TABLE 6.8

SYMMETRIC TRAJECTORY VEHICLE

WEIGHT SUMMARY FOR NUCLEAR INJECTION

	Weight (lbs)	Weight (lbs)
Earth Orbit Spacecraft		375,000
First Stage Injection Propellant	112,400	
First Stage Burnout		262,600
First Stage Perimeter Tanks	7,300	
Second Stage Ignition		255,300
Second Stage Injection Propellant	76,600	
Second Stage Burnout		178,700
First Stage Center Tank	8,000	
Injection Engine & Shield	18,300	
On-Orbit Spacecraft		152,400
Trajectory Correction Propellant	21,700	
Earth Approach Burnout		130,700
Radiation Shelter	40,000	
Living Modules	9,000	
On-Board Systems	35,300	
Second Stage Tanks	10,400	
Trajectory Correction Booster	2,400	
Earth Reentry System		33,600
Entry Propellant (First Stage)	11,100	
First Stage Entry Burnout		22,500
First Stage Booster	1,500	
Entry Propellant (Second Stage)	6,900	
Second Stage Entry Burnout		14,100
Second Stage Booster	900	
Aerodynamic Entry Vehicle		13,200

EMPIRE VEHICLE - SYMMETRIC TRAJECTORY - NUCLEAR INJECTION

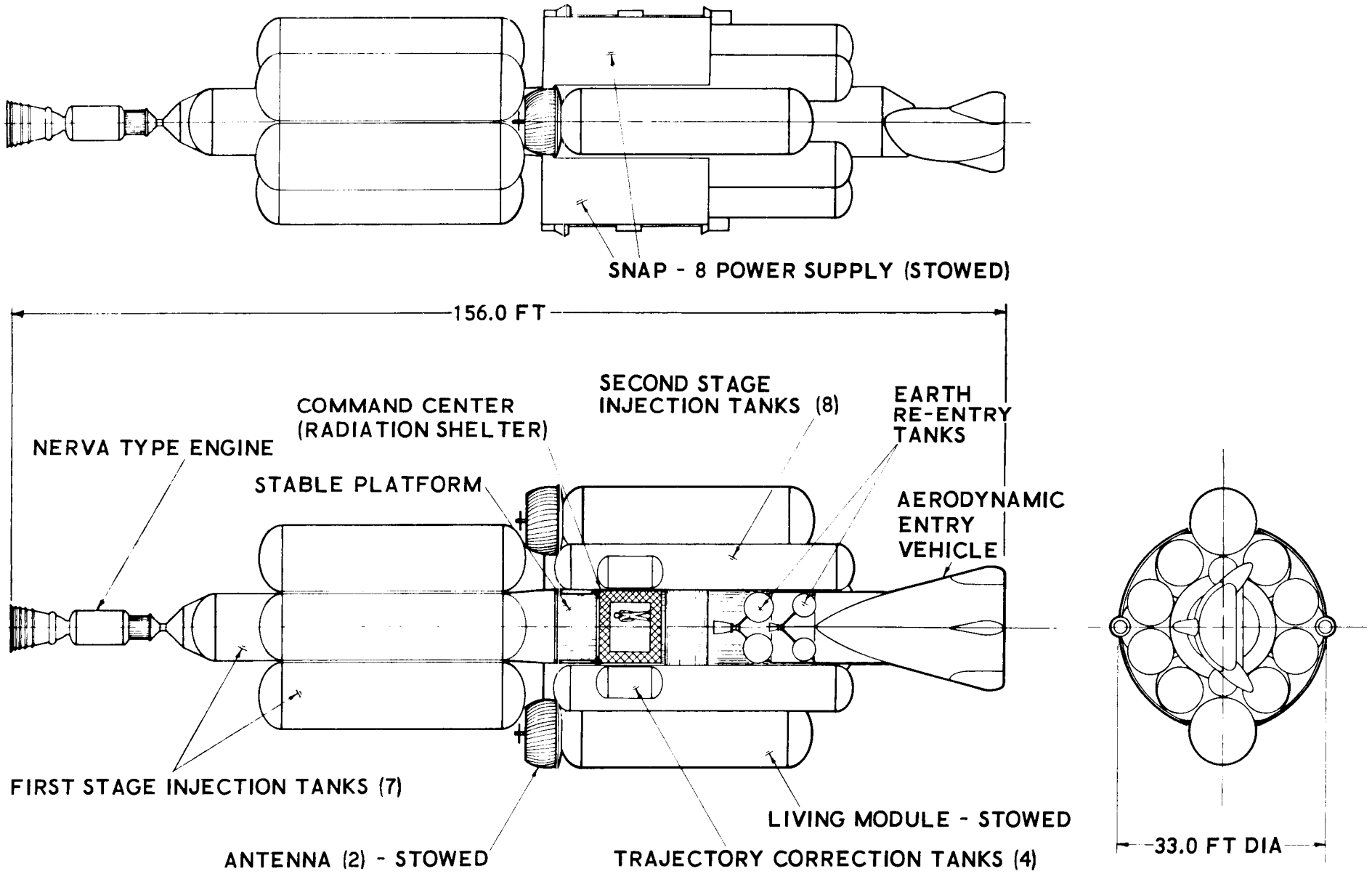

FIGURE 6-11

solar radiation is provided by 50 cm of polyethylene which completely surrounds the command center. An area set aside for an inertial platform and weightless experimentation is located just aft of the command center. Four chemical propellant tanks which provide trajectory correction energy are placed around the command center.

This entire core is surrounded by eight second stage injection tanks. These tanks are retained throughout the mission to provide meteoroid protection for the propellant systems contained within the core.

The top view depicts the vehicle before and during first stage injection. First stage injection propellant is contained in seven cylindrical tanks. The center tank also serves as structural support for the injection engine(s) assembly. The living modules are stowed, as they will be during Earth launch and injection. The antennas and SNAP-8 power supplied are also stowed until trajectory is attained.

Figure 6-12 shows the staging sequence employed from trajectory injection to Earth entry. The vehicle is shown during first stage injection with propellant from the seven tanks being fed into the main engine. The crew is located in the reentry (abort) vehicle. Abort is possible up to a distance of approximately 3 Earth radii. At the completion of first stage burning, the six peripheral tanks are jettisoned, leaving the center tank as structural carry-through between the injection engine and the remainder of the vehicle.

During second stage injection, the propellant in the second stage tanks is fed into the main engine. At the completion of second stage burning, the main engine and first stage center tank are jettisoned.

After trajectory has been established, one SNAP-8 power supply and the two living modules are deployed, and a spacecraft rotation of approximately 3 rpm begun. Midcourse correction and planetary approach correction is applied through small systems fed from four tanks located around the radiation shelter. A second SNAP-8 is carried to insure adequate power for the entire mission. In the event of a malfunction, the first SNAP-8 is jettisoned and the second deployed.

After Earth approach corrections are complete, the crew enters the reentry vehicle and the reentry system is separated by small posigrade solid units. The entry retro-pack decelerates the reentry vehicle to a velocity at which full aerodynamic entry is feasible.

EMPIRE VEHICLE - STAGING SEQUENCE - SYMMETRIC TRAJECTORY NUCLEAR INJECTION

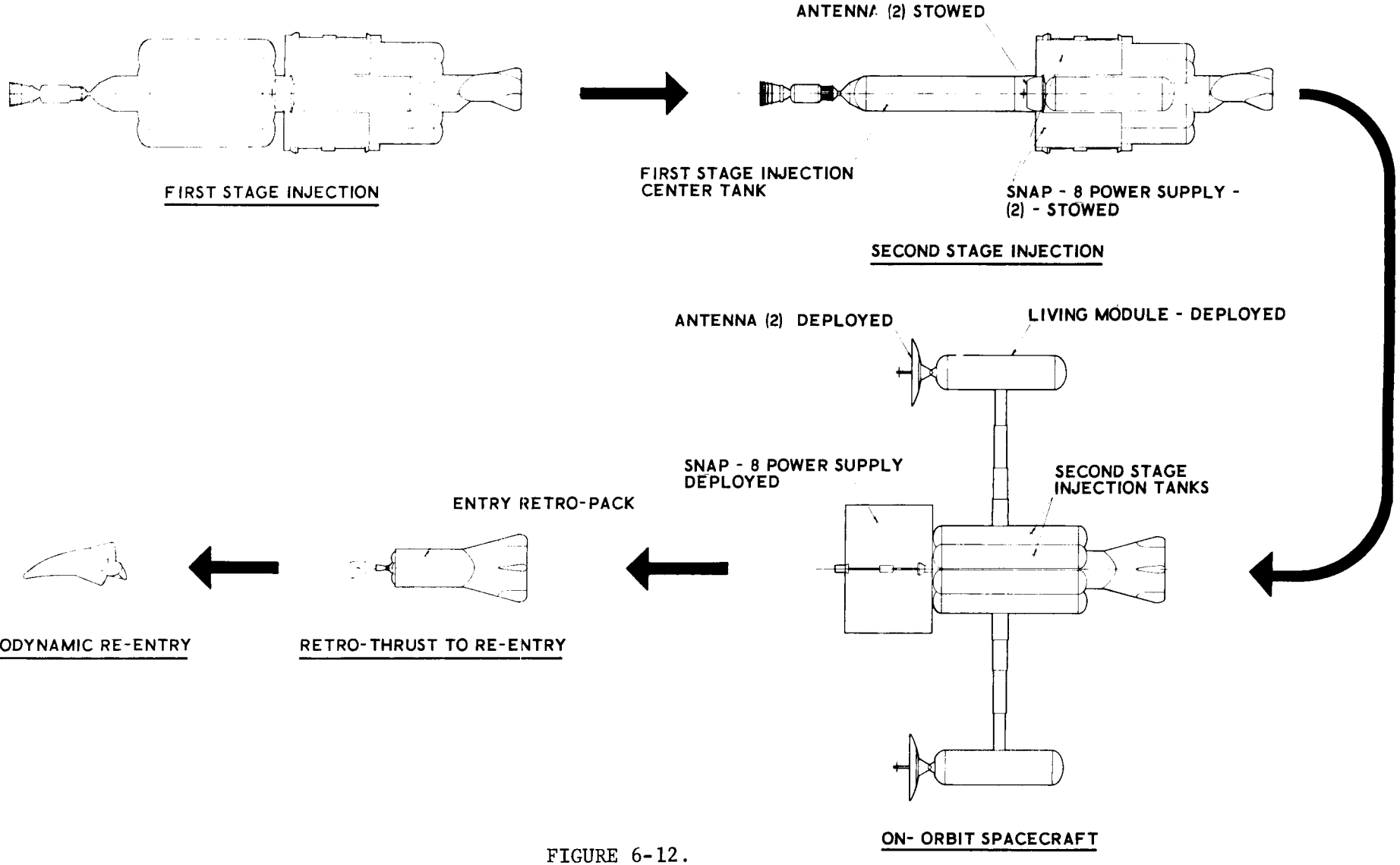

FIGURE 6-12.

(3) Trajectory Injection Engine Burning Time

Two of the most important parameters in nuclear engine performance are thrust and burning time. In the time available for EMPIRE mission development, nuclear engine thrusts above approximately 50,000 pounds appear to be questionable, therefore the burning time was calculated based upon that value. The burning time was calculated from:

$$t = \frac{W_8 I_{sp}}{F} \qquad 6\text{-}8$$

where t = burning time in seconds

W_8 = propellant weight in pounds

I_{sp} = specific impulse in lb sec/lb

F = thrust in pounds

$$t = \frac{(112{,}400 + 76{,}600)\ (760)}{50{,}000}$$

$$t = 2{,}873 \text{ seconds}$$

This exceeds current estimates of burning time, which are limited by reactor material considerations. The effect on burning time and spacecraft weight with variations in nuclear engine thrust were calculated. The values of fixed weights shown above in the derivation of the nuclear symmetric vehicle were used, along with nuclear engine and shield weights from Figure 6-8. The method used to develop these data was identical to that presented with the exception that weight increments for first and second stage tanks were included. The data are presented in graphical form in Figure 6-13. The curve shows that the nuclear engine burning time decreases with increasing thrust, while the overall increase in spacecraft weight for the wide range in thrust is not severe.

(4) Effect of Propellant Specific Impulse

During the early phases of this study program, it became quite apparent that the effect of the specific impulse of the various propellant systems used was significant. The data presented in Figure 6-14 were generated in order to determine the magnitude of this effect.

NUCLEAR ENGINE BURNING TIME & SPACECRAFT WEIGHT
AS FUNCTIONS OF ENGINE THRUST

SINGLE ENGINE I_{SP} = 760 SEC.

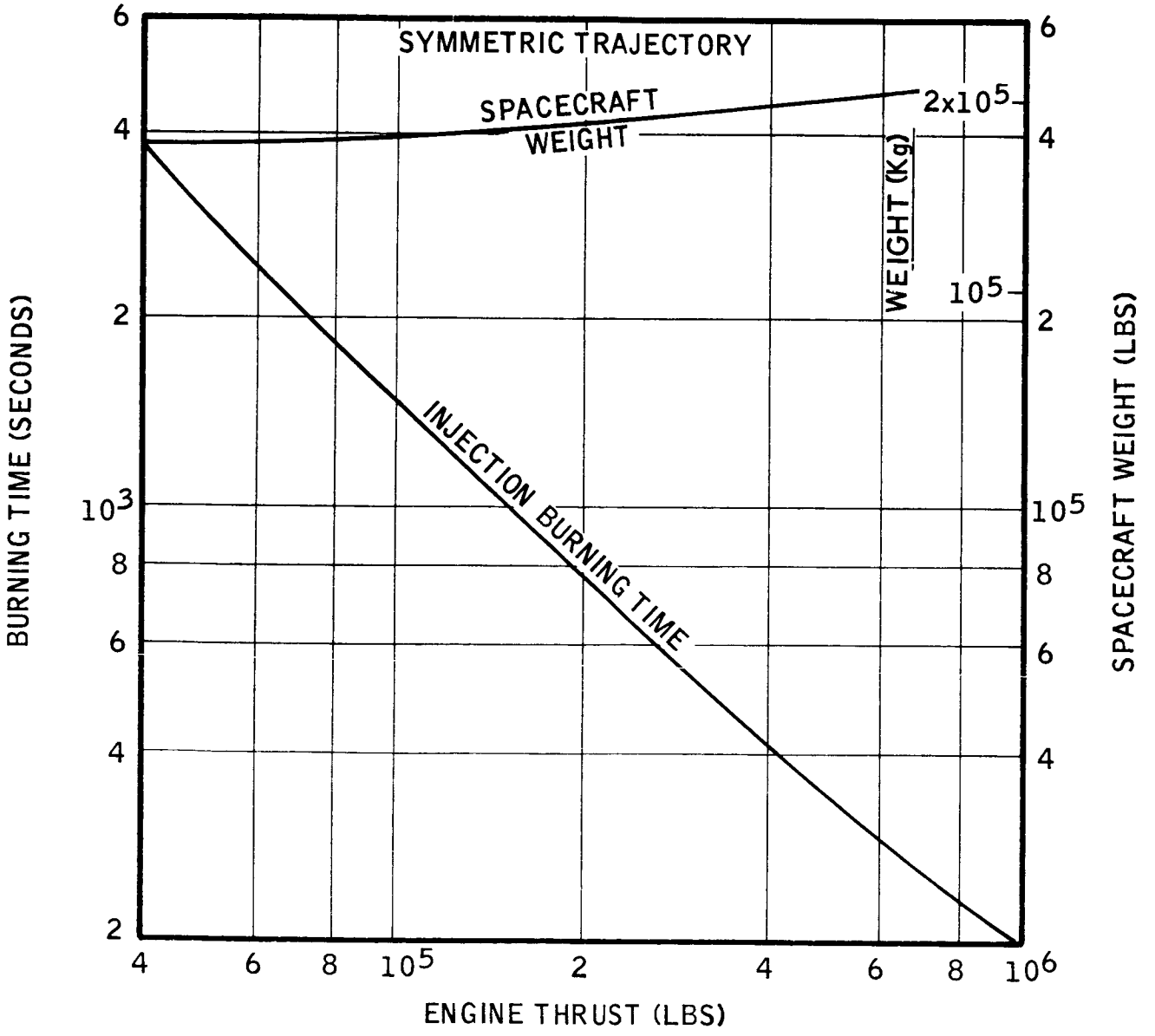

FIGURE 6-13

SYMMETRIC NUCLEAR VEHICLE WEIGHT AS A FUNCTION OF PROPELLANT LOADING FRACTION, R.V. & TRAJECTORY CORRECTION I_{SP}, AND NUCLEAR ENGINE I_{SP}

(SINGLE 50,000 LB_F ENGINE)

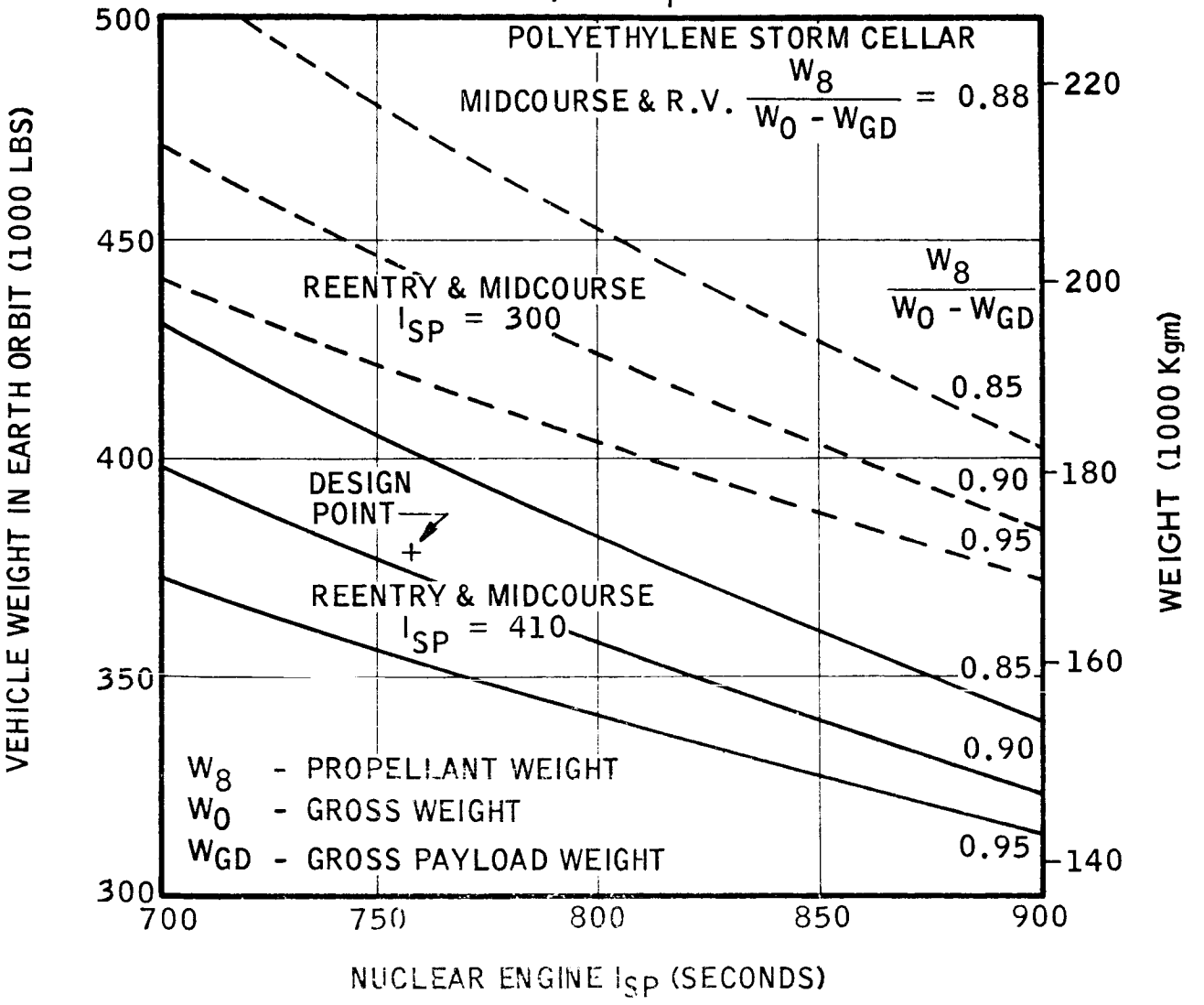

FIGURE 6-14

It can be seen that if the lower value of reentry and midcourse system specific impulse had been used, an on-orbit spacecraft weight in the neighborhood of 450,000 pounds would have resulted. Similarly, increases in the injection system specific impulse over the 760 seconds used would result in even further reduction of the spacecraft weight. The range of propellant loading fractions were included to provide an envelope of reasonable spacecraft weights for the systems considered.

b. Nuclear Crocco Injection Vehicle

(1) Weight Synthesis

The technique used to synthesize the weight and configuration of the symmetric trajectory vehicle was employed in sizing the Crocco trajectory vehicle. One major difference occurred, however, in that the extremely large abort velocity increment required (11.95 km/sec) resulted in abort system of considerable magnitude. This, in return, influenced the injection propulsion system and in conjunction with the relatively large injection velocity of the Crocco mission, resulted in an on-orbit spacecraft weight that was greatly in excess of that calculated for the Symmetric mission. A summary of the Crocco trajectory vehicle weight is given in Table 6.9.

(2) Spacecraft Configuration

This vehicle (see Figure 6-15) features nuclear propulsion systems for injection and abort, and chemical propulsion for trajectory correction and reentry. The reentry vehicle is oriented as shown to position the crew in an optimum manner for exposure to injection and abort or entry separation forces. The chemical reentry system is affixed to the pointed end of the reentry vehicle, and the abort system, using a single NERVA type engine, is attached to the reentry vehicle base. If abort is necessary, the reentry propulsion system can serve as a posigrade separation for the abort package. If abort is not required, the entire abort package may be jettisoned, or certain components retained if useful. The reentry retro-pack, trajectory correction propellant system, and command module/radiation shelter are located within the ring of second stage injection tanks, which are retained to provide meteoroid protection. Six first stage perimeter tanks are clustered about a center tank, which also serves as structural carry-through for the engine system. This center tank is retained throughout first and second stage injection and then jettisoned, complete with nuclear engine and shield.

TABLE 6.9

CROCCO TRAJECTORY VEHICLE

WEIGHT SUMMARY FOR NUCLEAR INJECTION

	Weight (lbs)	Weight (lbs)
Earth Orbit Spacecraft		2,243,000
First Stage Injection Propellant	1,225,000	
First Stage Burnout		1,018,000
First Stage Perimeter Tanks	121,000	
Second Stage Ignition Weight		897,000
Second Stage Injection Propellant	490,000	
Second Stage Burnout		407,000
First Stage Center Tank	15,000	
Injection Engine & Shield	44,300	
Abort-First Stage Propellant	92,000	
Abort-First Stage Booster	10,200	
Abort-Second Stage Propellant	39,000	
Abort-Second Stage Booster	4,250	
Abort-Engine & Shield	18,300	
On-Orbit Spacecraft		183,950
Trajectory Correction Propellant	27,900	
Earth Approach Burnout		156,050
Radiation Shelter	40,000	
Living Modules	7,500	
On-Board Systems	31,500	
Second Stage Tanks	55,950	
Trajectory Correction Booster	3,800	
Earth Reentry System		17,300
First Stage Entry Propellant	2,000	
First Stage Entry Booster	300	
Second Stage Entry Propellant	1,760	
Second Stage Entry Booster	240	
Aerodynamic Entry Vehicle		13,000

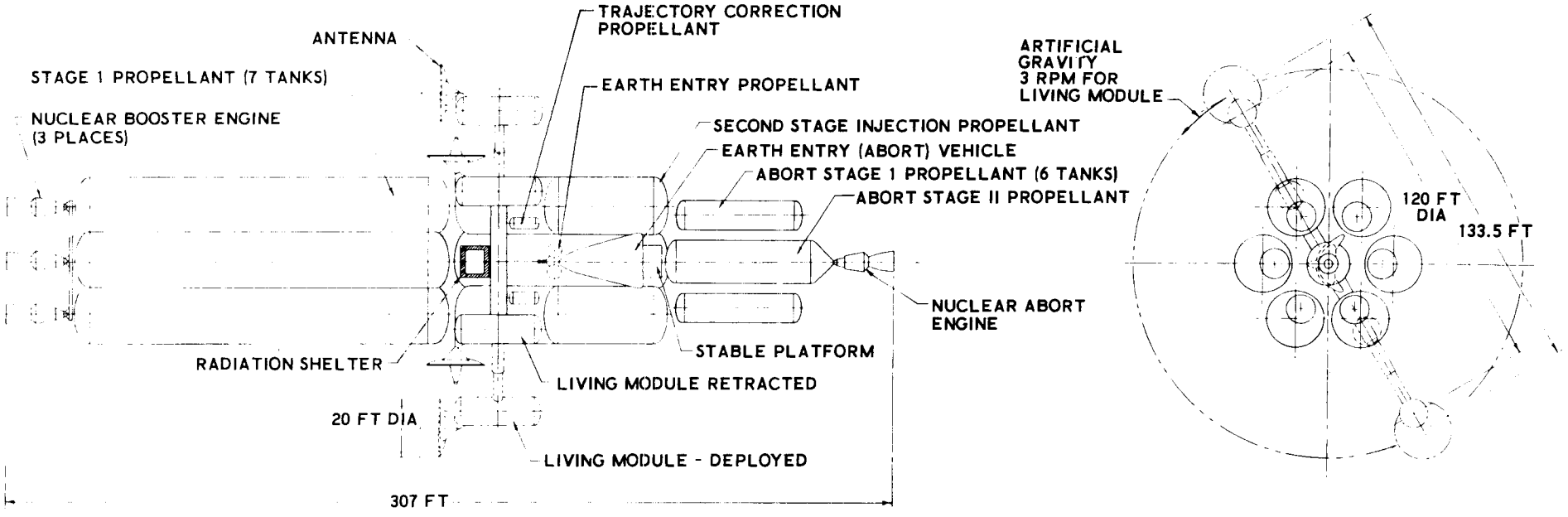
CROCCO TRAJECTORY DESIGN POINT VEHICLE
TRAJECTORY CORRECTION PROPELLANT
ANTENNA
EARTH ENTRY PROPELLANT
STAGE 1 PROPELLANT (7 TANKS)
NUCLEAR BOOSTER ENGINE (3 PLACES)
SECOND STAGE INJECTION PROPELLANT
EARTH ENTRY (ABORT) VEHICLE
ABORT STAGE 1 PROPELLANT (6 TANKS)
ABORT STAGE II PROPELLANT
NUCLEAR ABORT ENGINE
STABLE PLATFORM
RADIATION SHELTER
LIVING MODULE RETRACTED
20 FT DIA
LIVING MODULE - DEPLOYED
307 FT
ARTIFICIAL GRAVITY 3 RPM FOR LIVING MODULE
120 FT DIA
133.5 FT

FIGURE 6-15.

The living modules, shown in the stowed position for injection are extended, as is one of the two SNAP-8 power supplies and both communication antennas. Attitude control systems then orient the vehicle properly and rotation is initiated.

(3) Trajectory Injection Engine Burning Time

The burning time for the nuclear engine system used on the Crocco nuclear vehicle was calculated and found to be at least an order of magnitude above what seems to be the practical upper limit of current projections for nuclear reactor operational capability. Therefore, the need for increasing the engine thrust and reducing this burning time is of even greater importance if the Crocco trajectory is to be seriously considered. As in the case of the symmetric trajectory, values of fixed weight shown in Table 6.9 for the Crocco vehicle were used, and combined with nuclear engine and shield weights from Figure 6-8 along with injection tank weight increments, to derive the variation in spacecraft weight and nuclear engine burning time as a function of nuclear engine thrust. These data are presented graphically in Figure 6-16 and the most important information presented is that a 700,000 pound thrust engine is required to limit nuclear engine burning time to what appears to be the capability of current reactor design. This fact alone, in view of the criticality of the launch windows and limited thrust of the current reactor systems would render the Crocco trajectory vehicle technically infeasible. In view of these and other considerations, the Crocco trajectory vehicle was not given further effort in the present study.

c. Chemical Symmetric Injection Vehicle

(1) Weight Synthesis

The problem areas of nuclear engine thrust and burning time led to a consideration of utilizing more conventional chemical propulsion systems for the EMPIRE mission. The weight synthesis method described in this section for the nuclear symmetric vehicle was used in sizing two chemical symmetric vehicles. The chemical injection vehicles used the same specific impulse propellant systems for reentry (abort), trajectory correction, and injection. Table 6.10 summarizes the major weight items of the two vehicles.

NUCLEAR ENGINE BURNING TIME & SPACECRAFT WEIGHT AS FUNCTIONS OF ENGINE THRUST

SINGLE ENGINE I_{SP} = 760 SEC.

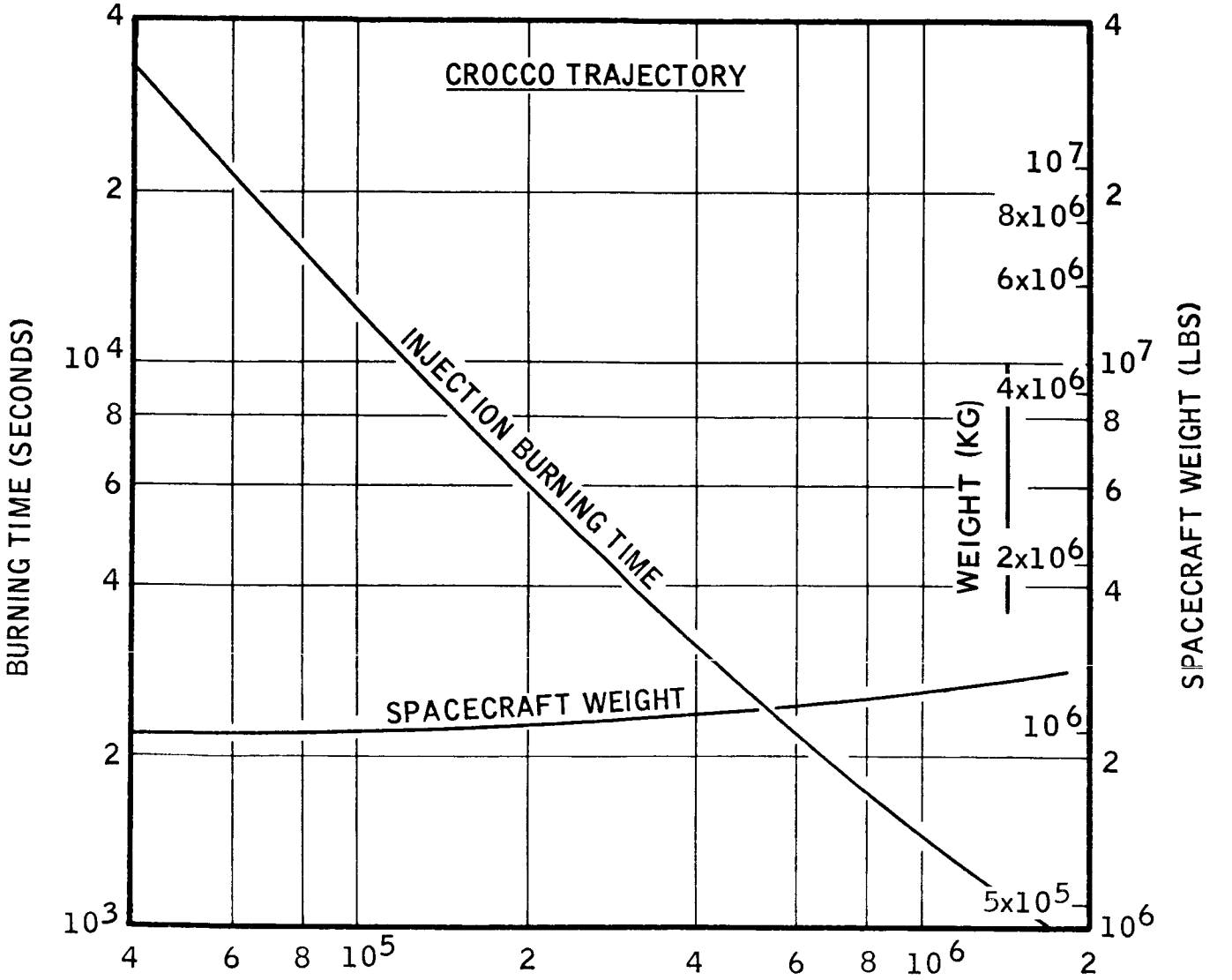

FIGURE 6-16

TABLE 6.10

SYMMETRIC TRAJECTORY VEHICLE

WEIGHT SUMMARY FOR CHEMICAL INJECTION

	WEIGHT IN POUNDS	
	I_{sp} = 300 sec	I_{sp} = 410 secs
Earth Orbit Spacecraft Weight	1,859,000	701,000
First Stage Burnout Weight	756,000	362,000
Second Stage Ignition Weight	576,000	316,000
Second Stage Burnout Weight	234,000	163,000
On-Orbit Spacecraft Weight	217,600	160,400
Earth Approach Burnout Weight	176,600	138,800
Earth Reentry System Weight	48,700	33,600
Aerodynamic Entry Vehicle	14,200	13,200

(2) Spacecraft Configurations

An in-board profile of the two vehicles is shown in Figure 6-17. The vehicles are generally arranged identical to the nuclear injection Symmetric vehicle with the exception that the first stage engine(s) and tank(s) are ejected at the completion of first stage burning. In both vehicles, the second stage engine(s) is ejected at the completion of burning while the tanks are retained to provide meteoroid protection for the trajectory correction and entry propulsion systems. A tunnel in the ring of second stage injection tanks provides ready access between the main areas of manned occupany and the reentry vehicle.

(3) Effect of Propellant Specific Impulse

The effect of propulsion specific impulse on chemical Symmetric vehicle weight was calculated and is presented graphically in Figure 6-18. Once again the significant reduction in spacecraft weight with specific impulse increase is apparent. The values of propellant loading fraction serve to establish the range of reasonable weights for the propulsion system selected. The two design point vehicles (specific impulses of 300 and 410 seconds) are shown on the curve at 1,859,000 pounds and 701,000 pounds respectively.

(4) Effect of Payload Weight Variation

In establishing the system and subsystem weights, (Section 6.2) it was realized that certain weight variations would occur. The data presented in Figure 6-19 was generated to show the variation in spacecraft weight for the Nuclear Symmetric and Chemical Symmetric (I_{sp} = 410 secs) vehicles, as the on-trajectory payload weight was varied. These data were generated by varying the weight of the spacecraft in its trajectory configuration and applying the payload ratios for trajectory correction and trajectory injection as shown for the nuclear Symmetric vehicle. From Figure 6-19, if the payload increased by 10,000 pounds, the nuclear Symmetric vehicle weight would increase from 375,000 to 401,000 pounds.

d. Configuration Summary and Comparison

The vehicle envelopes shown in Figure 6-20 serve to provide a general comparison of the size and weight of the various vehicles considered during the study. It is interesting to note that the

EMPIRE VEHICLE - COMPARISON OF CHEMICAL INJECTION SYSTEMS

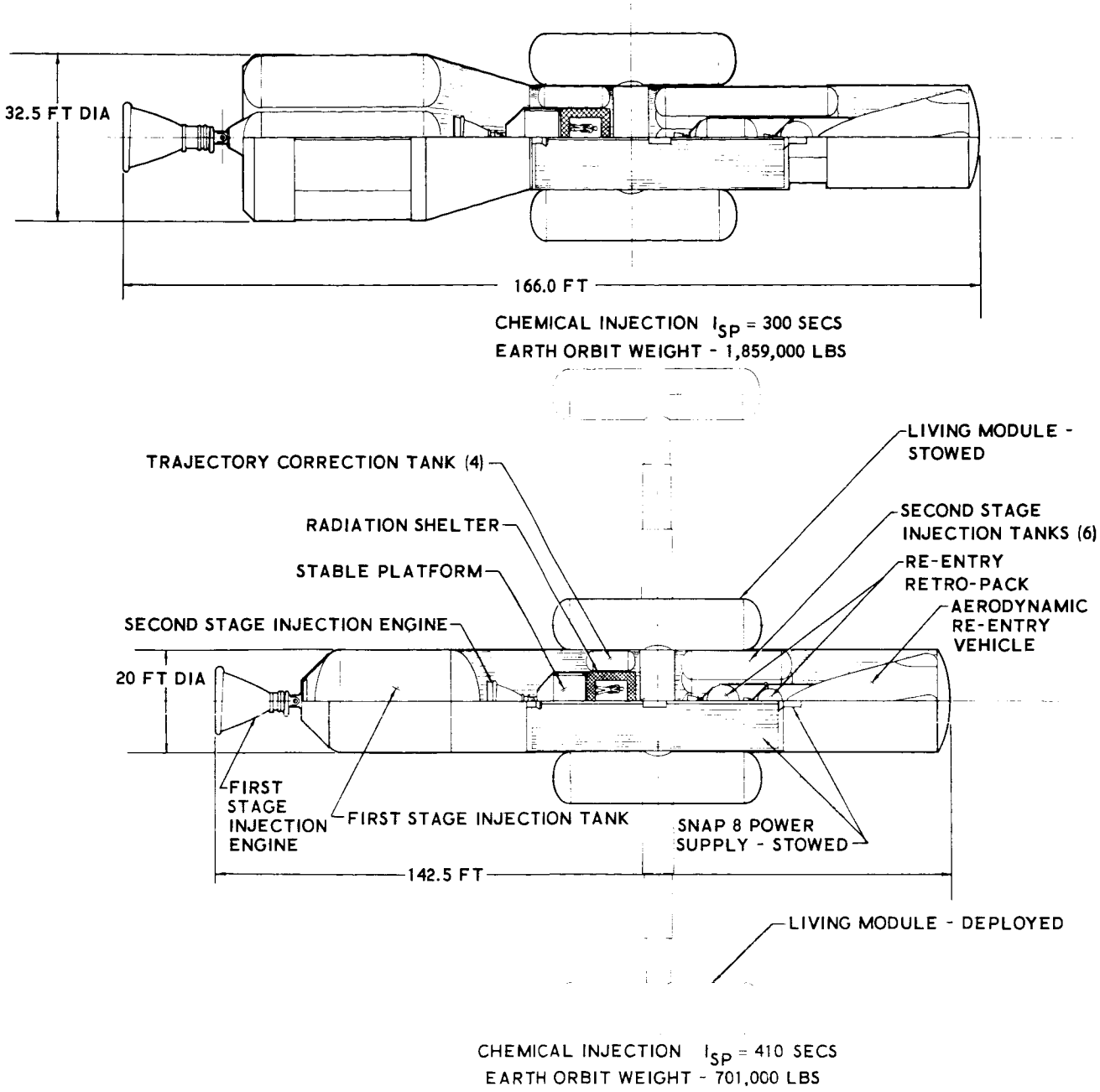

FIGURE 6-17.

SYMMETRIC CHEMICAL VEHICLE WEIGHT
AS A FUNCTION OF
SPECIFIC IMPULSE

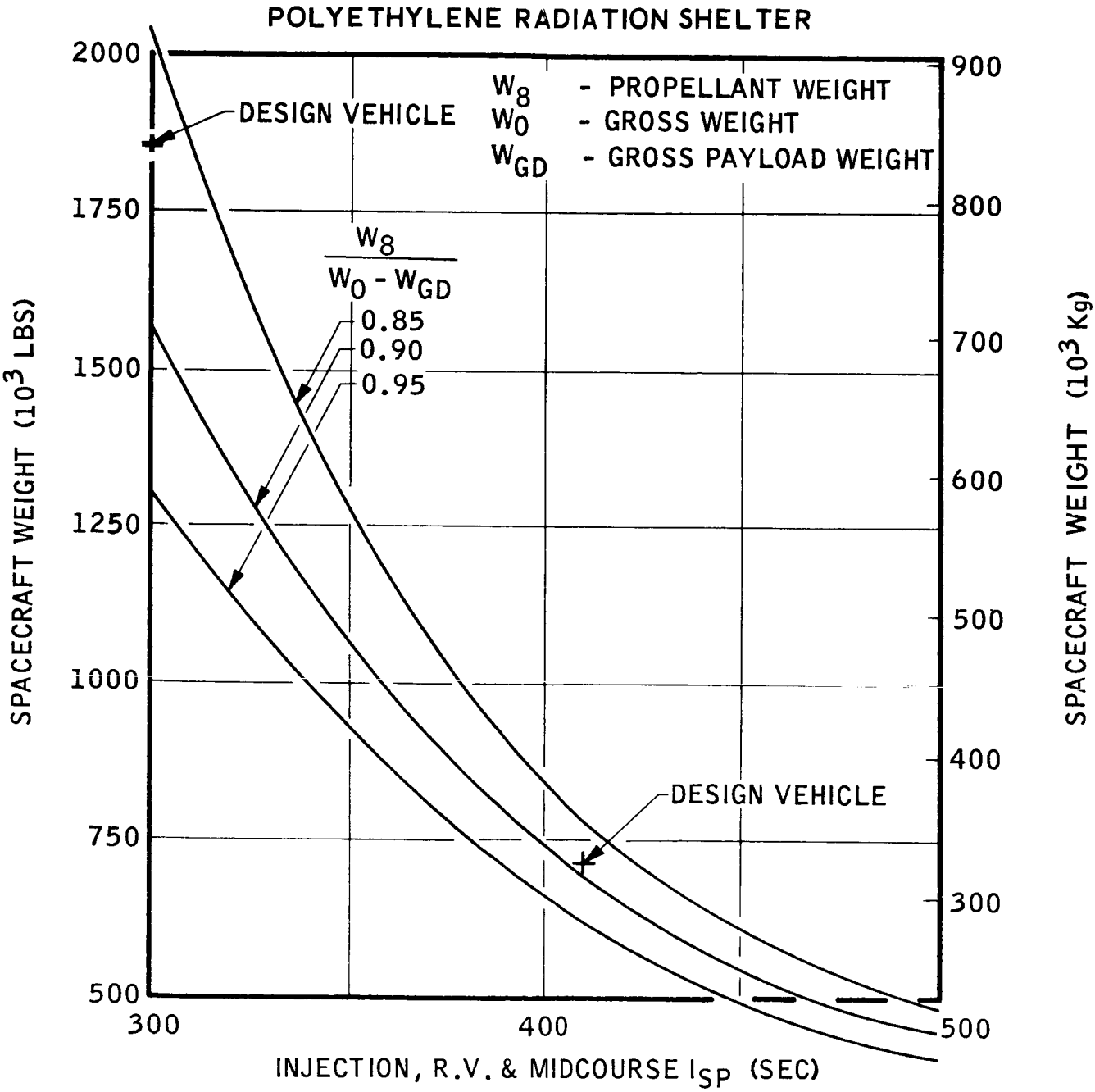

FIGURE 6-18

VEHICLE WEIGHT AS A FUNCTION OF PAYLOAD WEIGHT VARIATION

SYMMETRIC TRAJECTORY

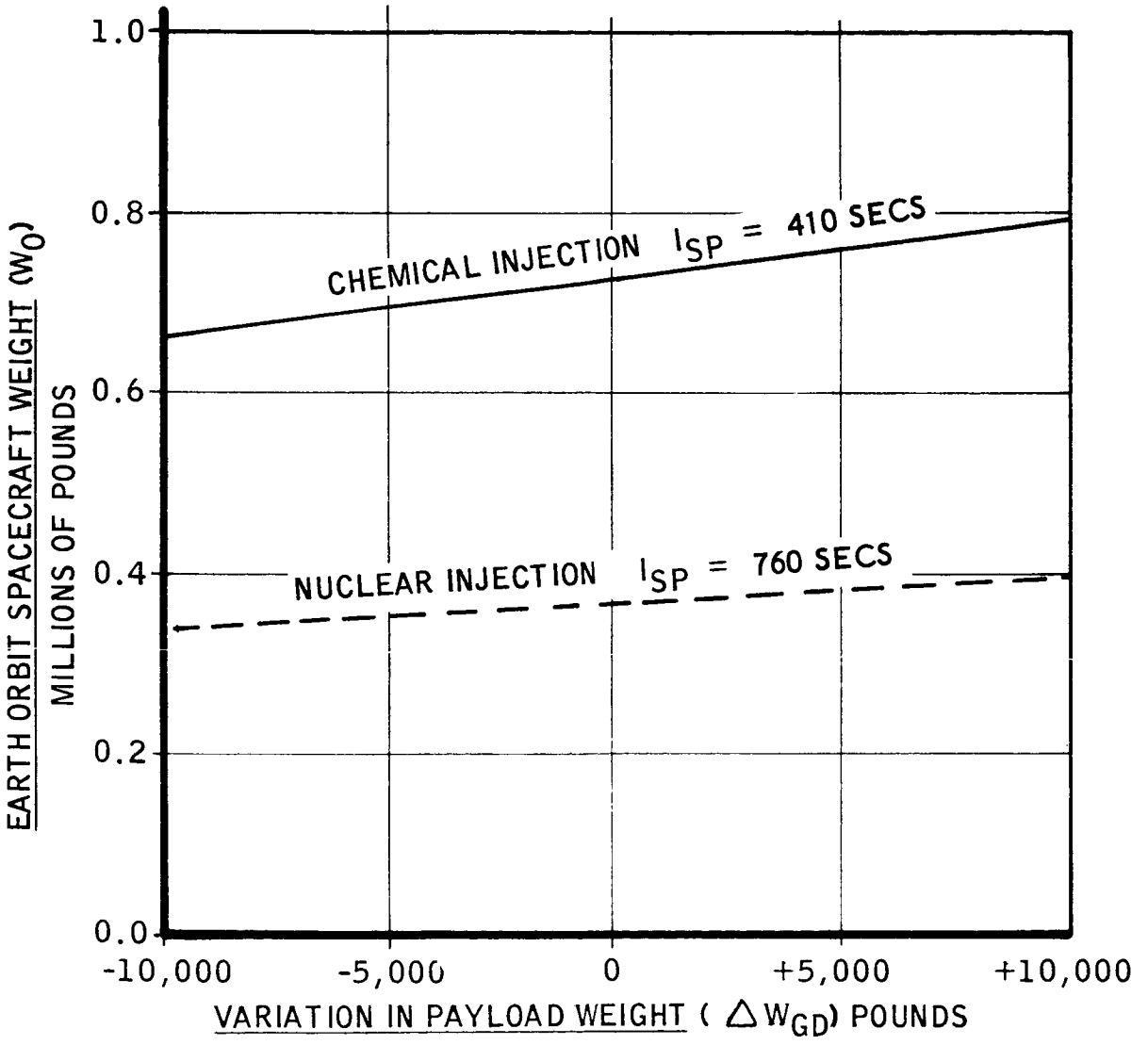

FIGURE 6-19

CONFIGURATION SUMMARY

NUCLEAR CROCCO

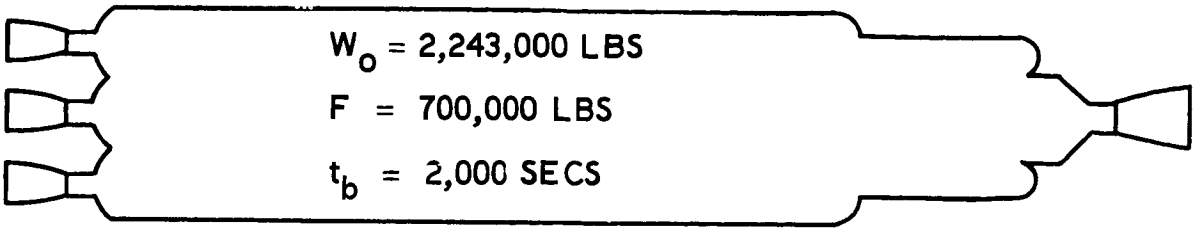

CHEMICAL SYMMETRIC (I_{SP} = 410 SECS)

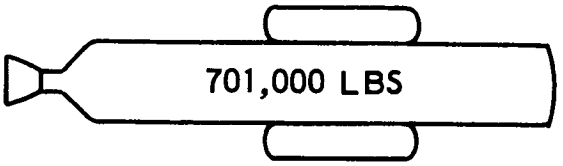

NUCLEAR SYMMETRIC

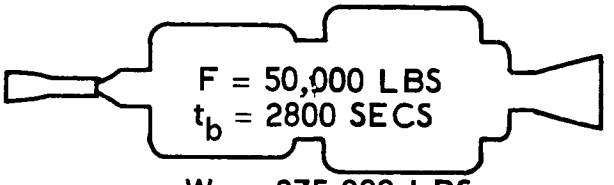

W_o = 375,000 LBS

CHEMICAL SYMMETRIC (I_{SP} = 300 SECS)

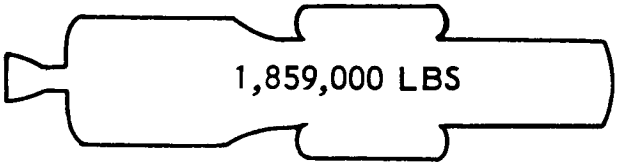

ATLAS-MERCURY

F = ENGINE THRUST

t_b = BURNING TIME

FIGURE 6-20

chemical Symmetric vehicles, though heavier, are as small, or smaller, than the nuclear Symmetric vehicle. This is primarily the result of the relatively dense propellant used in the chemical system (ρ = 60 lbs/ft^3) as compared with the nuclear system (ρ = 4.4 lbs/ft^3).

6.5 MISCELLANEOUS STUDIES

During the initial phase of the EMPIRE study program it appeared that propulsive Earth reentry would be required. Because of the large reentry energy requirement associated with the Crocco trajectory, it also appeared that nuclear propulsion, hence long term cryogenic storage, would be required. Accordingly a study of the cryogenic storage problem was made.

a. Cryogenic Storage in Space

The cryogenic storage study was made in two phases. During the first phase, problem areas were investigated and a study was made to determine optimum insulation thickness. Following this an investigation of liquefaction and refrigeration systems was made and a weight comparison was performed between the all insulation system and a refrigeration system.

The conclusions reached from these studies are summarized:

- The refrigeration system is lighter than the insulation only system for long term storage.
- Initial subcooling of liquid hydrogen is desirable.
- Artificial gravity for vapor-liquid phase separation is desirable.
- During the mission the vehicle should be oriented with its longitudinal axis along the vehicle-sun line.
- Planetary albedo and infrared heating contributions to boil-off are small compared to total solar heating during planetary passes greater than one planet radius.

(1) Configuration and Insulation Studies

The thermal evaluation of cryogenic storage starts with the launching of the propellant tanks from the Earth and the injection into the Earth orbit. The loaded tanks will be subjected to heating on

the launch pads, rocket booster heating during launch and orbit injection and aerodynamic heating while still in the atmosphere. After obtaining orbit the tanks will be subjected to direct solar radiation, the Earth albedo and the thermal (infrared) radiation emitted by the Earth and its atmosphere. While the solar direct and solar reflected radiation will be eliminated while the propellant tank is on the dark side of the planet, hence reducing the heating on the dark side, the thermal radiation emitted by the Earth and atmosphere will remain relatively constant. For the purpose of this study it has been estimated that the total time in Earth orbit to accomplish assembly, checkout, and interplanetary launch will be one month. During this period the hydrogen will exposed to the thermal environment just described and as a result some hydrogen will be lost. The vaporized hydrogen will increase the tank pressure or may be vented to space at a pre-determined tank vent pressure. While hydrogen vaporization does not represent a major consideration for the initial boost stages, it represents a monumental problem for long term hydrogen storage to provide midcourse and terminal (orbit ejection) velocity increments.

Following injection into the Mars-Venus interplanetary flyby orbit the vehicle will be exposed primarily to direct solar radiation. During a short time period passing Mars and Venus the vehicle will be exposed to the planet albedo and planet emitted infrared radiation. For this phase of the study it was anticipated that during the planetary bypass the vehicle will not come closer than one planet radius. Figure 6-21 shows that the view factor between the vehicle and either Mars or Venus is approximately 0.07. Considering the time in the vicinity of the planets and the very low view factor it appears that the planetary contribution to the total heating will be relatively small. The initial estimate of heating for determination of insulation, hydrogen boil-off and system weights is based on considering the planetary heat contribution negligible. For this initial estimate there were no trajectory data available so an average heat flux was selected from Figure 6-2. The average heat flux was purposely chosen large to cover the planetary input, vehicle misorientation and the effect of coming close to the Venus orbit on the outgoing and returning legs of the 18 month Crocco mission. Subsequent approximate trajectory data indicate that the estimate was indeed conservative. In addition it should be pointed out that the heat input to the cryogenic propellant is based upon maintaining a vehicle orientation with the minimum area (i.e., the end of the tanks) facing the sun.

CONFIGURATION FACTOR BETWEEN A SMALL CYLINDER AND A LARGE SPHERE

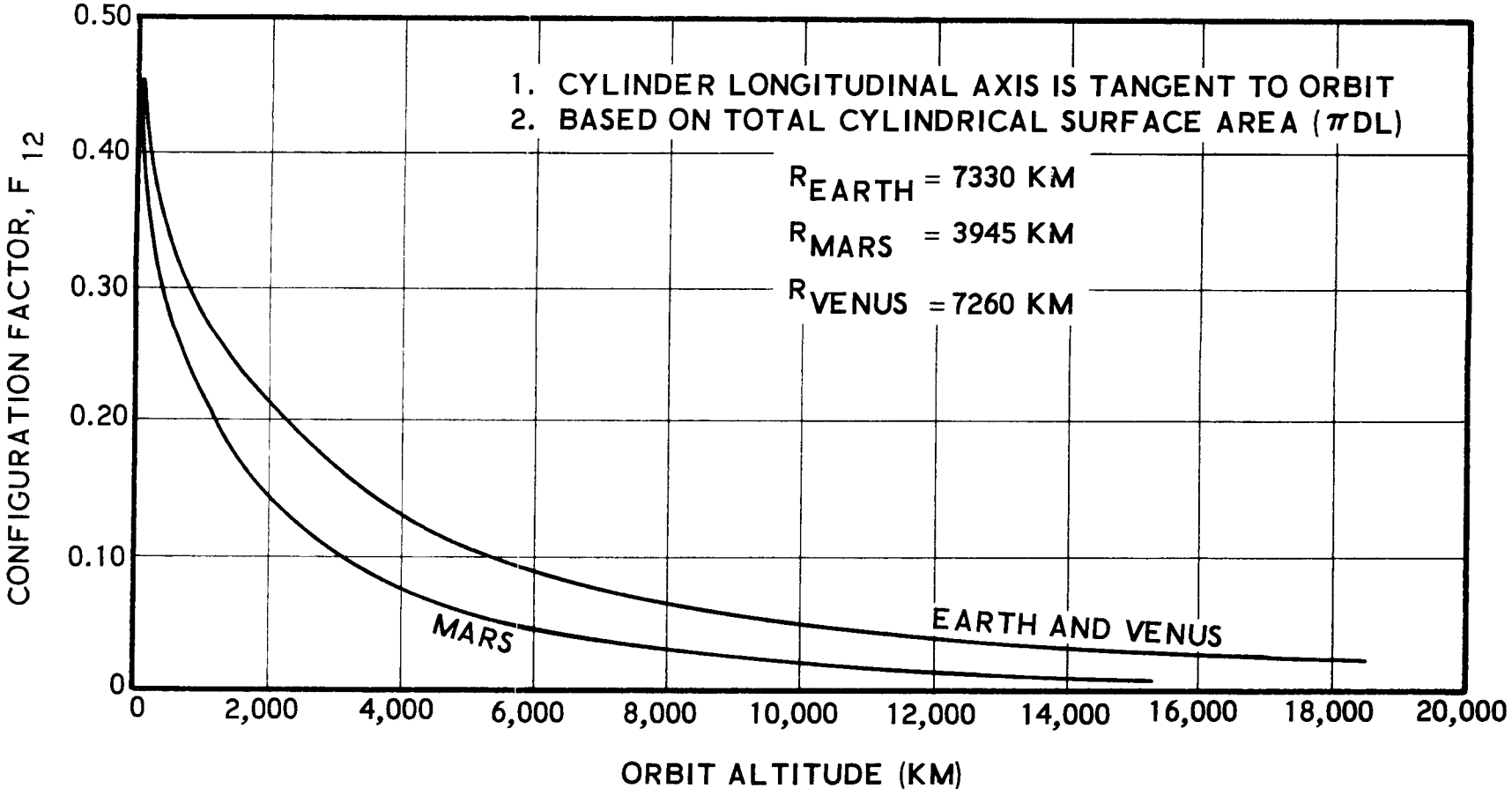

FIGURE 6-21

A dual wall tank with an L/D = 4 was selected for the initial estimate of hydrogen boil-off. A multilayer superinsulation such as Linde SI4 or NRC-2 with a thermal conductivity of 2.5×10^{-5} Btu/Ft-Hr^{o}F was used and assumed to be located between the double wall tank structure in a vacuum. The external surface was assumed to have a coating such as Rokide A providing an $\alpha / \epsilon = 0.2$. In lieu of detail tank design data is was assumed that the heat input through the tank structure would be equivalent to an increase of 50 percent of the heat coming through the insulation. Based on these assumptions and the estimated incident heat, the hydrogen boil-off was calculated as a function of the initial weight of hydrogen and the insulation thickness. These data are presented in Figures 6-22 and 6-23. The variation in the weight of hydrogen boil-off (W_{bo}) and cryogenic insulation weight (W_i) is shown as a function of mission duration and propellant quantity in Figure 6-24. The minimum values of the ratio $(W_{bo} + W_i)/(W_8 + W_i)$ represent optimum insulation thicknesses.

(2) Liquefaction and Refrigeration System Studies

Three active systems were analyzed: direct liquefaction of hydrogen, liquefaction of hydrogen using a modified Stirling Cycle, and refrigeration of hydrogen using a reverse Brayton Cycle. These systems were compared on a weight and power basis and the lowest mass system was then compared with a system consisting of tank insulation only.

- Direct Liquefaction of Hydrogen

Direct liquefaction of hydrogen is accomplished using an ideal vapor cycle. Hydrogen boil-off is compressed isentropically, condensed isobarically, and throttled back into the tank. Figure 6-25 shows a system schematic and a hydrogen phase diagram. Point 1 on the figure is the hydrogen boil-off. The hydrogen is taken from the tank through a valve (a constant enthalpy process) heated in a recuperator to remove all traces of liquid and them compressed. Condensation takes place in an external radiator. The condensed hydrogen is then throttled back into the storage tank through a valve.

Figure 6-26 shows mass, power, and radiator area as a function of boil-off rate for the direct system. The large radiator area is due to the very low radiating temperature (approximately 20^{o} Kelvin). A mass penalty of approximately 5 kilograms per square meter was assigned to the radiator and the large mass of the total system is a direct function of the radiator size. The number chosen for mass per unit area of the radiator could be either larger or smaller depending on the radiator design. A smaller number would result if existing structure was used. A larger number would result if the radiator was completely separate from existing vehicle structure. The power requirement for this system is very low primarily because of the low pressure ratios used in the cycle.

HYDROGEN BOILOFF 12 MONTH MISSION

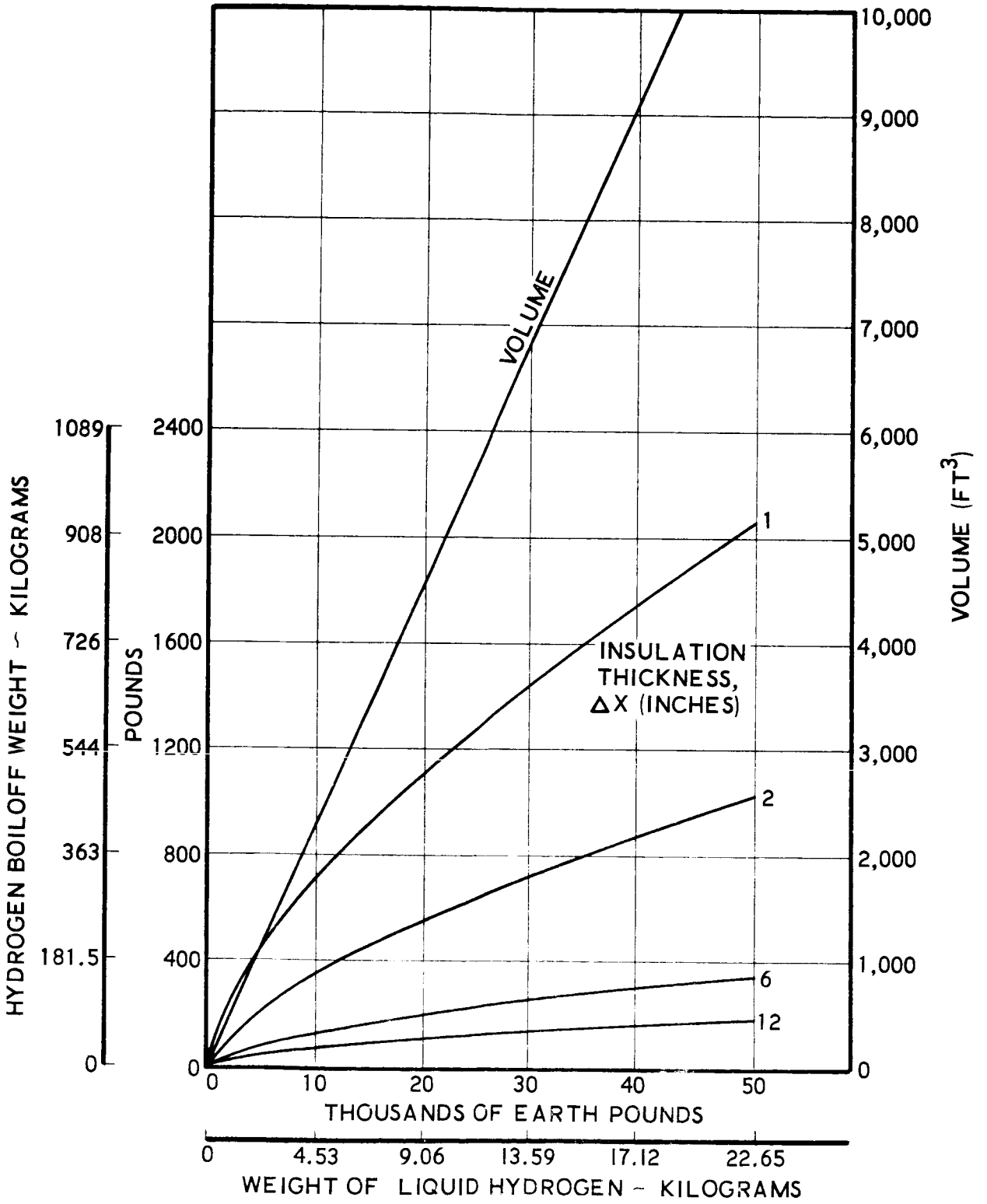

FIGURE 6-22

HYDROGEN BOILOFF 18 MONTH MISSION

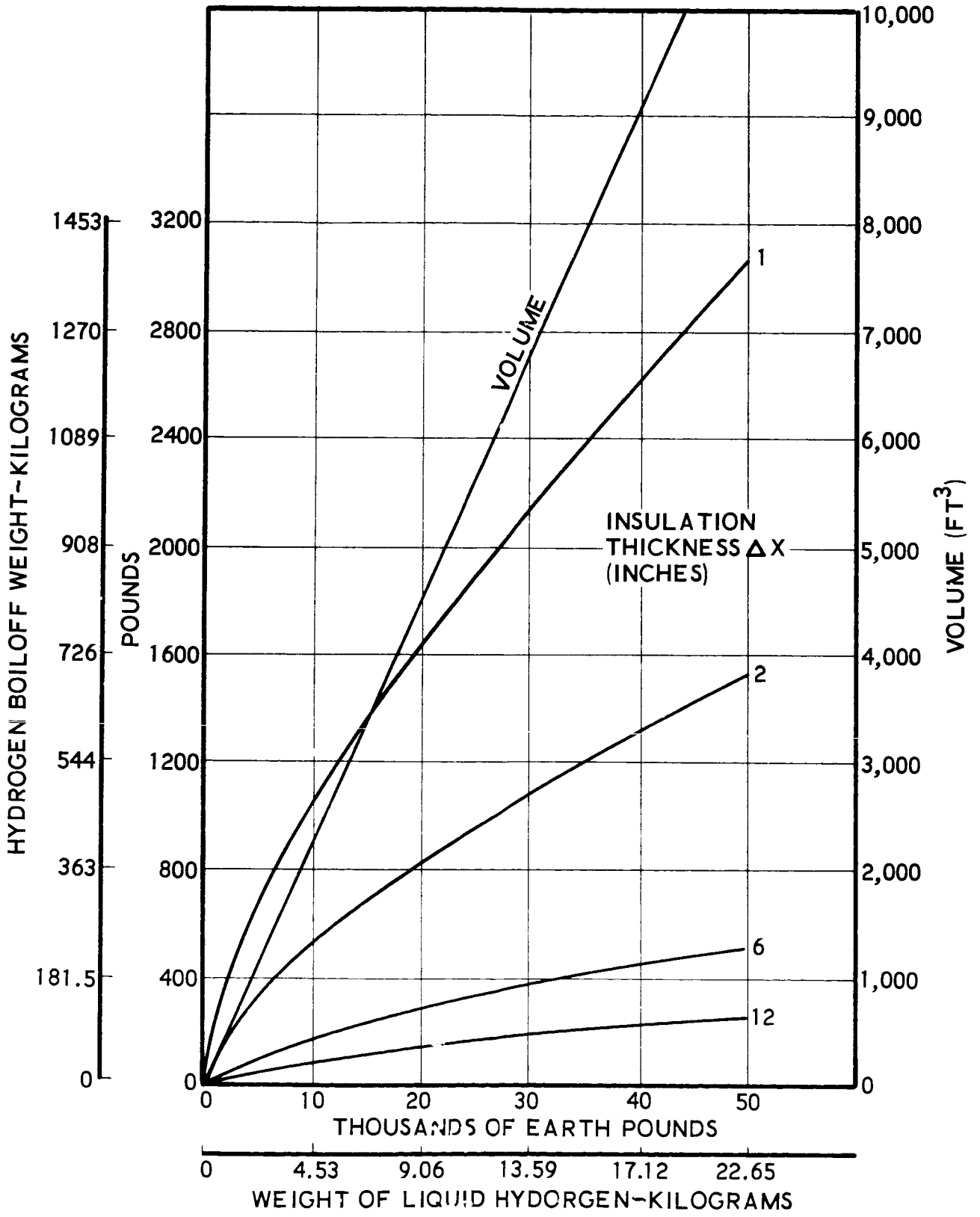

FIGURE 6-23

LIQUID HYDROGEN BOILOFF & INSULATION WEIGHTS
AS FUNCTIONS OF
INITIAL PROPELLANT WEIGHT & MISSION DURATION

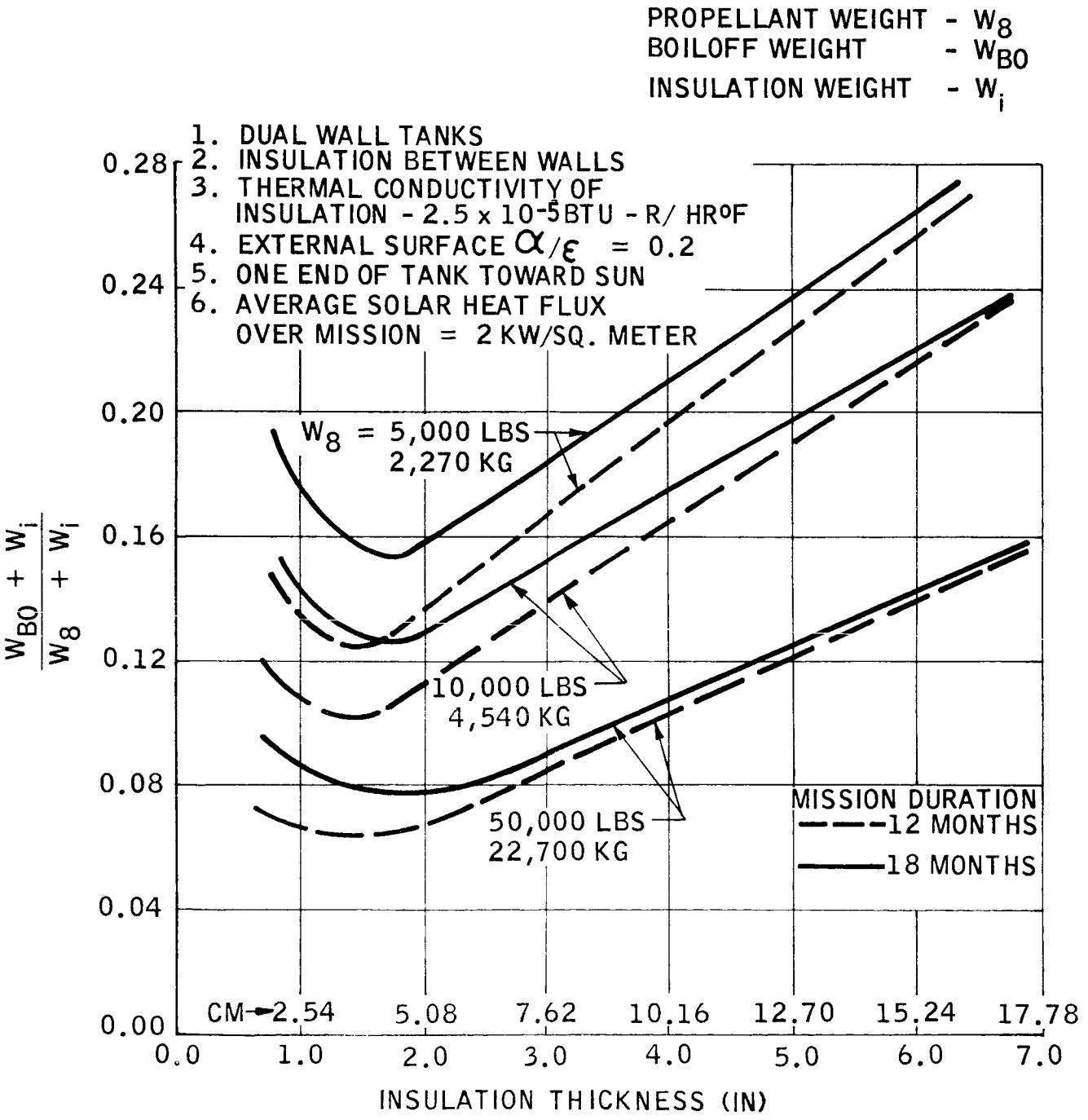

FIGURE 6-24

1. DIRECT LIQUEFACTION

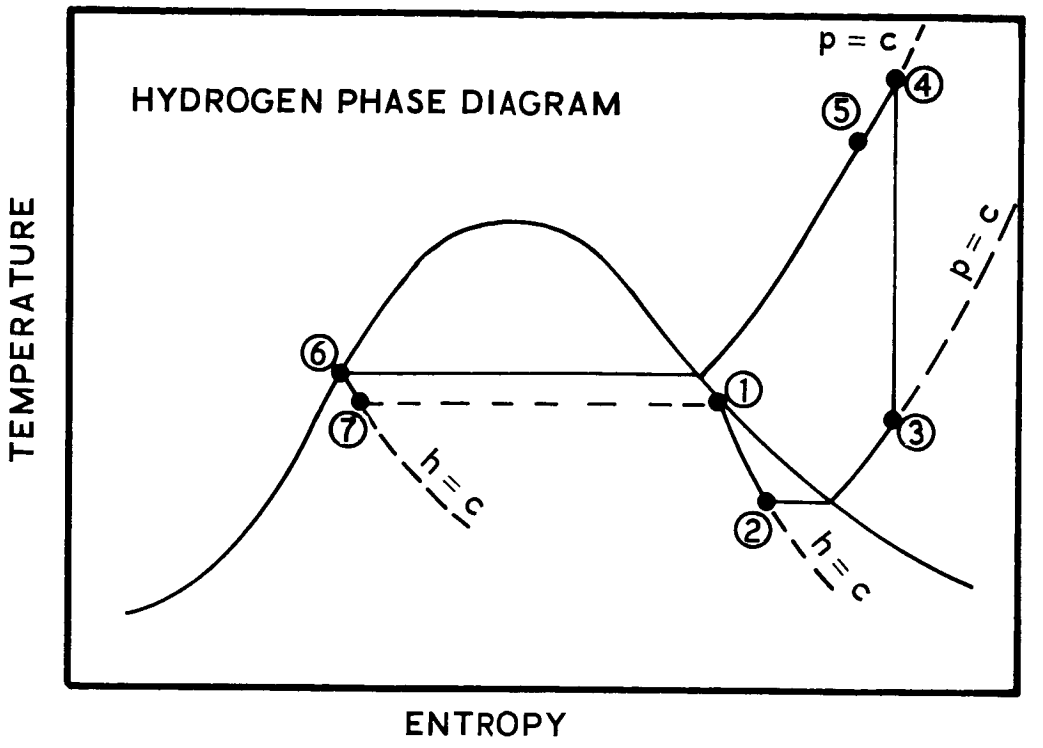

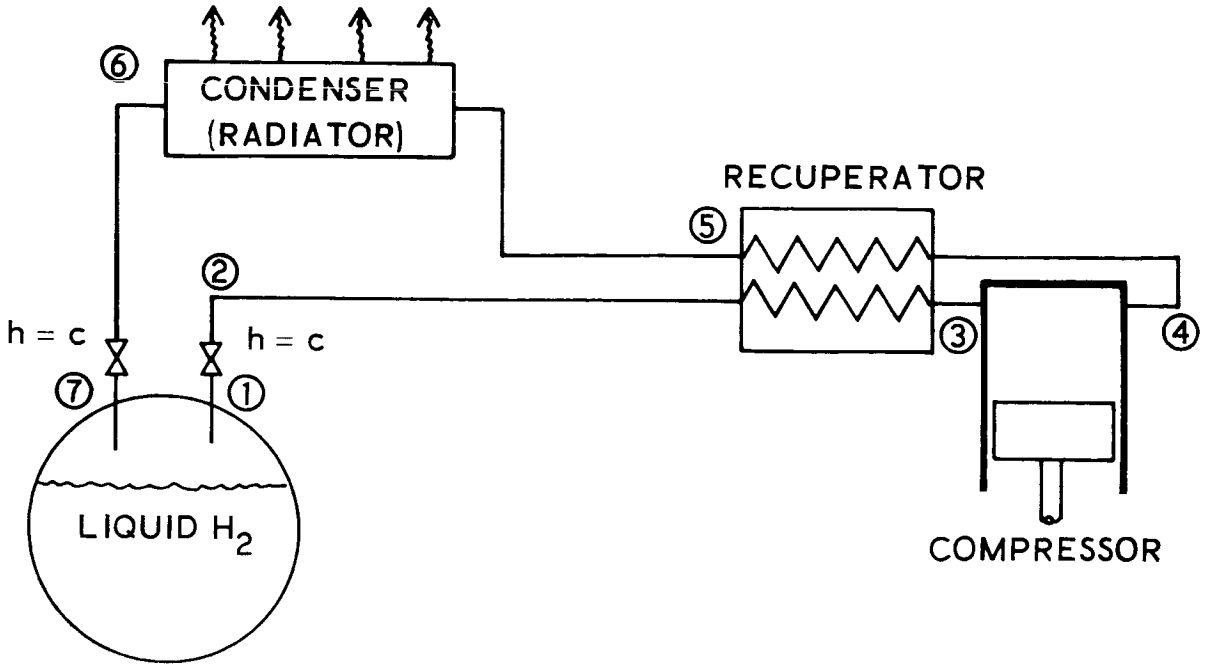

FIGURE 6-25

DIRECT LIQUEFACTION SYSTEM PARAMETERS
VERSUS
BOILOFF RATE

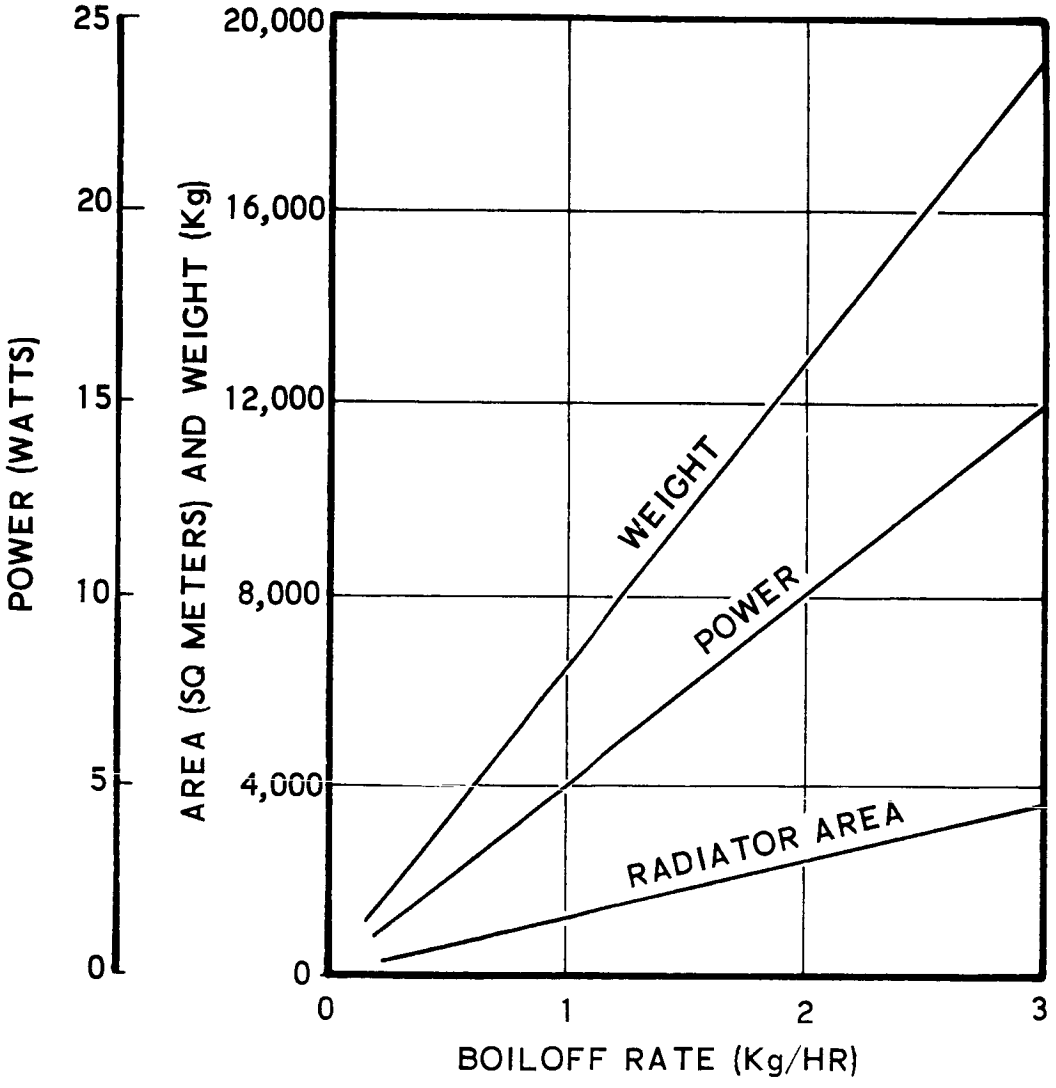

FIGURE 6-26

Since radiator size is inversely proportional to the fourth power of radiator temperature it is apparent that radiator size, hence total system weight, can be reduced by rejecting heat from the radiator at a higher temperature. The next step in the analysis was then to analyze heat pump systems.

- Modified Stirling Cycle

A modified Stirling Cycle engine was next analyzed (Refs. 14 and 15). Cold is produced in this machine by the reversible expansion of a gas. The working fluid, helium, goes through a cycle during which it is compressed at ambient temperature (approximately 300° Kelvin) and expanded at the desired low temperature (approximately 30° Kelvin). The transition between these two temperatures is accomplished by heat exchange between the working fluid going in the one direction and the other. The heat exchange process is aided by a regenerator which stores heat from the hot compressed gas going in one direction and then rejects it to the cold expanded gas going in the other.

Such a device called "A Closed Cycle Cryogenerator" has been developed by N. V. Phillips, of Eindhoven, Netherlands. Figure 6-27 shows the thermodynamic cycle of the working fluid and a schematic diagram of the cold producing device. Starting at point 1 and going through the cycle, the fluid is compressed in the compression space at constant temperature to point 2. Heat is removed during this process by the cooling jacket. At the end of the high temperature compression process the displacer is moved downward forcing the compressed gas through the regenerator. Heat is transferred into the regenerator during this constant volume process. The cooled gas is then expanded at the constant low temperature with heat being transferred into the working fluid from the liquefaction coils. Another constant volume displacement process follows during which the expended cold gas is forced back through the heated regenerator removing the stored heat.

Figure 6-28 shows a schematic diagram of this system along with a hydrogen phase diagram. Two cryogenerators are used in the system; one operating between 30° and 90° Kelvin and the other operating between 90° and 300° Kelvin. The reason for using two cryogenerators is that efficiency increases with decreasing temperature difference across the machine, and two systems operating between narrower temperature limits are much more efficient than a single system.

2. MODIFIED STIRLING CYCLE

(CLOSED CYCLE CRYOGENERATOR, N. V. PHILLIPS, EINDHOVEN, NETHERLANDS)

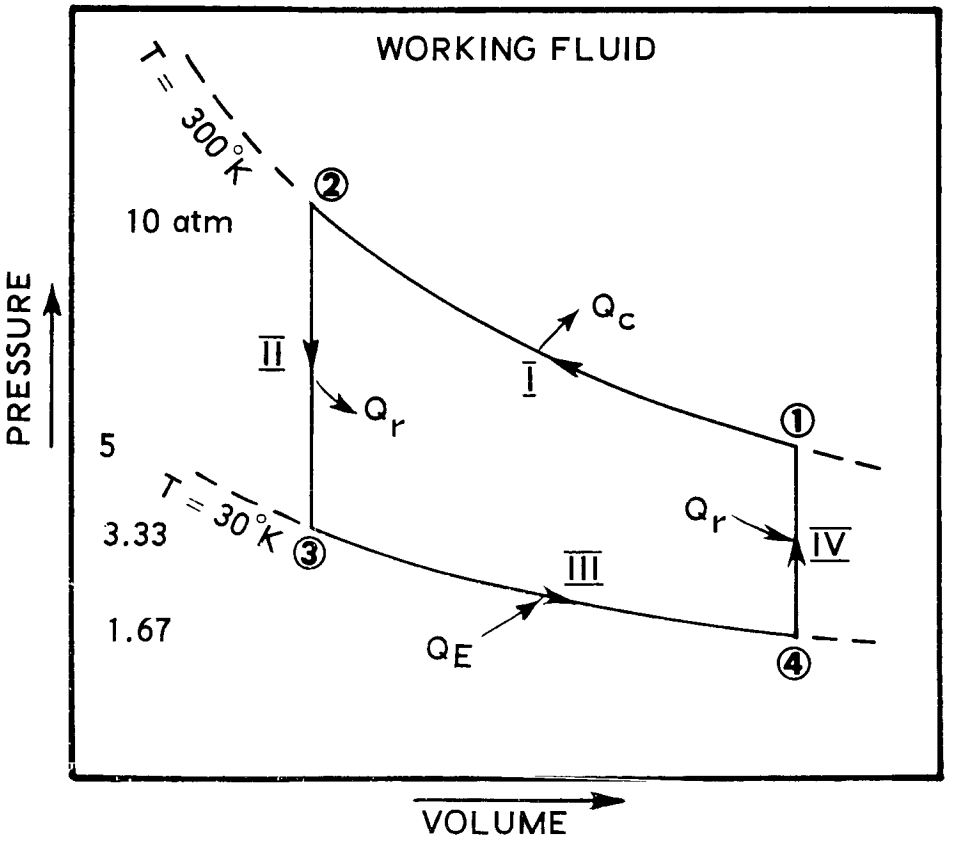

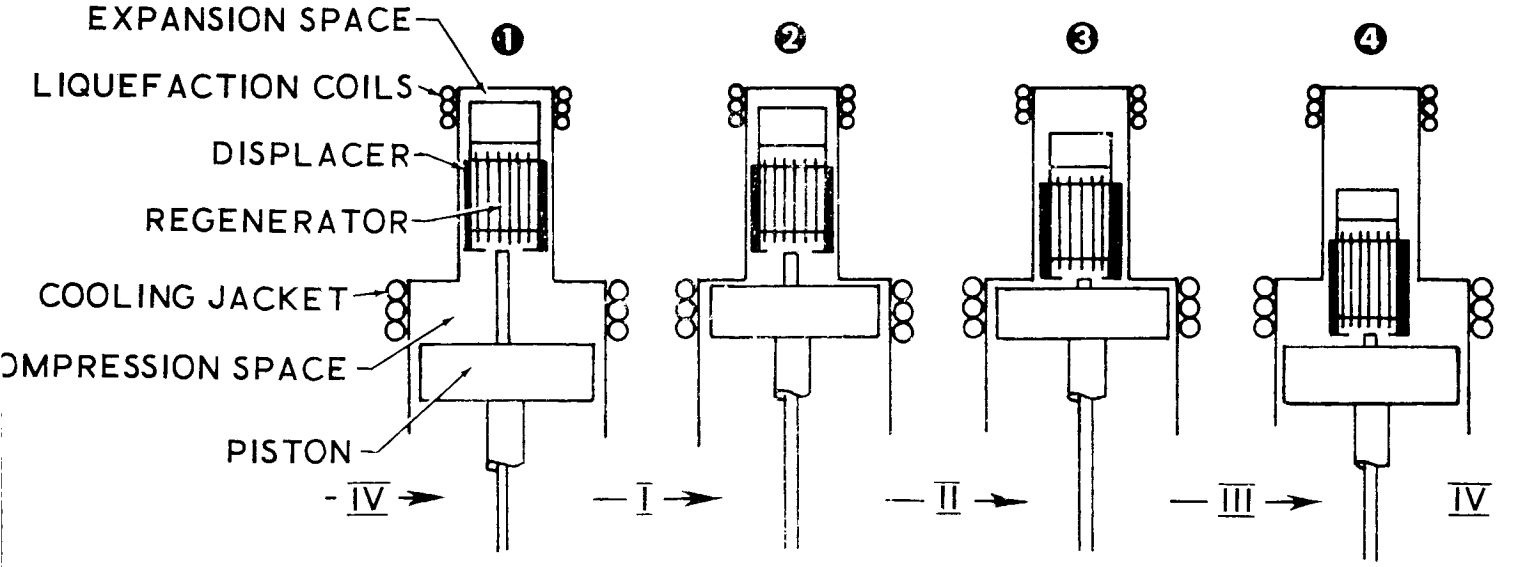

FIGURE 6-27

STIRLING CYCLE LIQUEFACTION SYSTEM

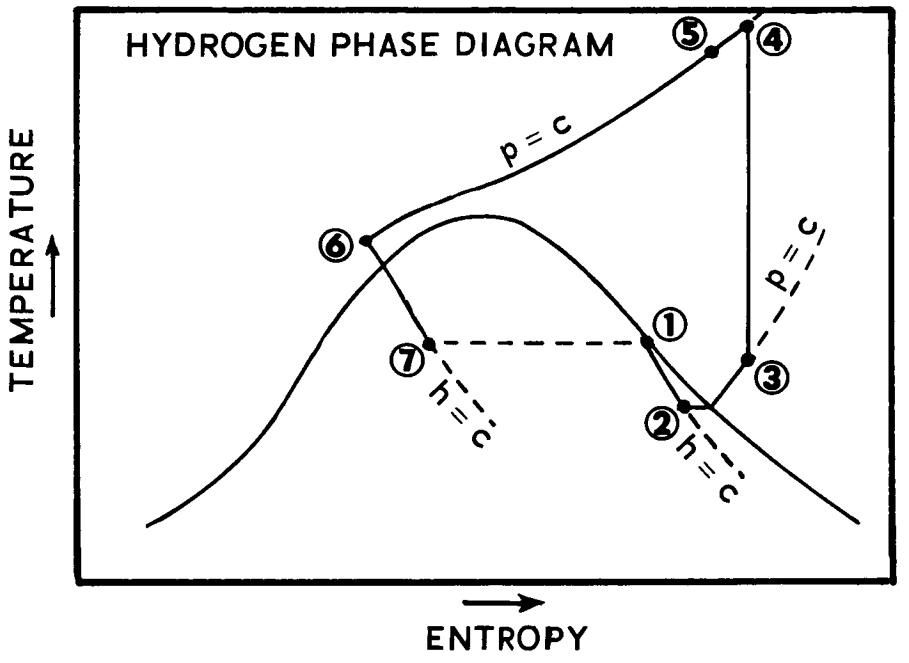

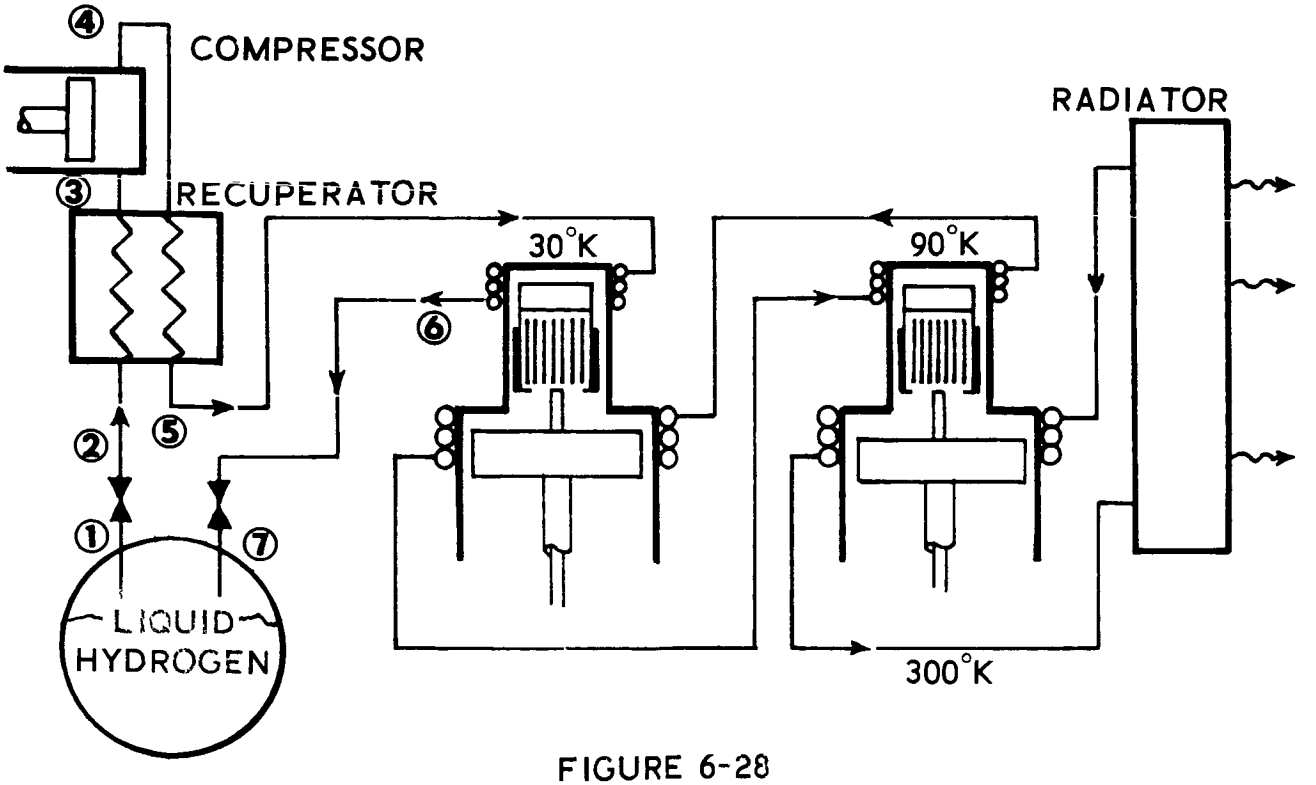

FIGURE 6-28

Hydrogen is reliquefied with the system as in the case of the direct system. Hydrogen is removed from the tank, compressed isentropically, cooled at constant pressure in the cryogenerator liquefaction coils and then expanded back into the tank. Heat is rejected from the system in the space radiator at approximately 300° Kelvin. Mass, radiator area, and power as a function of boil-off rate are shown in Figure 6-29. Also shown for comparison is mass of the direct cycle system. The Stirling Cycle system mass includes the power supply. Approximately 25 kilograms per kilowatt were assumed for the power supply weight.

- Reverse Brayton Cycle

A refrigeration technique using a reverse Brayton Cycle was also analyzed. This system was used to subcool rather than liquefy the hydrogen. The helium working fluid (Figure 6-30) is compressed at constant entropy, heat is removed at constant pressure and rejected overboard by a space radiator. The cooled working fluid is then expanded through an expansion engine where the energy level of the working fluid is further reduced. The very cold working fluid is then passed through coils within the liquid hydrogen. Power, radiator area, and weight for this system were computed as a function of refrigeration capacity.

- System Comparison

A comparison of radiator size for all three of the systems analyzed is shown in Figure 6-31 as a function of refrigeration. Two curves are shown for the Stirling Cycle system. The one for direct liquefaction of boil-off and the other for direct cooling. It can be seen that the Brayton system requires the smallest radiator. Figure 6-32 compares power requirements for the three systems as a function of refrigeration. The direct cycle is the lowest power system. The significance of this curve, however, is the comparison of Brayton and Stirling cycles. The Stirling cycle refrigeration system (direct cooling curve) requires nearly twice the power required by the Brayton cycle at the same refrigeration capacity. Figure 6-33 compares system mass for each of the systems as a function of refrigeration. The Brayton cycle system has the least mass penalty.

The Brayton refrigeration system is compared with a system using insulation only to determine the relative mass penalties. Figure 6-34 is a plot of system mass as a function of insulation thickness for a delivered propellant mass of 22,600 kilograms (18-month mission). The boil-off curve shows mass of insulation plus mass of boil-off during the

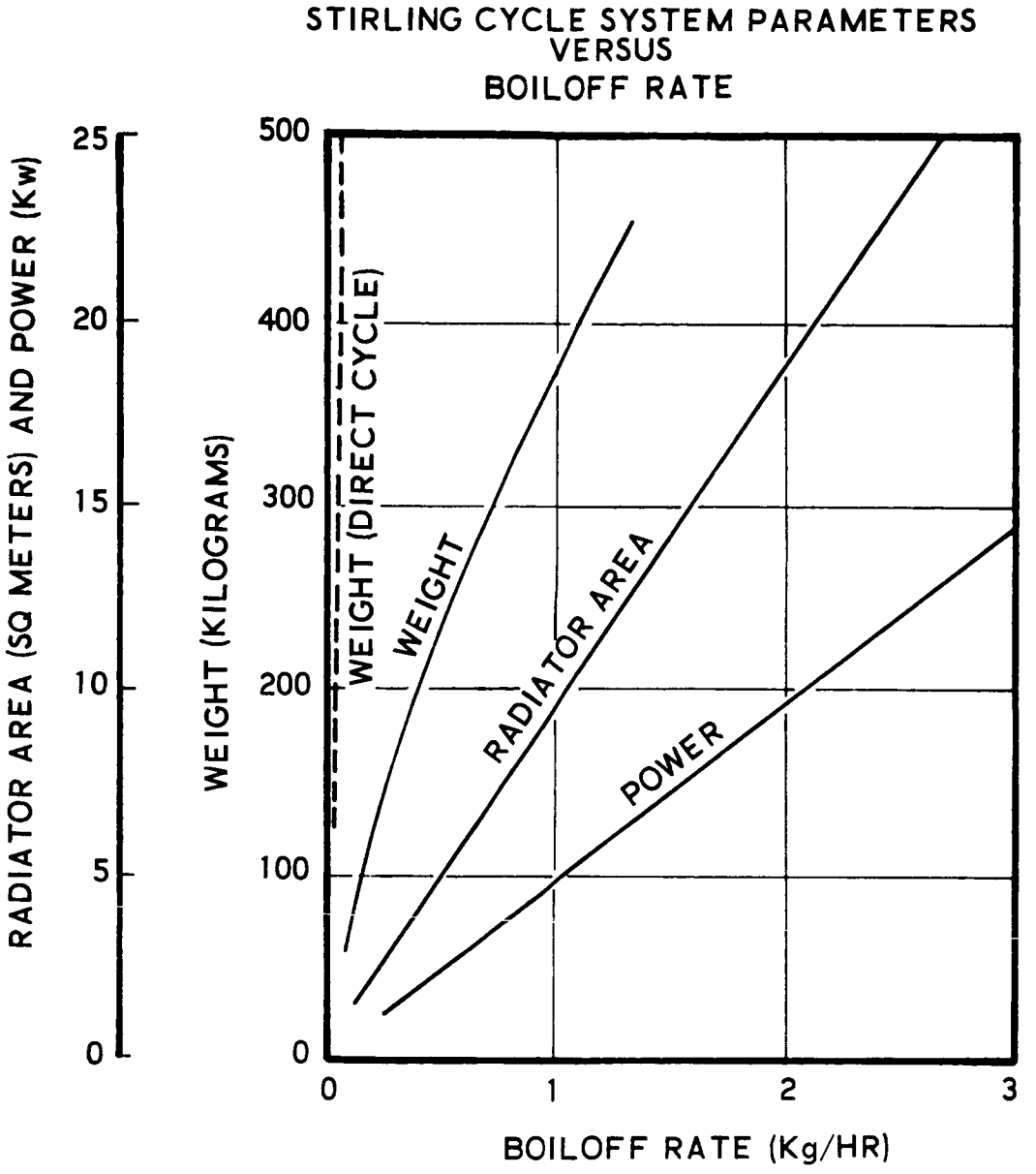
STIRLING CYCLE SYSTEM PARAMETERS
VERSUS
BOILOFF RATE
RADIATOR AREA (SQ METERS) AND POWER (Kw)
WEIGHT (KILOGRAMS)
BOILOFF RATE (Kg/HR)
WEIGHT (DIRECT CYCLE)
WEIGHT
RADIATOR AREA
POWER
0
5
10
15
20
25
0
100
200
300
400
500
0
1
2
3

FIGURE 6-29

REVERSE BRAYTON CYCLE REFRIGERATION SYSTEM

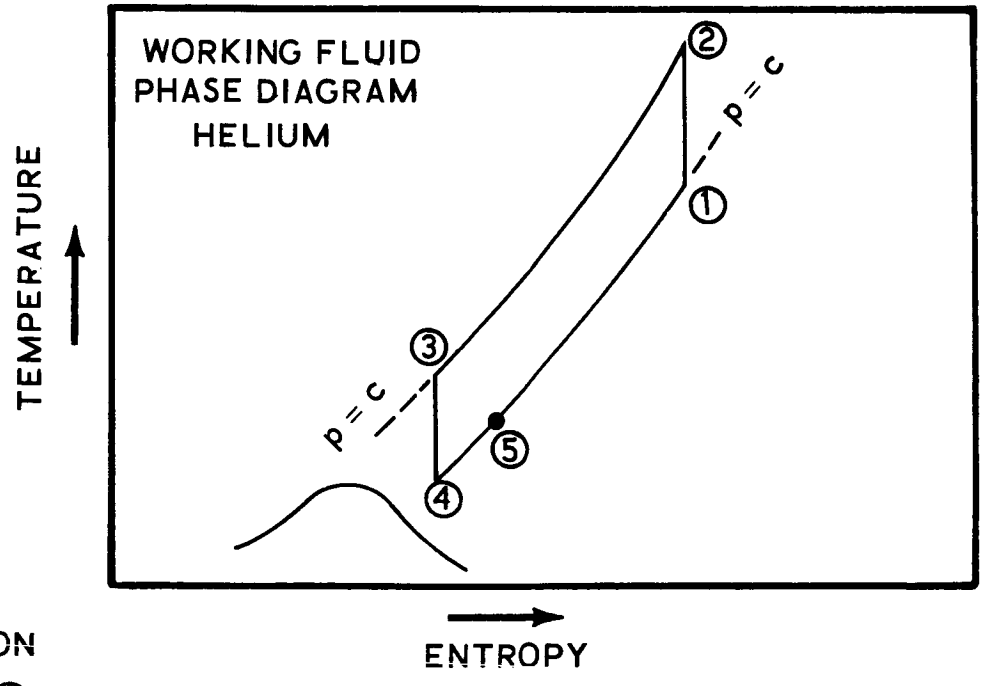

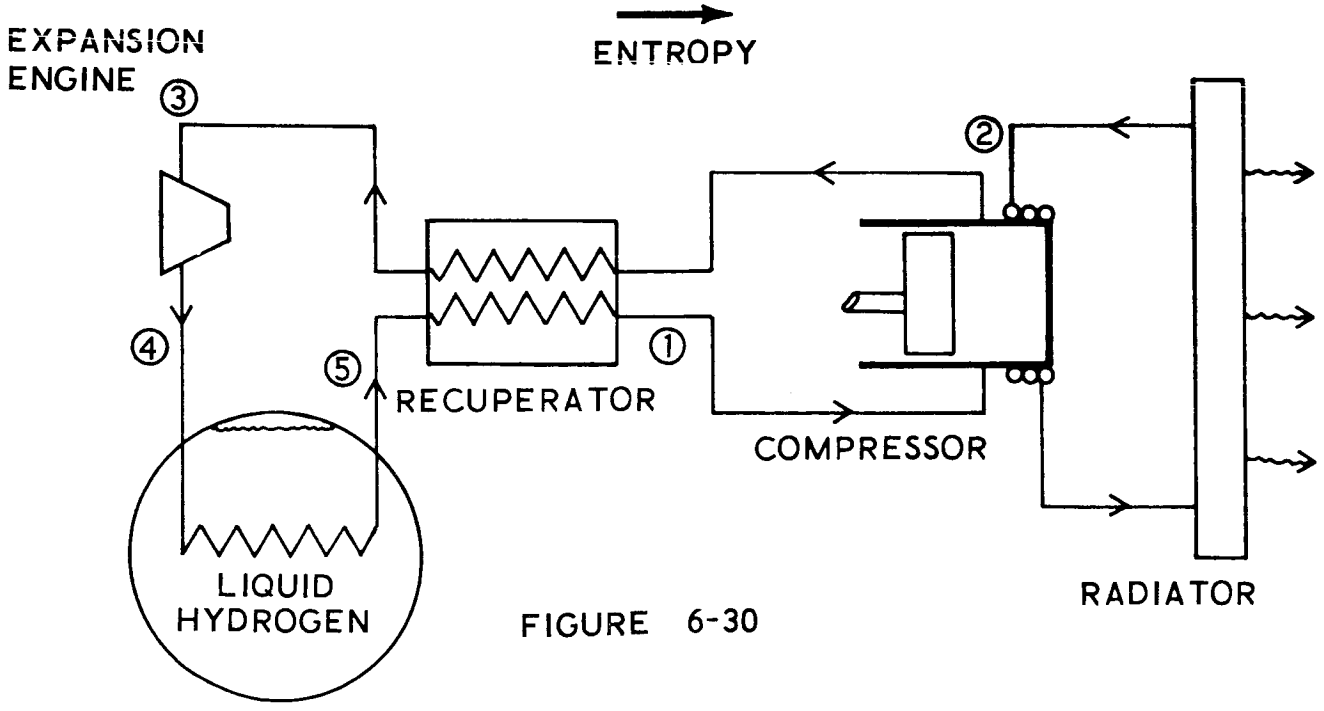

FIGURE 6-30

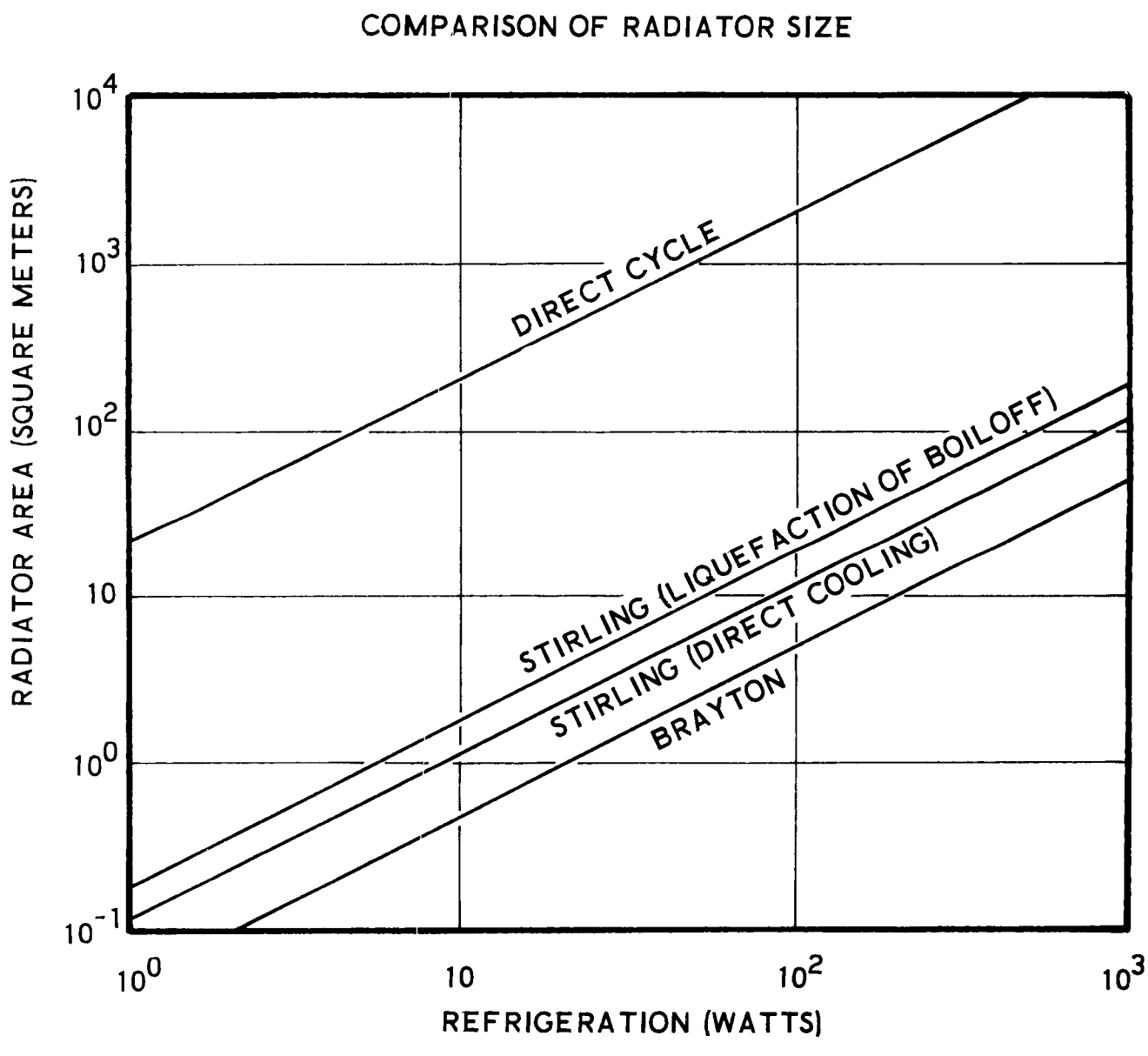
COMPARISON OF RADIATOR SIZE
RADIATOR AREA (SQUARE METERS)
10^4
10^3
10^2
10
10^0
10^{-1}
DIRECT CYCLE
STIRLING (LIQUEFACTION OF BOILOFF)
STIRLING (DIRECT COOLING)
BRAYTON
10^0
10
10^2
10^3
REFRIGERATION (WATTS)

FIGURE 6-31

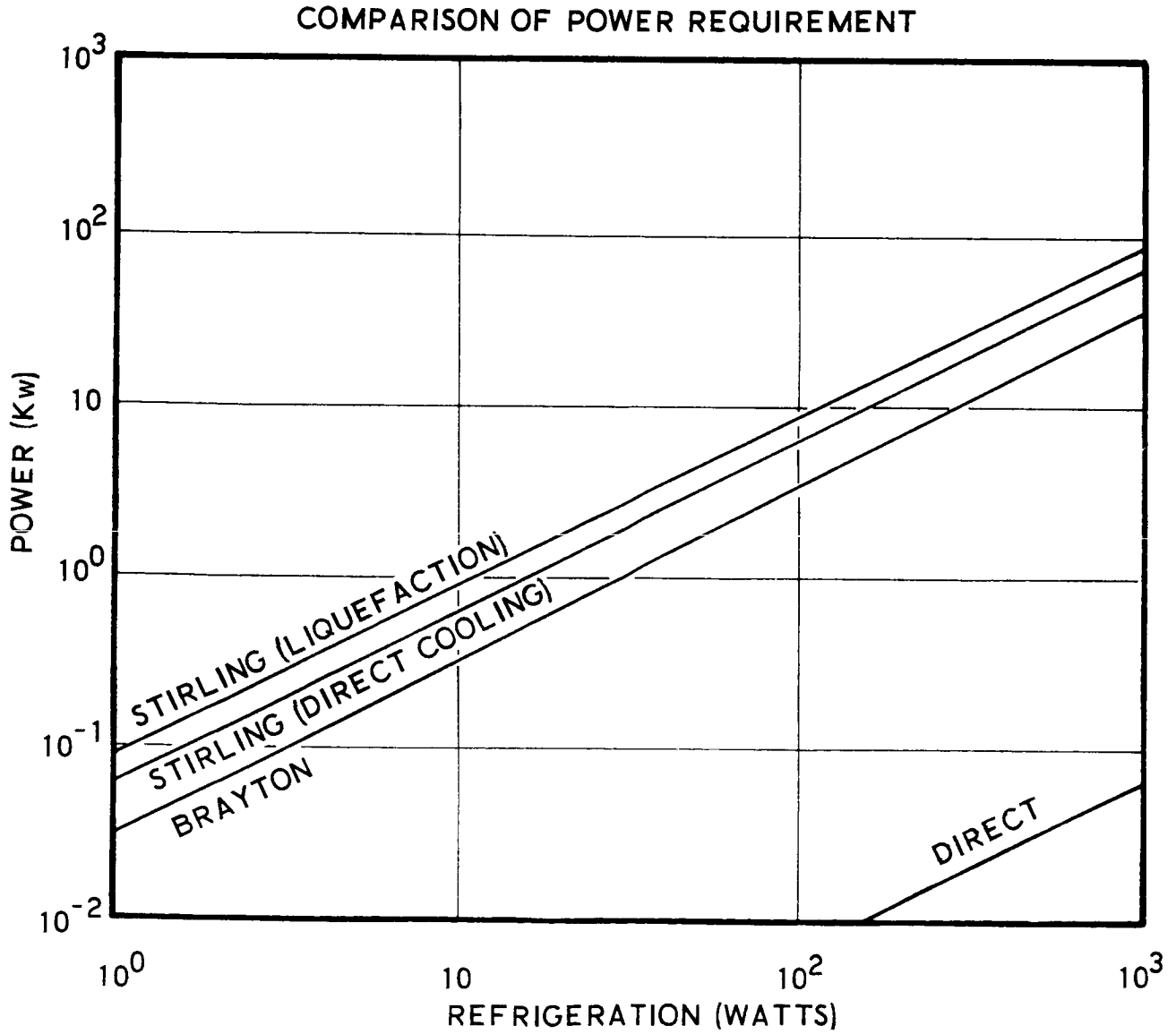
COMPARISON OF POWER REQUIREMENT
POWER (Kw)
10^3
10^2
10
10^0
10^{-1}
10^{-2}
STIRLING (LIQUEFACTION)
STIRLING (DIRECT COOLING)
BRAYTON
DIRECT
10^0
10
10^2
10^3
REFRIGERATION (WATTS)

FIGURE 6-32

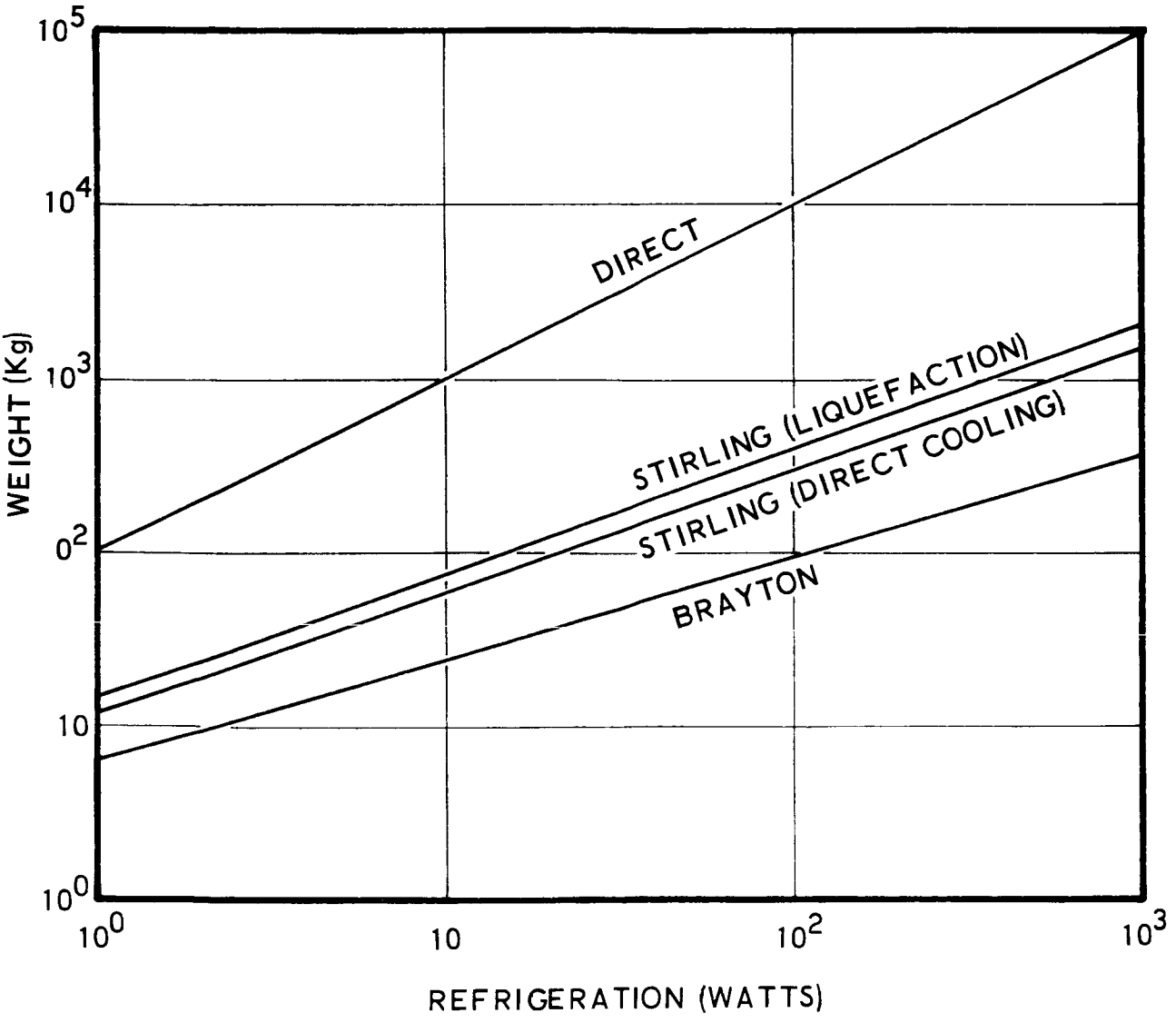
COMPARISON OF SYSTEM WEIGHT
WEIGHT (Kg)
10^5
10^4
10^3
0^2
10
10^0
DIRECT
STIRLING (LIQUEFACTION)
STIRLING (DIRECT COOLING)
BRAYTON
10^0
10
10^2
10^3
REFRIGERATION (WATTS)

FIGURE 6-33

EFFECT OF INSULATION ON BOILOFF LOSSES
AND REFRIGERATION SYSTEM WEIGHT

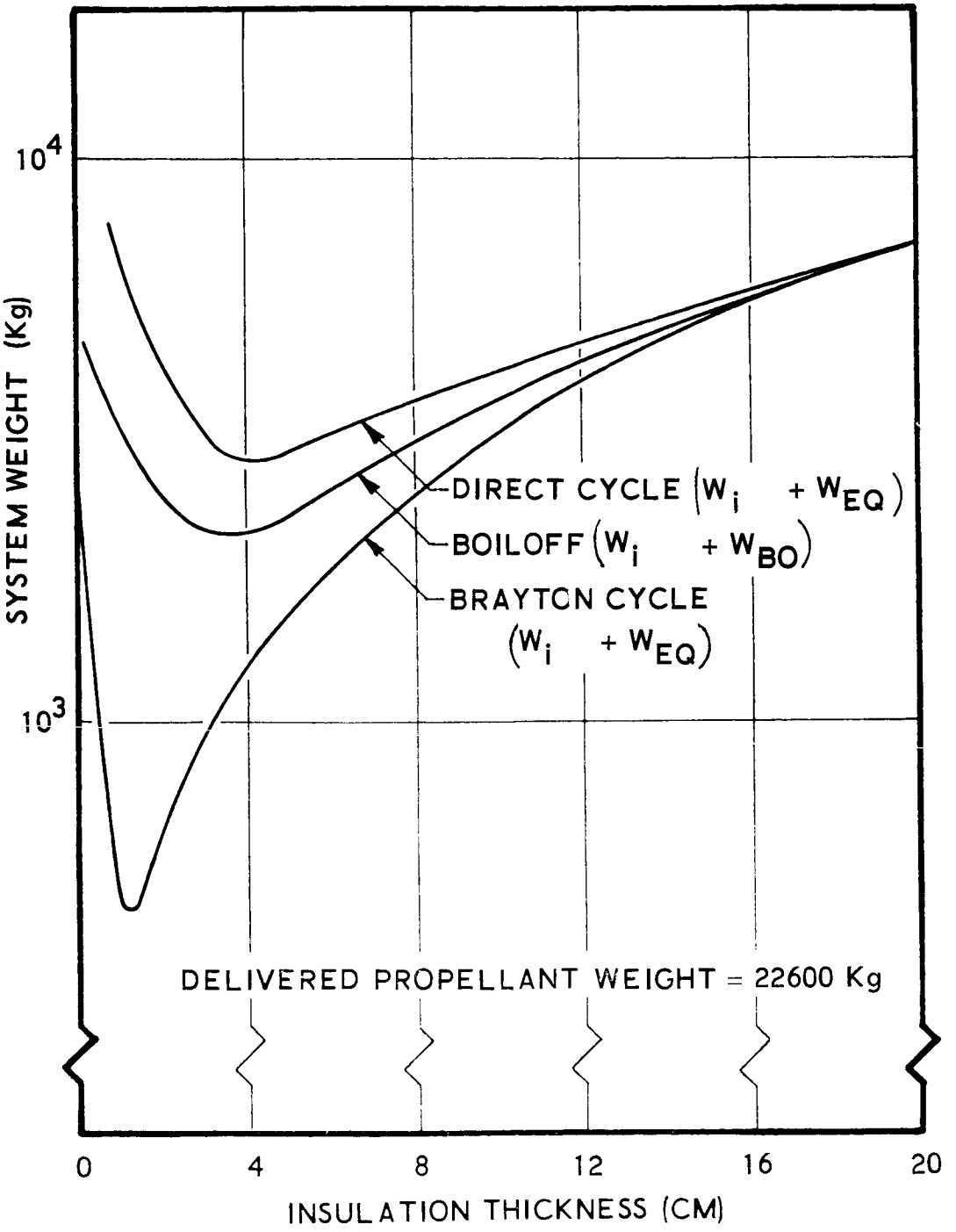

FIGURE 6-34

entire mission. Minimum mass points occur for all of the systems at a point between 2 and 5 centimeters of insulation thickness. The figure shown is representative of all delivered propellant masses analyzed.

A cross plot was made to compare the minimum Brayton cycle mass with the system using insulation only. Figure 6-35 shows this comparison. A more detailed analysis is required to verify the results of this preliminary investigation, however, it appears that for an 18-month mission an active system, where propellant is either refrigerated or reliquefied with no boil-off being allowed, is lighter than a system which utilizes insulation only.

SYSTEM WEIGHT REQUIRED TO DELIVER
A QUANTITY OF LIQUID HYDROGEN

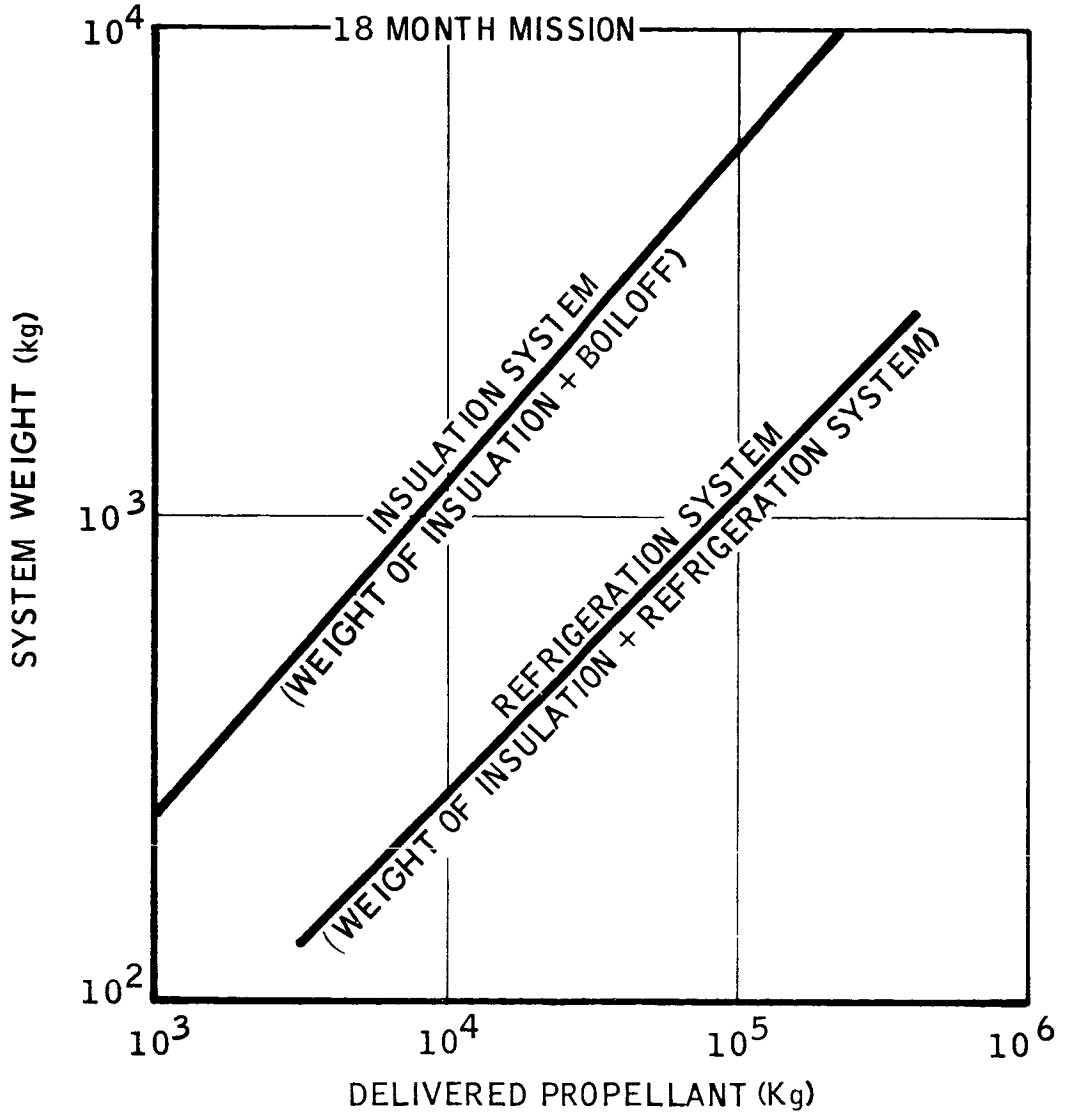

FIGURE 6-35

SECTION 6

REFERENCES

1. Younger, D. G., et al., "Multi-Wall Structure for Space Vehicles", WADD TR-60-503, 1960.

2. Koelle, H. H. ed., "Handbook of Astronautical Engineering", McGraw-Hill Book Company, 1961.

3. Panel on Psychology and Physiology, "Human Factors in Undersea Warfare", National Research Council, 1949.

4. Gantz, Lt. Col. K.F., USAF, ed., "Man in Space".

5. Rathert, George A., et al., "Minimum Crew Space Habitability for the Lunar Mission", ARS paper 2644-62.

6. Wilson, R. K., et al., "Report No. FZK-144", General Dynamics, Fort Worth, 1962.

7. Rom & Johnson, "Nuclear Rockets for Interplanetary Propulsion", paper presented at SAE National Aeronautic Meeting, April, 1959.

8. Johnson, Miser, & Smith, "Residual-Load-Plus-Powerplant Weights for Orbital-Launch Nuclear Rockets", NASA TN D-843.

9. Cavicchi, R. H., and Miser, J. W., "Determination of Nuclear-Rocket Power Levels for Unmanned Mars Vehicles Starting from Orbit About Earth", NASA TN D-474.

10. Parametric Engine Performance, Weight, and Envelope Data for Nuclear Rocket Propulsion Systems, Curves obtained from Aerojet-General Corp., Azusa, Calif., Conf. Restricted Data.

11. "Final Report NERVA Engine Development Program and Associated Tasks, for the period 10 July 1961 through 10 January 1962, Volume II - NERVA Engine System Appendix - specifications", Aerojet-General Corp., Report No. 2200, Feb. 1962, Secret-RD.

12. Slide Book, "Propellant State-of-the-Art", Rocketdyne BCL 62-136, Conf.

13. Irwin, R. E., "Optimization of Multistage Vehicles", Aeronutronic Memorandum SE-S-IBD-50, 20 October 1961.

14. Kohler, J.W.L., "Principles of Gas Refrigeration Machines", Proceedings of 1956 Cryogenic Engineering Conference, Advances In Cryogenic Engineering, Vol. 12.

15. Kovit, B., "Miniature Single-Stage Cryogenerator Reaches 30 deg. K", Space/Aeronautics, Jan. 1961.

16. Smolak, George R., Knoll, Richard H., and Wallner, Lewis E., "Analysis of Thermal-Protection Systems for Space-Vehicle Cryogenic-Propellant Tanks", NASA TR R-130.

17. Smolak, George R., and Knoll, Richard H., "Cryogenic Propellant Storage for Roundtrips to Mars and Venus", Aero/Space Engineering, June 1960.

18. Smolak, G. R., and Knoll, Richard H., "Cryogenic Propellant Storage for Roundtrips to Mars and Venus", IAS Paper No. 6023.

19. Ta Li, "Liquid Behavior in a Zero-G Field", IAS Paper No. 61-20.

20. Macklin, Martin, "Space Cooling Procedures", IAS Paper No. 61-18.

21. Love, Charles C., "Liquid Hydrogen Transport Time Limits in Space", ARS Paper 1087-60.

22. Ballinger, J. C., Elizalde, J. C., and Christensen, E. H., "Thermal Environment of Interplanetary Space", Convair Astronautics Paper.

23. Schwartz, E. W., "Liquid Behavior Investigations Under Zero and Low G Conditions", Convair Astronautics Paper.

24. Scott, Russell B., "Cryogenic Engineering", D. Van Nostrand Co., Inc., 1959.

25. Ehricke, Krafft A., "Space Flight--Environment and Celestial Mechanics", Vol. 1, D. Van Nostrand Co., Inc., 1960.

26. Threlkeld, J. L., "Thermal Environmental Engineering", Prentice-Hall, Inc., 1962.

27. Besserer, C. W., Merrill, Grayson, ed., "Principles of Guided Missile Design - Missile Engineering Handbook",D. Van Nostrand Company Inc., 1958.

28. Ehricke, Krafft A., "A Systems Analysis of Fast Manned Flights to Venus and Mars" Part II: Storage of Liquid and Solid Hydrogen on Nuclear Powered Interplanetary Vehicles", ASME Paper No. 60-AV-1. (Presented at 1960 ASME Semi-Annual Meeting and Aviation Conference, Dallas, Texas, June 5-9, 1960)

29. Emslie, A. G., "Gas Conduction Problem with Multilayered Radiation Shields", A. D. Little, Inc., Rep. No. 63270-04-01, April 1961. (NASA Contract No. NAS5-664.)

30. Emslie, A. G., "Radiation Transfer by Closely Space Shields", A. D. Little, Inc., Rept. No. 63270-04-02, May 1961. (NASA Contract No. NAS 5-664.)

31. Butler, C. P., and Inn, E.C.Y., "The Total Hemispherical Emissivity of Metals", Res. and Dev. Tech. Report, USNRLD-TR-327 BU. Aer., U. S. Naval Radiological Defense Laboratory, May 28, 1959.

32. Fonseca, E., "The Boomerang Project", XII I.A.C., Washington, D.C., 1961.

33. Goodwin, F., "The Exploration of the Solar System", Plenum Press, 1960.

34. Crocco, G. A., "One-Year Exploration Trip...", VII I.A.C., Rome, 1956.

35. Wallner, L. E., et al., "Radiation Shielding", NASA TN D-681, 1961.

36. Laning, J. H., et al., "Preliminary Consideration on the ... Reconnaissance of Mars", MIT Instrumentation Lab Report R-174, 1958.

37. Battin, R. H., "The Determination of Round Trip...," MIT Instrumentation Lab Report R-219.

38. Himmel, S. C., et al., "Study of Manned Nuclear...," Aero/Space Engineering, July, 1961.

39. Dugan, Duane W., "A Preliminary Study of a Solar-Probe Mission", NASA TN D783.

40. Brun, R. J., Livingood, J. N. B., Rosenberg, E. G., and Drier, D. W., "Analysis of Liquid-Hydrogen Storage Problems for Unmanned Nuclear-Powered Mars Vehicles", NASA TN D-587.

41. Olivier, J. R., and Dempster, W. E., "Orbital Storage of Liquid Hydrogen", NASA TN D-559.

42. Sirocky, Paul T., "Transfer of Cryogenic Fluids by an Expulsion-Bag Technique", NASA TN D-849.

43. Gray, V. H., Gelder, T. F., Cochran, R. P., and Goodykoontz, J. H., "Bonded and Sealed External Insulations for Liquid-Hydrogen-Fueled Rocket Tanks during Atmosphere Flight", NASA TN D-476.

44. Chelton, Dudley B., and Mann, Douglas B., "Cryogenic Data Book", National Bureau of Standards.

45. MacKay, D. B., and Bacha, C. P., "Space Radiator Analysis and Design", ASD Technical Rept. 61-30 Part 1.

46. "Radiation Heat Transfer Analysis", ASD Tech. Rept. 61-119 Part 1.

47. "Spacecraft Thermal Control", Lockheed Missiles and Space Division Progress Report, Sept. 1960.

48. Kramer, J. L., Lowell, H. H. and Roudebush, W. H., "Numerical Computations of Aerodynamic Heating of Liquid Propellants", NASA TN D-273, 1960.

49. Burry, R., "Liquid Propellant Storage in Earth Satellite Orbits", Rocketdyne Division of North American Aviation, Inc., (Paper presented at April 7, 1960, session of Institute of Environmental Sciences, Los Angeles, California.)

50. Edelbaum, T. N., "Comparison of Nonchemical....," United Aircraft Corporation, Res. Lab., R-1383, Oct. 1960.

51. Baker, R. M. L. Jr., et al., "Introduction to Astrodynamics", Academic Press, 1960.

52. Dedeon, G. S., "Round-trip Trajectories to Mars and Venus", AAS Preprint 62-30.

53. "The Atmosphere of Mars and Venus", National Academy of Sciences, Publication 944.

54. "Study of Interplanetary System" NAS8-2469 (Lockheed).

55. Weiss, D. C. "Computation Technique for Fast Transit Earth-Mars Trips", General Atomics, Rept. 2626.

56. Weiss, D. C. "Graphical Solution of Earth-Mars Interplanetary Roundtrips", General Atomics, Rept. 2661.

57. Moore, R. W. Jr., "Conceptual Design Study of Space Borne Liquid Hydrogen Recondensers for 10 and 100 watts capacity", A. D. Little, Inc.

58. Welch, Billy E., et al., "Bioengineering Experiments in the SAM Space Cabin Simulator", Paper presented at 17th Annual Meeting and Space Flight Exposition, ARS, Nov. 13-18, 1962.

59. Etherington, Harold, ed., "Nuclear Engineering Handbook", McGraw-Hill Book Co., Inc., 1958.

SECTION 7

LAUNCH AND ORBITAL OPERATIONS

7.1 INTRODUCTION

The requirements for Earth Launch Vehicles (ELV's) are studied by using projected reliability trends for the launch and orbital operations to derive overall mission success probabilities. Alternate ELV combinations are evaluated for four different EMPIRE mission vehicles during the early 1970's, including the effect on mission success of backup ELV's, duplicate nuclear upperstages and accelerated nuclear development.

The approach taken was to establish the minimum number of ELV's required for each mission, then to assign reliability trends for the ELV's, for orbital operations and for planetary injection. Assuming independence of the series of operations, a probability of success for the mission through injection becomes:

$$P = (R_{ELV})^{N} (R_{ORB})^{N-1} (R_{INJ}) \qquad (7\text{-}1)$$

where

P_{ELV} = Reliability of Earth launch vehicle

R_{ORB} = Reliability of Orbital operations (rendezvous, docking and assembly)

R_{INJ} = Reliability of injection into planetary orbit

N = Minimum number of ELV's required.

The probability, P, is increased by increasing the reliabilities, R's, and minimizing the number of ELV's required, N. However a smaller N is the consequence of larger ELV capability meaning higher costs (not considered in this analysis). The R's increase with later launch dates, but this evaluation should include the effects due to higher energy requirements and variation in solar radiation shielding requirements later in the 1970's.

The launch and injection reliabilities can be increased to a certain extent through accelerated programs. This is especially true for the nuclear upper stage (advanced NERVA) which appears as an improvement in R_{INJ}. An alternate method of increasing the reliability figures is to use duplication or backups. The reliability of two parallel and equivalent units over one is:

$$R_2 = 1 - (1 - R_1)^2 \qquad (7\text{-}2)$$

It will be shown later that duplication of upper stage nuclear units as well as program acceleration, and a duplicate backup of ELV's greatly increases the probability for a successful mission in the early 1970's.

7.2 REQUIREMENTS FOR VEHICLES

Weights previously were estimated for four EMPIRE mission vehicles to be placed into an Earth orbit and are listed in Table 7.1. The first vehicle weight in Earth orbit is that for the Crocco (one year) mission using nuclear final stages to inject it into the planetary orbit and is approximately 2¼ million pounds. Using Earth orbit capabilities of 100 tons, 250 tons, and 350 tons as conservative figures for the Saturn C-5, Nova and Super-Nova ELV's, respectively, the minimum number of boosters required for this mission are shown in Table 7.1. The requirement for twelve Saturn C-5's results in a very poor mission success as will be demonstrated shortly, and would require additional orbital launch facilities (OLF) (Ref. 1). The larger the number of boosters, the longer is the orbital assembly time which not only degrades the overall reliability, but also necessitates a higher orbital assembly altitude. Those cases requiring few ELV's can be placed into lower Earth orbit for assembly purposes, thus permitting some weight gain.

TABLE 7.1

MINIMUM NUMBER OF EARTH LAUNCH VEHICLES REQUIRED

Planetary Orbit	Injection Propulsion	Weight in Earth Orbit (lb.)	Saturn C-5 (100 tons)	Nova (250 tons)	Super-Nova (350 tons)
Crocco	Nuclear	2,243,000	12	5	3
Symmetric	Nuclear	375,000	2	1	1*
Symmetric	Chemical (I_{sp} = 410)	701,000	4	2**	1*
Symmetric	Chemical (I_{sp} = 300)	1,859,000	10	4	1***

* No additional orbital injection stage required
** Or 1 Nova and 1 Saturn C-5
*** Fourth stage required

The symmetric-orbit mission weights also are shown; one with nuclear upper staging and two using chemical upper staging (I_{sp} = 410 sec and I_{sp} = 300 sec). It is suggested that the symmetric mission could be accomplished with a Super-Nova without the need for additional staging (i.e., the Super-Nova final chemical stage would be restartable and capable of placing 80 tons into symmetric orbit). An interesting combination arises for the high specific impulse chemical vehicle using one Nova and one Saturn C-5 which takes advantage of the higher reliability for the Saturn. The present-day chemical (I_{sp} = 300 sec) system would require an additional stage on the Super-Nova, as its payload into the symmetric planetary orbit is in excess of 100 tons. The Crocco payload is only 90 tons into its planetary orbit, however the much higher injection velocity required eliminates the possible use of only one or even two Super-Novas.

7.3 RELIABILITY TRENDS

Figure 7-1 shows the projected reliability growth with time, or number of tests, for the three different Earth launch vehicles. It was obtained from a variety of sources (Ref. 2-5) and is consistent with data given by Koelle (Ref. 4). The operational dates used were 1967, 1970 or or 1971 for the Saturn C-5, Nova or Super-Nova, respectively. This assumes either Nova or Super-Nova, but not both, are to be developed. Thus, for the earliest time period being considered for the EMPIRE mission of mid-1970, the three ELV's are seen to have the following respective reliabilities: 0.75, 0.685, and 0.65.

The reliability growth trends for the subsequent orbital operations are shown combined in Figure 7-2. By this time period a considerable number of rendezvous and docking experiments will have been performed under the Gemini and Apollo programs. Orbital assembly will have been accomplished under both NASA and DOD programs. Thus, these operations should exhibit a high degree of reliability. This conclusion coincides with the data given in the OLO studies of Vought Astronautics (Ref. 1,6-9) and of Sperry Rand (Ref. 10).

Three orbital launch reliability trends also are shown for injection into a planetary orbit by nuclear or chemical systems. These are projections based upon the presently planned developmental schedules (Ref. 5, 11). The reliability trend for the higher specific impulse chemicals reflects confidence in expected state-of-the-art advances based on a variety of chemical possibilities and the relatively short development periods required. The much lower reliability trend for the nuclear system reflects the NERVA and RIFT schedules as presently set. Accelerating these programs and critical developments (in particular, the reactor core) would move the reliability curve upwards. The effect of this upon the mission success will be emphasized shortly, where translations of the curve to the left by one or two years will be considered.

7.4 PROBABILITY OF MISSION SUCCESS

A rather low probability of mission success is shown dashed in Figure 7-3 for the Crocco mission. (A chemical version of the Crocco mission requires such a tremendous orbital weight that it was immediately discarded as impractical.) As is evident in this figure and others which follow, the Super-Nova has the highest probability and the Saturn C-5 has the lowest because of the effect of the larger number of Earth launch vehicles and orbital rendezvous operations required in the latter case.

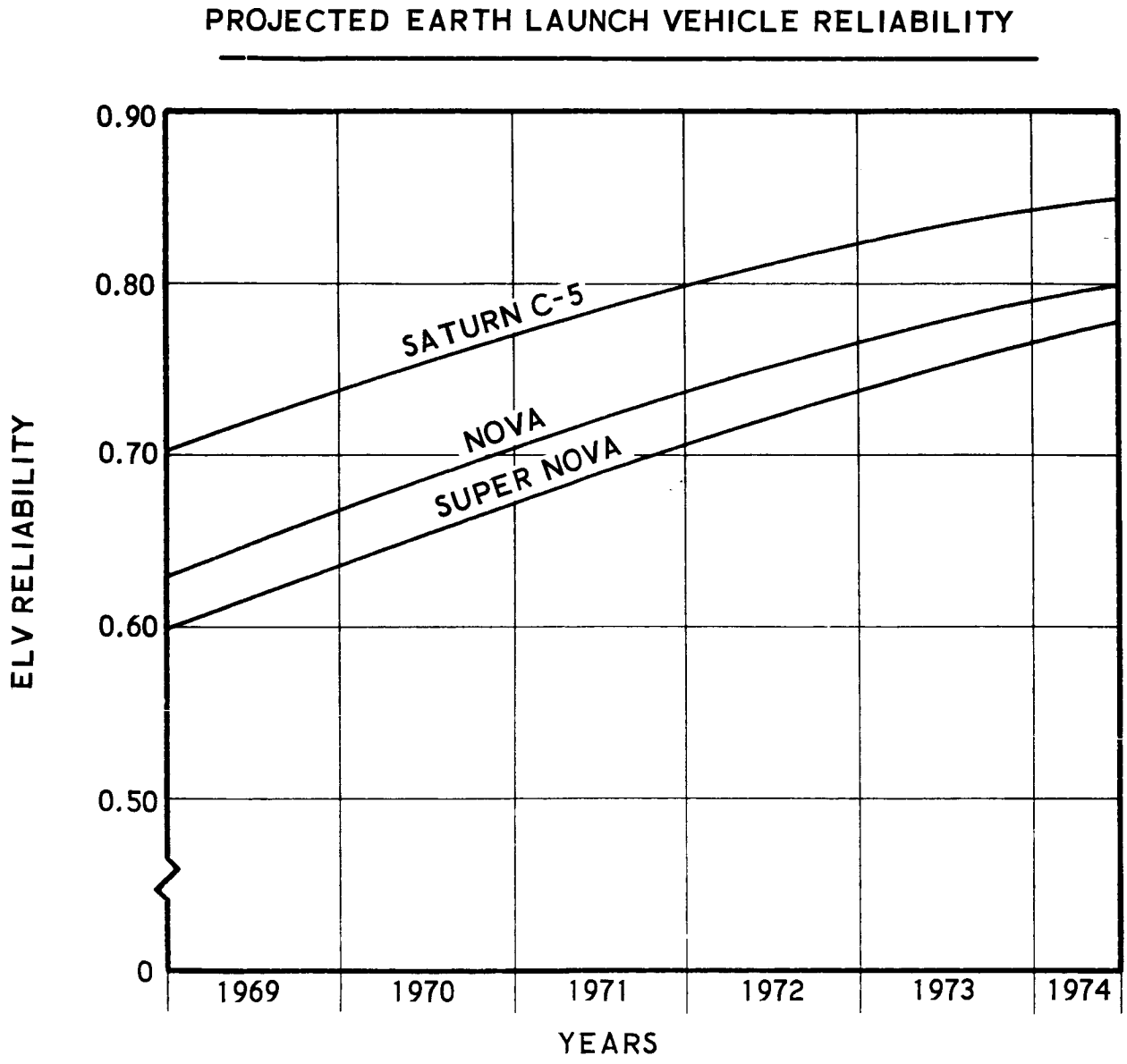
PROJECTED EARTH LAUNCH VEHICLE RELIABILITY
ELV RELIABILITY
0.90
0.80
0.70
0.60
0.50
0
SATURN C-5
NOVA
SUPER NOVA
1969
1970
1971
1972
1973
1974
YEARS

FIGURE 7-1.

PROJECTED ORBITAL OPERATIONAL RELIABILITY TRENDS

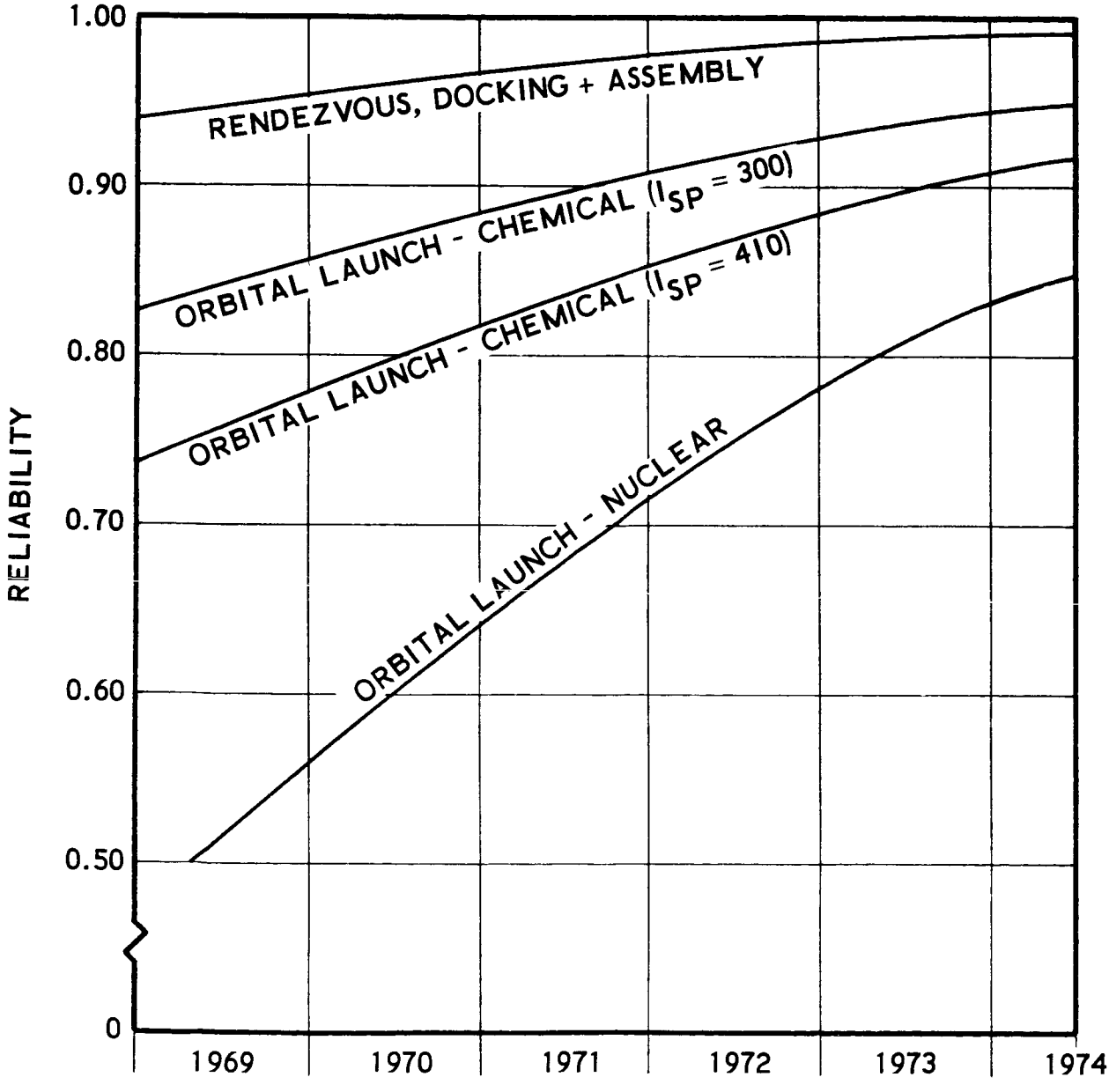

FIGURE 7-2.

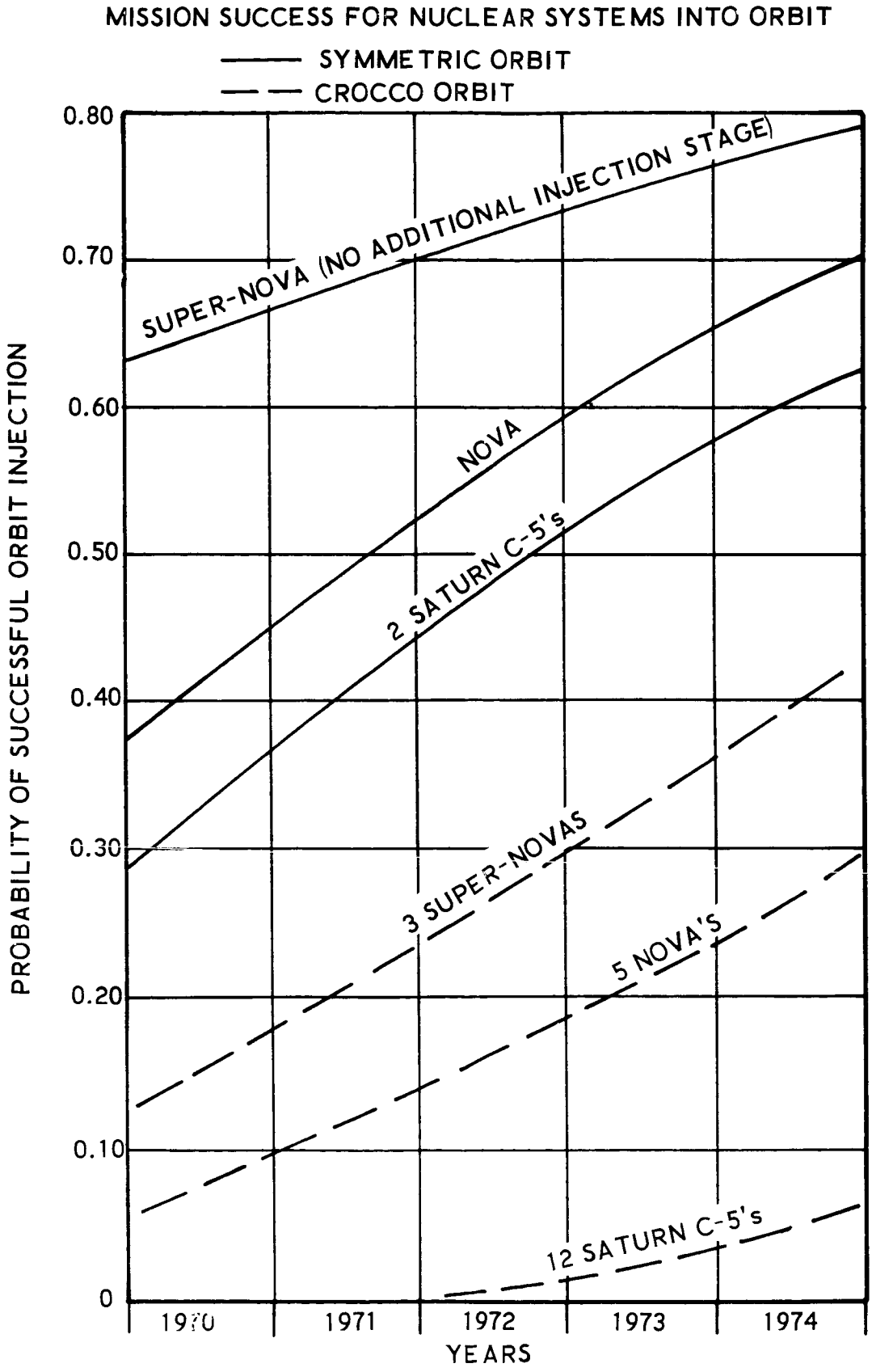
MISSION SUCCESS FOR NUCLEAR SYSTEMS INTO ORBIT
SYMMETRIC ORBIT
CROCCO ORBIT
PROBABILITY OF SUCCESSFUL ORBIT INJECTION
0.80
0.70
0.60
0.50
0.40
0.30
0.20
0.10
0
SUPER-NOVA (NO ADDITIONAL INJECTION STAGE)
NOVA
2 SATURN C-5's
3 SUPER-NOVAS
5 NOVA'S
12 SATURN C-5's
1970
1971
1972
1973
1974
YEARS

FIGURE 7-3.

The symmetric EMPIRE mission shown in Figure 7-3 has the highest probability of success using a nuclear final staging for injection into the planetary orbit. Recall that this vehicle system had the lowest orbital weight requirement which was 375,000 lbs. Again the Super-Nova shows the highest trend which was due to the elimination of the final nuclear staging by using an upper stage chemical restart. The single Nova does require final nuclear staging. Two Saturn C-5's were required for this mission. Thus, an injection system probability of success of 65 percent appears feasible for the 1970 EMPIRE mission if the Super-Nova were chosen over the Nova. If Nova is chosen then a figure of about 42 percent is feasible in 1970 provided NERVA is pressed hard to meet this schedule. Use of backup ELV's and duplicate nuclear injection stages will make the Saturn more attractive as will be shown in a subsequent figure.

It is quite evident that abort capability is necessary from these figures. Provisions have been made for abort both during Earth launch as well as during the orbital operations sequence, and in particular during planetary injection, so that the probability of survival of the crew will run at least as high as 99 percent. In cases where the Earth orbiting payload is launched as separate packages, such as the case above using two Saturn C-5's, the unmanned portions would be launched first followed by backup launches where failures occur. Then the final package would contain the crew with a smaller abort capability requirement than in the case of single payload launches by Nova or Super-Nova. If abort occurred, a second Saturn and crew should be prepared to launch and take over the mission (or the second ELV could launch the first crew later).

The use of a high specific impulse chemical upperstaging (shown by solid curves in Figure 7-4) instead of the nuclear units, reduces the injection reliability of the symmetric mission from about 5 to 10 percent. Recall this case requires an orbital launch weight of 701,000 lb. One Super-Nova, two Novas or four Saturn C-5's would be required. An interesting vehicle combination is shown using one Nova and one Saturn C-5 which would result in an injection system reliability of about 40 percent in the 1970 period. Using the Nova to launch the unmanned payload first, including backup Novas and unmanned payloads, if necessary, increases the mission reliability to:

$$P = (R_{SAT}) (R_{ORB}) (R_{INJ}) = (0.75) (0.96) (0.80) = 0.58 \qquad (7\text{-}3)$$

The Super-Nova approach is identical to that on the previous figure since no planetary injection staging or parking orbit is necessary.

MISSION SUCCESS FOR CHEMICAL SYSTEM INTO SYMMETRIC ORBIT

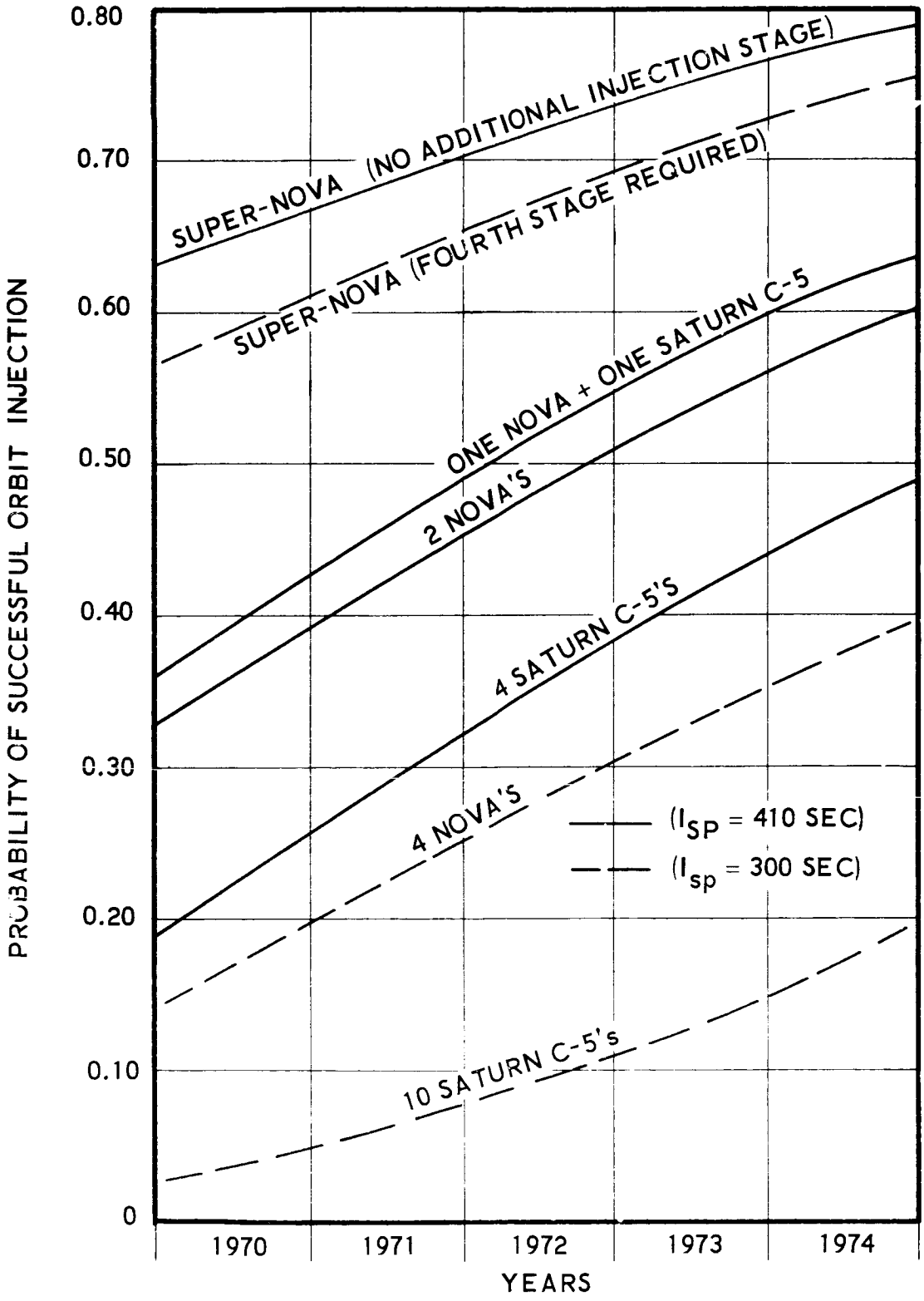

FIGURE 7-4.

7.5 PROBABILITY OF MISSION SUCCESS USING REDUNDANT SYSTEMS

It has been demonstrated that the highest probability of mission success during the 1970 launching into a symmetric planetary orbit would be about 65 percent, and then only if the Super-Nova ELV were to go into an immediate development program. The Nova or Saturn C-5 ELV's would necessitate nuclear upperstages for injection into the symmetric planetary orbit and even then would only result in probabilities of about 42 percent or 33 percent, respectively, in 1970.

The advantage of launching separate payload packages, with the crew in the last launch, was discussed. Two advantages are evident; that of separating the crew from previous payload packages (requiring abort only on the crew package); and the advantage of using backup ELV's to increase overall mission success, however, it does considerably increase the cost of the ELV's, necessitating both duplication in cost of units as well as the requirement for a certain amount of duplication in launch facilities. This must be weighed, in a subsequent analysis, against the cost of the larger Nova unit and its developmental costs.

The lowest solid curves in Figure 7-5 indicate the success probability growth with the number of Saturn C-5's used for the symmetric mission in 1970. Recall that a minimum of 2 Saturns were necessary for the nuclear injection vehicle, whereas 4 Saturns were required for the chemical (I_{sp} = 410 sec) vehicle. Complete duplication, 4 and 8 Saturns, respectively, really increase the liklihood of mission success. Larger quantities of ELV's offer diminishing returns as the probabilities now are limited by the injection reliabilities.

Figure 7-5 shows sizable increases in mission success by duplication (or triplication) of upperstage propulsion units, particularly in the case of the nuclear propulsion. The reliability of a single nuclear unit is 0.60 in 1970 from Figure 7-3. Duplication increases this, by equation 7-2, to:

$$R_2 = 1 - (1 - 0.60)^2 = 0.84 \qquad (7\text{-}4)$$

or triplication would be:

$$R_3 = 1 - (1 - 0.60)^3 = 0.936 \qquad (7\text{-}5)$$

These effects on overall mission success are shown by the upper solid curves in Figure 7-5. The design of duplicated or triplicated

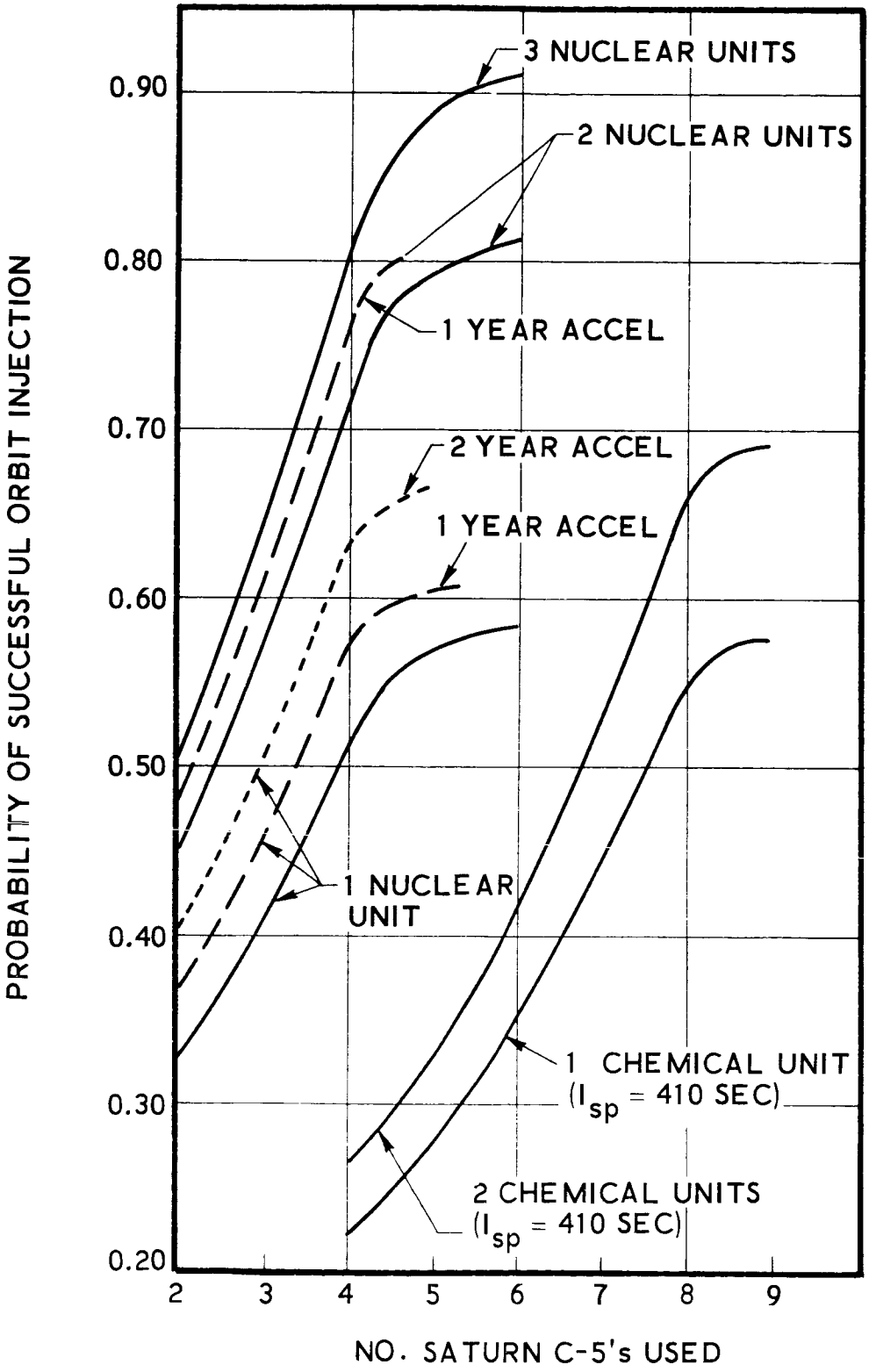
3 NUCLEAR UNITS
2 NUCLEAR UNITS
1 YEAR ACCEL
2 YEAR ACCEL
1 YEAR ACCEL
1 NUCLEAR UNIT
1 CHEMICAL UNIT (I_{sp} = 410 SEC)
2 CHEMICAL UNITS (I_{sp} = 410 SEC)
PROBABILITY OF SUCCESSFUL ORBIT INJECTION
0.90
0.80
0.70
0.60
0.50
0.40
0.30
0.20
2
3
4
5
6
7
8
9
NO. SATURN C-5's USED

FIGURE 7-5.

units, including possible pitching effects from off-center alignment, cross-radiation effects, and added structure is reserved for a future study, however the additional weight penalties seem to be small compared to the reliability gains (Ref. 11).

Shown dashed and dotted in Figure 7-5 are the effects of accelerating the nuclear development program by one or even two years by 1970. Some decided improvements are evident, however, duplication of the nuclear units gives the more significant improvement. The acceleration of the nuclear development program by one year and duplication of ELV's as well as injection stages results in a probability of mission success of 75 percent in 1970, using 4 Saturn C-5's.

Figure 7-6 demonstrates the effects of duplication and nuclear program acceleration using Novas or combinations of Novas and Saturn C-5's. Using two Novas and two accelerated nuclear units would result in a probability of success of 80 percent in 1970. A combination of two Novas and two Saturn C-5's would be about equivalent to this performance if chemical units were used. Thus, a Nova is roughly equivalent in relative success to two Saturn C-5's (compare Figures 7-5 and 7-6), and roughly twice as many ELV's are required for chemical injection compared to nuclear injection.

Figure 7-7 shows the success trends for a Crocco far flyby mission in 1970 using Saturns or Novas. The far flyby would pass each planet at distances about equal to their respective radii, rather than at the nominal three-tenths radii, and would require approximately 800 tons into Earth orbit (recall the nominal weight was about 1100 tons). Assembling eight packages in Earth orbit using a complete backup of ELV's thus totaling 16 Saturn C-5's, appears to be approaching the limit of orbital operations capability. Therefore this is a definite requirement for Nova should a Crocco trajectory be desired.

Figure 7-8 shows the trends for the symmetric mission in 1972 using Saturns or Novas and nuclear upperstages. The same payload weights into Earth orbit were assumed as previously used, so that this would amount to a more distant flyby of the planets (about one-half their respective radii). Some weight penalty results from higher energy requirements but this is offset some by the lower solar protection requirements. Comparing this mission with the 1970 mission, the differences reflect the ELV and injection reliability figures for the 1972 period which are about 15-18 percent higher.

SYMMETRIC MISSION SUCCESS IN 1970 USING NOVAS

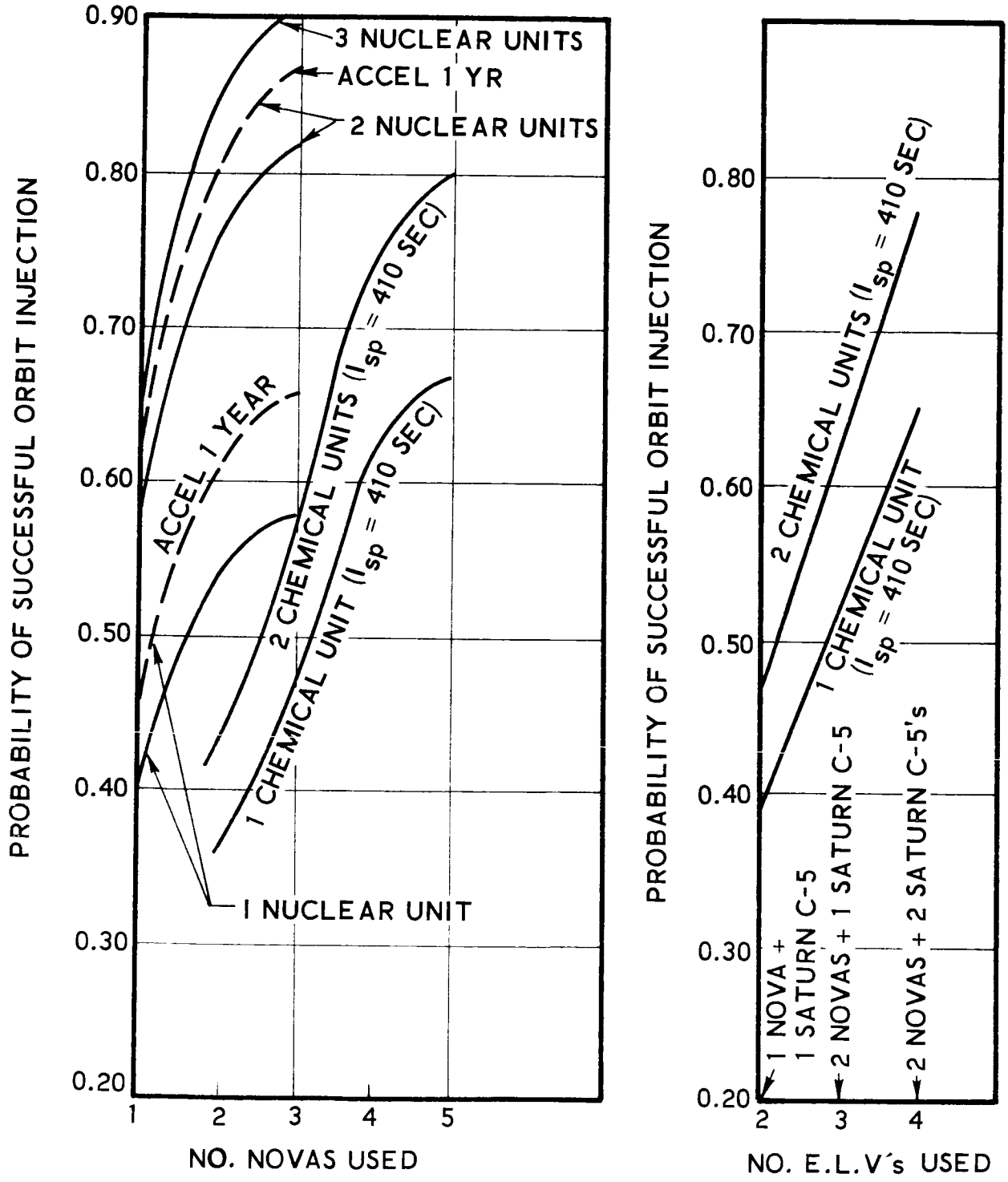

FIGURE 7-6

CROCCO FAR FLYBY MISSION SUCCESS IN 1971

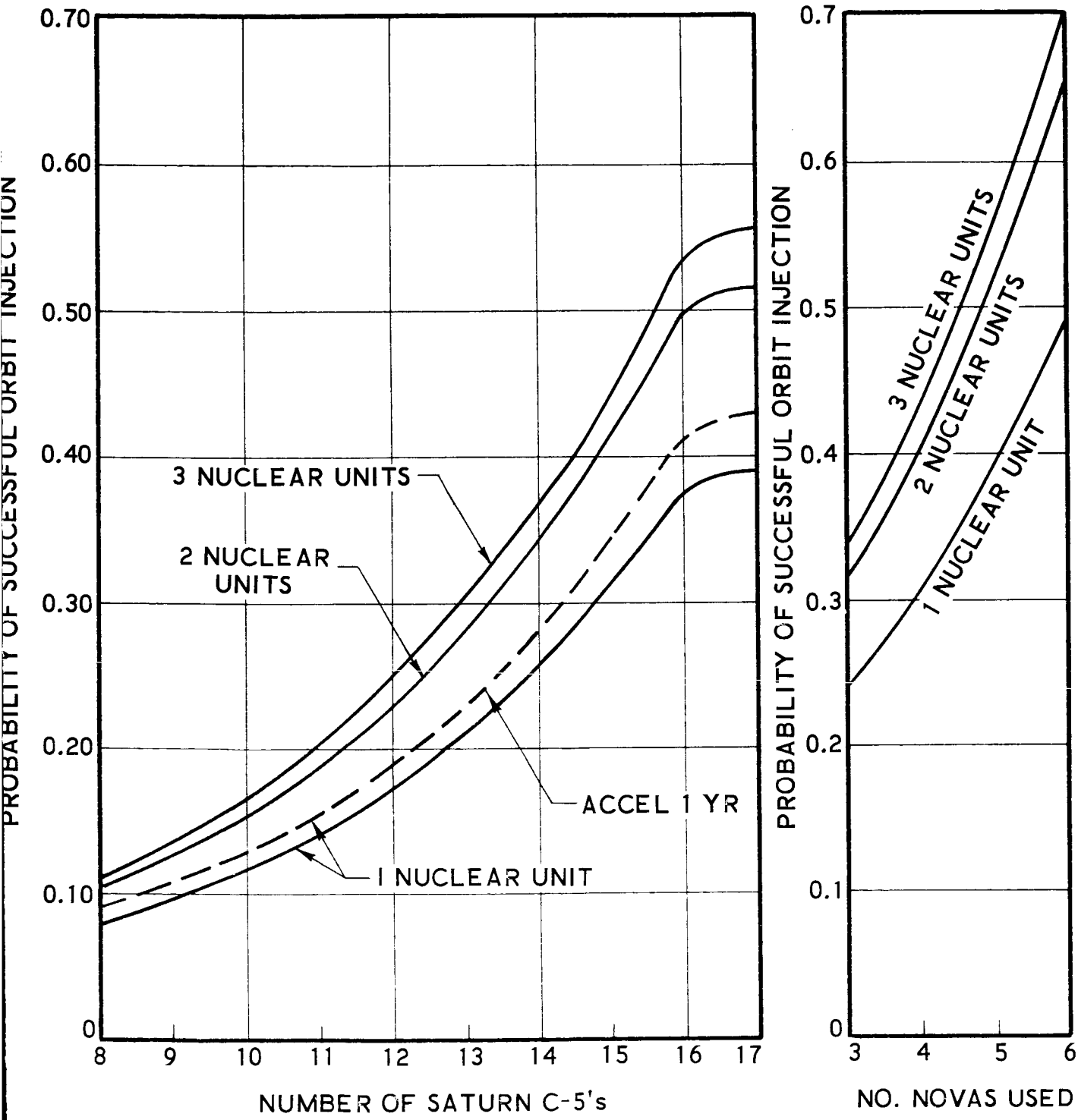

FIGURE 7-7.

SYMMETRIC MISSION SUCCESS IN 1972

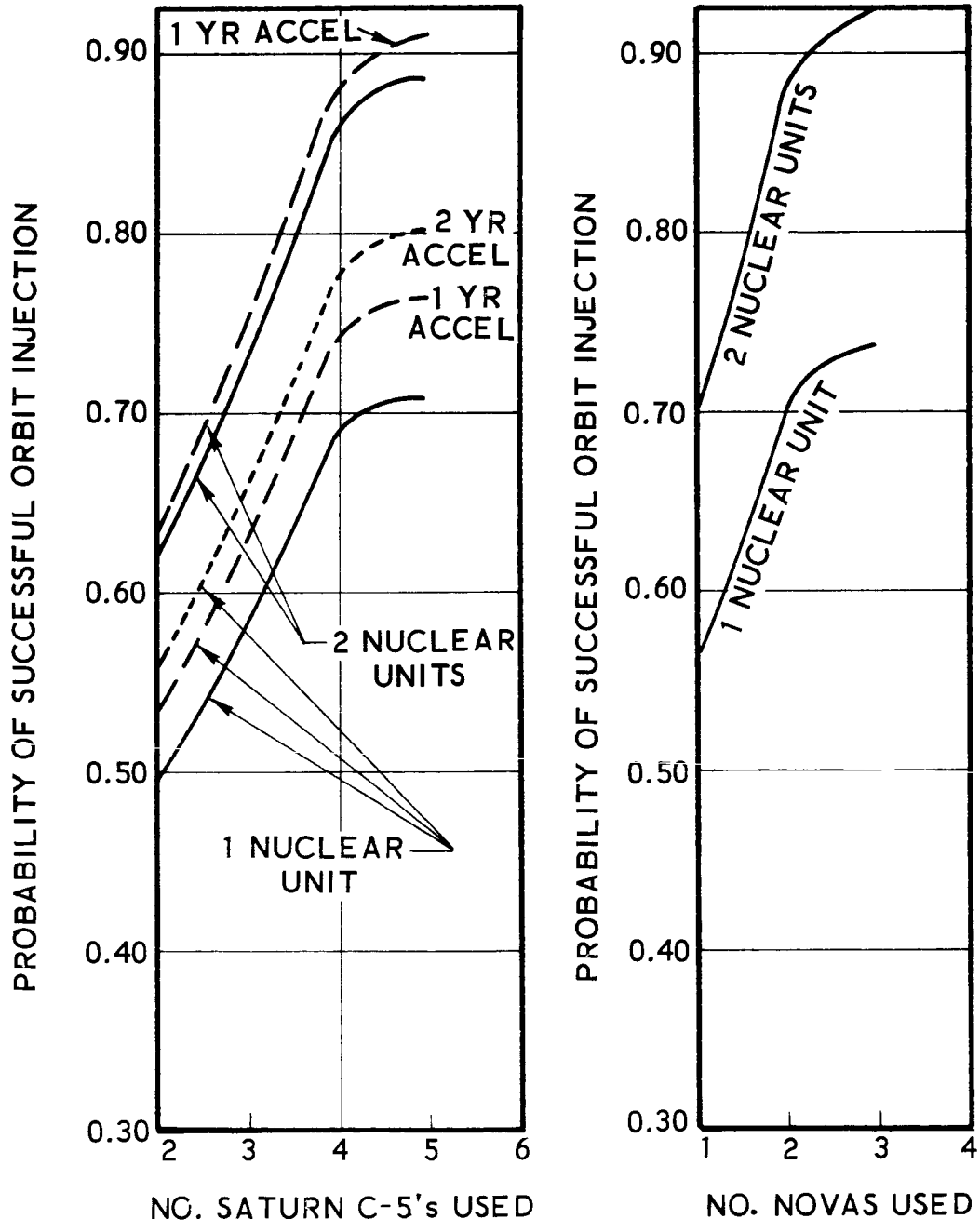

FIGURE 7-8.

7.6 CONCLUSIONS

The conclusions which can be drawn from this phase of launch and orbital operations based upon probability of mission success are:

- Super-Nova offers the highest probable mission success of 2 out of 3 in 1970 without duplication or backup ELV's.
- Nuclear injection staging outperforms chemical staging.
- Saturn C-5 ELV's appear practical only with the use of nuclear injection.
- Pairing of Nova and Saturn does show some promise for chemical injection.
- Abort capability is required on manned payloads.
- Largest penalty in mission success is due to ELV reliability and injection reliability; not due to the orbital operations of rendezvous, docking, and assembly.
- Backup ELV's significantly increase mission success.
- Duplication of nuclear injection stages can offer significant increases in mission success, if feasible.
- Acceleration of the nuclear development program also offers definite increases in mission success.
- Nova is roughly equivalent to two Saturn C-5's based upon mission success.
- Approximately twice as many ELV's are required for chemical injection having the same success as nuclear injection.
- Nova is required for the Crocco mission in 1971.

7.7 RECOMMENDATIONS

Recommendations from this phase of the study are:

- Accelerate nuclear development program at least one year from that presently planned for a 1970 mission.
- Initiate design studies of optimal staging taking into account the feasibility of designing duplicate nuclear upperstages.
- Perform cost and schedule analyses for the more promising vehicle combinations to evaluate which type and number of ELV's are most efficient.
- Consider relaxation of certain less critical requirements which would lessen payload weight such as the more distant flyby missions.
- Coordinate such changes with other aspects of the program such as selection of experiments which are feasible at the more distant flyby missions.

SECTION 7

REFERENCES

1. "Study of Orbital Launch Operations: Vol. I - Summary", Rept. No. 00.26 (C-V), Phase II Progr. Rept., Vought Astronautics Div., 16 Jan. 1962 (Conf.).

2. "Sixth Annual World Missile/Space Encyclopedia", Missiles and Rockets, July 30, 1962.

3. "Astrolog", Missiles and Rockets, Nov. 1962.

4. Koelle, H. H., "Missiles and Space Systems - 1962", Astronautics, Nov. 1962.

5. Private Communication, A. Ford, Rocketdyne, Div. of North American Aviation, Oct. 11, 1962.

6. "Study of Orbital Launch Operations: Vol. II - Rendezvous and Escape Windows", Rept. No. 00.26 (C-V), Phase II Progr. Rept., Vought Astronautics Div., 16 Jan. 1962 (Conf.).

7. "Study of Orbital Launch Operations: Vol. III - Orbital Operational Techniques", Rept. No. 00.26 (C-V) - Phase II Progr. Rept., Vought Astronautics Div., 16 Jan. 1962 (Conf.)

8. "Study of Orbital Launch Operations: Vol. VI - Operational Feasibility Rept. No. 00.26 (C-V) - Phase II Progr. Rept., Vought Astronautics Div., 16 Jan. 1962 (Conf.)

9. "Study of Orbital Launch Operations: Vol. III - Additional Study Recommendations", Rept. No. AST/Eir-13491 - Interim Progr. Rept., 14 June 1961.

10. "Orbital Launch Operations: Vol. I - Summary", Publ. No. AB 1210 0004-1, Sperry Rand Corporation, Jan. 1962.

11. Private Communication, S. Gunn, Rocketdyne, Div. of North American Aviation, Nov. 1, 1962.

SECTION 8

PROGRAM DEVELOPMENT PLAN

8.1 INTRODUCTION

The proposed development plan presents the results of a planning effort to determine if it is feasible to accomplish a manned, non-stop, Mars and Venus flyby, close encounter mission in the 1970 to 1972 time span.

Additional constraints, assumptions, and considerations important to this planning effort are as follows:

(1) The mission state-of-the-art requirement shall, generally, not greatly exceed those of the Apollo mission.

(2) Earth return mode considerations:

- direct atmosphere entry
- rocket braking and atmospheric entry in combination
- crew safety, landing area control, land/water recovery, etc.

(3) Utilization of the Apollo command module, if feasible.

(4) Feasibility of desirable scientific missions

(5) Mission earth staging to be accomplished from the AMR.

(6) Program funding requirement shall not include research and development costs for Saturn, Nova, Apollo mission, nuclear rocket engine, nuclear electrical power unit, etc. equipment.

The initial planning effort was devoted to the selection of a mission trajectory and related vehicle configuration. In addition to development lead time considerations, state-of-the-art, parametric trade-off, and mission probability of success considerations (presented in previous sections of this report) were the key factors of constraint in identifying the various configurations selected. A comparative analysis of the prime development tasks for the non-symmetrical (Crocco) trajectory and symmetrical trajectory missions, utilizing nuclear propulsion for final orbital injection, was accomplished. This analysis served as the basis for final selection of a particular mission trajectory and vehicle configuration. Development and production activity scheduling and related program cost analysis identified the fact that the subject mission could be accomplished in the 1970 to 1972 time span.

It is important to note, however, that the feasibility of this accomplishment in the years under study is contingent upon immediate action to expedite nuclear development programs currently in process.

8.2 MISSION DEVELOPMENT TASK CONSIDERATIONS

An analysis of both the non-symmetrical, "Crocco" trajectory and the symmetrical trajectory missions, utilizing nuclear propulsion for final orbital injection, identified the following development task considerations as important factors to the selection of a mission trajectory and vehicle configuration.

a. Crocco, Non-Symmetric Mission Tasks

(1) Prime Tasks

. Spacecraft*

. Booster vehicles**

---

* Includes reentry/abort vehicle development.

** Development flight test and operational pre-injection boost vehicles.

- Earth-entry spacecraft development (identical to the Crocco spacecraft abort vehicle)
- Crew training program (Apollo extension)
- AMR mission staging base
- Earth-orbit mission staging base
- Earth-orbit staging base personnel training programs
- Deep space instrumentation and world-wide tracking system (existing facilities modified)
- One man "back-pack"vehicle (under development)
- Space suits (under development)
- Earth-based logistics vehicles

(2) Subtasks

Definition of important subtasks pertinent to the above development considerations are presented in Appendix A for Section 8.

b. Symmetric Mission Tasks

(1) Prime Tasks

- Spacecraft*
- Booster vehicles**
- Crew training programs (Apollo extension)
- AMR mission staging base

---

* Includes reentry/abort vehicle development.

** Development flight test and operational, pre-injection boost vehicles.

- Deep space instrumentation and world-wide tracking system (existing facilities modified)
- Earth-reentry vehicle recovery (water and land)
- Space suits (under development)
- One man "back-pack" vehicle (under development)

(2) Subtasks

Definition of important subtasks pertinent to the above development considerations are presented in Appendix B for Section 8.

A comparative analysis of the above noted key development tasks and related scheduling and funding considerations for the non-symmetric and symmetric, nuclear injection missions resulted in the selection of the symmetric trajectory, nuclear injection mission as having the highest probability of successful mission accomplishment for the 1970 to 1972 time span.

Spacecraft and booster development considerations, key to the comparative analysis process, are presented in Table 8.1. Support system development considerations are presented in Table 8.2. Scheduling considerations are identified in Subsection 8.5. Funding considerations are identified in Subsection 8.6.

8.3 SYMMETRIC MISSION DEVELOPMENT TEST PLAN

The definition and analysis of a development test program represents a significant portion of the effort devoted to the analysis of mission development considerations presented in the previous subsection (8.2) of this report. Development ground and flight test programs for the proposed symmetric trajectory mission are defined, briefly, in Tables 8.3 and 8.4.

It is important to note the following philosophical foundation upon which the above defined test programs were based:

(1) Man rating of all systems shall be accomplished as a prerequisite to any manned flight operations.

TABLE 8.1

COMPARATIVE SUMMARY - CROCCO AND SYMMETRIC MISSIONS*

PRIME DEVELOPMENT TASKS
(Spacecraft and Booster Vehicles)

	Crocco Mission	Symmetric Mission
Spacecraft	Life Support and Command Modules	Life Support and Command Modules
	Reentry/Abort Vehicle (Including Nuclear Propulsion)	Reentry/Abort Vehicle
	Guidance and Control	Guidance and Control
	Telecommunications	Telecommunications
	Nuclear Electrical Power Unit	Nuclear Electrical Power Unit
	Nuclear Propulsion - Stages I, II, III and IV	Nuclear Propulsion - Stages I and II
	Flight Termination	Flight Termination
	Thermal Control	Thermal Control
Booster Vehicles	Nova - Stages I and II (13 required)	Nova - Stages I and II (10 required)
	C-5 Saturn - Stages I & II (10 required)	C-5 Saturn - Stages I & II (4 required)
	C-1 Saturn - Stages I & II (3 required)	C-1 Saturn - Stages I & II (5 required)

* Nuclear injection

TABLE 8.2

COMPARATIVE SUMMARY - CROCCO AND SYMMETRIC MISSIONS*

PRIME DEVELOPMENT TASKS
(Support Systems)

	Crocco Mission	Symmetric Mission
Earth-Orbit Staging Base	Life Support and Command Modules	None Required
	Telecommunications	
	Guidance and Control	
	Electrical Power	
	Air Conditioning	
	Spacecraft Maintenance Platforms	
	Intercommunications	
	Hydrogen Liquefaction	
	Hydraulic and Pneumatic Power	
AMR Mission Staging Base	4 Checkout Stations	1 Checkout Station
	2 Launch Sites and Related Equipment	1 Launch Site and Related Equipment
Spacecraft Propulsion Development Test Facilities		
Ground Test (Nevada)		
Battleship Tests	1 Test Stand - Stages I and II Propulsion	1 Test Stand - Stages I and II Propulsion
	1 Test Stand - Stages** III and IV Propulsion	
Captive Tests	1 Test Stand - Stages I and II Propulsion	1 Test Stand - Stages I and II Propulsion
	1 Test Stand - Stages III and IV Propulsion	

* Nuclear injection
** Reentry/abort vehicle propulsion

TABLE 8.3

SYMMETRIC MISSION DEVELOPMENT GROUND TEST PLAN**

I. Spacecraft

1. Aerothermodynamic - Reentry/Abort Vehicle (Model Tests)
2. Space Simulation (Model Tests)
3. Subsystem and System*

Structural - static and dynamic loading
Battleship - cold flow (contractor "back-yard")
Battleship - hot firings (AEC Nevada)
Physical, RF and Electrical compatibility
Captive Vehicle - cold flow (contractor "back-yard")
Capture Vehicle - hot firings (AEC Nevada)
Reentry/Abort Vehicle - captive/hot firings (EAFB)

II. Nova Booster

Subsystem and System*

Structural - static and dynamic loading
Battleship - cold flow and hot firings (contractor facility)
Physical, RF and Electrical Compatibility
Captive Vehicle - cold flow and hot firings (contractor and Mississippi)

III. Reentry/Abort Vehicle and C-1 Saturn Booster

Captive Vehicle - stage I hot firing (Mississippi and AMR)

IV. Spacecraft and C-5 Saturn Booster

Captive Vehicle - stage I hot firing (Mississippi and AMR)

V. Spacecraft and Nova Booster

Captive Vehicle - stage I hot firing (Mississippi and AMR)

* Includes "buy" item acceptance, design qualification, flight certification and life expectancy/parametric test-to-failure.

** Nuclear injection

TABLE 8.4

SYMMETRIC MISSION DEVELOPMENT FLIGHT TEST PLAN*

I. Reentry/Abort Vehicle - drop tests (EAFB)

II. Ballistic Trajectory Tests (AMR)

Nova Booster

Reentry/Abort Vehicle (utilizing C-1 Saturn Booster)

Spacecraft (less reentry vehicle - utilizing C-5 Saturn Booster)

Spacecraft (utilizing Nova Booster)

III. Earth-Orbit Tests

Reentry/Abort Vehicle (utilizing C-1 Saturn booster)

Spacecraft and Nova Booster (unmanned)

Spacecraft and Nova Booster (manned)

* Nuclear injection

(2) All flight and support systems hardware shall be qualified in accordance with subsystem, system and interface specifications as a prerequisite to system man rating.

(3) All subsystem, system and interface specifications shall be proven, utilizing development ground and flight test data as a prerequisite to system man rating.

(4) Component, subassembly, assembly, module, and subsystem life expectancy/parametric test-to-failure tests of selected hardware shall serve as the prime basis for demonstration of system reliability.

(5) Design qualification testing shall be initiated at the low or component level with each successive level of testing (i.e., component, subassembly, assembly, etc.) for a given subsystem serving as prerequisite to tests for the following levels. This continues on up the level scale to, and including, physical, radio frequency, and electrical compatibility tests involving all subsystems and systems.

(6) All design qualified, production hardware shall be acceptance tested in accordance with acceptance specifications.

(7) All flight hardware shall be flight certified prior to integration with any subsystem and/or system equipment.

8.4 SYMMETRIC MISSION VEHICLE AND SUPPORT SYSTEM REQUIREMENTS

Vehicle and support system requirements for both mission development test and operational activity are key "footstones" in the mission implementation process. Flight hardware, ground support equipment and facility requirements (with the exception of requirements for logistics activity) are presented in Tables 8.5 and 8.6. Delivery dates pertinent to these requirements are identified in Figure 8-1.

Logistics system requirements in support of "factory-to-launch" and mission orbital activity were not identified. However, this activity and related vehicle and support system requirements were, in terms of generalized functional requirements, considered. The "factory-to-launch"

TABLE 8.5

SYMMETRIC MISSION FLIGHT HARDWARE REQUIREMENTS

	Delivery Requirements (Units)						
	1964	1965	1966	1967	1968	1969	1970
I. Spacecraft	--	--	2	5	4	4	--
Reentry/Abort Vehicle	--	--	3	5	4	4	--
Nuclear Rocket Engine	--	--	4	5	4	3	--
Nuclear Electrical Power Unit	--	--	4	5	4	3	--
II. Booster Vehicles							
C-1 Saturn (S-1 and S-4B)	--	--	1	4	--	--	--
C-5 Saturn (S-1B and S-4B)	--	--	1	3	--	--	--
Nova (Steps I & II)	--	--	2	4	4	4	--

* Nuclear injection

Note: Nova booster, nuclear rocket engine and nuclear electrical power unit development items not included.

TABLE 8.6

SYMMETRIC MISSION BASIC FACILITY REQUIREMENTS

Engineering, Manufacturing and Test/Checkout*

Crew Training Facilities (MSC and AMR)*

Development Ground Test Facilities

- Contractor "Back-Yard"
- Nevada Test Complex
- Mississippi Test Site
  - C-1 Saturn Test Complex*
  - C-5 Saturn Test Complex*
  - Nova Test Complex

Development Flight Test Facilities (AMR)

- C-1 Saturn Launch Site*
- C-5 Saturn Launch Site*
- Nova Hangar and Launch Site
- Spacecraft Assembly and Checkout

Operational Flight Facilities (AMR)

- Mission Staging Site
- Deep Space Instrumentation Facilities*
- World-Wide Tracking Net*

Reentry/Abort Vehicle Land Recovery Site

* Modification of existing facilities

sequence of activity is presented in Table 8.7 . Orbital logistics system requirement were identified as follows:

(1) Earth launched space rescue system (includes an eight-man reentry vehicle)

(2) Earth launched space supply system (includes small, medium and large payloads)

(3) Support systems for the above items (1) and (2)

8.5 SYMMETRIC MISSION DEVELOPMENT SCHEDULE

Another important factor in the selection of a mission trajectory and vehicle configuration for the accomplishment of the subject mission was the development schedule, presented in Figure 8-1. The time allocation and sequencing for the accomplishment of previously identified development events (Sections 8.2 and 8.3) is an important indicator of feasibility of mission accomplishment; that is, where a fixed span of time for development is an absolute constraint. An important product of the effort is the identification of those development tasks having relatively short lead times as compared to existing development schedules for these tasks. In this case, existing development programming of various spacecraft subsystems will require expediting. An investigation of these development processes yielded evidence that such expeditious action is feasible. A summary of expedite development requirements is presented in Table 8.8.

8.6 SYMMETRIC MISSION FUNDING REQUIREMENT FOR A 1970-72 LAUNCH

The funding requirement resulting from a cost analysis for the research and development and production of spacecraft, booster vehicle and support systems is presented in Figure 8-2.

A program cost analysis statement is presented in Table 8.9. The cost premises which serve as a basis for this cost analysis is presented in Table 8.10. A funding schedule breakdown is presented in Table 8.11.

TABLE 8.7 SYMMETRIC MISSION - FACTORY-TO-LAUNCH SEQUENCE

Spacecraft	Reentry/Abort Vehicle	Booster Vehicle (Steps I & II)
Factory subsystem tests*	Factory Subsystem tests	Factory subsystem tests
Factory composite acceptance test	Factory composite acceptance test	Factory composite acceptance test
Preparation for transport	Preparation for transport	Preparation for transport
Transport to AMR	Transport to AMR	Transport to "backyard" static test stand
Receive & inspect at hangar	Receive and inspect at hangar	Perform flight readiness firing
Repair as required	Repair as required; install spacecraft interface adapter	Prepare for transport to factory
Assemble spacecraft	Hangar checks	Transport to factory
Hangar checks	Transport to explosive safe facility	Adjustments and cleanup
Prepare for transport	Install explosives	Prepare for transport to AMR
Transport to radiation & explosive safe facility	Complete hangar checks	Receive and inspect
Install nuclear rocket engine & elec. power unit	Prepare for transport	Repair and required
Complete hangar checks	Transport to launch complex	Hangar checks
Prepare for transport	Erect on spacecraft	Prepare for transport
Transport to launch complex	Pre-launch tests	Transport to launch complex
Erect on booster adapter, align and weigh	Final service and checks	Erect step I on launch stand & step II on step I adapter
Pre-launch tests		Align and weigh
Final service and checks		Pre-launch tests
		Final service and checks

* Includes nuclear propulsion, propellant feed system cold-flow/blow-down tests.

PROJECT EMPIRE
SYMMETRIC MISSION (NUCLEAR INJECTION) DEVELOPMENT SCHEDULE

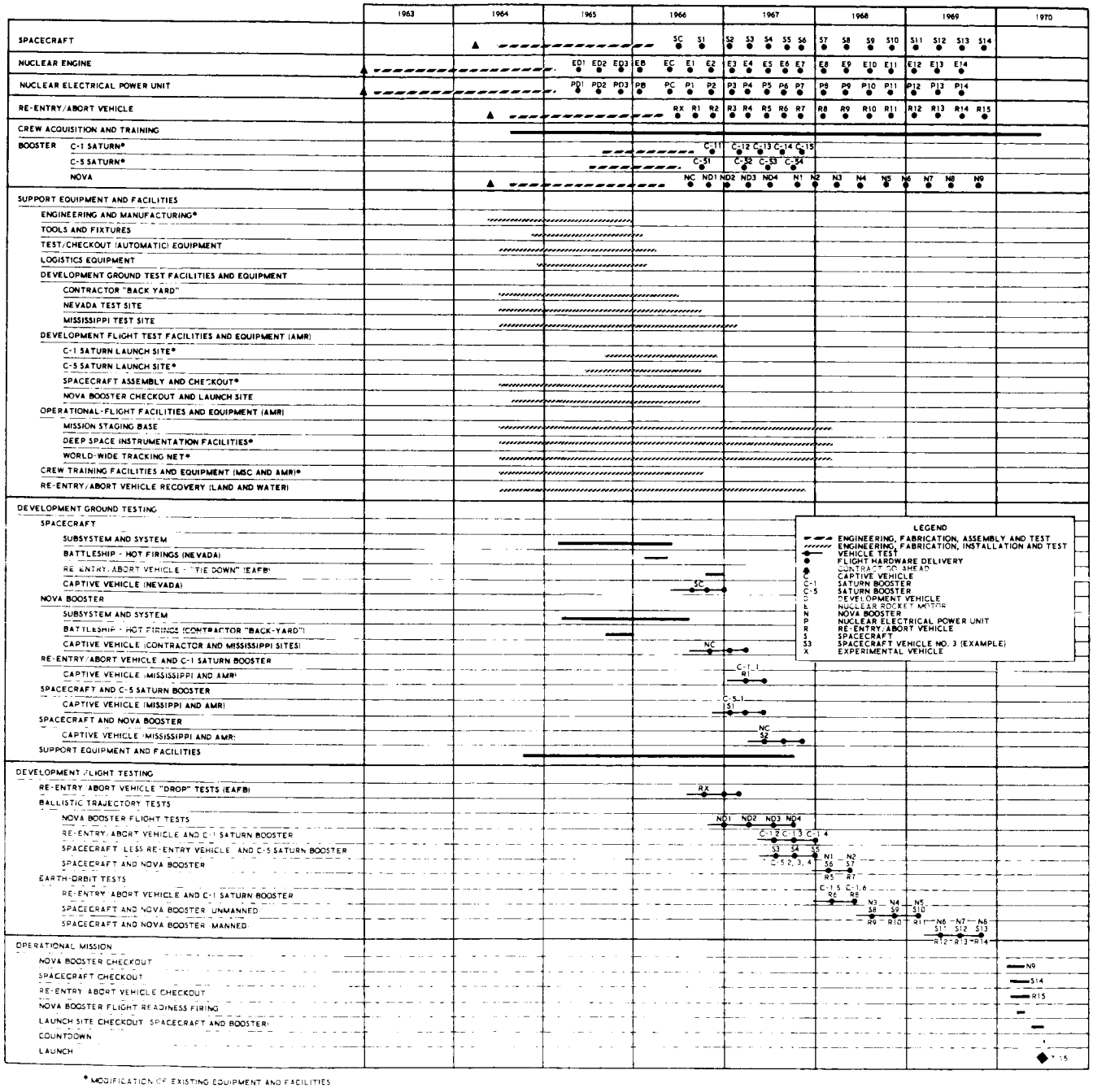

* MODIFICATION OF EXISTING EQUIPMENT AND FACILITIES

FIGURE 8-1.

TABLE 8.8

PROPOSED EXPEDITE DEVELOPMENT EFFORT

- Nuclear rocket engine development for man rating by 1969 - also increased thrust level and/or nominal burn time
- Non-cryogenic, tripropellant rocket engine development for increased specific impulse (I_{sp}) by mid 1967
- Nova engine development consistant with Nova development requirement
- Snap-8 life time extension or development of a solar-generator power unit
- Materials technology development for high reentry vehicle velocity design application by mid 1964

SYMMETRIC MISSION (NUCLEAR INJECTION)
FUNDING REQUIREMENT FOR 1970 LAUNCH

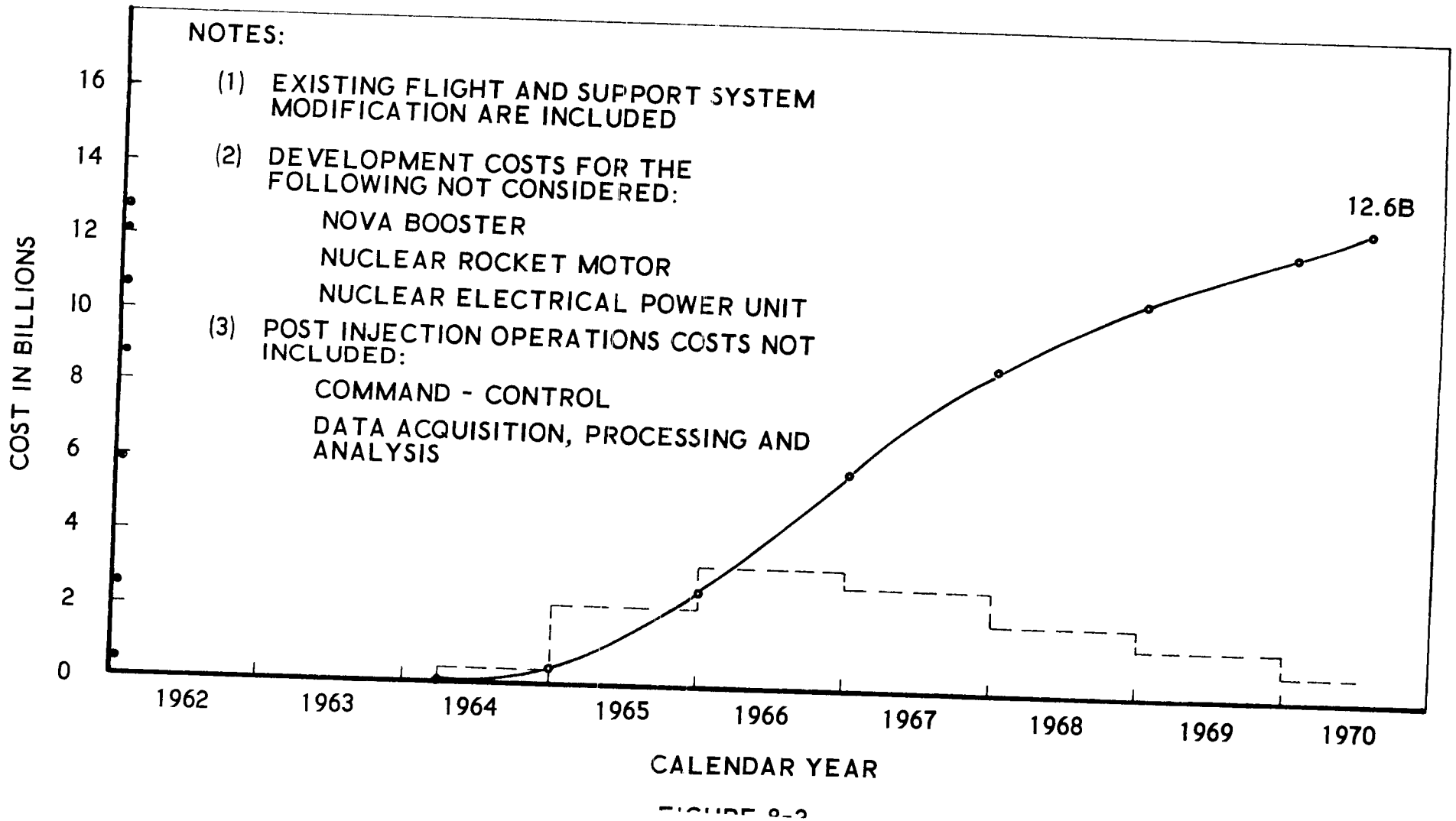

FIGURE 8-2

TABLE 8.9

SYMMETRIC MISSION (NUCLEAR INJECTION)

Cost Analysis

		Cost (Billions)	
I.	Flight Hardware & GSE		
	1. Spacecraft		
	a. Living Module and Radiation Shielding	$1.930	
	b. Reentry/Abort Vehicle	.236	
	c. Spacecraft Stages I & II Booster (less engine and EPU)	.042	
	d. Nuclear Engines	.105	
	e. Nuclear Electrical Power Unit (EPU)	.068	
	TOTAL		$2.381
	2. Booster Vehicles		
	a. Nova Booster (11 required - Stages I & II)	1.780	
	b. Saturn Boosters		
	C-1 (6 required - Stages I & II)	.065	
	C-5 (5 required - Stages I & II)	.425	
	TOTAL		2.270
	SUMMARY TOTAL		$4.651

II. (See next page)

TABLE 8.9 (Cont.)

II. Total Program Costs (less post injection costs) Reference 1

$$37\% \ (x) = 4.650 \times 10^9 \text{ dollars}$$

$$x = 12.6 \times 10^9 \text{ dollars}$$

Cost Breakdown	% Total	Cost (Billion $)
Engineering	43	5.40
Research	3	.376
Systems Analysis	2	.255
Flight Hardware	33	4.140
Ground Support Equipment	4	.502
Facilities	9	1.130
Mission and Payload Integration	3	.376
Launch Operations	3	.376
TOTAL	100	12.555

TABLE 8.10

SYMMETRIC MISSION COST ANALYSIS

Cost Premises

I.	Booster Vehicles	
	a. Developed Chemical Booster & Related GSE	- $10.00/lb Thrust
	b. Undeveloped Spacecraft Nuclear Booster (less engine)	- $5,000/lb Vehicle*
	c. Developed Spacecraft Nuclear Booster	- $375.00/lb Vehicle
	d. Nuclear Engine Costs	- 6.2 million each
II.	Spacecraft (less nuclear booster)	
	a. Spacecraft Living and Command Modules Development Costs and Reentry/Abort Vehicle	- $3,000/ lb Vehicle*
	b. Nuclear Electrical Power Unit	- 2.0 million each
III.	Modified Existing Flight Hardware and Related Facilities and Equipment Costs	- 1/.37 (developed booster cost)
IV.	Deep Space Instrumentation and World-Wide Tracking Net Modification Costs	- No additional cost considered. Assumed that Apollo, Ranger & Mariner programs would require a significant portion of this modification and improvement.

* Yields total program R&D cost.

TABLE 8.11 SYMMETRIC MISSION FUNDING SCHEDULE

	1964 *	1964 **	1965		1966		1967		1968		1969		1970	
Engineering	5	.26	20	1.06	30	1.57	15	.755	15	.755	10	.52	5	.26
Research	15	.056	50	.168	35	.132	--		--		--		--	
Systems Analysis	10	.026	30	.077	25	.064	20	.051	10	.026	5	.013	--	.013
Flight Hardware	--		5	.207	15	.596	35	1.400	25	1.015	20	.828	--	
Ground Support Equipment	--		5	.024	60	.301	35	.177	--		--		--	
Facilities	--		5	.555	60	.652	35	.370	--		--		--	
Mission and Payload Integration	15	.056	30	.113	5	.019	5	.019	20	.075	15	.056	10	.038
Launch Operations	--		--		--		--		5	.019	15	.056	80	.300
TOTALS		.398		2.204		3.334		2.772		1.885		1.473		.611

TOTAL FUNDING 12.6 billion

* Per cent
** Billions

REFERENCE

1. Based on typical funding distribution presented in Table 1.12, page 1-64 of the Handbook of Astronautical Engineering, McGraw-Hill Book Company, 1961.

SECTION 8

APPENDIX A

CROCCO NON-SYMMETRIC MISSION DEVELOPMENT TASKS

Subtasks pertinent to the subject mission prime development tasks are presented as follows:

Tasks	Table No.
Spacecraft	A8.1
Booster Vehicles	A8.2
AMR Mission Staging Base	A8.3
Earth-Orbit Mission Staging Base	A8.4
Logistics Vehicles	A8.5
Crew Training Program	A8.6
Earth-Orbit Staging Base	A8.7

TABLE A8.1

NON-SYMMETRIC MISSION

SPACECRAFT DEVELOPMENT TASKS

Nuclear Rocket Engine

Airframe	. Stages I & II propellant feed and pressurization - nuclear propulsion.
	. Stages III & IV propellant feed and pressurization - nuclear propulsion (Abort Propulsion attached to the reentry/abort vehicle)
Life Support & Command Modules	. Living module (including basic life support provisioning) & command control module/radiation shelter
	. Physical conditioning
	. Recreation
	. Medical center
	. Pressurization and air conditioning
	. Intercom
	. Command controls
	. Data acquisition, processing & display
Earth reentry/abort vehicle*	. Airframe
	. Propulsion (Nuclear and chemical storables)
	. Life support

*Expected to be the same as the Earth-Orbit base, Earth return vehicle.

TABLE A8.1 (cont.)

- . Intercom
- . Command controls
- . Data acquisition, processing and display
- . Guidance and control
- . Telecommunications
- . Thermal control and cockpit conditioning
- . Recovery aids (water and land)

Guidance and Control

Telecommunications (spacecraft-to-earth communications, spacecraft position and scientific data acquisition)

Electrical power supply (nuclear or solar generator)

Flight termination

Thermal control

Scientific experiments

Spacecraft Maintenance kits

Production facilities, tooling, fixtures and test/checkout equipment

Support systems (AMR and earth-orbit Mission staging bases)

Development test facilities

- . Contractor development laboratories
- . Contractor backyard "cold flow" facilities
- . Nevada battleship captive test facility

TABLE A8.1 (cont.)

- . Mississippi captive test facility (modified C-1 & C-5) Saturn and Nova test stands
- . AMR 4 checkout station facility (same as mission staging base) Also, modified C-1 & C-5 Saturn & Nova (Steps I & II) facilities
- . AMR launch pads (modified C-1 & C-5 Saturn and a 2 launch pad staging base)

Crew and support personnel training aids

Spacecraft assembly, servicing, and maintenance procedures

TABLE A8.2

NON-SYMMETRIC MISSION

BOOSTER VEHICLE DEVELOPMENT TASKS

C-1 and C-5 Saturn booster, Step II modification (to be utilized in early development flight test activity)

C-1 and C-5 Saturn booster, AMR support facilities and equipment modifications

Nova booster (Steps I & II)

- Engine (chemical existing engine modification) & controls
- Airframe (includes propellant feed and pressurization)
- Electrical power supply
- Flight termination
- Data acquisition

Nova booster (Steps I & II) production facilities, tooling fixtures and test/checkout equipment*

Nova booster (Steps I & II) ground support facilities and equipment* (includes Mississippi captive and AMR flight test facilities and equipment)

Support personnel training aids

Test/checkout, servicing and maintenance procedures

TABLE A8.3

NON-SYMMETRIC MISSION

AMR MISSION STAGING BASE

Spacecraft assembly and checkout facility (including four checkout stations - with mobile vehicle support structure/gantry)

Operations center

Communications center

Spacecraft radiation and explosive-safe facility

- Nuclear rocket and electrical power unit storage and checkout laboratory
- Nuclear rocket and electrical power unit installation facility
- Chemical propulsion laboratory

Launch complex

- Blockhouse
- Gantry (four required - includes vehicle support structure - see Item 1 above)
- Umbilical tower (four required)
- Launch stand (two required)
- Launch control center (two required)
- Instrumentation center
- Communication center

Crew briefing center

TABLE A8.4

NON-SYMMETRIC MISSION

EARTH-ORBIT MISSION STAGING BASE

Basic structure - including:

- Living quarters
- Physical conditioning
- Medical center

Telecommunications (staging base to ground/staging base to spacecraft)

Guidance and control

Electrical power

Air conditioning

Spacecraft assembly, checkout, servicing, and staging platforms

- Crocco mission vehicle
- Earth-entry vehicle
- Space logistics vehicles (utility, etc.)

Intercommunications

- Intercom system
- Operational phones
- Operation interconnection (includes base-to-earth communications)
- Vehicle staging control (spacecraft docking and launch)

Thermal control & liquefaction (hydrogen & oxygen)

Hydraulic and pneumatic power systems

Scientific experiments

Support equipment - spacecraft

TABLE A8.4 (cont.)

- Tools
- Fixtures - alignment
- Systems test/checkout
  - Control
  - Simulation
  - Instrumentation

Earth-orbit base maintenance kits

Ground support systems

Development test facilities

Support personnel training aids

Base assembly, servicing and maintenance procedures

Base production facilities, tooling, fixtures and test/checkout equipment

TABLE A8.5

NON-SYMMETRIC MISSION

LOGISTICS VEHICLES

Space Rescue Vehicle

- Rescue vehicle (reentry type)
- Booster vehicle*
- Support system*
  - Ground support equipment
  - Facilities (development test & operational)

Supply transportation vehicles (small, medium, and large)

- Spacecraft
- Booster vehicles*
- Support systems*
  - Ground support equipment
  - Facilities (development test & operational)

---

*Modified existing equipment

TABLE A8.6

NON-SYMMETRIC MISSION

CREW TRAINING PROGRAM

Spacecraft simulator (living module and abort vehicle)

Spacecraft mockup (includes reentry vehicle)

Crew conditioning equipment (Apollo extension)

MSC & AMR support facilities (Apollo extension)

Training aids

Spacecraft operation and maintenance procedures

TABLE A8.7

NON-SYMMETRIC MISSION

EARTH-ORBIT STAGING BASE PERSONNEL TRAINING PROGRAM

Staging base simulators

- Command-control module
- Spacecraft assembly and checkout module
- Earth-reentry/abort vehicle
- Space utility vehicle

Staging base mockup

Crew conditioning equipment

MSC and AMR support facilities

Training aids

Operations and maintenance procedures

SECTION 8

APPENDIX B

SYMMETRIC MISSION DEVELOPMENT TASKS

Subtasks pertinent to the subject mission prime development tasks are presented as follows:

Tasks	Table No.
Spacecraft	B8.1
Booster Vehicles	B8.2
Support Systems	B8.3
Logistics Vehicles	B8.4
Crew Training Program	B8.5

TABLE B8.1

SYMMETRIC MISSION

SPACECRAFT DEVELOPMENT TASKS

Nuclear Engine	
Airframe	. Stages I & II propellant feed and pressurization
Life Support and Command Modules	. Living module (including basic life support provisioning)
	. Command-control module/radiation shelter
	. Physical conditioning
	. Recreation
	. Medical center
	. Pressurization and air conditioning
	. Intercom
	. Command controls
	. Data acquisition, processing and display
Reentry/abort vehicle	
	. Airframe
	. Propulsion (chemical - storables)
	. Life support
	. Intercom
	. Command-controls
	. Data acquisition, processing and display

TABLE B8.1 (cont.)

- Guidance and control
- Telecommunications
- Thermal control and cockpit conditioning
- Recovery aids (water and land)

Guidance and control

Telecommunications (spacecraft-to-earth communications, spacecraft position and scientific data acquisition)

Electrical power supply (nuclear or solar electric)

Thermal control

Flight termination

Scientific experiments

Spacecraft maintenance kits

Production facilities, tooling, fixtures and test/checkout equipment

Ground support system* (includes logistics)

Development test facilities and related equipment*

- Contractor development laboratories
- Contractor "back-yard" cold flow facilities
- Nevada captive test facility

---

*Duplicate (or similar) automatic tests/checkout and related data acquisition, processing, and display equipment employed at all test/checkout locations.

TABLE B8.1 (cont.)

- Mississippi captive test facility (modified C-5 Saturn and Nova test stand)
- AMR single station checkout facility (part of mission staging base)
- AMR launch pads (modified C-1 & C-5 Saturn and one staging base, Nova type launch)

Crew and support personnel training aids

Spacecraft assembly, servicing, and maintenance procedures

TABLE B8.2

SYMMETRIC MISSION

BOOSTER VEHICLE DEVELOPMENT TASKS

C-1 and C-5 Saturn booster, Step II modification (to be utilized in early development flight test activity)

C-1 and C-5 Saturn booster, AMR support facilities and equipment modifications

Nova Booster (Steps I & II)

- Engine (chemical - existing engine modification) & controls
- Airframe (includes propellant feed and pressurization)
- Electrical power supply
- Flight termination
- Data acquisition

Nova Booster (Steps I & II) production facilities, tooling fixtures and test/checkout equipment*

Nova Booster (Steps I & II) ground support facilities and equipment* (includes Mississippi captive and AMR flight test facilities and equipment)

Support personnel training aids

Test/checkout, servicing and maintenance procedures

---

*Duplicate (or very similar) automatic test/checkout and related data acquisition, processing and display equipment employed at all test/checkout locations.

TABLE B8.3

SYMMETRIC MISSION

AMR MISSION STAGING BASE*

Spacecraft assembly and checkout facility (single station includes mobile vehicle support structure)**

Operations center

Communications center

Spacecraft radiation and explosive-safe facility

- Nuclear rocket and electrical power unit storage and checkout laboratory
- Nuclear rocket and electrical power unit installation facility
- Chemical propulsion laboratory

Launch complex

- Blockhouse**
- Gantry
- Umbilical tower — included as part of Item 1
- Launch stand
- Launch control center
- Instrumentation center
- Communication center

Crew briefing center

---

*In addition to NASA and PAA operated central control, telemeter ground station, radar tracking, impact prediction, etc. equipment.

**Duplicate (or very similar) automatic test/checkout and related data acquisition, processing, and display equipment employed at all test/checkout locations.

TABLE B8.4

SYMMETRIC MISSION

LOGISTICS VEHICLES

Space Rescue Vehicle

- Rescue vehicle (reentry type)
- Booster Vehicle*
- Support system*
  - Ground support equipment
  - Facilities (development test & operational)

Supply transportation vehicle (small, medium and large)

- Spacecraft
- Booster Vehicles*
- Support systems*
  - Ground support equipment
  - Facilities (development test & operational)

---

*Modified existing equipment

TABLE B8.5

SYMMETRIC MISSION

CREW TRAINING PROGRAM

Crew Training Program

- Spacecraft simulator (living module and reentry/abort vehicle)
- Spacecraft mockup (including reentry/abort vehicle)
- Crew conditioning equipment (Apollo extension)
- Training aids (in addition to those stated above)
- Spacecraft operation & maintenance procedures

SECTION 9

CONCLUSIONS AND RECOMMENDATIONS

9.1 REQUIREMENTS FOR THE 1970-72 LAUNCH

It is evident from the preceding data that a launch in July 1970 appears within technological reach of a plausible development program--provided certain problem areas are attacked immediately. The most critical areas include nuclear rocket engines, auxiliary power supplies of the SNAP or solar turboelectric varities, development of the Nova booster or C-5 Earth orbital operations capability, development of storable non-cyrogenic (or mild cryogenic) tripropellants with $I_{sp} \approx 410$ seconds, reentry materials and technology improvements, and immediate allocation of funds. These would be essential to a successful launch in the 1970 window. Slippage beyond August of 1970 would not be acceptable without uprating of the system to meet a 1972 launch for a similar mission and for this reason the program would have very stringent delivery date requirements which must be successfully met.

The early definition of a suitable advanced nuclear rocket engine (at least 200,000 pounds thrust burning for 800 seconds or 50,000 pounds thrust burning for 3600 seconds) must be made and development started before July 1963. Immediate development of a high I_{sp} storable liquid propellant and oxidizer is also necessary to meet the EMPIRE requirements. For Nova, continued development of the F-1, M-1, and J-2 engines is called for with the chosen engines to be integrated into a booster system starting in mid-1964. Of course, the alternative of using Saturn C-5 with rendezvous, docking, assembly, and fueling orbital operations is also feasible. The areas of interest not specified as critical also require active development, but are either represented by programmed developments or have apparent solutions within reach.

9.2 USE OF PROGRAMMED HARDWARE

In keeping with a conservative approach, it would be desirable to use the Saturn C-5, Apollo Command Module, NERVA nuclear rocket engine, and other hardware under development. Much of this approach has been integrated into this EMPIRE study. However, use of the Apollo reentry system, as currently envisioned, is not compatible with the six-man crew and mission characteristics. Use of C-5 is a definite possibility, but requires operations that tend to degrade mission success, especially when compared with a larger booster such as Nova. This is because rendezvous is not essential for the Nuclear Symmetric Mission using Nova for its boost vehicle. NERVA in its programmed form is not capable of providing enough total impulse without an extension of its burning time to an hour.

These and other considerations are all important. The major point to be made here is that use of present hardware capabilities could be a requirement for later study. In addition, it appears that a mission could be performed in 1970 or 1972 with this restriction. However, the cost would be greater due to the less efficient hardware approach, as well as the higher energy requirements for 1972 versus 1970.

9.3 LAUNCHES AFTER 1970-72

It should be noted that a detailed search for launch windows was not performed after 1 January 1972. It is believed that a mission of the Symmetric type exists in 1972 and 1975. It would be extremely desirable to perform an analysis of requirements for low energy multiple planet flyby and stopover missions from 1970 to 1990 in order to expose any useful or problem areas. Also, low energy single planet flyby's and stopovers should be explored with the future goals of manned landings on Mars and Venus.

There is no doubt that orbiting and landing missions require greater propulsion capabilities and larger weights at interplanetary injection than the flyby missions. For this and other reasons the ultimate goal of landing men on the other planets should be held as a long range objective. However, a logical first step could be a low energy flyby (the dual planet mission is not much harder to accomplish than a single planet encounter). If properly integrated into the overall space effort, such a mission could be achieved early and could lead directly to development of those areas of technology required for landings. This is without the more stringent requirements of the landing programs at relatively early dates.

The real importance of an integrated program is the financial and temporal savings to be accomplished by this approach. Also, the requirements of the lunar programs should not preclude an early attack on planetary missions, in view of the greater costs as time elapses into the 1970's for missions involving Mars. These statements emphasize the necessity for immediate overall evaluation of requirements for a Lunar and Planetary Program in the 1964-1990 time period.